Titre: Title:	Biomechanical Response of Trunk Under Perturbations and in Challenged Seated Balance
Auteur: Author:	Ali Shahvarpour
Date:	2015
Type:	Mémoire ou thèse / Dissertation or Thesis
Référence: Citation:	Shahvarpour, A. (2015). Biomechanical Response of Trunk Under Perturbations and in Challenged Seated Balance [Thèse de doctorat, École Polytechnique de Montréal]. PolyPublie. https://publications.polymtl.ca/1931/

URL de PolyPublie: PolyPublie URL:	https://publications.polymtl.ca/1931/
Directeurs de recherche: Advisors:	Aboulfazl Shirazi-Adl
Programme: Program:	Génie mécanique

UNIVERSITÉ DE MONTRÉAL

BIOMECHANICAL RESPONSE OF TRUNK UNDER PERTURBATIONS AND IN CHALLENGED SEATED BALANCE

ALI SHAHVARPOUR

DÉPARTEMENT DE GÉNIE MÉCANIQUE

ÉCOLE POLYTECHNIQUE DE MONTRÉAL

THÈSE PRÉSENTÉE EN VUE DE L'OBTENTION

DE DIPLÔME DE PHILOSOPHIAE DOCTOR

(GÉNIE MÉCANIQUE)

NOVEMBRE 2015

UNIVERSITÉ DE MONTRÉAL

ÉCOLE POLYTECHNIQUE DE MONTRÉAL

Cette thèse intitulée :

BIOMECHANICAL RESPONSE OF TRUNK UNDER PERTURBATIONS AND IN CHALLENGED SEATED BALANCE

présentée par : SHAHVARPOUR Ali

en vue de l'obtention du diplôme de : Philosophiae Doctor

a été dûment acceptée par le jury d'examen constitué de :

M. LAKIS Aouni, Ph. D., président

M. SHIRAZI-ADL Aboulfazl, Ph. D., membre et directeur de recherche

M. ÉTIENNE Stéphane, Doctorat, membre

M. DESCARREAUX Martin, Ph. D., membre externe

DEDICATION

To my family

ACKNOWLEDGEMENT

Foremost, I would like to express my sincere gratitude to my supervisor Prof. Aboulfazl Shirazi-Adl for his guidance, encouragement, patience, knowledge, and his unwavering support throughout this work.

I express my gratefulness to Dr. Christian Larivière for his continuous support and invaluable advice during this research. I sincerely thank Dr. Babak Bazrgari and Dr. Navid Arjmand for their assistance.

I would like to thank the members of my thesis jury, Prof. Aouni Lakis and Prof. Stéphane Étienne from École Polytechnic de Montréal and Prof. Martin Descarreaux from Université du Québec à Trois-Rivières for dedicating time to my thesis.

I thank the technical staffs at institut de recherche Robert-Sauvé en santé et en sécurité du travail, Mr. Hakim Mecheri, Ms. Cynthia Appleby and Ms. Sophie Bellefeuille.

I would like to take this opportunity to thank my former advisor at Sharif University of Technology, Tehran, Iran, Prof. Mohamad Parnianpour who introduced me to spine biomechanics and inspired me with his knowledge and encouragement to explore a new path in my life.

I am grateful of all my friends who encouraged and helped me during these years, Shabnam, Farshad and my many friends at University of Montréal.

I owe my deepest gratitude to my family, my parents to whom I dedicate this thesis for their unconditional love, support and patience, to my loveliest sisters Azadeh, Shideh, Fahimeh and Attieh, to my kindest brothers Mohammad, Saman and Simon, to my dearest aunt Nargues and my sweetest niece and nephews Rashno, Ahura and Radin.

For last but not least, I offer my special gratefulness to my beloved Shaghayegh for her love, patience and support that she has offered me throughout these years.

The financial supports from institut de recherche Robert-Sauvé en santé et en sécurité du travail (IRSST-Québec) and the Natural Sciences and Engineering Research Council of Canada (NCERC-Canada) are sincerely acknowledged.

RÉSUMÉ

Les maux de dos sont reconnus comme un problème de santé répandu et ayant un grand impact socio-économique. Des programmes de prévention, de réadaptation et de traitement devraient être fondés sur une bonne compréhension des fonctions neuro-biomécaniques de la colonne vertébrale dans des conditions normales et de blessure. En raison de difficultés techniques, de coûts excessifs et des enjeux éthiques aux mesures in vivo et in vitro, la modélisation biomécanique a été reconnue comme un outil complémentaire et puissant à cet égard.

Une perturbation du tronc qui peut se produire lors du chargement/déchargement soudain ou le déplacement rapide du tronc (ex. chutes et glissades) a été identifié comme un facteur de risque de mal de dos. Les effets d'inertie ainsi que les grandes réponses réflexives des muscles ont le potentiel de générer des charges vertébrales excessives qui peuvent causer des blessures à la colonne vertébrale. En effet, le risque de blessure augmente dans les cas ayant une faible marge de stabilité ou une réponse réflexive neuromusculaire altérée. La rigidité intrinsèque des tissus passifs et des muscles préactivés ainsi que les réponses réflexives de ces muscles permettraient d'améliorer la stabilité et l'équilibre du tronc. Les charges produisant la perturbation, les conditions préexistantes ainsi qu'un dysfonctionnement dans le contrôle des rigidités intrinsèques et réflexives influencent les forces musculaires et les charges imposées sur la colonne vertébrale.

L'équilibre postural du tronc en position assise instable a été suggérée autant en réadaptation que pour l'étude des mécanismes de contrôle neuromusculaire de la colonne vertébrale. L'avantage de cette tâche ou exercice pour l'étude de la stabilité de la colonne vertébrale est qu'elle permet d'éliminer l'apport des membres sur le contrôle de la colonne vertébrale en positon assise. En d'autres mots, seul le mouvement de la colonne lombaire permet de rétablir l'équilibre, ce qui en fait une tâche très spécifique. Puisque les réponses réflexes des muscles sont essentielles au contrôle de la colonne vertébrale, un contrôle altéré en raison de la douleur ou d'un dysfonctionnement neuromusculaire peut causer de plus grandes forces réflexives et charges sur la colonne vertébrale qui peuvent augmenter le risque de blessure. Il est important d'estimer les charges sur la colonne vertébrale afin d'évaluer la sécurité relative de cette tâche autant chez des sujets sains que chez des sujets lombalgiques.

Trois objectifs ont été poursuivis dans cette thèse. Le premier est de déterminer l'effet des conditions préexistantes et de la grandeur de la charge de perturbation (charge soudaine) sur la réponse biodynamique de la colonne vertébrale. On pose l'hypothèse que les conditions initiales du tronc (c.-à-d. la posture, coactivité antagoniste et précharge) et la grandeur de la charge de perturbation affecteront la réponse biodynamique de la colonne vertébrale, c.-à-d. la cinématique, les forces musculaires, la stabilité du tronc et le chargement de la colonne vertébrale. Le deuxième objectif est de vérifier si la position assise sur une chaise instable est suffisamment sécuritaire autant chez des sujets sains que chez des sujets lombalgiques chroniques. Le troisième objectif est de vérifier si les forces musculaires et le chargement de la colonne vertébrale pendant l'équilibration sur la chaise instable peuvent être utilisées pour différencier des sujets sains et lombalgiques chroniques.

Dans la première étude, l'effet de la précharge, de la flexion initiale du tronc, de la préactivation antagoniste des muscles abdominaux et de la grandeur de la charge de perturbation ont été étudiés chez 12 sujets asymptomatiques de sexe masculin. Ils étaient dans une posture semi-assise et la charge soudaine était appliquée au niveau T8 à l'aide d'un harnais. La précharge et la charge de perturbation appliquées sur le tronc ainsi que la translation du tronc au niveau T8 ont été mesurées. L'électromyographie (EMG) de 12 muscles (6 muscles bilatéraux) a également été enregistrée avant, pendant et après la perturbation. Les signaux EMG ont été normalisés par rapport à l'EMG maximal recueilli lors de contractions isométriques maximales volontaires (MVC) produites au début des séances. Les données cinématiques et cinétiques enregistrées ont été introduites dans un modèle non linéaire d'éléments finis qui considère le poids spécifique de chaque sujet. Le modèle a produit des estimations des forces musculaires, des charges imposées sur la colonne vertébrale et de la stabilité du tronc chez tous les 12 sujets. Pour étudier l'effet de la grandeur de la perturbation et des conditions préexistantes, des analyses statistiques ont été réalisées pour chaque variable dépendante, soit la cinématique du tronc, c'est-à-dire son déplacement, sa vitesse et son accélération angulaires, l'EMG normalisé et les forces musculaires actives / passives, le chargement de la colonne vertébrale et l'indice de la stabilité du tronc; tout ceci avant et après la perturbation.

Dans la deuxième étude, 6 hommes sains et 6 hommes lombalgiques chroniques ont été choisis (parmi 36 sujets testés dans une étude déjà publiée) afin de s'approcher du gabarit (taille

et poids) considéré par le modèle d'éléments finis. Tous les sujets avaient effectué 60 s d'une tâche d'équilibre posturale en position assise alors que la cinématique angulaire de différents segments du tronc (sacum, T12 et C7) et du siège a été enregistrée. La position du centre de pression et la force de réaction ont également été mesurées avec une plate-forme de force. Les cinématiques du tronc et du siège ont été introduites dans un modèle d'éléments finis tridimensionnel de la colonne vertébrale. Les forces musculaires et les charges de la colonne vertébrale ont été estimées. L'analyse statistique a été réalisée pour étudier si la présence d'un mal de dos influence la réponse des muscles et les charges imposées sur la colonne vertébrale.

Les résultats de la première étude sur le chargement soudain du tronc ont montré que le préchargement du tronc n'a pas affecté le déplacement du tronc alors que sa vitesse et son accélération ont diminué de façon statistiquement significative. Les EMG et les forces des muscles du dos ont augmentées avant la perturbation, ceci afin de contrebalancer la précharge appliquée antérieurement. Les EMG enregistrées des muscles n'ont pas été affectées après la perturbation. Par contre, les forces musculaires prédites par le modèle ont diminué de façon statistiquement significative, mettant de l'avant l'effet bénéfique de la précharge sur la stabilité du tronc (avant la perturbation); ce qui a d'ailleurs été confirmé par l'indice de stabilité. Le chargement de la colonne vertébrale, de leur côté, n'ont pas été affectées par la précharge, ceci autant avant qu'après la perturbation. La flexion initiale du tronc n'a pas affecté le déplacement relatif du tronc, bien que la vitesse et l'accélération maximales ainsi que la charge relative de perturbation (i.e. la charge maximale après la perturbation moins la charge appliquée au tronc à l'instant de la perturbation) aient augmenté de façon statistiquement significative. En raison des grandes déformations lorsque le tronc est initialement fléchi, la contribution des tissus passifs avant et après la perturbation était plus élevée. Ainsi, avant la perturbation les EMG enregistrées et les forces actives prévues par le modèle ont augmenté afin de résister contre la gravité. Les forces passives / actives des muscles ont amélioré la stabilité tel que confirmé par l'indice de stabilité. La latence du réflexe des muscles a été retardée, bien que le pic des réflexes (EMG) n'ait pas été affecté. Les forces musculaires actives calculées par le modèle étaient significativement plus grandes lorsque le tronc était initialement fléchi, ce qui s'explique par le besoin d'équilibrer le moment net de flexion qui augmente avec la flexion du tronc. La plus grande contribution des composantes passives de la colonne vertébrale et des forces actives / passives musculaires ont amélioré la stabilité avant et après les perturbations, c.-à-d. pendant toute la durée du mouvement.

Par contre, les charges plus élevées imposées sur la colonne vertébrale impliquent un risque accru de blessure dû à une perturbation soudaine lorsque le tronc est déjà en position fléchie. La préactivation des muscles abdominaux a augmenté la préactivation des EMG et les forces des muscles dorsaux avant la perturbation. Le plus petit indice de stabilité estimé avant la perturbation et au début de la période post-perturbation a montré une stabilité améliorée. La cinématique du tronc, le pic de réflexe EMG, les forces musculaires et le chargement imposé sur la colonne vertébrale estimés par le modèle n'ont pas été influencés par la préactivation des muscles abdominaux. Comme prévu, une plus grande charge de perturbation n'a pas affecté l'activité des muscles avant la perturbation; mais elle a augmenté le déplacement, la vitesse et l'accélération maximales, le pic de réflexe EMG, les forces musculaires prévues et le chargement de la colonne vertébrale. La stabilité a été améliorée après la perturbation, ceci dû à une plus grande activité réflexive des muscles dorsaux. Bien que le risque d'instabilité ait été réduit, le risque de blessure associé au chargement plus élevé de la colonne vertébrale a augmenté.

Pour résumer les résultats de la première étude, on a constaté que (1) la stabilité du tronc a été améliorée dû à la plus grande contribution des composantes actives-passives lorsqu'une précharge est appliquée, lorsque l'angle de flexion initiale du tronc est augmenté et lorsqu'il y a préactivation des muscles abdominaux; (2) les conditions initiales (pré-perturbation) ont influencé la réponse du tronc avant et après la perturbation; (3) la précharge a augmenté la rigidité intrinsèque active et diminué l'activité réflexive des muscles du dos; (4) la demande de réponse réflexive a augmenté sous la posture fléchie initiale en dépit de la rigidité intrinsèque active-passive plus élevée, ceci parce que l'effet de la gravité sur le tronc a détérioré la stabilité; ce qui a eu comme conséquence d'augmenter de façon significative le chargement de la colonne vertébrale; (5) la préactivation des muscles abdominaux n'a pas modifié les forces musculaires mais la coactivation prolongée des muscles qui a disparu progressivement après la perturbation a amélioré la stabilité avant et après la perturbation; (6) l'augmentation de la charge de perturbation a simultanément amélioré la stabilité et augmenté le chargement de la colonne vertébrale; (7) la sensibilité de la vitesse et l'accélération du tronc aux variables indépendantes est plus élevée par rapport aux EMG enregistrés des muscles, ce qui souligne la capacité du modèle d'éléments finis à décoder la cinématique en entrée et à prévoir l'effet de différentes variables sur les forces musculaires, le chargement de la colonne vertébrale et la stabilité du tronc.

Les résultats de la deuxième étude portant sur l'équilibre postural du tronc en position assise n'ont montré aucune différence statistique entre les groupes de sujets sains et lombalgiques chroniques. Les moyennes (pics entre parenthèses) de compression, des forces de cisaillement antéro-postérieur et mid-latéral ont été estimées 1139 N (1946 N), 437 N (790 N) et 6 N (239 N), respectivement. Les forces moyennes de compression et de cisaillement de la colonne vertébrale ont augmenté d'environ 50% par rapport à la position assise au repos (en position stable). Cependant, elles sont demeurées assez basses pour ne pas augmenter le risque de blessure.

Dans la première étude, les forces musculaires normalisées par rapport à la force musculaire maximale (0,6 MPa × PCSA (mm^2)) ont été comparées à l'EMG normalisé pour des fins de validation du modèle. Les variations dans le temps étaient similaires. Les forces musculaires étaient retardées par rapport aux EMG normalisées, ce qui s'expliquerait par le délai électromécanique. Dans la deuxième étude, la position du centre de pression ainsi que la force de réaction verticale mesurées par la plate-forme de force ont montré des corrélations satisfaisantes avec les estimations du modèle.

En conclusion, les perturbations soudaines du tronc ont considérablement augmenté le chargement de la colonne vertébrale et par conséquent le risque de blessure. Le risque de blessure augmente davantage en présence d'une posture fléchie adoptée avant la perturbation et de plus grandes charges de perturbation. Bien que toutes les conditions préexistantes aient augmenté la rigidité intrinsèque de la colonne vertébrale en phase de pré-perturbation, la réponse réflexive a été déterminée comme essentielle au maintien de l'équilibre et de la stabilité du tronc après la perturbation. Les estimations du modèle lors de la tâche d'équilibre posturale en position assise n'ont pas permis de distinguer les sujets sains des sujets lombalgiques chroniques mais révèlent qu'il s'agit d'un exercice sécuritaire en raison des forces faibles à modérées imposées à la colonne vertébrale.

ABSTRACT

Back pain is known as a prevalent health crisis with large socioeconomic impact on societies. Effective prevention, rehabilitation and treatment programs should be founded on solid understanding of the spine functional neuro-biomechanics in normal and injured conditions. Due to technical difficulties, excessive cost and ethical concerns with in vivo and in vitro measurements, in silico biomechanical modeling has been recognized as a complementary and powerful tool in this respect.

Trunk perturbation that may happen in sudden loading/unloading or rapid displacement of trunk (during falls and slips for example) has been found as a risk factor for back pain. Inertial effects as well as large reflexive response of muscles could generate excessive spinal loads that may cause back pain or spinal injuries. The risk of injury further increases in cases with low margin of stability or impaired neuromuscular reflex response. Intrinsic stiffness of passive tissues and active muscles along with muscles reflexive responses have been suggested as the mechanisms that enhance stability and balance of the trunk. Perturbation load, pre-perturbation conditions as well as dysfunction in any of active-passive mechanisms alter their contributions in balance control and as a result influence muscle forces and spinal loads. The risk of pain and injury likely increases as well.

Challenged sitting has been suggested as an approach for therapeutic applications as well as investigation of the neuromuscular control mechanisms of spine. The advantage of this method in studying spine stability is in eliminating the effect of lower extremities that are fixed to the seat on the control of the spine in seated subjects. Since muscle reflex responses are essential in control of the trunk, impaired control due to pain or neural dysfunction cause larger reflexive forces and spinal loads that may increase the risk of injury and pain. It is important to estimate the spinal loads in order to assess the relative safety of a task for both healthy and chronic low back pain (CLBP) groups.

Three objectives are set in this study. The first one is to determine the effect of pre-perturbation conditions and perturbation load magnitude on the spine biodynamics response subject to sudden loads. It is hypothesized that the trunk initial conditions (i.e. posture, antagonistic coactivity and preload) and perturbation load magnitude affect the spine

biodynamics response, i.e. kinematics, muscle forces, trunk stability and spinal loads. The second objective is to verify if the challenged seated position on a wobble chair is safe enough for both healthy and CLBP groups. The third objective is to verify if muscle forces and spinal loads profiles during the challenged balance sitting can be employed to differentiate healthy and CLBP groups.

In the first study, the effect of preload, initial trunk flexion, antagonistic preactivity of muscles and perturbation load magnitude were investigated on twelve asymptotic male subjects in a semi-seated upright posture under sudden loads applied at the T8 level via a harness. Applied preload and perturbation load on the trunk as well as generated trunk translation at the T8 level were measured. Electromyography (EMG) of 12 bilateral muscles was also recorded throughout before and after perturbations. EMGs were normalized to maximum isometric voluntary contractions (MVC) that were initially collected before experiments. A validated nonlinear musculoskeletal kinematics-driven finite element (FE) model of spine, driven by collected kinematics-kinetics was employed to compute muscle forces, spinal loads and trunk stability of all 12 subjects accounting for their individual body weight. To investigate the effect of perturbation magnitude and pre-perturbation conditions on collected results, statistical analyses were performed on kinematics of trunk, i.e. displacement, velocity and acceleration, muscle normalized EMG and muscles active/passive force, spinal loads and trunk stability index pre- and post- perturbation.

In the second study, 6 healthy and 6 CLBP males (among 36 subjects tested in an earlier study) with body height and weight close to our FE model were chosen. All the subjects had performed 60-sec challenged seated stability task while Euler rotations of the trunk at the S1, T12 and C7 as well as seat were recorded. Loci of the center of pressure and the reaction force were also measured with a force plate. The kinematics of trunk and the seat were prescribed into a three-dimensional kinematics-driven FE model of spine; and muscle forces and spinal loads were estimated. Statistical analysis was performed to investigate if back pain status had any influence on computed muscles response and spinal loads.

Results of the first study on sudden loading revealed that preloading the trunk did not affect trunk displacement; however its velocity and acceleration decreased significantly. Back muscles EMG and force prior to the perturbation increased to counterbalance the anterior

preload. Recorded muscles EMG were not affected post-perturbation, but model-predicted muscle forces decreased significantly highlighting the improving effect of preload on trunk stability pre-perturbation that was confirmed with the stability index. Spinal loads however remained unaffected pre- and post-perturbation. Initial trunk flexion did not affect relative displacement of trunk although peak velocity and acceleration as well as the relative perturbation load (peak load minus perturbation load at the perturbation instance) increased significantly. Due to larger deformations when the trunk was initially flexed, contribution of passive tissues before and after perturbation was higher. Recorded EMG and model-predicted active forces increased in order to resist against the gravity before perturbation. Higher passive/active muscle forces improved stability that was confirmed by the stability index. Muscles reflex latency was delayed although EMG reflex-peak was unaffected. Model-predicted muscle active forces were significantly larger when trunk was initially flexed that is due to the effect of gravity in larger flexion angles that increases back muscle forces. Larger contribution of spine passive components and larger active/passive muscle forces improved the stability before and after perturbations during the entire motion time. Significantly higher spinal loads indicate greater risk of injury due to sudden perturbation in a flexed posture. Abdominal muscles preactivation increased muscles EMG preactivity and model-predicted back muscle forces pre-perturbation. Smaller stability index found before perturbation and early post-perturbation period showed enhanced stability. Post-perturbation kinematics, EMG reflex-peak, calculated muscle forces and spinal loads however remained unaffected. As expected, the magnitude of the perturbation load did not affect activity in muscles pre-perturbation; however, it increased post-perturbation displacement, peak velocity and acceleration, EMG reflex-peak, calculated muscle forces and spinal loads. Stability was improved after perturbation due to larger reflexive activity of muscles. Although the risk of instability was reduced but the risk of failure under larger spinal loads increased.

To summarize the findings of the first study, it was found that (1) trunk stability was improved due to larger contribution of active-passive components when preload, initial trunk flexion angle and abdominal preactivation increased; (2) initial (pre-perturbation) conditions influenced the trunk response both pre- and post-perturbation; (3) preload caused higher active intrinsic stiffness and decreased back muscles reflexive activity; (4) the demand for reflex response increased under initial flexed posture in spite of higher intrinsic active-passive stiffness

as upper body gravity deteriorated stability; spinal loads increased significantly in consequence; (5) abdominal preactivation did not alter muscle forces but the prolonged muscles coactivity that disappeared gradually after perturbation enhanced stability pre- and post-perturbation; (6) higher perturbation load magnitude increased both the margin of stability and the spinal loads; (7) higher sensitivity to independent variables found in trunk velocity and acceleration profiles as compared to collected muscle EMG, highlighted the capability of the kinematics-driven FE model in decoding the input kinematics and in predicting the effect of changing variables on muscle forces, spinal loads and stability.

The results of the second study on challenged sitting on a wobble chair revealed no statistical difference between healthy and CLBP groups. The mean (peak) compression, anterior-posterior and right-left shear forces reached 1139 N (1946 N), 437 N (790 N) and 6 N (239 N), respectively. The average spinal compression and shear forces increased (by about 50%) relative to relaxed sitting. They remained nevertheless low enough to cause any injury.

In the first study, the muscle forces normalized to maximum muscle force (0.6 MPa × PCSA (mm^2)) were compared to normalized EMG for validation. The temporal patterns were found in good agreement. The muscle forces were delayed with respect to muscles normalized EMG that indicates the muscles electromechanical delay (EMD). In the second study, the loci of the center of pressure and the vertical reaction force calculated at the base compared to measurements via a force plate showed satisfactory correlations.

In conclusion, external sudden perturbations considerably increased spinal loads and consequently the risk of injury. The risk of injury further increases in presence of a pre-perturbation flexed posture and under higher perturbation loads. Although all pre-perturbation conditions increased spine intrinsic stiffness pre-perturbation, reflex response is found essential in maintaining the balance and stability after the perturbation. Challenged seated stability task could not distinguish between healthy and CLBP groups while it is a safe exercise due to low to moderate spinal forces.

TABLE OF CONTENTS

LIST OF TABLES

LIST OF FIGURES

LIST OF SYMBOLS AND ABBREVIATIONS

AGLR	Approximated generalized likelihood-ratio
ANOVA	Analyses of variance
AP	Anteroposterior
CLBP	Chronic low back pain
CMRR	Common mode rejection mode
CNS	Central nervous system
CoM	Center of mass
CoP	Center of pressure
ECG	Electrocardiogram
EO	External oblique
EMG	Electromyography
FE	Finite element
FEM	Finite element model
EMD	Electromechanical delay
HHT	Hilber-Hughes-Taylor
IAR	Instantaneous axis of rotation
IC	Iliocostalis
ICPL	Iliocostalis lumborum pars lumborum
ICPT	Iliocostalis lumborum pars thoracic
IDP	Intradiscal pressure
IO	Internal oblique
IP	Iliopsoas
JEK	Journal of Electromyography and Kinesiology
KDM	Kinematics-driven model
LBP	Low back pain
LG	Longissimus
LGPL	Longissimus thoracis pars luborum
LGPT	Longissimus thoracis pars thoracic
MF	Multifidus
MVC	Maximum voluntary contraction

PCSA	Physiological cross sectional area
PD	Proportional-derivative
QCT	Quantitative computed tomography
QL	Quadratus lumborum
RA	Rectus abdominis
RMS	Root mean square
RSI	Repetitive strain injury
SD	Standard deviation

LIST OF APPENDICES

CHAPTER 1 INTRODUCTION

1.1. Low back pain impacts

Low back pain (LBP) has devastating impacts on both the inflicted individuals in terms of sufferance and loss of quality of life and the whole society in terms of loss of productivity and health care costs. Epidemiological studies (Table 1.1) reveal that 84% of Canadians living in Saskatchewan have experienced low back pain in their life (Cassidy et al., 1998). 14.4% and 16.7% of, respectively, male and female Canadians (accounting for more than 2 million people) were experiencing LBP when they were surveyed with one third of them suffering from chronic low back pain (CLBP) (Ramage-Morin and Gilmour, 2010). The prevalence of serious back and spine problems reaches 4.4% among Canadians while the total number of disability days (sick leaves) is estimated at 21 million annually (Lee et al., 1985). Back strain injuries affect 18.5% of people in Canada with 54.6% of them reported to be work-related happening during repetitive and forceful movements, heavy lifting and exposure to vibration (Tjepkema, 2003). According to a survey in US, the total cost relating to LBP exceeded $100 billion annually of which two-third was related to indirect costs (Table 1.2) (Crow and Willis, 2009; Katz, 2006). Physical therapy and inpatient services comprise the biggest portion (17%) of the direct cost of LBP followed by pharmacy and primary care (13%) (Dagenais et al., 2008). The total number of cervical and lumbar fusion surgeries performed in US attained 281300 in 2003 showing a considerable 170% increase in 13 years (Kurtz, 2006). The huge financial and social impacts of low back pain and spinal disorders have motivated the health care practitioners and researchers to focus their efforts on the investigation of the biomechanical behavior of the spinal column in intact and injured conditions in order to gain better understanding of the functional biomechanics of spine towards more effective injury prevention programs as well as rehabilitation and treatment strategies.

Table 1.1 Prevalence of low back pain in different countries (Ghaffari, 2007)

Country	Results	
	Duration	**Prevalence**
Canada (Cassidy et al., 1998)	Lifetime:	84.1%
	6 months	48.9%
	Point Prevalence	28.4%
USA (Lawrence et al., 1998)	Lifetime	70%
	Annual	56%
Sweden (Linton et al., 1998)	1 year for men	63%
	1year for women	69%
United Kingdom (Papageogiou et al., 1995)	1 month for men	35%
	1 month for women	42%
Iran (Ghaffari et al., 2006)	1 year for men	20%
	1 year for women	27%
	1 week	8%
Turkey (Oksuz, 2006)	Life-time	44%
	1 year	34%
	Point Prevalence	19.7%

Table 1.2 Direct and indirect cost of low back pain in different countries (Ghaffari, 2007) given in million US$ with % of total cost in brackets.

Cost Categories	United Kingdom	Sweden	The Netherlands
Direct Costs	385 (11.5)	213 (8)	368 (7.4)
Indirect Costs	2948 (88.5)	2262 (92)	4600 (92.6)
Total	3333	2475	4968

CHAPTER 2 LITERATURE REVIEW

2.1. Spine functional biomechanics

2.1.1. Spine anatomy

A brief description of the functional anatomy and biomechanics of the spine is given in this section; nonetheless more details could be found elsewhere (Adams et al., 2012; Bogduk, 2012; McGill, 2007; White and Panjabi, 1978). Spine is a column made of thirty three vertebrae interconnected by intervertebral discs and ligaments (Figure 2.1). It has three main functions: supporting head, trunk and upper extremities, providing flexibility and movement to perform daily tasks and protecting spinal cord and nerve roots. Spinal column is divided into 5 regions; the most distal one is coccyx with very limited range of motion. The next is sacrum made of 5 vertebrae fused to each other. Resting on top of the sacrum, the lumbar spine consists of 5 vertebrae shaped a curvature called lordosis in the sagittal plane. Lumbar spine has a substantial contribution to the movement of the upper body. Lumbar vertebrae are bigger and stronger than those at other regions (Kurtz and Edidin, 2006). Twelve vertebrae forming kyphosis curvature make the thoracic region. Since they are reinforced by the rib cage, their range of motion is much smaller than that of adjacent regions. Finally and the most proximal region, the cervical spine is made of 7 vertebrae and supports the head. Due to the structure of the vertebrae and the intervertebral discs, it has the largest range of motion relative to the other levels.

Each bony vertebra consists of the anterior body, the vertebral arch including lamina and pedicle and seven processes (Figure 2.2). Each vertebra is made of cancellous (trabecular) bone within a dense thin shell of cortical bone with the average thickness of about 0.35 mm (Ashton-Miller and Schultz, 1997). The superior and inferior edges of anterior vertebral body, averaged less than 0.5 mm thick, called vertebral endplates and attaches the body to the adjacent intervertebral discs. The vertebrae provide pathway for nerves and blood veins as well as attachment surfaces for muscles and ligaments. The vertebrae transfer compression and shear loads as well as moments through the vertebral column.

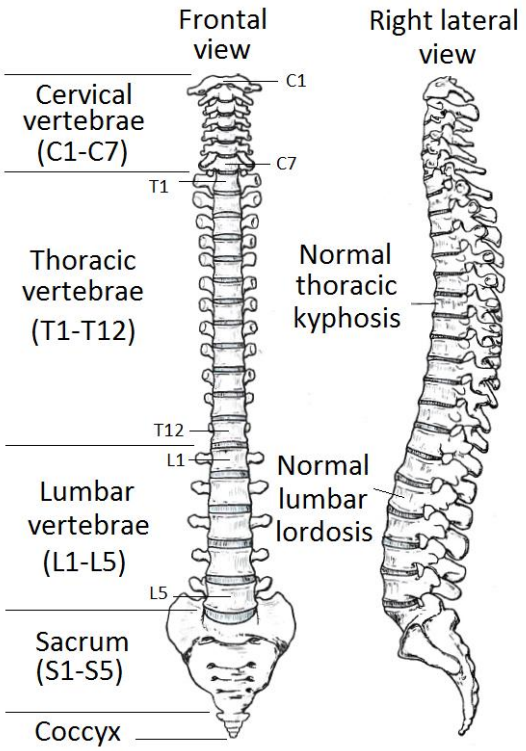

Figure 2.1 Spine with 33 vertebrae is anatomically divided into 5 regions, coccyx, sacrum, lumbar spine, thoracic spine and cervical spine (modified from (Vieira et al., 2009)).

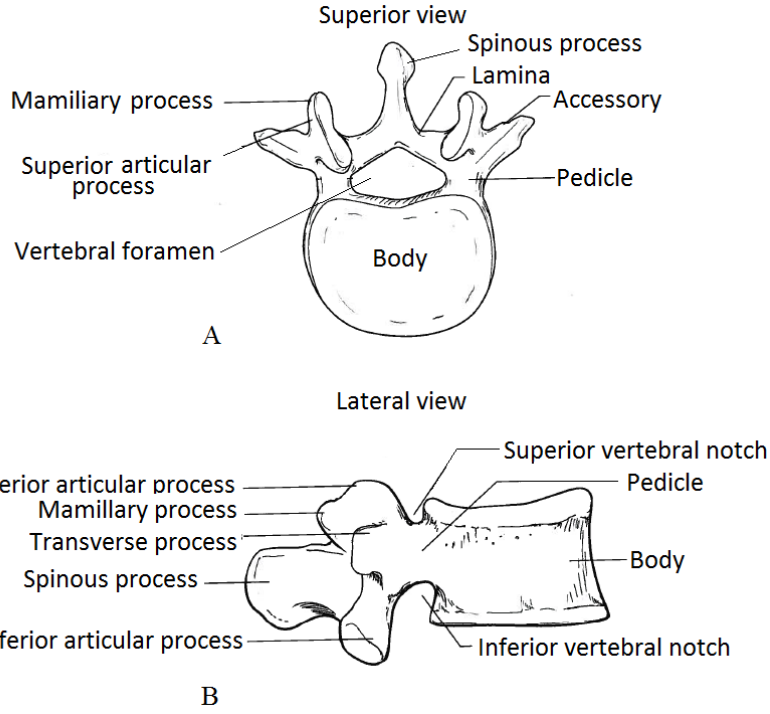

Figure 2.2 Superior and lateral view of a lumbar vertebra (adapted from (Moulton, 2009))

Mechanical properties of each vertebra depend on its architecture and density (Stokes and Iatridis, 2005). Kopperdahl et al. (2002) showed that the modulus of elasticity increases linearly with the quantitative computed tomography (QCT) density of the trabecular centrum. The elasticity moduli of the vertebral trabecular bone in compression and tension are reported identical (Kopperdahl and Keaveny, 1998) at 319 ± 189 MPa (Kopperdahl et al., 2002). However, yield strain of the bone is significantly higher in compression (0.84 ± 0.06%) than in tension (0.78 ± 0.04%) (Kopperdahl and Keaveny, 1998). The vertebrae strength decreases due to aging while bone matrix becomes more anisotropic (Figure 2.4) (Mosekilde and Mosekilde, 1986). The relative contribution of the vertebral body shell is only 10% relative to the body centrum implying the dominant role of the body centrum in carrying the compression (Silva et al., 1997). With aging, elasticity modulus and strength of vertebra decrease due to osteoporosis.

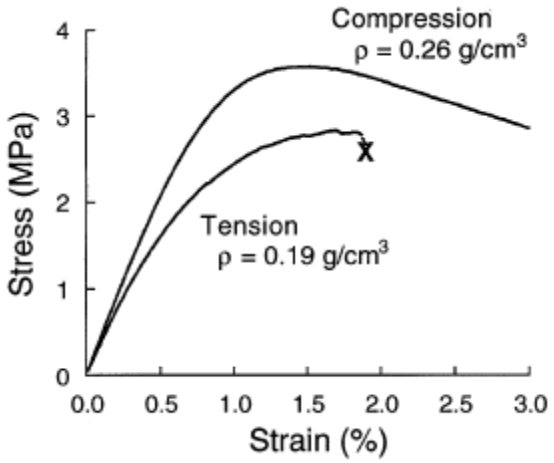

Figure 2.3 Stress-strain curves in compression and tension of two human vertebrae reported in (Kopperdahl and Keaveny, 1998). The vertebra tested in tension had lower density suggesting lower modulus and strength.

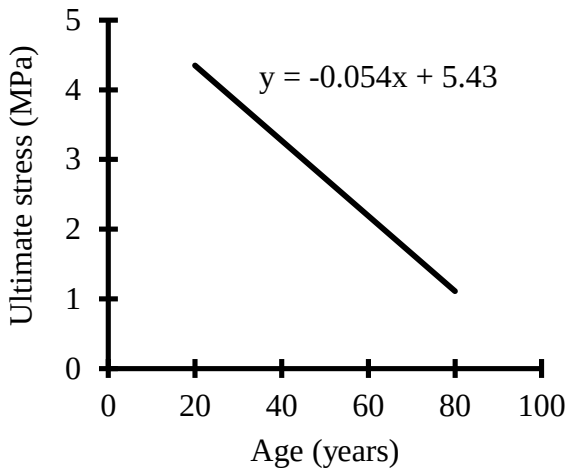

Figure 2.4 Ultimate compressive stress of the vertebra decreases with age (Mosekilde and Mosekilde, 1986)

The intervertebral discs placed in between two thin cartilaginous endplates consist of two central regions of nucleus pulposus and annulus fibrosus (Figure 2.5). The nucleus pulposus possesses (by weight) 70-90% of water, 25% of collagen (mainly types I and II) and some proteins (Antoniou et al., 1996). Due to its composition, the normal nucleus acts as an incompressible fluid with hydrostatic state of stress. Some studies have modeled the nucleus as an incompressible inviscid fluid (Shirazi-Adl et al., 1986b) while some others have modeled it as a biphasic material (Laible et al., 1993; Laible et al., 1994; Simon et al., 1985). Mechanical behavior of the nucleus pulposus in shear (Greene et al., 2001; Sato et al., 1999) and tension reveals its viscoelastic behavior (Stokes and Iatridis, 2005), which makes it capable of absorbing shocks when the structure is under impact or cyclical loads. Bulk modulus of the nucleus pulposus has been estimated around 0.3 MPa (Stokes and Iatridis, 2005); while its tensile and shear moduli are, respectively, reported 0.04 MPa (Panagiotacopulos et al., 1987) and 0.025 MPa (Iatridis et al., 1997), respectively. Loading frequency and degeneration highly affects mechanical properties of the nucleus pulposus (Stokes and Iatridis, 2005).

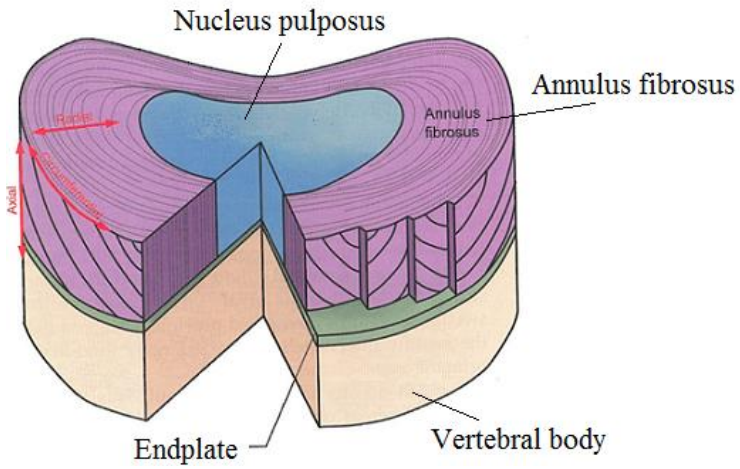

Figure 2.5 Intervertebral discs attaches to vertebral body through the very dense cartilage tissue called endplates (adapted from (Guerin and Elliott, 2006))

Annulus fibrosus is composed of about 20 strong connected layers reinforced by collagen fibrils running obliquely in circumferential orientations, layer thickness increases from 0.1 mm at the periphery to 0.4 mm at the inner area (Cassidy et al., 1989; Marchand and Ahmed, 1990). Lamina collagen angles change from 60 to 45 degrees (to the spinal axis) from the outer to the inner annulus (Stokes and Iatridis, 2005). Annulus fibrosus is a nonlinear, heterogeneous, anisotropic and viscoelastic material stronger in tension. Its mechanical properties are influenced by its state of hydration (Galante, 1967). Aggregate compression (at equilibrium) and tensile modulus of elasticity of annulus fibrosus are 0.56 MPa (Iatridis et al., 1998) and 20 MPa (Acaroglu et al., 1995), respectively. The high tensile modulus of elasticity of the annulus fibrosus is the result of its fibrous nature. Shear modulus of annulus fibrosus is estimated at 0.1 MPa (Iatridis et al., 1999).

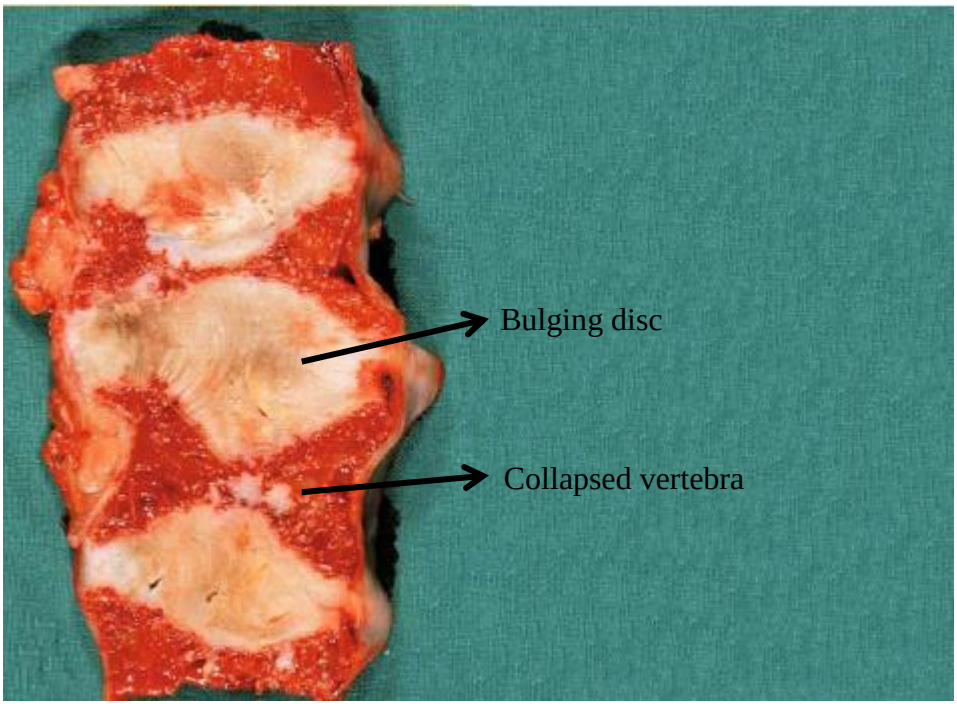

Figure 2.6 Collapse of degraded structure of human vertebra causes bulging of intervertebral disc (from (Sukthankar et al., 2008))

Two layers of hyaline cartilage connect the superior and inferior intervertebral disc to the vertebral body (Roberts et al., 1989). Its thickness is approximately 0.8 mm at the periphery that decreases towards the center (Zhao et al., 2009). Vertebral endplates distribute the load uniformly between the discs and vertebrae. The permeability and diffusivity of the endplates allow for the transport (diffusion and convection) of water and solutes between the vertebral bodies and adjacent discs (Ferguson, 2008); it also controls evacuation of degraded matrix products and waste materials from the disc (Stokes and Iatridis, 2005). Restraining fluid flow with low permeability, endplates also maintain fluid pressure within the nucleus pulposus (Zehra et al., 2015). High compressive loads pressurize nucleus pulposus that causes bulging of endplates. A compressive load of 7500 N deflects the endplate by 0.5 mm (Ashton-Miller and Schultz, 1997; Brinckmann et al., 1983). In the event of a central endplate fracture under large compression, the nucleus material could extrude into the fractured vertebra causing vertical disc herniation called "Schmorl's node" (Hilton et al., 1976). It is generally believed that the occurrence of these fractures predispose the discs to accelerated degeneration that may be the cause of low back pain (Roaf, 1960; White and Gordon, 1982).

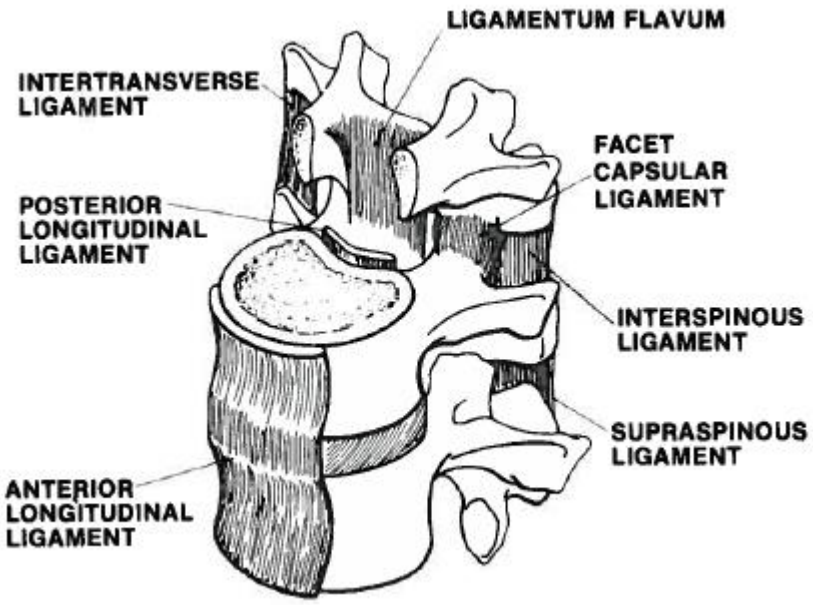

Figure 2.7 A lumbar motion segment illustrating two vertebrae with the intervertebral disc, facet joints and seven ligaments. They provide flexibility to the entire intervertebral column while constraining the motion and providing the structure with sufficient stiffness and stability to safely perform daily tasks (from (White and Panjabi, 1990)).

2.1.2. Motion segment

The relative motion between two vertebrae is constrained by an intervertebral disc, two pairs of facet articulations with adjacent vertebrae and seven intervertebral ligaments. An intervertebral disc is placed between anterior vertebral bodies. Facet joints are articular joints between the inferior processes of the upper vertebra and the superior processes of the lower vertebra. Each pair of vertebrae with intervening disc, ligaments and facet joints constitute the building block of the entire spine and is called a motion segment (Figure 2.7).

Table 2.1 expresses the maximum range of rotation of lumbar motion segments in flexion/extension, lateral bending, and axial rotations. Lumbar flexibility and range-of-motion are larger in forward flexion relative to backward extension (Shirazi-adl, 1994a). L4-L5 rotation is the largest among lumbar motion segments when subject to similar sagittal moments; in other word L4-L5 stiffness is the smallest; under lateral moment no difference is seen between rotation at L2-L3, L3-L4 and L4-L5 (Shirazi-adl, 1994a). The lumbar spine demonstrates much greater compliance than the thoracic spine that is stiffened by the rib cage; the contribution of lumbar

motion segments in trunk movements is more than the contribution of thoracic motion segments (White and Panjabi, 1990). Thoracic region is often taken as a rigid body in modeling the trunk though recent works have suggested that about 16-20% of the total trunk forward rotation originates from the thoracic discs (Hajibozorgi and Arjmand, in press).

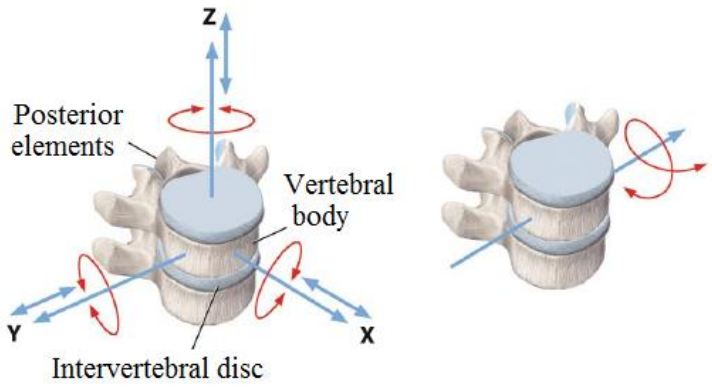

Figure 2.8 Each motion segment has three translational and three rotational degrees of freedom (from (Ferguson, 2008))

Providing six degrees of freedom, a motion segment is the basic unit of the spine structure that gives flexibility and load carrying capacity to the spine (Figure 2.8). The mechanical behavior of the motion segment depends on that of its constituents; disc, vertebrae, facet joints and ligaments. Stiffness of spinal motion segments in all planes increases nonlinearly with deformation (Schmidt et al., 2013), i.e. flexion-extension, lateral bending, axial rotation and axial/shear deformation, that is verified both experimentally (Berkson et al., 1979; Markolf, 1972; Miller et al., 1986; Schultz et al., 1979) and in model studies (Shirazi-Adl, 2006; Shirazi-Adl et al., 1986a; Shirazi-Adl et al., 1986b; Shirazi-Adl et al., 1984) of human and other species (Figure 2.9) (Stokes et al., 2002; Wilke et al., 1997). This is partly due to the higher resistance of collagen fibers when stretched under loads and internal nucleus pressure (Schmidt et al., 2013; Shirazi-Adl, 2006). Presence of axial compression preload further stiffens the motion segment (Figure 2.10) (Adams and Dolan, 1991; Edwards et al., 1987; Stokes and Gardner-Morse, 2003), albeit with reducing the nonlinearity of the load-deformation relationship (Janevic et al., 1991). Higher axial load pressurizes the nucleus and causes disc bulging in the horizontal plane (Figure 2.11). Higher stress in outermost annular fibers stiffens the disc due to nonlinear stress-strain properties of the annular fibers (Broberg, 1983; Shirazi-Adl, 2006).

Table 2.1 Maximum range of rotation of lumbar motion segments in three anatomical planes; sagittal, frontal, and transverse (from (White and Panjabi, 1990))

Motion segment	Combined flexion/extension (±y-axis rotation) degrees	One sided lateral bending (x-axis rotation) degrees	One sided axial rotation (z-axis rotation) degrees
T12-L1	12	8	2
L1-L2	12	6	2
L2-L3	14	6	2
L3-L4	15	8	2
L4-L5	16	6	2
L5-S1	17	3	1

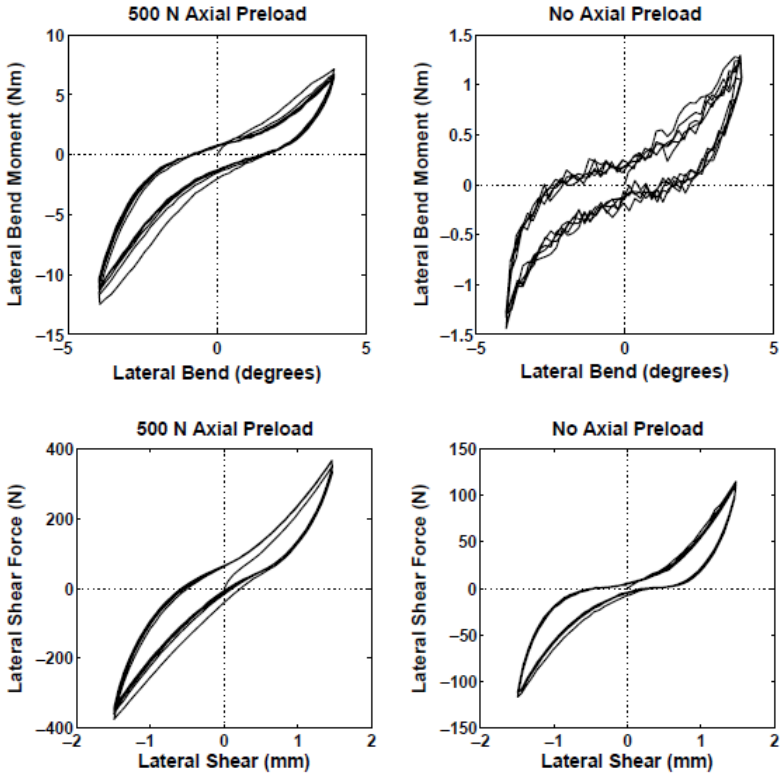

Figure 2.9 The measured motion segment stiffness increases in lateral bending (top) and lateral shear (bottom) when 500 N axial force applied to the motion segment of a pig lumbar spine (from (Stokes et al., 2002)).

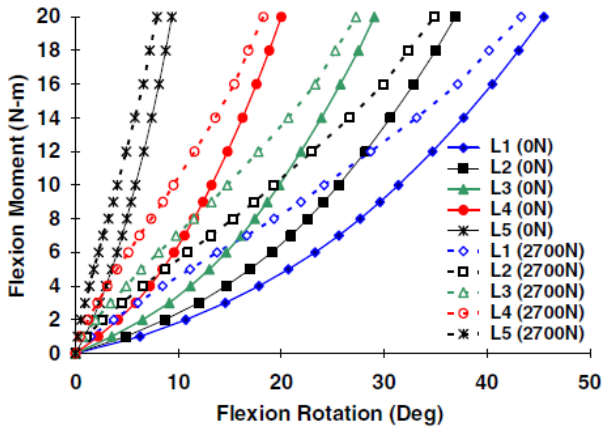

Figure 2.10 Lumbar segments stiffen in flexion moment when compression preload increases from 0 N to 2700 N (from (Shirazi-Adl, 2006)).

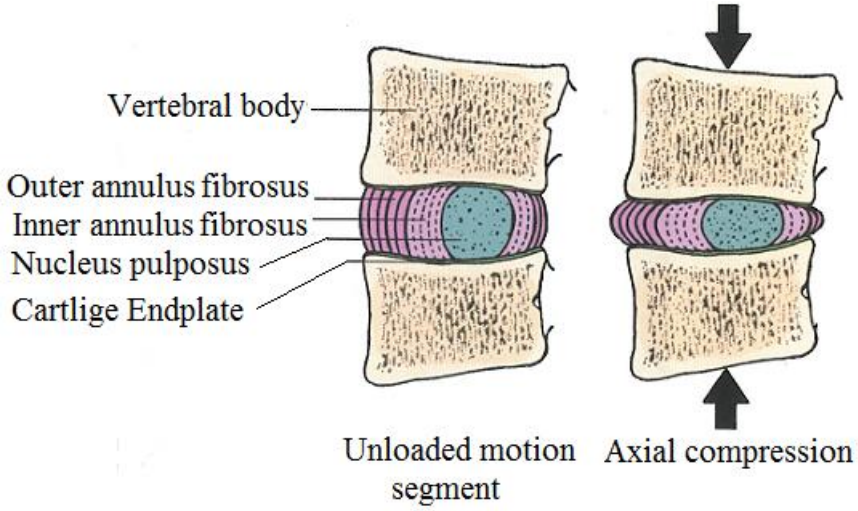

Figure 2.11 Compression on the spine motion segment increases stress in annulus collagen fibers that in turn stiffen the spine segments (from (Guerin and Elliott, 2006)).

When the load-deformation relationship is linearized, a six-order symmetric tangent stiffness matrix, $[K]$, could describe the mechanical behavior of the motion segment: $\{F\} = [K]\{X\}$, in which $\{F\}$ is the vector of loads, i.e. three forces and three moments, and $\{X\}$ is the vector of displacements, i.e., three translations and three rotations. Evidently, this tangent stiffness matrix is valid only in the vicinity of the operating state, i.e. configuration and loading, of the motion segment. The six diagonal elements relate forces/moments to corresponding displacements/rotations for each degree of freedom. Some terms are zero because of the structure's symmetry about the sagittal plane; for instance, axial compression load does not cause

displacement in lateral direction. However, there are non-zero off-diagonal elements due to coupling of load and deformation in different degrees of freedom. Goel (1987) measured two primary off-diagonal elements relating the rotation in the sagittal and frontal planes to shear forces. Other studies have attempted to determine all elements of a linear stiffness matrix for the motion segment (Gardner-Morse and Stokes, 2004; Meng et al., 2015; Panjabi et al., 1976).

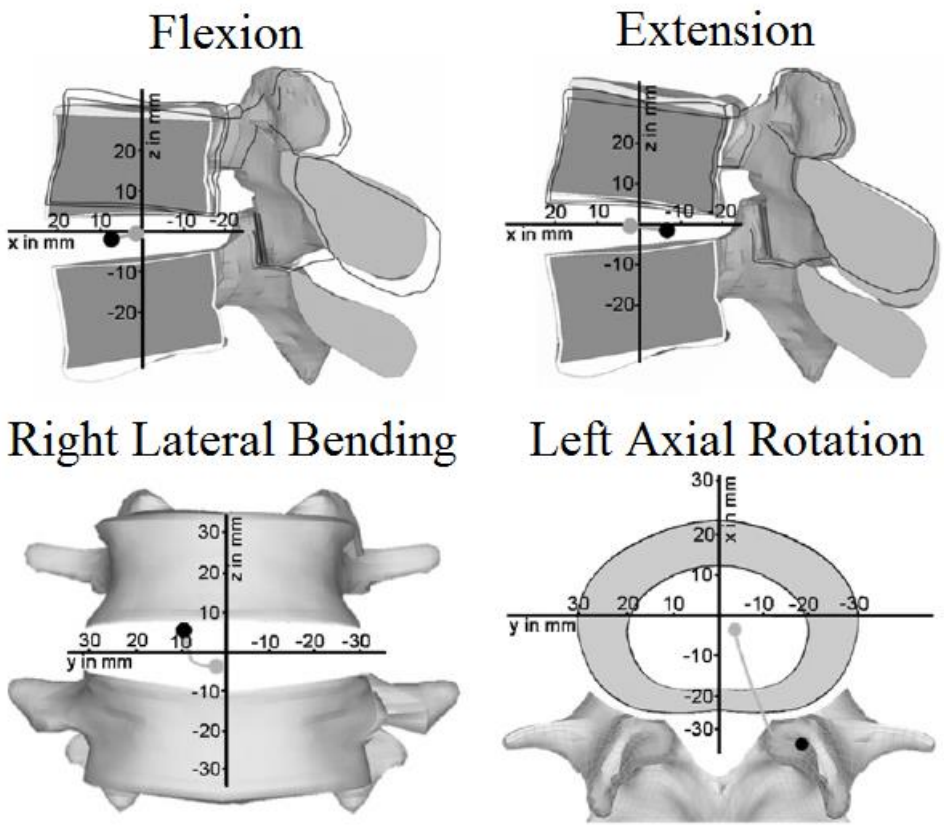

Figure 2.12 Movement of the instantaneous axis of rotation when the motion segment is subject to flexion, extension, lateral bending and axial rotation. Gray and black dots represent, respectively, the primary and displaced positions of the axis of rotation (from (Schmidt et al., 2008))

When motion segment deforms, the position of the instantaneous axis of rotation (IAR) changes accordingly (Figure 2.12). The findings on the position of the axis of rotation diverge (Bogduk et al., 1995; Rousseau et al., 2006; White and Panjabi, 1990). In vitro studies revealed that IAR, which primarily passes through the disc nucleus, moves posteriorly under flexion moment (Rousseau et al., 2006). This is however in contrast with a FE model study reporting that

IAR moves anteriorly as the resistance of the posterior ligaments and annulus fibers increases while the facet joints remain unloaded (Schmidt et al., 2008). Correspondingly, the axis of rotation moves posteriorly in large extension angles (Schmidt et al., 2008). Similarly, when lateral bending moment increases, the instantaneous axis of rotation moves posteriorly and toward the ipsilateral side of the disc. In axial rotation, however, uneven loading of facet joints plays a more significant role. When the motion segment is rotated axially, the opposite facet joint is compressed. Therefore, as vertebra rotates axially, the instantaneous axis of rotation moves outside the disc approaching the compressed facet joint (Schmidt et al., 2008; Shirazi-Adl et al., 1986b).

Intervertebral disc and facet joints transmit load between vertebrae; however, their contribution depends on the direction and magnitude of the load. FE model studies of lumbar spine devoid of musculature reveal that under 15 Nm flexion moment, largest (~0.68 MPa) and smallest (~0.25 MPa) intradiscal pressures (IDP) are generated, respectively, at L1-L2 and L4-L5 (Shirazi-adl, 1994a); while the contact forces at facet joints are very small at all levels. In contrast, 10 Nm extension moment generates considerably large loads at facet joints (170 N at L2) while decreasing the IDP (Figure 2.13) (Shirazi-adl, 1994a; Shirazi-Adl et al., 1986a). The axial compressive load is transmitted primarily by intervertebral disc. Facet joints only carry 1% to 5% of the 5000 N compression load in neutral or flexed position; while the contribution of the facet joints increases considerably to 10-30% with much smaller compression load (1000 N) (Shirazi-Adl and Drouin, 1987). When lumbar spine devoid of musculature was subject to 10-Nm lateral moment the contact force on the ipsilateral facet joint is found smaller than its pair on higher vertebral levels; then at lower levels the pattern changes such that the relative contact force in ipsilateral facet joint at L5 is substantially larger than force at the other facet joint (Shirazi-adl, 1994a). When the lumbar spine is subject to 10 Nm axial torque IDP varies between 0.10 to 0.20 MPa; and total contact forces at fact joints are larger at higher levels (93 - 125 Nm) decreasing at lower levels (26 - 78 Nm) (Shirazi-Adl, 1994b).

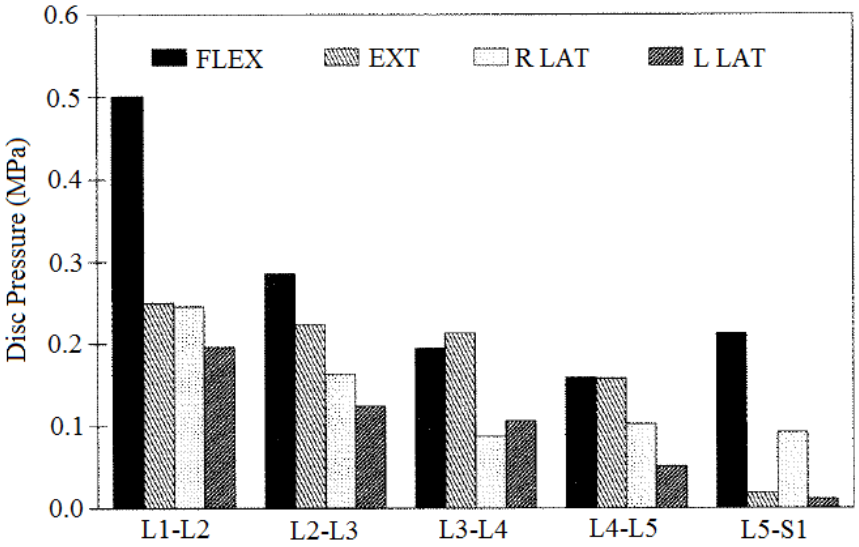

Figure 2.13 Lumbar intradiscal pressure when lumbar is subject to 10 Nm bending moment at different directions: flexion, extension, right and left lateral bending (from (Shirazi-adl, 1994a)).

2.1.3. Spinal loads

Lumbar compression loads have been estimated by measuring in vivo the intradiscal pressure IDP (Andersson et al., 1977; Nachemson, 1960; Nachemson and Elfström, 1970; Nachemson and Morris, 1964; Nachemson, 1981; Polga et al., 2004; Sato et al., 1999; Schultz et al., 1982; Schultz et al., 1979; Takahashi et al., 2006). Wilke et al. (1999) measured IDP in one subject at various diurnal activities (Figure 2.14). While minimum IDP is found in lying supine and on the side (approximately $1/4$ of IDP in standing), its peak happens in stoop lifting with IDP 4.5 times larger than that in standing. The IDP during stoop lifting is 1.3 times larger than that of squat lifting. The IDP in relaxed sitting without rest is almost equal to IDP in standing, while flexion increases it and slouching back decreases it. In walking, jogging with hard shoes, climbing and walking down stairs IDP varied between 0.53-0.65, 0.35-0.95, 0.50-0.70 and 0.38-0.60 MPa, respectively.

Spinal compressive force, F_{Comp}, may be estimated from IDP by accounting for the disc cross-sectional area, *Area*, including both nucleus pulposus and annulus fibrosus, and a correction factor, C_{Corr}, accounting for non-uniform load transfer across the disc cross-section.

$$F_{Comp} = IDP \times Area \times C_{Corr} \quad (1.1)$$

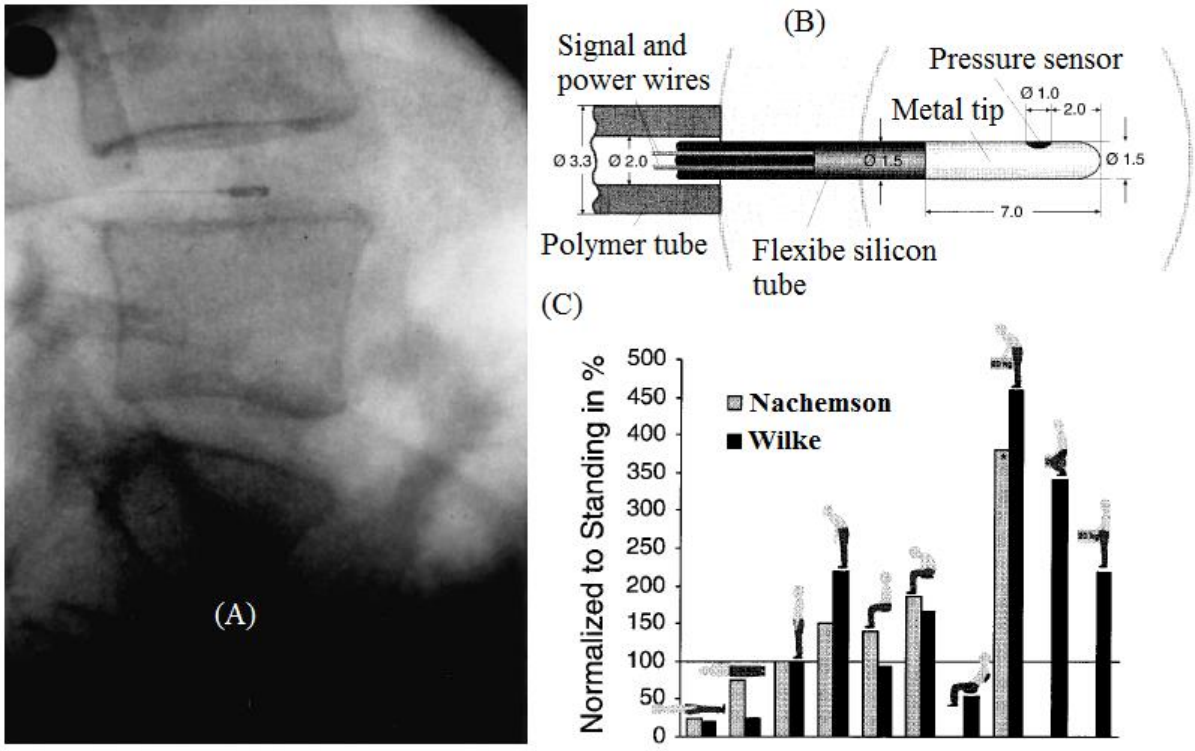

Figure 2.14 (A) A pressure transducer (shown in B) was inserted into the L4-L5 disc of a 45-year-old male. The IDP was measured at different postures, conditions and tasks. (C) IDP was measured during (from left to right) lying supine (IDP = 0.1 MPa), lying on the side (IDP = 0.12 MPa), relaxed standing (IDP = 0.5 MPa), standing bent forward (IDP = 1.10 MPa), sitting relaxed without backrest (IDP = 0.46 MPa), sitting with maximum flexion (IDP = 0.83 MPa), sitting slouched into the chair (IDP = 0.27 MPa), lifting 20 Kg bent over with round back (IDP = 2.30 MPa), squat-style lifting 20 Kg (IDP = 1.70 MPa) and holding 20 Kg close to the body (IDP = 1.10 MPa). In the graph the IDPs are normalized to the IDP at relaxed standing posture. They are compared to values reported in (Nachemson, 1992; Nachemson and Morris, 1964), in which weight is 10 Kg in lifting tasks. The dimensions in B are in mm. (from (Wilke et al., 1999))

Taking 0.66 for C_{Corr}, Nachemson (1960) estimated the compressive force in standing posture equal to 500 N. Other correction factors varying between 0.55 – 0.77 have been suggested in other studies (Brinckmann and Grootenboer, 1991; Nachemson, 1981). A recent FEM study (Dreischarf et al., 2013) has however revealed that more accurate geometry of disc

and individualized correction factor are needed to minimize the error of spinal load estimation from IDP measurement.

Spine compression has been estimated by measuring IDP in healthy controls and patients (Sato et al., 1999). Results reveal that IDP reduces according to the degree of disc degeneration. Takahashi et al. (2006) measured IDP, muscles EMG and trunk kinematics of subjects instructed to bend forward, stay in maximum flexion in 1-2 sec and extend back to upright position. Spinal loads were estimated with a simple inverted pendulum representing the spine pinned at the L4-L5 and a single-equivalent muscle model. Compression was also estimated using the measured IDP and correction factor of 1. Both methods show that flexing forward increases compression; however, model-predicted compression is 40% smaller than IDP-calculated compression. Oversimplifying the spine model or using correction factor of 1 could be the reason of this disagreement.

Spinal load has been measured by instrumented vertebral replacements in patients (Rohlmann et al., 2013). The daily activities with maximum spinal load have been reported as (the maximum of compression among 5 patients): lifting weight from ground (1649 N), straight arm elevation forward with weight in hands (1467 N), moving a weight in front of the body with hanging arms (1434 N), standing up/sitting down (1213 N), staircase walking (1145 N), tying shoes (1095 N) and trunk flexion (1075 N), moving from lying to sitting (858 N), walking (833 N) (Rohlmann et al., 2014). Maximum shear force, bending moment and torsional moment are, respectively, 123 N in lifting weight from ground, 6.23 Nm in upper body flexion and 3.51 Nm in tying shoes (Rohlmann et al., 2014).

Due to the difficulty in measuring IDP, compression and shear forces, computational models have been developed to estimate muscle forces and spinal loads (Anderson et al., 1985; Chaffin, 1969; Gracovetsky et al., 1977), with validation noted to be of concern (van Dieen and de Looze, 1999). Employing an EMG-assisted model of spine, Granata and Marras (1993) estimated compression, AP and lateral shear in asymmetric trunk extension; compression exceeded 3kN while peak AP and lateral shear reached over 300 N and 60 N, respectively. Using the same technic, spinal loads were predicted during symmetric and asymmetric dynamic lifting with different velocities (Granata and Marras, 1995). Lifting in asymmetric posture increased significantly the spinal loads. Compression increased significantly with lifting velocity but AP

and lateral shear were not affected. Maximum compression, AP and lateral shear increased significantly with lateral lifting velocity (Marras and Granata, 1997). Compression was estimated around 7 kN in weight lifting tasks while movement asymmetry significantly affected the spinal loads (Granata et al., 1999). Using a linked segment model of spine, Cholewicki et al. (1991) estimated the average compressive forces up to 17 kN for powerlifters. Using an EMG-assisted optimization-based model of spine, McGill et al. (1996) proposed a polynomial function estimating L4-L5 compression in 3D loading and motion of trunk.

Using FE model studies, compression and shear forces at the L5-S1 in upright posture without any load in hands were estimated to reach 570 N and 190 N, respectively (Arjmand and Shirazi-Adl, 2006a). They increased to ~700 N and ~250 N, accordingly, when 1.7% antagonist coactivity was considered; another 20% increase in spinal loads was reported when the level of antagonistic coactivation was doubled (El-Rich et al., 2004). When 180 N load is held in hands, the compression and shear increase 35% and 50%, respectively (Arjmand and Shirazi-Adl, 2006a). Over 200% increase in compression has been reported when trunk is flexed 40º (Arjmand and Shirazi-Adl, 2006a). The compression and AP shear forces at the L5-S1 in 65º forward flexion with 180 N load in hands are 3850 N and 708 N, respectively. Spinal loads are found higher in lordotic and smaller in kyphotic lumbar posture relative to free posture which was argued to be due to alterations in muscles line of action and disc inclination along with changes in passive-active force components of spine (Arjmand and Shirazi-Adl, 2005). Accordingly, spinal load measurement by instrumented vertebral replacement reveals that considerable changes of the spine lordosis may decrease or increase the spinal load depending on the posture (Srbinoska et al., 2013).

Apart from static postures, spinal loads have been evaluated in dynamic tasks using dynamic modeling that accounts for inertial effects too. Transient finite element kinematics-driven model studies of trunk in lifting report compression (shear) of 4.8 kN (1.6 kN) in stoop lifting of 180-N weight that is 20% (15%) larger than the compression (shear) in squat lifting of the same weight (Bazrgari et al., 2007). Higher inertial effects in fast movements and larger muscle forces increase spinal loads comparing to slow movements. Compression and shear forces at the L5-S1 reach (averaged over three subjects) ~4.4 kN and 1.3 kN, accordingly, in fast pace showing around 70% increase relative to slow motions. Spine passive moment, mainly dependent

on deformation, of ~35 Nm was reported in fast movement that was higher ~9% comparing to slow movement (Bazrgari et al., 2008c). Spinal loads have also been estimated in seated vibration environment. Four Hz excitation escalate substantially the compression (shear) forces from 0.5 kN (0.2 kN) in static sitting to 3.5 kN (1.2 kN) (Bazrgari et al., 2008a, b). Interestingly, augmenting the excitation frequency from 4 Hz to 20 Hz decreases both compression and shear by ~44%. When trunk is subject to sudden forward load perturbation, L5-S1 passive moment, compression and AP shear force reach (averaged over three subjects) 21.2 Nm, 3.7 kN and 1 kN, respectively (Bazrgari et al., 2009a). In another study, perturbation was caused when a static posterior load was suddenly removed; compression and AP shear force increased abruptly 60% and 100%, respectively, right after load release (Bazrgari et al., 2009b). Compression increase is the result of muscles activation that kicks in for maintaining the balance; however, shear load was more influenced by inertial effects in AP direction (Bazrgari et al., 2009b).

2.2. Spine stability

Spine stability is a challenging subject, and as such numerous models have been developed to gain further insight. The spine is subject to large compression loads of 1000-6000 N in various recreational and occupational activities (Arjmand, 2006; Bazrgari et al., 2009b; Cholewicki et al., 1991; Granata et al., 1999), while the passive (devoid of muscles) ligamentous lumbar or thoracolumbar spines, on the other hand, become unstable under much smaller compression forces of about 90 N (Crisco, 1989) or 20 N (Lucas and Bresler, 1960), respectively. The dilemma is therefore how the spine is stabilized in order to safely carry out various daily physiological activities. A large number of studies have hence focused on mechanisms that could enhance the compression load-carrying capacity of the spine. On the other hand, spine is also subject to sudden external loading/unloading and displacement/inertial effects. In addition, any contamination in neuromuscular sensory and motor signal-dependent noise may further deteriorate spine stability. Better understanding of the spine stability and the mechanisms involved has hence the potential to help prevent spinal disorders and injuries.

In order to maintain a safe level of stability, the central nervous system (CNS) controls trunk stiffness via different mechanisms (Panjabi, 1992, 2003). The passive ligamentous spine provides the spine structure with some passive stiffness. The contribution of the passive

components, which is a function of the trunk posture and loading, is smaller at or near upright postures; but it increases with trunk flexion angle (Arjmand and Shirazi-Adl, 2006a; Cholewicki et al., 2000b; Granata and Rogers, 2007; McGill et al., 1994). The trunk stiffness substantially increases by 38% and 44% at forward flexions of 60° and 90°, respectively whereas the reflex gain decreases by 31% and 45% (Figure 2.15) (Granata and Rogers, 2007).

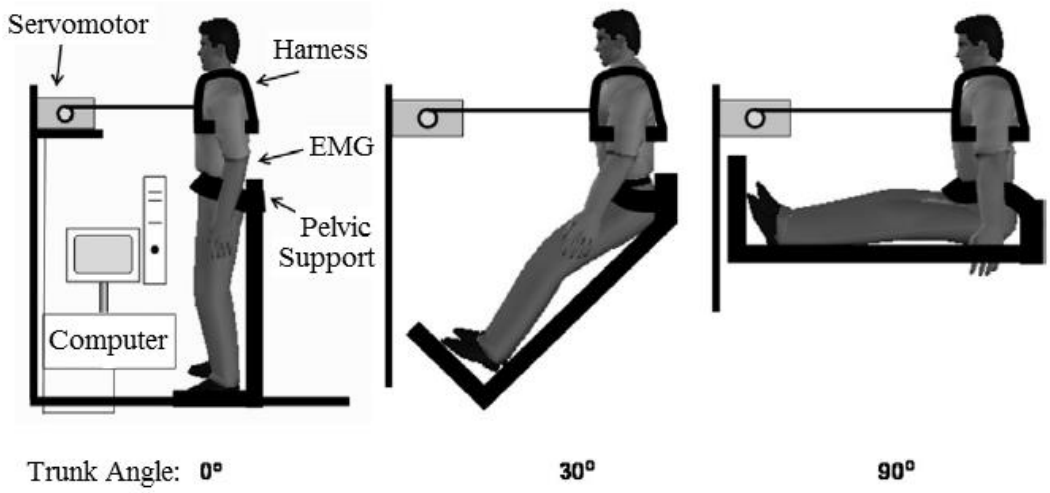

Figure 2.15 Experimental setup used in (Granata and Rogers, 2007) to measure the effect of trunk forward flexion on trunk stiffness and muscles reflexive response.

Empirical and model studies show that the spine passive stiffness increases at higher spine compression forces (Figure 2.9) (Adams and Dolan, 1991; Edwards et al., 1987; Janevic et al., 1991; Stokes and Gardner-Morse, 2003); albeit the disc load-displacement behavior becomes more linear as compression load increases (Figure 2.10) (Gardner-Morse and Stokes, 2003). Higher axial load pressurizes the nucleus and causes disc bulging in the horizontal plane (Figure 2.11). Higher stress in outermost annular fibers stiffens the disc due to nonlinear stress-strain properties of the annular fibers (Broberg, 1983; Shirazi-Adl, 2006).

In addition, muscle stiffness also increases at higher muscle activation level (Cholewicki and McGill, 1995; Joyce and Rack, 1969; Lawrence et al., 2006) as the number of cross-bridges increases (Ma and Zahalak, 1985). Larger exertions of paraspinal muscles against external load, increase trunk stiffness (Brown and McGill, 2008; Cholewicki et al., 2000b; Gardner-Morse and Stokes, 2001) and improve its stability (Figure 2.16). The effect of voluntary activation of different agonist/antagonist muscle groups on trunk stiffness and stability has been studied.

Trunk stiffness increases significantly when backward and forward preload on the trunk alters from 100 N to 170 N (Lee et al., 2007; Moorhouse and Granata, 2005) (Figure 2.16). Smaller post-perturbation trunk displacement when trunk was preloaded could be interpreted as a sign of enhanced spine stability (Granata et al., 2004; Krajcarski et al., 1999).

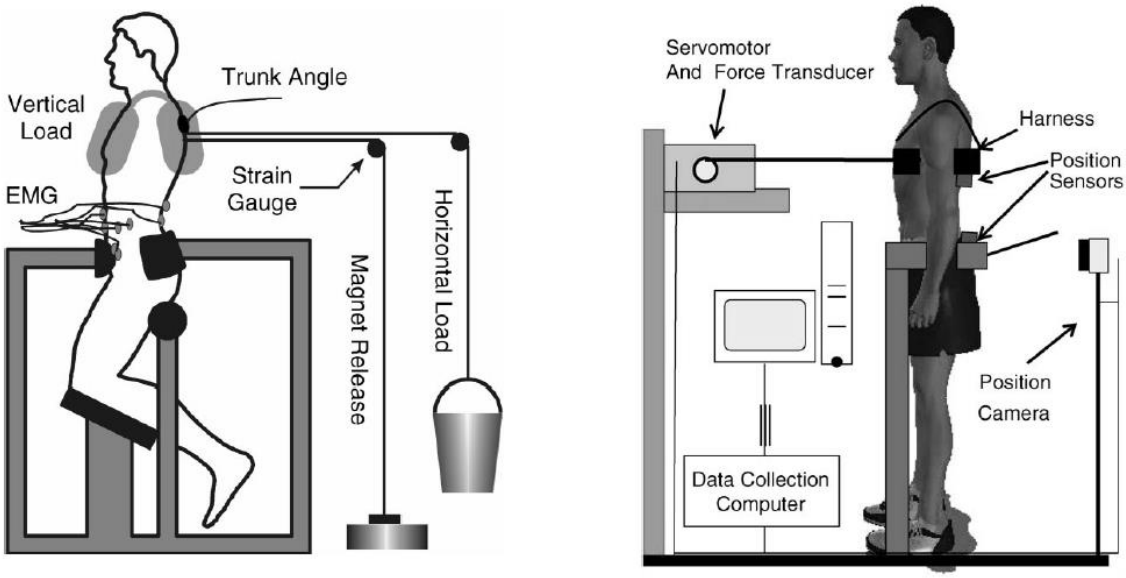

Figure 2.16 Experimental setups used in (Cholewicki et al., 2000b) (left) to study the effect of load direction and magnitude and in (Moorhouse and Granata, 2005) (right) to study the effect of preloading the trunk on trunk stiffness and stability.

Antagonist coactivation also increases the trunk stiffness (Brown et al., 2006; Vera-Garcia et al., 2006) and hence the spinal stability (Andersson et al., 2004; Brown and McGill, 2009; Gardner-Morse and Stokes, 1998; Van Dieen et al., 2003b) albeit at the cost of higher spinal loads that tend to deteriorate the trunk stability margin (Arjmand and Shirazi-Adl, 2006a; El Ouaaid et al., 2009; Granata and Marras, 2000) and as a consequence, it increases the risk of injury. Previous studies found that antagonistic coactivation may increase in anticipation of an external preload (Brown et al., 2003; Granata and Orishimo, 2001; Granata et al., 2001). Higher intra-abdominal pressure caused by abdominal muscles contraction improves spine stability (Mokhtarzadeh et al., 2012; Stokes et al., 2011) although its contribution is found posture and task specific (Arjmand and Shirazi-Adl, 2006b).

The essential role of muscle reflexive response in stability is evident when passive/active intrinsic stiffness is not enough to maintain a sufficient margin of stability (Brown and McGill,

2009; Moorhouse and Granata, 2007). Reflex dynamics may contribute up to 42% of the measured torso stiffness (Moorhouse and Granata, 2007). When trunk intrinsic active/passive stiffness is not sufficient to maintain the trunk balance against external perturbations and neuromuscular noise, muscles reflex becomes necessary (Andersen et al., 2004; Brown and McGill, 2008; Cholewicki et al., 2000b; Granata and Rogers, 2007; Stokes et al., 2000). Some studies have revealed that when active/passive intrinsic stiffness increases due to agonist/antagonist preactivation/coactivation, muscle reflex response as a result decreases (Granata and Rogers, 2007; Granata et al., 2004).

To investigate the role (intrinsic and reflexive) of muscles in the trunk stability, Bergmark (1989b) suggested that the muscles action could be modeled by linear springs with stiffness, K, that is proportional to muscle's instantaneous force (Morgan, 1977) and inversely proportional to its instantaneous length, $K = q\,{}^{F}/_{L}$, where q is a proportional constant. Some studies considered q the same for all muscles while others calculated a unique q for each muscle. Bergmark (1989b) suggested q = 40; while values varying from 0.5 to 42 have been cited (Cholewicki and McGill, 1995; Zeinali-Davarani et al., 2008).

Stiffness coefficient q directly affects the system margin of stability. For a given set of muscle forces at a posture and trunk loading, smaller stiffness coefficient decreases muscle and spine stiffness and consequentially deteriorates trunk stability. In contrast, higher q values increase the load-carrying capacity of the vertebral column and improve the stability. Two approaches have been taken to assess trunk stability based on Bergmark's stiffness coefficient q. In the first approach, critical stiffness coefficient, q_{cr}, is determined at each instance of time when muscle forces at a specific trunk posture and loading (El-Rich et al., 2004) are known. The q_{cr} is the minimum stiffness coefficient for which the trunk remains stable. Smaller values than q_{cr} makes the system unstable meaning that the spine would exhibit hypermobility upon small perturbations. Critical stiffness coefficient q_{cr} naturally remains always positive ($q_{cr} \geq 0$). Posture, loading condition and the level of coactivity change q_{cr}. A system state, defined by a trunk posture, loading and muscles activation level, with smaller q_{cr} indicates higher margin of stability over another state with higher q_{cr}. When q_{cr} is zero, the stiffness coming from muscle activation is not needed for the trunk stability although the muscle forces are still necessary for equilibrium

(Arjmand and Shirazi-Adl, 2005, 2006a; Bazrgari et al., 2008c). In another word, the contribution of the passive ligamentous spine is sufficient to maintain the trunk stability.

In order to assess the trunk stability in upright posture with and without load in hands, El-Rich et al. (2004) have employed a finite element model (FEM) of spine with 7 rigid bodies representing T1-T12 (as a single rigid body) and L1 to S1 vertebrae. Six deformable beam elements with nonlinear load-displacement behavior interconnected the adjacent vertebrae. To calculate muscle forces as well as spinal loads at a prescribed kinematics and given external load, an iterative optimization-based algorithm is used in which muscle forces are computed at each vertebral level satisfying equilibrium equations. Stability analysis is subsequently performed with all muscles replaced by linear springs with adequate stiffness. The critical stiffness coefficient q_{cr} at each posture and external loading condition is then determined using perturbation method. Antagonistic coactivity as well as larger back muscles exertion due to loading increased spine stiffness and stability, albeit at higher spinal loads. Using improved similar methodology, Arjmand and Shirazi-Adl (2005) have studied the influence of lumbar curvature on the spine stability. It is observed that a kyphotic lifting increases passive stiffness whereas a lordotic lifting increases active muscle forces. With smaller q_{cr}, margin of stability is higher in a lordotic lifting; nevertheless, larger axial compression and shear forces at L5-S1 disc is estimated is this lifting style. Larger trunk flexion angles in forward bending substantially enhance the trunk stability (Arjmand and Shirazi-Adl, 2006a; Bazrgari et al., 2008c). In addition, wrapping of global spinal musculature, i.e. erector spinae group, slightly increases the spinal stability in flexed postures (Arjmand et al., 2006). This latter study shows that much larger muscle forces and spinal loads are estimated when wrapping mechanism is neglected. The kinematics-driven approach applied in a dynamic loading condition reveals that faster unconstrained extension-flexion movements in upright standing substantially increases spinal loads, muscle forces and trunk stability margin (Bazrgari et al., 2008c). The estimated peak spinal loads when body was subject to base vibration were found around 4 kN at 4-Hz excitation frequency that decreased in larger frequencies (Bazrgari et al., 2008b) (Figure 2.17). Trunk response and stability after sudden trunk loading and unloading has also been investigated (Bazrgari et al., 2009a; Bazrgari et al., 2009b). Foregoing studies have highlighted the crucial role of posture, perturbation load and initial agonist/antagonist muscle activities on the trunk stability margin under sudden loads.

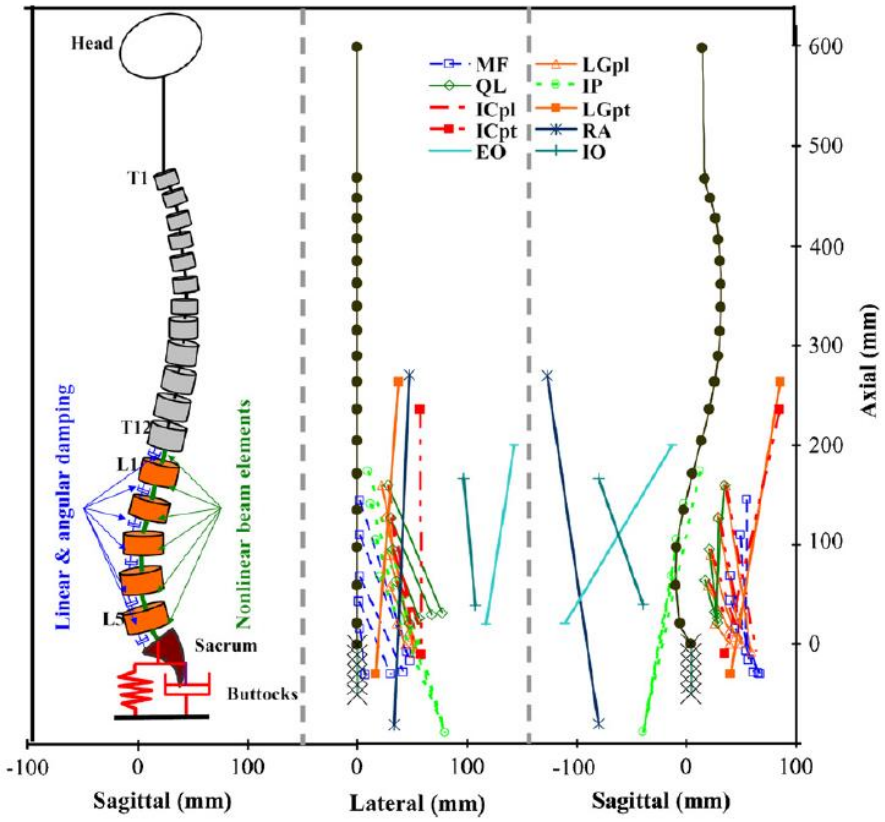

Figure 2.17 FE model of the spine which includes rigid bodies representing vertebrae and thoracic spine as well as deformable beams representing motion segments. ICPL = iliocostalis lumborum pars lumborum, ICPT = iliocostalis lumborum pars thoracic, IP = iliopsoas, LGPL = longissimus thoracis pars luborum, LGPT = longissimus thoracis pars thoracic, MF = multifidus, QL = quadratus lumborum, IO = internal oblique, EO = external oblique, and RA = rectus abdominis are shown (from (Bazrgari et al., 2008b))

The second alternative approach to quantify spine stability based on stiffness coefficient q is to set a-priori a q value and calculate the required activation level (or force) of agonist and antagonist muscles in order to satisfy both equilibrium and stability requirements of the trunk. In this approach a Lyapunov function is defined and the requirement for satisfaction of stability is considered as a constraint in an optimization problem that solves the kinetic redundancy of the system to determine muscle forces. Granata and Wilson (2001) have estimated muscle forces by optimizing sum of muscle stresses in a simplified model of spine with a double inverted pendulum and two muscle groups, one agonist and one antagonist, for each degree of freedom (Figure 2.18). In this model the stiffness coefficient was set at 10 for all muscle groups. The

optimization was constrained to yield a semi-positive Hessian matrix of the trunk potential energy. This study finds that due to higher activation level the asymmetric postures are more stable than symmetric ones. In addition, it is found that as the system approaches upright neutral posture, larger muscle forces are required to satisfy the stability constraint. Brown and Potvin (2005) have applied a hybrid EMG-optimization technic to estimate muscle forces while the second derivate of the trunk potential energy is constrained to remain positive. Using the same technic, Zeinali-Davarani et al. (2007) have linearized the trunk dynamics around a trajectory and estimated the muscle forces while constraining the state matrix of the trunk to be negative definite. This model is able to predict antagonistic coactivity based on different values of stiffness coefficient q during a fast dynamic extension/flexion (Zeinali-Davarani et al., 2008; Zeinali-Davarani et al., 2011). The effect of consideration of the trunk stability as an additional constraint equation alongside equilibrium equations when computing spinal loads has also recently been investigated in a trunk musculoskeletal model study under a number of isometric tasks (Hajihosseinali et al., 2014). Despite the estimation of antagonistic activity in some tasks, the spinal loads altered by less than 15% when this stability condition is also incorporated in the optimization algorithm.

Kinematic variability has also been used to evaluate the spine stability. Using posturography method that measures the trunk sway during different movements it has been found that the trunk sway angle and velocity increases with age (Baloh et al., 1998; Overstall et al., 1977; Prieto et al., 1996) suggesting likely deteriorations in the vestibular system, CNS and hence postural control with ageing (Enrietto et al., 1999; Fernie et al., 1982). Blaszczyk (2008) suggested a new measure called sway ratio for evaluating stability which is the ratio of anteroposterior (AP) displacement of the body center of mass (CoM) to AP displacement of the feet center of pressure (COP). These global measures although beneficial in evaluating the stability, particularly in a clinical setting, they do not however shed insight into the role of individual neuro-musculoskeletal components contributing to the trunk stability.

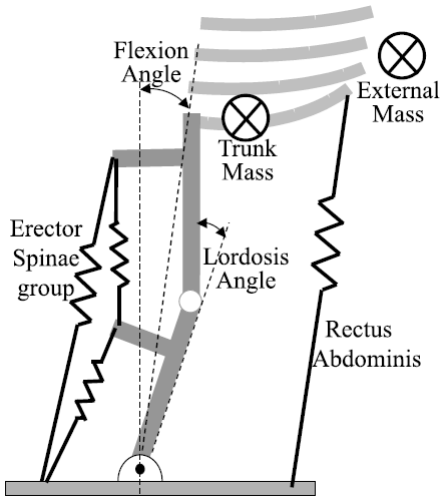

Figure 2.18 Constrained optimization estimated muscle forces in a simplified model of spine with a double inverted pendulum and two groups of agonist and antagonist muscles for each degree of freedom (from (Granata and Wilson, 2001)).

Another technic to quantify trunk stability margin is based on kinematics variability by calculating maximum Lyapunov exponent. This technic measures whether the dynamical sphere of kinematics variability, whose center is at the actual state of the system, is growing or shrinking along different dimensions. A Lyapunov exponent calculated for each direction determines how the sphere diameter is changing along that direction. Each Lyapunov exponent will be positive or negative if the sphere, respectively, grows or shrinks along the corresponding direction. Therefore, the system's dynamics possesses a spectrum of Lyapunov exponents; the stability measure is the summation of all Lyapunov exponents as an indication of alterations in the sphere as it deforms (probably to an ovoid) with time. Positive summation indicates an increasing volume and instability while a negative summation reveals a shrinking sphere and a stable system. In regular activities, the system is evidently stable as the subject's spine does not buckle or lose balance and control, the volume alteration (i.e. exponents' summation) is never positive. In this case, the biggest exponent corresponds to the least stable (growing) dimension; and is the most dominant one too. Although finding the entire spectrum of the Lyapunov exponents based on recorded in vivo data is not possible, fortunately there are technics to detect the largest exponent called maximum Lyapunov exponent (Rosenstein et al., 1993). Smaller maximum exponent is an indication of bigger margin of stability. Lyapunov exponent measures provide an intra-session comparison of torso stability (Lee and Granata, 2008). They have been exploited in

many investigations including torso and limb movements (Gsell et al., 2015) as well as gait stability (Bruijn et al., 2012; Bruijn et al., 2009; England and Granata, 2007).

The maximum Lyapunov exponent in asymmetric spatial trunk movement has been estimated to be smaller than that in symmetric sagittal movements (Granata and England, 2006) implying that asymmetric movements are more stable. Faster movements are found less stable as a result of higher demand for the muscular effort that deteriorates the fine control (Fitts, 1954; Harris and Wolpert, 1998). On the other hand, fast movement pace might decline the neuromuscular system ability to respond against disturbances in a short period of time (Granata and England, 2006). Maximum Lyapunov exponent decreases with higher load during repetitive lifting due to higher muscle activation and spinal load (Graham et al., 2011). Maximum Lyapunov exponents in cyclic tasks has also been estimated to increase after fatigue indicating the destabilizing role of fatigue (Granata and Gottipati, 2008).

Tanaka (Tanaka et al., 2009) has developed a mathematical model of the spine to determine its basin of stability. In this study, a computational model of trunk seated on a wobble chair with variable rotational stiffness is developed (Figure 2.19). The potential energy of the system in the sagittal plane for different chair stiffness values representing task difficulty is calculated. Basin of stability was defined based on variation of the potential energy versus angle and angular velocity for each task difficulty (chair stiffness). The predicted basin of stability is found in good agreement with experimental observations; the subjects seated on the wobble chair are not able to stabilize their trunks when the stiffness drops too low or the angular position is far from the neutral posture.

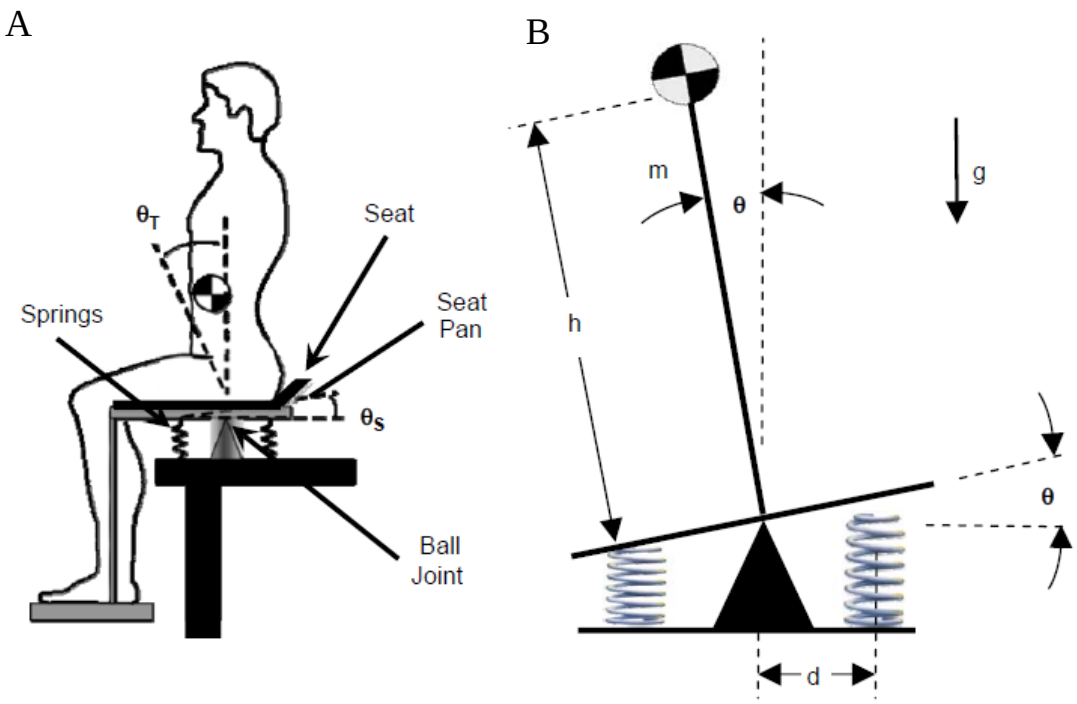

Figure 2.19 (A): The trunk seated on the wobble chair, the legs are fixed such that they could not participate in movement, θ_S and θ_T are the seat rotation from the horizontal line and the trunk rotation plane from the neutral position, respectively, both measured in the sagittal plane; (B): the simplified model of the seated trunk, θ, h, m, and g are sagittal rotation from neutral position, the height of the trunk center of gravity from the chair pivot, body mass, and gravity acceleration, respectively. d is the distance of springs from the center of pivot. Increasing d, as the independent variable in this investigation, decreases task difficulty (Tanaka et al., 2009).

Basin of stability of trunk for the case in which a human is seated on a wobble chair has been determined using a computational model of the trunk (Tanaka et al., 2010). The system is modeled with two rigid bodies joined at the lumbosacral disc; the upper one represents the upper extremity while the lower one includes chair, thighs and legs fixed vertically to minimize their effect on the trunk stability (Figure 2.20). The pivoted chair to ground could only rotate in the sagittal plane. A simple proportional-derivative (PD) controller determines the torque representing the muscular moment at the lumbosacral joint based on the angular position and velocity of the system. Therefore, placing the system (time = 0) at every state, i.e. bodies' angular position and velocity, leads the system over time through a trajectory in the state pace. In theory, if the trajectory always remains in a vicinity around the initial state, that state is stable and

belongs to the basin of stability. If a state of the system is not stable, it will be unstable. Since finite-time simulation may not provide sufficient information to employ this theory, Tanaka et al. (2010) calculated finite-time Lyapunov exponents at each node in a subset of system's state space. The ridges defined as the connected set of local maxima in the field of finite-time Lyapunov exponents represent the boundary that separates stable and unstable behavior (Shadden et al., 2005) (Figure 2.21).

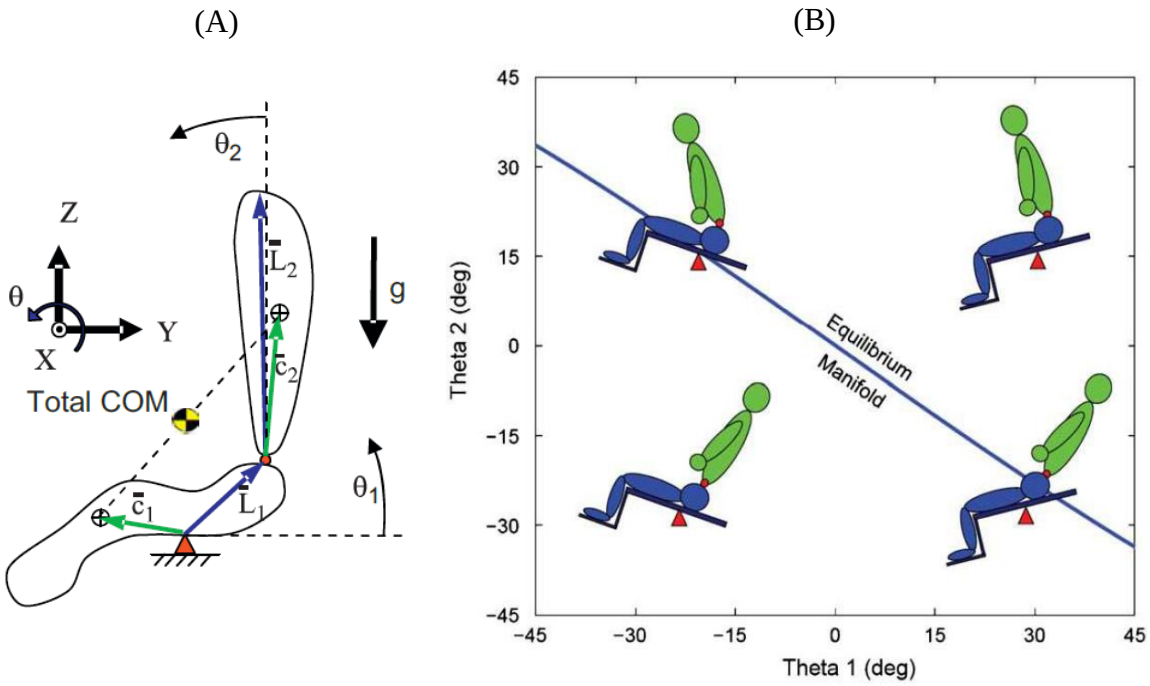

Figure 2.20 (A) Model of human body sitting on a wobble chair with two degrees of freedom in the sagittal plane: Θ_1 represents the rotation of the chair, lower extremities and buttocks while Θ_2 is the rotation of torso, head and upper extremities. The required control torque for equilibrium is calculated through a PD controller. The four-dimensional state space $[\theta_1, \dot{\theta}_1, \theta_2, \dot{\theta}_2]$ is meshed and stability is assessed at each node (configuration and velocity) calculating the Lyapunov exponent (B) Equilibrium manifold for motion in the sagittal plane (from (Tanaka et al., 2010)).

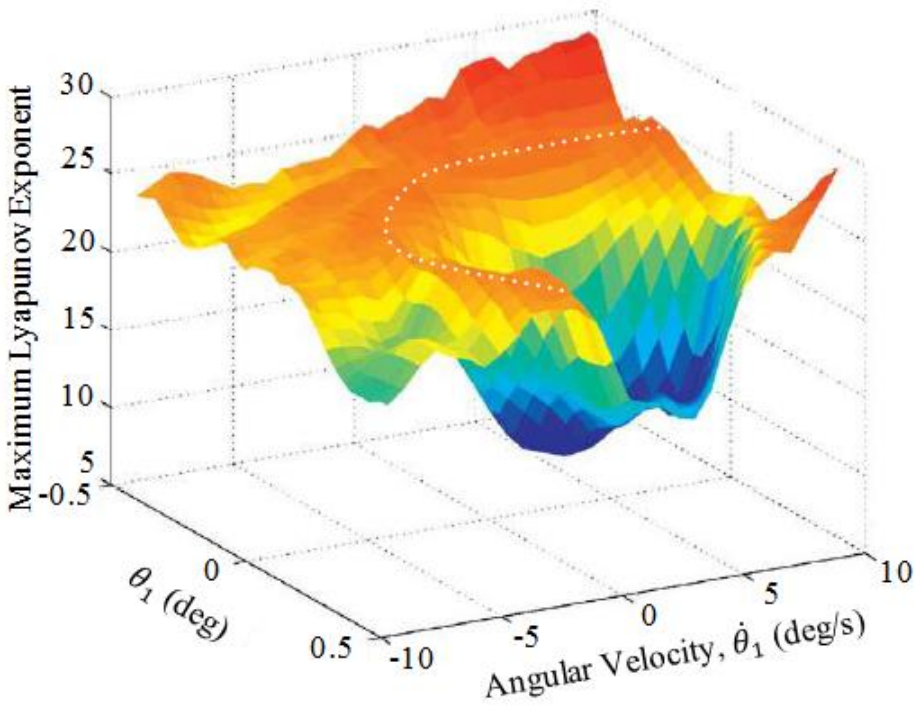

Figure 2.21 Finite time Lyapunov exponents and the boundary (white dotted line) of the basin of stability illustrated when $\theta_2 = \dot{\theta}_2 = 0$ (from (Tanaka et al., 2010)).

2.3. Trunk perturbation

Epidemiological studies have identified trunk perturbations as risk factors of LBP and spinal disorders (Lavender et al., 1989; Magora, 1973; Manning et al., 1984; Marras et al., 1987). Perturbation may happen in forms of sudden trunk loading/unloading and sudden movements associated with large inertial effects. Such conditions may happen during daily activities, in sports or at work place causing excessive strains and tissue injuries especially when spine margin of stability is low and reflexive recovery actions are absent, not sufficient or excessive (Knutsson, 1944; White and Panjabi, 1990). Lower active/passive intrinsic stiffness due to existing prior tissue injury or back pain may also increase the risk. Higher reflexive muscle efforts are then needed to maintain stability albeit at greater spinal loads and hence risk of tissue injury. On the other hand, impaired neuromuscular reflexive response aggravates postural control and stability. Antagonistic coactivation could also enhance pre-perturbation spine stiffness in such circumstances (Franklin and Granata, 2007; Granata et al., 2001). Dysfunction, disorder and degeneration in any of contributing mechanisms demand compensatory increases in the

contribution of other mechanisms that could increase spinal loads, decrease stability margin and increase risk of further injuries.

Large spinal loads have been predicted when the trunk is exposed to perturbations. External force, inertial effects and large muscle exertions are huge sources of escalating spinal loads. Previous model-estimations have reported compressions and shear forces at the L5-S1 over 3.1 kN and 1kN, respectively, under sudden loadings (Bazrgari et al., 2009a). The compression at the same level in sudden unloading reaches over 2 kN (Bazrgari et al., 2009b). Posterior trunk perturbation causes 2.5 kN compression at the L4-L5 level that markedly increases to 4 kN in presence of 30% antagonistic coactivation (Vera-Garcia et al., 2006). This emphasizes the negative effect of antagonistic coactivation on increasing the spinal loads in spite of its positive role in improving the spinal stability.

Reflexive response of muscles to perturbation is influenced by pre-perturbation trunk conditions as well as the perturbation itself. Larger perturbation amplitudes increases as expected muscle reflexive effort for balance and stability (Granata et al., 2004; Krajcarski et al., 1999). Muscles reflexive response decreases in presence of preload (Granata et al., 2004) suggesting the effect of trunk initial stiffness. Higher antagonistic coactivity also decreases muscles reflexive response to perturbation. Zedka et al. (1998) have investigated muscles reflexive activity in trunk perturbation in sitting posture. The recruitment pattern of left and right muscles is similar during perturbation in the sagittal plane. However, when the trunk is perturbed in the frontal plane left and right muscles are recruited separately in consecutive time periods, likely with over laps, corresponding to the required moment for equilibrium. Anticipatory and reflexive activities of muscles decrease with prior knowledge of an unloading perturbation (Brown et al., 2003). It is observed that when unloading is self-triggered, muscles anticipatory activity is present and responsive activity is minimized. Fatigue (Dupeyron et al., 2010) and muscle creep (Sanchez-Zuriaga et al., 2010) increase reflex amplitude and affect postural strategy (Wilson et al., 2005) after a perturbation. Reflex amplitude is also reported higher in women relative to men (Olson, 2014).

Muscles respond to perturbations but only after a delay called reflex latency with values reported varying from 20 to 80 ms (Granata et al., 2004; Vera-Garcia et al., 2006; Zedka et al., 1999). Responses with latencies beyond 150 ms are suggested to be voluntary rather than

reflexive (Cholewicki et al., 2005). Delayed reflex latency likely caused by prior back injuries impairs adequate control and stability of the trunk (Cholewicki et al., 2005; Hodges and Richardson, 1996; Magnusson et al., 1996; Radebold et al., 2000; Radebold et al., 2001; Wilder et al., 1996) increasing tissue strains and stresses (Reeves et al., 2009) and hence risk of further injuries. Previous studies have reported that reflex latency of abdominal muscles is shorter than that of back muscles (Cresswell et al., 1994; Olson, 2014) while latency in thoracic muscles are significantly shorter than in lumbar muscles (Sanchez-Zuriaga et al., 2010). It is reported that fatigue does not affect muscles reflex latency (Dupeyron et al., 2010) (Sanchez-Zuriaga et al., 2010); however, muscle creep increases it (Sanchez-Zuriaga et al., 2010) suggesting that prolonged spinal flexion may impair sensorimotor control mechanisms. The reflex latency in females is found shorter than in males (Miller et al., 2010; Olson, 2014). Reflex latency significantly increases in presence of preload (Granata et al., 2004). Evidently, muscles reflex latency is crucial in the trunk equilibrium and stability when fast response of muscles is needed in response to sudden changes in loading and movement.

In addition to the muscle reflex latency, muscle electromechanical delay (EMD) prolongs delays in muscle force generation in the response to perturbations. It is defined as the time between the onset of muscle activation to the onset of muscle force generation (Cavanagh and Komi, 1979), nevertheless, other definitions have been suggested too (Marras, 1987; van Dieen et al., 1991). Large discrepancy is seen among the reported EMD values from 20 to 120 ms (Vos et al., 1990). EMD for vastus lateralis is reported 41 ms (Houston et al., 1988) while another study reports 117.9 ms (Horita and Ishiko, 1987) during the same task. Definitions and methods of measurement may influence the reported EMD. For instance, the measured force and muscle activity (EMG) could be influenced by the parameters in data acquisition (like sampling frequency) and signal preparation (like filtering, resampling). In addition, the method of onset detection, e.g. definition of the onset threshold, may affect the EMD. EMD is found smaller in spastic muscles (Granata et al., 2000) whereas muscle stretching increases EMD (Esposito et al., 2011). Marras (1987) reports that EMD in static lifts is similar to dynamic lifts with 30 deg / sec velocity; EMD increases in lower velocities and reduces with higher velocity. No significant difference is reported between sexes (Johnson et al., 2012).

2.4. Musculoskeletal trunk modeling

As mentioned earlier, since direct measurement of muscle forces and spinal loads is unethical and difficult if not impossible, computational models of spine have emerged as alterative feasible approach. Using in vivo measurements, such as kinematics and/or muscles EMG, that can be measured non-invasively and in a large number of subjects, postures, loading and tasks, muscle forces, spinal loads and trunk stability have been estimated. However, musculoskeletal modeling faces some challenges. Firstly, our knowledge on anatomical geometry, tissue material properties, biomechanical and physiological mechanisms, etc. is limited. Secondly, some parameters such as genetics, aging, nutrition, sport, etc. may change anthropometry and tissue properties between individuals. The third issue is that the spine is redundant that means the number of muscles needed for equilibrium exceeds the number of equations. A physiologically-meaningful method is needed to partition the required force among muscles. The third issue is validation of these models that need in vivo measurement (van Dieen and de Looze, 1999). To overcome the redundancy and determine unknown muscle forces and spinal loads, there are a number of approaches that have been proposed and used in the literature that are briefly presented and evaluated below.

2.4.1. Single-equivalent muscle model

In order to overcome the kinetic redundancy of spine, the agonist muscles are modeled as a single synergetic group defined by a sole force acting through its line of action. By reducing the number of unknown muscle forces, this approach allows for a deterministic solution (Chaffin, 1969; Morris et al., 1961). Due to much smaller lever arm of muscles compared to external loads, it is found that muscle forces have major contribution to spinal loads (Morris et al., 1961). These models could approximately estimate spinal loads although the results considerably vary with assumptions on muscles line of action (van Dieen and de Looze, 1999).

2.4.2. EMG-assisted models

EMG-assisted models use recorded surface EMGs at select muscles to drive the model and predict muscle forces using a Hill-type (Hill, 1938) muscle model (Granata and Marras, 1993). The muscle tensile force is taken proportional to the normalized EMG, which represents the activity level of muscle and muscle cross sectional area while being modulated by muscle

force-length and force-velocity relations. A gain factor, which is interpreted as the muscle force per unit area, is introduced to match the measured external moments with internal ones estimated by muscle forces and possibly passive spine. The equilibrium is often satisfied at a single spinal level that likely violates equilibrium at other joints (Arjmand et al., 2007). The contribution of passive ligamentous spine is often neglected.

Because of the subject-specific muscle EMG activity, this approach is a biologic-based one able to predict the inter- and intra-subject variation in activities. For instance, the compression and shear forces are higher in subjects with psychosocial stress (Marras et al., 2000) and job complexity (Davis et al., 2002), in LBP patients comparing to asymptomatic individuals (Marras et al., 2004) and in males comparing to females (Marras et al., 2002; Marras et al., 2003). This method has been employed to evaluate muscle forces and spinal loads in forward bending (Granata and Marras, 1993, 1995; Marras and Sommerich, 1991), lateral bending (Marras and Granata, 1997), axial rotation (Marras and Granata, 1995) and repetitive exertion task (Granata et al., 1999) (Mirka and Marras, 1993). Disadvantages of this method include infeasibility of electromyography of deep muscles, high influence of fat and skin tissues on recorded superficial EMG, cross-talk issues of adjacent muscles, collection of EMG data on limited number of muscles, measurement of EMG at maximum voluntary contractions especially in patients with pain and nature of assumed force-EMG relations.

2.4.3. Optimization-based models

Optimization methods have been exploited to solve kinetic redundancy of spine and find paraspinal muscle forces in different postures, loading conditions and movements. In this method, the required moments for equilibrium of spine at different levels (or a single level) are partitioned among the muscles while minimizing one or many objective functions (Crowninshield and Brand, 1981; Schultz et al., 1982; van Dieen, 1997). Although predicted spinal loads vary with different cost functions (Hughes, 2000; Parnianpour et al., 1997), however, only 1.1% and 1.5% difference are found in peak and average compression forces when minimum muscle stress or minimum L3-L4 compression were used as objective function (Hughes, 2000). The results are more physiologically acceptable with nonlinear optimization methods especially when they are related to movement dynamics (Tsirakos et al., 1997). Predicted muscle forces during trunk flexion to 40º and 65º with 180-N load in hands agree well

with recorded EMG during the same tasks when $\sum \text{stress}^3$, $\sum \text{stress}^2$, fatigue (Dul et al., 1984) and double-linear objective functions (Bean et al., 1988) are minimized in the optimization procedure (Arjmand and Shirazi-Adl, 2006c). Arjmand and Shirazi-Adl (2006c) suggests that $\sum \text{stress}^3$ and $\sum \text{stress}^2$ could be adequate to estimate physiologically-plausible results. The former criterion has been found to be compatible with maximization of endurance (Crowninshield and Brand, 1981).

Previous studies have observed optimality in human body movement (Figure 2.22) (Jordan and Wolpert, 1999; Uno et al., 1989) suggesting that CNS recruits the muscles while optimizing a cost function (Todorov and Jordan, 2002). It is believed that movement optimality is the result of evolution, learning and adaptation (Scott, 2004; Todorov, 2004). Kinematic cost functions such as movement jerk (Flash and Hogan, 1985; Hoff, 1992; Hogan, 1984), dynamic cost functions like the summation of joints torque (Uno et al., 1989) and movement variance cost functions (Harris and Wolpert, 1998) have been exploited in investigation of the human body movement. These studies support the use of optimization models in human trunk modeling.

Optimization methods are however criticized for not being able to represent inter- and intra-subject variations in performance. They have been also criticized that they are not able to predict antagonistic coactivity. Therefore, stability-constrained optimization methods have been developed to address this shortcoming, in which the time derivative of a Lyapunov function such as the potential energy of the system is constrained to be negative definite in optimization (Granata and Wilson, 2001; Zeinali-Davarani et al., 2008).

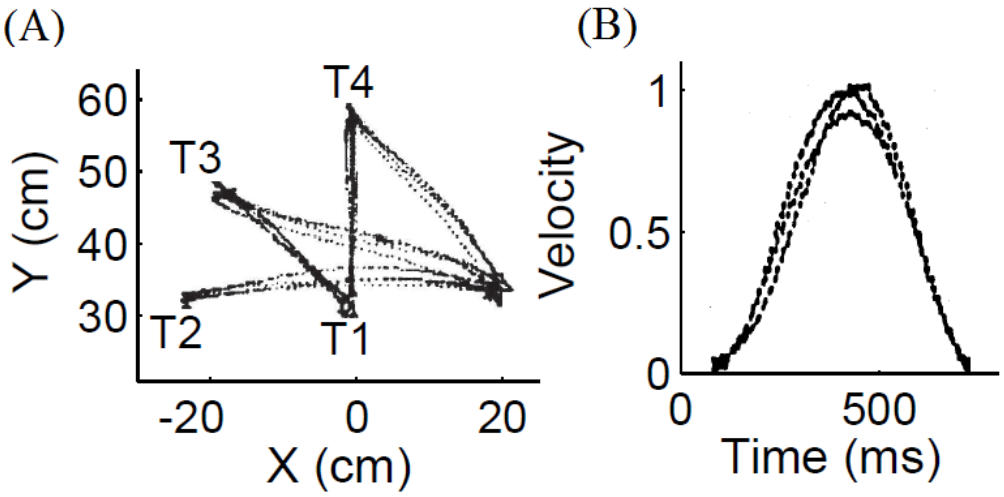

Figure 2.22 (A) Paths and (B) bell-shaped velocity profiles of hand during point-to-point movements suggesting minimum jerk behavior. The coordinate system is centered on the shoulder with x and y in lateral and anterior directions (from (Uno et al., 1989)).

2.4.4. EMG-assisted optimization based models

Comparison of EMG-based and optimization-based approaches on spinal forces remains contradictory as some find small differences (van Dieen and Kingma, 2005) while other report much larger variations (Cholewicki et al., 1995). A hybrid EMG-assisted optimization method has been developed in order to integrate the advantages of both EMG-assisted and optimization-based approaches (Cholewicki and McGill, 1994; Cholewicki and McGill, 1996). In this method, muscle forces are estimated primarily by recorded EMG of muscles (Granata and Marras, 1993); then equations of motion are satisfied while minimizing changes in computed muscle forces. It is suggested that this method yields more realistic muscle forces comparing to EMG-assisted or optimization-based models (Gagnon et al., 2001).

2.5. Wobble chair experiments

A wobble chair, which is pivoted to its base or placed on a hemisphere, provides an unstable support useful for investigating trunk balance and stability control. To minimize the contribution of lower extremities in balance and stability on wobble chair, they are fixed on the chair to rigidly follow it. Neuromuscular mechanisms involved in balance and stability of the upper body have been studied with wobble chair (Cholewicki et al., 2000a). This method has

been used to investigate the effect of impaired neural control in LBP patients in balance and stability (Radebold et al., 2001). Trunk stiffness, evaluated for subjects sitting on a wobble chair, is reported higher in LBP patients that could be related to a compensatory strategy to decrease pain and prevent further injuries (Freddolini et al., 2014c). Another study found that antagonistic coactivation reduces postural control due to neuromuscular signal-dependent noise (Reeves et al., 2006). Posturography of individuals sitting on a wobble chair has showed higher hip range of rotation and smaller spine range of rotation in LBP patients relative to healthy controls. These differences are likely due to compensatory strategies in patients in order to diminish the risk of further injury (Freddolini et al., 2014a). Unbalanced sitting has been used to evaluate the threshold of trunk stability (Tanaka et al., 2009; Tanaka et al., 2010) based on the method of finite-time Lyapunov exponent (Ross et al., 2010).

2.6. Concluding remarks

Epidemiological studies reveal the marked impact of back pain and spinal disorders on individuals and societies. Understanding spine biomechanics when exposed to mechanical inputs is essential in preventing injuries and providing efficient treatment and rehabilitation programs. The mechanisms involved in balance control and stability maintenance have been studied; however, there remain still many unanswered questions. On the one hand, these mechanisms are affected by injuries, pain or neuromuscular dysfunctions. Alterations in contribution of any of these mechanisms increase the demand for contribution of others. That may influence the entire neuromuscular behavior and escalate the injury and pain. Experimental investigations are limited by technical or ethical limitations. Although muscles activation has been measured by surface EMG, experimental models are not able to estimate muscle force and spinal loads. Spinal loads recorded in vivo by instrumented vertebral replacements for few subjects, tasks and postures also provide a partial picture of loads on the spine. Therefore, realistic complex neuro-musculoskeletal modeling, in combination with in vitro studies, should help us reveal and quantify the mechanisms involved in stability when the trunk responds to perturbations or recovers its balance. The current study aims towards such combined investigations.

2.7. Objectives and thesis organization

2.7.1. Effect of pre-perturbation conditions and perturbation load magnitude on trunk response and stability

The principle goal of this part of study is to evaluate the effect of pre-perturbation conditions and load magnitude on trunk kinematics, muscles activity and spine stability. Kinematics of trunk along with muscles EMG are measured in normal young male subjects with the trunk subject to forward sudden loads. The effect of preloading the trunk, initial trunk flexion, preactivation of antagonistic muscles and perturbation load magnitude as independent variables are investigated. To achieve the goal three objectives are set.

The first objective is to investigate how trunk kinematics and muscles EMG alter with pre-perturbation conditions and perturbation load magnitude. It is hypothesized that the trunk responses (i.e., muscle activation, trunk kinematics, reflex delay and amplitude) to sudden perturbations are influenced by trunk initial conditions (i.e., preload, posture and coactivation) as well as sudden load magnitude.

The second objective is to estimate muscle forces and spinal loads before and after perturbation and investigate changes due to initial conditions and perturbation load magnitude. The in vitro results obtained in earlier step are prescribed into a musculoskeletal finite element kinematics-driven model in order to get more insight into spine biomechanics. Earlier studies have shown the reliability and accuracy of a kinematics-driven finite element model in predicting temporal pattern of muscle forces, spinal loads and passive moments during different dynamic motion scenarios (Bazrgari et al., 2007; Bazrgari et al., 2008b; Bazrgari et al., 2008c) as well as sudden trunk loading (Bazrgari et al., 2009a) and unloading (Bazrgari et al., 2009b). The same modeling approach is exploited here to estimate muscle forces and spinal loads in 12 subjects. Changes in peak muscle forces, muscles force latency and spinal loads are quantified as independent variables, i.e. preload, initial trunk flexion, abdominal antagonistic preactivation and load magnitude are altered. It is hypothesized that the kinematics-driven FE model would be sensitive (1) to identify the effect of various pre-perturbation and sudden loading conditions and (2) to demonstrate that the trunk muscle reflex activity and spinal loads drop in conditions associated with higher pre-perturbation intrinsic stiffness.

The third objective is set to determine in earlier perturbation tasks (1) how trunk stability changes before and after perturbation and (2) how initial trunk conditions and load magnitude affect stability. Temporal profile of the critical stiffness coefficient (Bazrgari et al., 2009a; Bergmark, 1989a) as a measure of trunk stability is calculated before and after perturbation in all conditions for 12 subjects. It is hypothesized that trunk stability will be influenced with pre-perturbation conditions and perturbation load.

2.7.2. Trunk biodynamics for subjects sitting on a wobble chair

The final objective of this study is to estimate muscle forces and spinal loads when subjects are sitting on a wobble chair maintaining their balance and stability. A three-dimensional finite element model was developed. Measured kinematics of control and patient groups collected in a recent study are input into the model and muscle forces and spinal loads are calculated for 12 subjects. The differences are investigated to examine if the kinematics driven model could discriminate between healthy and control groups.

CHAPTER 3 ARTICLE 1: TRUNK RESPONSE TO SUDDEN FORWARD PERTURBATIONS - EFFECTS OF PRELOAD AND SUDDEN LOAD MAGNITUDES, POSTURE AND ABDOMINAL ANTAGONISTIC ACTIVATION

Ali Shahvarpour [a], Aboulfazl Shirazi-Adl [a], Hakim Mecheri [b], Christian Larivière [b]

[a] Division of Applied Mechanics, Department of Mechanical Engineering, École Polytechnique, Montreal, Quebec, Canada

[b] Occupational Health and Safety Research Institute Robert-Sauvé, Montreal, Quebec, Canada

Article published in
Journal of Electromyography and Kinesiology (2014)

3.1. Abstract

Unexpected loading of the spine is a risk factor for low back pain. The trunk neuromuscular and kinematics responses are likely influenced by the perturbation itself as well as initial trunk conditions. The effect of four parameters (preload, sudden load, initial trunk flexed posture, initial abdominal antagonistic activity) on trunk kinematics and back muscles reflex response were evaluated. Twelve asymptomatic subjects participated in sudden forward perturbation tests under six distinct conditions. Preload did not change the reflexive response of back muscles and the trunk displacement; while peak trunk velocity and acceleration as well as the relative load peak decreased. Sudden load increased reflex response of muscles, trunk kinematics and loading variables. When the trunk was initially flexed, back muscles latency was delayed, trunk velocity and acceleration increased; however, reflex amplitude and relative trunk displacement remained unchanged. Abdominal antagonistic preactivation increased reflexive response of muscles but kinematics variables were not affected. Preload, initial flexed posture and abdominal muscles preactivation increased back muscles preactivity. Both velocity and acceleration peaks of the trunk movement decreased with preload despite greater total load. In contrast, they increased in the initial flexed posture and to some extent when abdominal muscles

were preactivated demonstrating the distinct effects of pre-perturbation variables on trunk kinematics and risk of injury.

Keywords: Trunk, Forward perturbation, Preactivation, EMG, Reflex.

3.2. Introduction

Unexpected alterations in trunk loading and/or position have been identified as risk factors for low-back pain (LBP) (Lavender et al., 1989; Manning et al., 1984; Marras et al., 1987). Such conditions are transient involving important inertial loads and could occur in the event of sudden external loading/unloading, fall/slip and internal (corrupted) neural reactions. In the absence of sufficient stiffness (i.e., margin of stability) and depending on the perturbation characteristics, the trunk may in such events undergo excessive strains causing tissue injuries (White and Panjabi, 1990). Large spinal forces have been estimated in sudden loading with moderate magnitudes (Bazrgari et al., 2009a).

Trunk response is governed by the individual and combined contributions to the overall stiffness of the passive ligamentous spine, musculature and neural control often referred to as intrinsic passive, active voluntary (feed forward) and reflexive (feedback) systems, respectively (Panjabi, 1992). The role of each of these components on the spinal response and stability has been stressed (Reeves et al., 2009). The contribution of passive tissues in trunk stability, though smaller at and around the neutral upright posture (Cholewicki et al., 2000b), substantially grows under larger compression loads and as forward flexion increases (Arjmand and Shirazi-Adl, 2006a; McGill et al., 1994; Shirazi-Adl, 2006). Using system identification method, reflex gain is found to diminish in larger torso flexion angles suggesting the crucial contributions of the passive spine and active musculature to the trunk stiffness (Granata and Rogers, 2007). Antagonistic coactivitation, for example due to an anticipated sudden load (Brown et al., 2006; Granata et al., 2001; Vera-Garcia et al., 2006), increases the joint stiffness and hence the spinal stability (Gardner-Morse and Stokes, 1998; Granata and Orishimo, 2001; Van Dieen et al., 2003b) albeit concurrent increases in the loads on the spine that diminish the trunk stability margin (Arjmand and Shirazi-Adl, 2006a; El Ouaaid et al., 2009; Granata and Marras, 2000) and consequently, may augment the risk of injury. Although muscle preactivation reduces trunk displacement (Krajcarski et al., 1999; Stokes et al., 2000), reflex feedback response is also needed in some

instances despite existing coactivity (Andersen et al., 2004; Brown and McGill, 2008; Cholewicki et al., 2000b; Granata and Rogers, 2007; Stokes et al., 2000).

The reflexive response of the neuromuscular system kicks in however with a delay after the stimuli. Based on the definition and methodology used for the detection of EMG onset (relative to the onset of trunk movement or applied force), various reflex latencies have been reported (Hodges and Bui, 1996; Staude, 2001; Vera-Garcia et al., 2006); some as low as 20 ms (Zedka et al., 1999) while latencies beyond 150 ms are more voluntary than reflexive (Cholewicki et al., 2005). Delayed reflex latency likely caused by prior back injuries impairs adequate control and stability of the trunk (Cholewicki et al., 2005; Hodges and Richardson, 1996; Radebold et al., 2000). Accurate determination of muscle reflex latency and reflex amplitude (gain) as well as factors affecting them is hence important for improved comprehension of the neural mechanisms of movement control in both asymptomatic and low-back pain subjects.

In the event of a sudden perturbation, the trunk response is dependent on the individual and coupled roles of each of its sub-systems and as a consequence alters with changes in not only the perturbation characteristics but also the trunk conditions prior and during perturbation. In the current study, the trunk kinematics, e.g. displacement, velocity and acceleration profiles, as well as muscle voluntary and reflexive activities were investigated in 12 asymptomatic male volunteers. The magnitude of preload and sudden load as well as initial trunk posture and abdominal coactivity were considered as independent parameters. It was hypothesized that the trunk responses (i.e., muscle activation, trunk kinematics, reflex delay and amplitude) to sudden perturbations are influenced by trunk initial conditions (i.e., preload, posture and coactivation) as well as sudden load magnitude.

3.3. Method

3.3.1. Experiment

Twelve young male subjects (weight 73.0 ± 3.9 kg and height 177.7 ± 3.0 cm) with no current or prior history of LBP participated voluntarily in the study. All subjects signed consent forms for the measurement protocol approved by the institutional review board. The subjects were initially positioned in a semi-seated posture in a trunk dynamometer and performed two

isometric maximum voluntary contraction (MVC) trials in 6 directions: flexion-extension, right-left lateral, and right-left axial rotations, as detailed elsewhere (Larivière et al., 2009).

Superficial EMG signals of 12 muscles were recorded during the isometric MVCs and subsequent perturbation tasks. After shaving and abrading the electrode sites on the skin, twelve active single-differential dry surface electrodes [Model DE-2.3, DelSys Inc., Wellesley, MA; preamplification gain 1000; bandwidth 20 ± 5 Hz to 450 ± 50 Hz, 12 dB/oct, CMRR > 80 dB; noise < 1.2 μV (RMS, R.T.I.)] composed of two parallel silver bars (10 mm long, 1 mm wide) spaced 10 mm apart, were positioned bilaterally over following trunk muscles: longissimus (LG) ~3 cm lateral to the midline at the L1, iliocostalis (IC) ~6 cm lateral to the midline at the L3, multifidus (MF) ~2 cm lateral to the midline at the L5, rectus abdominus (RA) ~3 cm lateral to the midline above the umbilicus, external oblique (EO) ~10 cm lateral to the midline above umbilicus and aligned with muscle fibers and finally internal (IO) oblique ~2 cm below and 7 cm medial to the anterior superior iliac spine according to earlier works (Axler and McGill, 1997; De Foa et al., 1989; McGill, 1991). The difficulty in recording EMG of MF with surface electrodes has been indicated (Stokes et al., 2003). As for the EMG of IO, the electrodes collect activity of the transverse abdominus as well (Marshall and Murphy, 2003). The signals were collected by a system (Biotel 99, from Glonner electronic GMBH, Planegg, Germany) with active electrodes not introducing additional built-in filters.

Subjects started the perturbation experiments after an hour of rest from the completion of the MVCs and some static lifting tests in upright posture carried out for a separate project (El Ouaaid et al., 2013). They were semi-seated in a perturbation apparatus with the pelvis fixed in all directions; and a harness placed at the T8 level (Figure 3.1). A cable connected the harness to an arm system in front that supported the dropping weights. A load cell was placed along the cable in series with the weights to measure the load transmitted to subjects. A potentiometer was connected to the harness on the back to measure the displacement of the trunk at the T8 level. The weights dropped when the magnetic lock of the arm was triggered off by the experimenter. Before each perturbation, a screen provided the subject with his trunk position feedback in all conditions as well as the biofeedback of the EO normalized EMG activity in condition 6. The signals of all measurement devices (dynamometer, EMG, load cell, potentiometer) were collected at a 1024 HZ sampling rate on a common data acquisition board.

Three preliminary preparation trials were performed for each subject. Each subject had to initially position his trunk comfortably at vertical, which represented the “zero” reference position, and visualized with the feedback system. Then without any notification and randomly during 5 s, the perturbation was applied by unlocking the weights. Each volunteer was instructed to resist the forward movement once the sudden load was applied. Six experimental conditions were considered (

Table 3.1). In conditions 1-4 (C1-C4) the effects of changes in preload and sudden load were studied. Two preload values of 5 N and 50 N were considered, the minimum 5 N preload ensured the subject-harness continuous contact. In condition 5 (C5), the subject was requested to flex forward (10 cm anterior translation at the T8, using the feedback system, leading to about 20° of trunk flexion) before perturbation. In this condition, pre- and sudden loads were the same as in C1. Finally in C6 under loads similar to C2, the subject preactivated abdominal muscles, attempting to keep the activity of EO at 10% using the visual biofeedback on the screen while keeping the upright reference posture. The order of tests was chosen randomly for each subject. Each condition was repeated five times (5 trials) in a row, with 30-s rest between trials and 2-min rest between experimental conditions.

3.3.2. Trunk movement and force perturbation

The measured displacement of the trunk and perturbation force were low-pass filtered by a second order Butterworth filter (cutoff frequency for displacement and force was set at 10 Hz and 50 Hz, respectively). Linear velocity and acceleration of the trunk at the T8 level were calculated from the measured translation profile using forward difference method. The relative peak of displacement at T8 (Rel-Displacement) was computed by subtracting its initial position (reference configuration in all cases except C5 where the flexed position was considered) from its recorded first peak value. The first peak of velocity (Max-Vel) and acceleration (Max-Accel) were also determined. The first peak of perturbation load Total-Load along with the Rel-Load defined as its peak value minus the average load in a 100-ms period before the onset of perturbation were identified for comparison (see Table 3.2).

3.3.3. EMG signals

All EMG signals were further band-pass filtered (30-450 Hz; 8th order zero-lag Butterworth IRR filter) to remove high-frequency noise and low-frequency movement and ECG artifacts. ECG is dominant in torso EMG signals (Redfern et al., 1993), which mandated the use of a high-pass cut-off frequency (30 Hz) that is above what is proposed to remove movement artefacts (10 Hz as indicated in JEK standards for reporting EMG data). The reflex latency was defined as the period between the onset of trunk movement and the onset of muscle EMG burst (Larivière et al., 2010). The onset of muscles reflex was detected using two distinct algorithms. The SD algorithm detected the onset when the standard deviation of the signal became 2 times larger than that of its base line (Hodges and Bui, 1996). To use the SD method, EMG was dual pass filtered with a 6^{th} order Butterworth low-pass filter with a 50-Hz cutoff frequency. An alternative algorithm, the AGLR (approximated generalized likelihood-ratio), was also used that is less affected by the background EMG activity (Staude, 2001; Staude and Wolf, 1999). The AGLR method evaluates log-likelihood ratio of variation in sliding windows along the signal, which indicates the probability of abrupt variation of the signal (Staude, 2001; Staude and Wolf, 1999). Latencies out of the range of 30-150 ms were considered non-reflexive and consequently removed from subsequent calculations. Two variables were defined to quantify the preactivation level and reflex amplitude of muscles. The preactivation level was the root mean square (RMS) of the EMG signal in a 250-ms time-window preceding the onset of force perturbation. It was normalized to the maximal EMG RMS value (500-ms time-windows; 90% overlap) computed over the EMG signals of the MVCs. Reflex-Peak was defined as the peak of the rectified and filtered EMG signal (second-order low-pass Butterworth filter with 25 Hz cut-off frequency) in a 200 ms time-window following the reflex onset. It was normalized to the corresponding maximal EMG value (same signal processing) extracted from the MVCs. Both variables were normalized to muscle maximal EMG recorded during MVCs (Table 3.2). Preliminary analyses demonstrated no reflexive activity in abdominal muscles in all conditions including C6 where preactivated abdominal muscles became silent sometime after the perturbation. Therefore, except for the preactivation in C6 (Figure 3.8), recorded activity in abdominal muscles was not considered when calculating preactivation, reflex latencies and Reflex-Peaks.

3.3.4. Statistical analyses

Preliminary statistical analyses rejected a difference between the EMG activity of muscle pairs (left and right) as well as learning between trials. Therefore, all muscle-based measures were averaged across both sides (left and right) and 5 trials. Kinematics, loading and muscle activity measures were statistically analyzed using NCSS software (NCSS 8. NCSS, LLC. Kaysville, Utah, USA. www.ncss.com), using a significance level (alpha) of 0.05. One- and two-way repeated measures analyses of variance (ANOVA), involving one (trunk flexion or EO antagonistic preactivation) or two (preload and sudden load) within-factors, were carried out to test the effect of preload (C1-2 vs C3-4), sudden load (C1-3 vs C2-4), trunk flexion (C1 vs C5 and C3 vs C5) and abdominal antagonistic pre-activation (C2 vs C6 and C4 vs C6) on trunk kinematics, back muscle reflex and loading variables.

3.4. Results

Results for various subjects and conditions follow similar profiles as those shown in Figures 2.2 and 2.3.

3.4.1. Effects of preload and sudden load

Interactions of preload and sudden load did not affect the muscles activity prior or after the perturbation, except for Reflex-Peak of LG. Pre-perturbation activity of back muscles was significantly affected by preload (Figure 3.4a, Table 3.3) whereas abdominal muscles were not affected. Latencies and Reflex-Peak were not influenced by preload, except for the SD latency of IC (Figure 3.4b, Table 3.3), which increased with higher preload although AGLR latency did not show any effect. Greater sudden load significantly increased the Reflex-Peak but not latencies (Figure 3.4b, Table 3.3). One-way ANOVA for six distinct cases (3 muscles x 2 preloads) showed significant increase in Reflex-Peak for all cases except LG-5 N and MF-5 N.

Preload did not influence trunk displacements while sudden load increased it significantly ($p<0.001$) (Figure 3.5a). Max-Vel and Max-Accel, occurring 150-180 ms and 29-73 ms respectively after the trunk movement onset, decreased significantly with preload (Figures 2.5b and c, Table 3.3). Both Max-Vel and Max-Accel increased however significantly when sudden load increased (Figures 2.5b and c, Table 3.3).

Total-Load and Rel-Load were significantly affected by preload and sudden load (Table 3.3). As expected, increasing either preload or sudden load increased Total-Load (Figure 3.5d). The same trend was observed for Rel-Load when sudden load increased (Figure 3.5e); however, as preload increased, Rel-Load dropped significantly irrespective of the sudden load magnitude.

3.4.2. Effect of initial flexed posture (IFP)

"Here under 50 N sudden load, cases with different initial conditions (C1, C3 and C5) were considered. While background EMG of only back muscles was significantly higher in C5 (with flexed posture) relative to C1 and C3 (with upright postures), Reflex-Peak remained unaffected (Figures 2.6a and b, Table 3.4). On the other hand, longer reflex latencies were observed in C5 (Figures 2.6c and d) with respect to those in C1 and C3; though one-way ANOVA yielded significant effect only for LG and MF. Good agreement was noted between the two methods (SD and AGLR) of onset detection.

Trunk displacement (Rel-Displacement) at T8 level did not vary between C1 (10.11 ± 4.28 cm), C3 (9.50 ± 5.61 cm) and C5 (10.20 ± 3.52 cm). Max-Vel and Max-Accel were higher when the subject was initially flexed in C5 compared to both C1 and C3 (Figures 2.7a and b); Max-Vel occurred at 151 ± 48 ms in C1, 153 ± 99 ms in C3 and 158 ± 50 ms in C5 after the onset of movement (averaged over subjects). The instance of the acceleration peak (Max-Accel) in C1 and C3 was 61 ± 16 ms and 29 ± 8 ms, respectively, which were significantly shorter than 100 ± 44 ms in C5. Due to the initial forward flexion, peak total displacement was significantly greater in C5 compared to C1 and C3 (Figure 3.7a). Total-Load (Figure 3.7d) and Rel-Load did not significantly change in C5 vs C1 and C3.

3.4.3. Effect of abdominal antagonistic preactivation (APA) on reflexive response

Here under 100 N sudden load, cases with different initial conditions (C2, C4 and C6) were considered. Antagonistic pre-activation of the abdominal muscles resulted in significantly higher preactivation in all abdominal muscles in C6 vs both C2 and C4 (Figure 3.8a, Table 3.5). Preactivation of all back muscles was found higher in C6 relative to C2; however compared to C4, only IC muscle showed higher preactivity. Abdominal antagonistic pre-activation did not affect the latency of back muscles (Figures 2.8c and d, Table 3.5), but significantly increased the

Reflex-Peak (Figure 3.8b) of IC and MF back muscles in C6 compared to C2 and C4. Finally, although antagonistic coactivation did not affect any of the trunk kinematics and loading variables with respect to C2, Max-Vel and Max-Accel in C4 was found significantly smaller than those in C6. Moreover, no significant difference was observed in Total-Load (Table 3.5, Figure 3.9). Rel-displacement reached 14.24 ± 3.76 cm in C2, 15.37 ± 4.49 cm in C4 and 13.63 ± 3.08 cm in C6.

3.5. Discussion

Trunk muscle, kinematics and loading responses were investigated in this study under sudden loading perturbations, accounting for a number of variables: preload level (5 N vs 50 N), sudden load magnitudes (50 N vs 100 N), initial trunk posture (upright standing vs flexed posture) and abdominal antagonistic preactivation (none vs 10% at EO). In brief, the results demonstrated that preloading expectedly increased back muscles preactivation; did not change the peak displacement and reflex responses but decreased peak trunk velocity and acceleration as well as the relative load peak. Increasing the sudden load neither affected reflex latencies but increased the Reflex-Peak as well as all trunk kinematics and loading variables. Trunk flexion increased extensor muscles preactivation, latencies of LG and MF muscles, trunk velocity and acceleration, but did not affect Reflex-Peak and loading variables. Abdominal antagonistic preactivation increased muscles preactivation but did not affect reflex, trunk kinematics or loading variables except for Reflex-Peak of IC and MF muscles, which significantly increased. Two distinct methods of EMG onset detection (SD and AGLR) were employed in this study that yielded comparable results.

3.5.1. Effects of preload and sudden load

Higher preload, as expected, increased the background EMG activity in back muscles (Figure 3.4a) that likely stiffens the trunk intrinsically (El-Rich et al., 2004). Higher stiffness of the spinal column was found in some studies to lower the demand for reflexive response under perturbations (Brown and McGill, 2009; Brown and McGill, 2008; Granata et al., 2004; Moorhouse and Granata, 2007). However, in the current study and with the exception of SD latency of IC, no effect of preload on reflex responses was noted (Figure 3.4b) that is in agreement with Krajcarski et al. (1999) using a similar perturbation set up. In addition, some other studies also found the reflexive response unaffected with changes in muscle preactivation

(Andersen et al., 2004; Stokes et al., 2000). It should be noted that these observations are likely affected by alterations in the ratio of sudden load to preload, the level of muscles preactivation, the direction of applied forces, the temporal pattern of applied sudden force and the experimental set up in various studies.

In contrast to our finding of no significant changes in trunk peak displacement under higher preload, previous findings showed smaller trunk rotation (Granata et al., 2004; Krajcarski et al., 1999). Significantly smaller trunk peak velocities and accelerations along with larger peak applied force were however found under higher preload that may indicate a greater trunk margin of stability. Lack of alterations in reflex activity of muscles and in trunk displacement despite substantial reductions in the trunk velocity and acceleration points to the relative sensitivity of displacement derivatives to changes in intrinsic stiffness. Moreover, this demonstrates the potential of the kinematics-driven models (Bazrgari et al., 2009a; Bazrgari et al., 2009b) in predicting the muscle forces and spinal loads since velocity and acceleration profiles are considered as direct input data. Earlier studies did not report alterations in the velocity and acceleration when the trunk was perturbed.

In contrast to the preload, higher sudden load increased trunk peak displacements, velocities and accelerations. It also significantly increased the back muscles reflex amplitude that concurs with previous findings (Granata et al., 2004; Krajcarski et al., 1999). Measured tensile force in the cable (Total-load) varied with the pre- and sudden loads as it depends on the dropping weights, inertia, trunk active/passive stiffness and damping. In the current study, the Total-Load peak increased with both preload and sudden load. The relative load peak (preload subtracted) also increased significantly when the sudden load increased but on the contrary and in agreement with earlier observations (Vera-Garcia et al., 2006) higher preload diminished the relative load peak (Figure 3.5e). This drop in the relative load at higher preloads should be interpreted positively with the likelihood to diminish the spinal loads.

3.5.2. Effect of trunk flexion:

When the trunk is flexed as in C5 compared to C1, the intrinsic stiffness from both passive and active components is expected to increase (Arjmand and Shirazi-Adl, 2006a; Granata and Rogers, 2007; Granata and Wilson, 2001; McGill et al., 1994) which likely reduces the need for reflexive stiffness contribution. Results showed that the reflex amplitude and relative

displacement remained unchanged although the reflex latency increased that supports a higher initial intrinsic stiffness with a diminished need for a reflexive response. It is also important to note that an identical muscle activity generates smaller force in a flexed posture when the extensor muscles are in the descending stretched portion of their active force-length relation. In addition, larger gravitational moments in flexed postures as well as longer reflex latencies (Figures 2.6c and d) tend to deteriorate the trunk control and stability (Cholewicki et al., 2005; Franklin and Granata, 2007; Reeves et al., 2009) and hence, act to counteract the effect of augmented initial trunk stiffness. They may also explain larger peaks of velocity and acceleration in C5 vs C1 and C3.

3.5.3. Effect of abdominal antagonistic preactivation:

Abdominal muscles coactivation in C6 significantly increased all back muscles preactivation compared to C2 but augmented the preactivation of only IC muscle relative to C4 (Table 3.5). It however influenced neither the trunk kinematics variables nor the peak load; effects that are found generally opposite to those under greater preloads (Table 3.3). Reflex-Peak of IC and MF muscles increased in C6 compared to C2 and C4. It appears that after the onset of perturbation the activity in both abdominal and extensor muscles further increased (Figure 3.3) that may substantially increase spinal loads during the critical early post-perturbation period. This prolonged antagonistic coactivity during post-perturbation period could affect the response and be the reason not to observe significant changes in kinematics and load output variables in C6 vs C2. With abdominals preactivation, extensor muscles showed greater activity more than when the preload was increased to 50 N, which explains why Reflex-Peak increased here and not when the preload was increased. Preactivation of a muscle at low to moderate levels has been reported to increase its reflex response (Lee et al., 2006), an observation that appears to contradict the expectation that increasing coactivity increases stiffness (Gardner-Morse et al., 1995) and hence lowers the need for a reflexive response. It should be noted that preactivation in agonist muscles may have different effects on post-perturbation response than that in antagonist muscles. In line with this hypothesis, additional analyses comparing C6 (antagonist preactivation) with C4 (agonist preactivation) demonstrated significantly different reflex amplitude and kinematics results. Moreover various preactivation routines might have distinct effects on the subject anticipation of perturbations and hence on the trunk response."

The current results help identify likely mechanisms influencing equilibrium and stability of the human trunk. The measured EMG signals revealed that, in contrast to expectation and due likely to alterations in the total load and total displacement, higher initial trunk intrinsic stiffness in cases with initial flexed posture and greater preload did not reduce reflexive response of muscles. The trunk velocity and acceleration peaks both dropped with greater preload despite greater total load but increased with initial posture due likely to larger total displacement. Decoding of trunk kinematics (displacements, velocities and accelerations) by kinematics driven musculoskeletal models would have the potential to reveal complementary information on the interplay between external loads, posture, muscle activity and passive resistance of the trunk. Such information would likely play an important role in the prevention and management of back injuries.

In summary, effects of increasing the preload, sudden load, trunk flexion and abdominal preactivation were studied on reflex responses, trunk kinematics (displacement, velocity and acceleration) and loading variables under sudden forward trunk perturbations. Preload, initial flexed posture and muscle preactivation increased pre-perturbation muscle activity and consequently trunk stiffness. Although preload and initial posture did not affect back muscles reflexive response and relative trunk displacements, trunk velocity and acceleration were decreased with the former but increased with the latter. Increased muscle preactivation did not affect any measured parameters except reflex peak. Changes in sudden load magnitude affected both muscles reflex and kinematics. Further insight into the behavior of the human trunk under sudden loads as well as the evaluation of crucial spinal loads and stability margins should await future musculoskeletal model studies that are driven by recorded kinematics and loads.

Conflict of interest

None to declare.

Acknowledgements

This study has been supported by grants from the Institut de recherche Robert-Sauvé en santé et en sécurité du travail (IRSST-Québec) and the Natural Sciences and Engineering Research Council of Canada (NCERC-Canada). Authors thank Dr. André Plamondon for his

support and advice, as well as Sophie Bellefeuille and Cynthia Appleby for their technical assistance during tests at the IRSST laboratory.

3.6. References

Andersen TB, Essendrop M, Schibye B. Movement of the upper body and muscle activity patterns following a rapidly applied load: the influence of pre-load alterations. European Journal of Applied Physiology. 2004;91:488-92.

Arjmand N, Shirazi-Adl A. Model and in vivo studies on human trunk load partitioning and stability in isometric forward flexions. Journal of Biomechanics. 2006;39:510-21.

Axler CT, McGill SM. Low back loads over a variety of abdominal exercises: Searching for the safest abdominal challenge. Medicine and Science in Sports and Exercise. 1997;29:804-11.

Bazrgari B, Shirazi-Adl A, Lariviere C. Trunk response analysis under sudden forward perturbations using a kinematics-driven model. Journal of Biomechanics. 2009a;42:1193-200.

Bazrgari B, Shirazi-Adl A, Parnianpour M. Transient analysis of trunk response in sudden release loading using kinematics-driven finite element model. Clinical Biomechanics. 2009b;24:341-7.

Brown SH, McGill SM. The intrinsic stiffness of the in vivo lumbar spine in response to quick releases: implications for reflexive requirements. Journal of Electromyography and Kinesiology. 2009;19:727-36.

Brown SHM, McGill SM. How the inherent stiffness of the in vivo human trunk varies with changing magnitudes of muscular activation. Clinical Biomechanics. 2008;23:15-22.

Brown SHM, Vera-Garcia FJ, McGill SM. Effects of abdominal muscle coactication on the externally preloaded trunk: Variations in motor control and its effect on spine stability. Spine. 2006;31:E387-E93.

Cholewicki J, Silfies SP, Shah RA, Greene HS, Reeves NP, Alvi K, et al. Delayed trunk muscle reflex responses increase the risk of low back injuries. Spine. 2005;30:2614-20.

Cholewicki J, Simons APD, Radebold A. Effects of external trunk loads on lumbar spine stability. Journal of Biomechanics. 2000;33:1377-85.

De Foa JL, Forrest W, Biedermann HJ. Muscle fiber direction of longissimus, iliocostalis and multifidus: landmark-drived reference lines. Journal of Anatomy. 1989;163:243-7.

El-Rich M, Shirazi-Adl A, Arjmand N. Muscle activity, internal loads, and stability of the human spine in standing postures: combined model and In vivo studies. Spine. 2004;29:2633-42.

El Ouaaid Z, Shirazi-Adl A, Plamondon A, Larivière C. Trunk strength, muscle activity and spinal loads in maximum isometric flexion and extension exersions: A combined in vivo computational study. Journal of Biomechanics. 2013;Under press.

Franklin TC, Granata KP. Role of reflex gain and reflex delay in spinal stability-a dynamic simulation. Journal of Biomechanics. 2007;40:1762-7.

Gardner-Morse M, Stokes IAF. The effects of abdominal muscle co-activation on lumbar spine stability Spine. 1998;23:86-91.

Gardner-Morse M, Stokes IAF, Laible JP. Role of muscles in lumbar stability in maximum extesion efforts. Journal of Orthopaedic Research. 1995;13:802-8.

Granata KP, Marras WS. Cost-benefit of muscle cocontraction in protecting against spinal instability. Spine. 2000;25:1398-404.

Granata KP, Orishimo KF. Response of trunk muscle coactivation to changes in spinal stability. Journal of Biomechanics. 2001;34:1117-23.

Granata KP, Orishimo KF, Sanford AH. Trunk muscle coactivation in preparation for sudden load. Journal of Electromyography and Kinesiology. 2001;11:247-54.

Granata KP, Rogers EL. Torso flexion modulates stiffness and reflex response. Journal of Electromyography and Kinesiology. 2007;17:384-92.

Granata KP, Slota GP, Bennett BC. Paraspinal muscle reflex dynamics. Journal of Biomechanics. 2004;37:241-7.

Granata KP, Wilson SE. Trunk posture and spinal stability. Clinical Biomechanics. 2001;16:650-9.

Hodges PW, Bui BH. A comparison of computer-based methods for the determination of onset of muscle contraction using electromyography. Electroencephalography and clinical Neurophysiology. 1996;101:511-9.

Hodges PW, Richardson CA. Inefficient muscular stabilization of the lumbar spine associated with low back pain - A motor control evaluation of transversus abdominis. Spine. 1996;21:2640-50.

Krajcarski SR, Potvin JR, Chiang J. The in vivo dynamic response of the spine to perturbations causing rapid flexion: effects of pre-load and step input magnitude. Clinical Biomechanics. 1999;14:54-62.

Larivière C, Forget R, Vadeboncpeur R, Bilodeau M, Mecheri H. The effect of sex and chronic low back pain on back muscle reflex responses. European Journal of Applied Physiology. 2010;109:577-90.

Larivière C, Gagnon D, Genest K. Offering proper feedback to control for out-of-plane lumbar moments influences the activity of trunk muscles during unidirectional isometric trunk exertions. Journal of Biomechanics. 2009;42:1498-505.

Lavender SA, Mirka GA, Schoenmarklin RW, Sommerich CM, Sudhakar LR, Marras WS. The effects of preview and task symmetry on trunk muscle response to sudden loading. Human Factors. 1989;31:101-15.

Lee PJ, Rogers EL, Granata KP. Active trunk stiffness increases with co-contraction. Journal of Electromyography and Kinesiology. 2006;16:51-7.

Manning DP, Mitchell RG, Blanchfield LP. Body movements and events contributing to accidental and nonaccidental back injuries. Spine. 1984;9:734-9.

Marras WS, Rangarajulu SL, Lavender SA. Trunk loading and expectation. Ergonomics. 1987;30:551-62.

Marshall P, Murphy B. The validity and reliability of surface EMG to assess the neuromucular response of the abdominal muscles to rapid limb movement. Journal of Electromyography and Kinesiology. 2003;13:477-89.

McGill SM. Electromyographic activity of the abdominal and low back musculature during the generation of isometric and dynamic axial trunk torque: Implications for lumbar mechanics. Journal of Orthopaedic Research. 1991;9:91-103.

McGill SM, Seguin J, Bennett G. Passive stiffness of the lumbar torso in flexion, extension, lateral bending and axial rotation, Efect of belt wearing and breath holding. Spine. 1994;19:696-704.

Moorhouse KM, Granata KP. Role of reflex dynamics in spinal stability: Intrinsic muscle stiffness alone is insufficient for stability. Journal of Biomechanics. 2007;40:1058-6.

Panjabi MM. The stabilizing system of the spine. Part I. Function, dysfunction, adaptation, and enhancement. Journal of Spinal Disorders 1992;5:383-9.

Radebold A, Cholewicki J, Panjabi MM, Patel TC. Muscle response pattern to sudden trunk loading in healthy individuals and in patients with chronic low back pain. Spine. 2000;25:947-54.

Reeves NP, Cholewicki J, Narendra KS. Effects of reflex delays on postural control during unstable seated balance. Journal of Biomechanics. 2009;42:164-70.

Shirazi-Adl A. Analysis of large compression loads on lumbar spine in flexion and in torsion using a novel wrapping element. Journal of Biomechanics. 2006;39:267-75.

Staude GH. Precise onset detection of human motor responses using a whitening filter and the log-likelihood-ration test. IEEE Transactions on Biomedical Engineering. 2001;48:1292-305.

Staude GH, Wolf W. Objective motor response onset detection in surface myoelectric signals. Medical Engineering and Physics. 1999;21:449-67.

Stokes IAF, Gardner-Morse MG, Henry SM, Badger GJ. Decrease in trunk muscular response to perturbation with preactivation of lumbar spinal musculature. Spine. 2000;25:1957-64.

Stokes IAF, Henry SM, Single RM. Surface EMG electrodes do not accurately record from lumbar multifidus muscles. Clinical Biomechanics. 2003;19:9-13.

Van Dieen JH, Kingma I, van der Bug JCE. Evidence for a role of antagonistic cocontraction in controlling trunk stiffness during lifting. Journal of Biomechanics. 2003;36:1829-36.

Vera-Garcia FJ, Brown SH, Gray JR, McGill SM. Effects of different levels of torso coactivation on trunk muscular and kinematic responses to posteriorly applied sudden loads. Clinical Biomechanics. 2006;21:443-55.

White AA, Panjabi MM. Clinical Biomechanics of the Spine. Philadelphia: J.B. Lippincott; 1990.

Zedka M, Prochazka A, Knight B, Gillard D, Gauthier M. Voluntary and reflex control of human back muscles during induced pain. Journal of Physiology. 1999;520:591-604.

Table 3.1 Parameters in the six experimental conditions considered in this work

Condition	Pre Load (N)	Sudden Load (N)	Initial posture	EO preactivation
C1	5	50	Upright	No
C2	5	100	Upright	No
C3	50	50	Upright	No
C4	50	100	Upright	No
C5	5	50	10 cm Anterior Translation	No
C6	5	100	Upright	10%

Table 3.2 List of variables for evaluating trunk kinematics and muscles responses

Variable	Definition
Latency (ms)	Delay period between the onset of muscle reflex and the onset of trunk movement
Max-Accel (cm/s^2)	Maximum linear acceleration of trunk at T8 level
Max-Vel (cm/s)	Maximum linear velocity of trunk at T8 level
Preactivation (%MVC)	RMS of the EMG signal in a 250-ms time-window preceding the onset of force perturbation (normalized to muscle MVC)
Reflex-Peak (%MVC)	Peak of filtered EMG signal in a 200-ms time-window following the reflex onset (normalized to muscle MVC)
Rel-Displacement (cm)	Peak of trunk displacement at T8 relative to reference posture: upright for C1[a] to C4 and C6, and flexed forward for C5
Rel-Load (N)	Total-Load minus the average load in a 100-ms window before the onset of perturbation
Total-Load (N)	Peak of the perturbation force applied to the trunk

[a] Conditions C1 to C6 are defined in Table 3.1.

Table 3.3 p-Values (ANOVA) for the effects of the preload and sudden load on muscles activity, trunk kinematics and loading variables [a].

Factor	**Muscle**	**Preactivation**	**Latency [SD]**	**Latency [AGLR]**	**Reflex-Peak**
Preload	LG	0.012	0.400	0.629	0.952
	IC	0.059	0.027	0.111	0.344
	MF	0.003	0.367	0.114	0.844
Sudden-Load	LG	0.643	0.854	0.091	0.014
	IC	0.693	0.989	0.263	0.006
	MF	0.422	0.728	0.378	0.019
Preload*Sudden Load	LG	0.236	0.167	0.510	0.044
	IC	0.506	0.201	0.290	0.977
	MF	0.491	0.728	0.762	0.642

Factor	Max-Vel	Max-Accel	Total-Load	Rel-Load
Preload	<0.001	0.016	0.005	<0.001
Sudden-Load	<0.001	<0.001	<0.001	<0.001
Preload*Sudden Load	0.802	0.806	0.828	0.954

[a] Statistics carried out using C1 to C4 experimental conditions; statistically significant differences ($p < 0.05$) are identified in bold characters, while trends ($0.05 < p < 0.1$) are underlined.

Table 3.4 p-Values (ANOVA) for the effect of preload and pre-perturbation trunk posture when sudden load was 50 N on muscles activity, trunk kinematics and loading variables*

Conditions	Muscle	Preactivation	Latency [SD]	Latency [AGLR]	Reflex-Peak
C1 vs C5	LG	<0.001	0.035	<0.001	0.763
	IC	<0.001	0.218	0.538	0.112
	MF	<0.001	0.015	0.010	0.705
C3 vs C5	LG	0.040	0.037	0.070	0.165
	IC	0.037	0.824	0.502	0.437
	MF	0.024	0.078	0.478	0.414

	Max-Vel	Max-Accel	Total-Load	Rel-Load
C1 vs C5	0.002	<0.001	0.522	0.391
C3 vs C5	<0.001	<0.001	0.150	0.007

*Statistics carried out using C1, C3 and C5 experimental conditions; statistically significant differences ($p < 0.05$) are identified in bold and trends ($0.05 < p < 0.1$) are underlined.

Table 3.5 p-Values (ANOVA) for the effect of preload and abdominal muscles pre-activation when sudden load was 100 N on trunk kinematics and loading variables [a].

Conditions	Muscle	Preactivation	Latency [SD]	Latency [AGLR]	Reflex-Peak
C2 vs C6	LG	0.004	0.450	0.890	0.114
	IC	0.002	0.370	0.850	0.003
	MF	<0.001	0.301	0.656	0.050
	RA	0.002			
	EO	<0.001			
	IO	<0.001			
C4 vs C6	LG	0.513	0.268	0.481	0.642
	IC	0.009	0.354	0.111	0.002
	MF	0.298	0.766	0.198	0.028
	RA	<0.001			
	EO	<0.001			
	IO	<0.001			

Factor	Max-Vel	Max-Accel	Total-Load	Rel-Load
C2 vs C6	0.437	0.510	0.448	0.415
C4 vs C6	0.002	<0.001	0.161	<0.001

[a] Statistics carried out using C2, C4 and C6 experimental conditions; statistically significant differences ($p < 0.05$) are identified in bold.

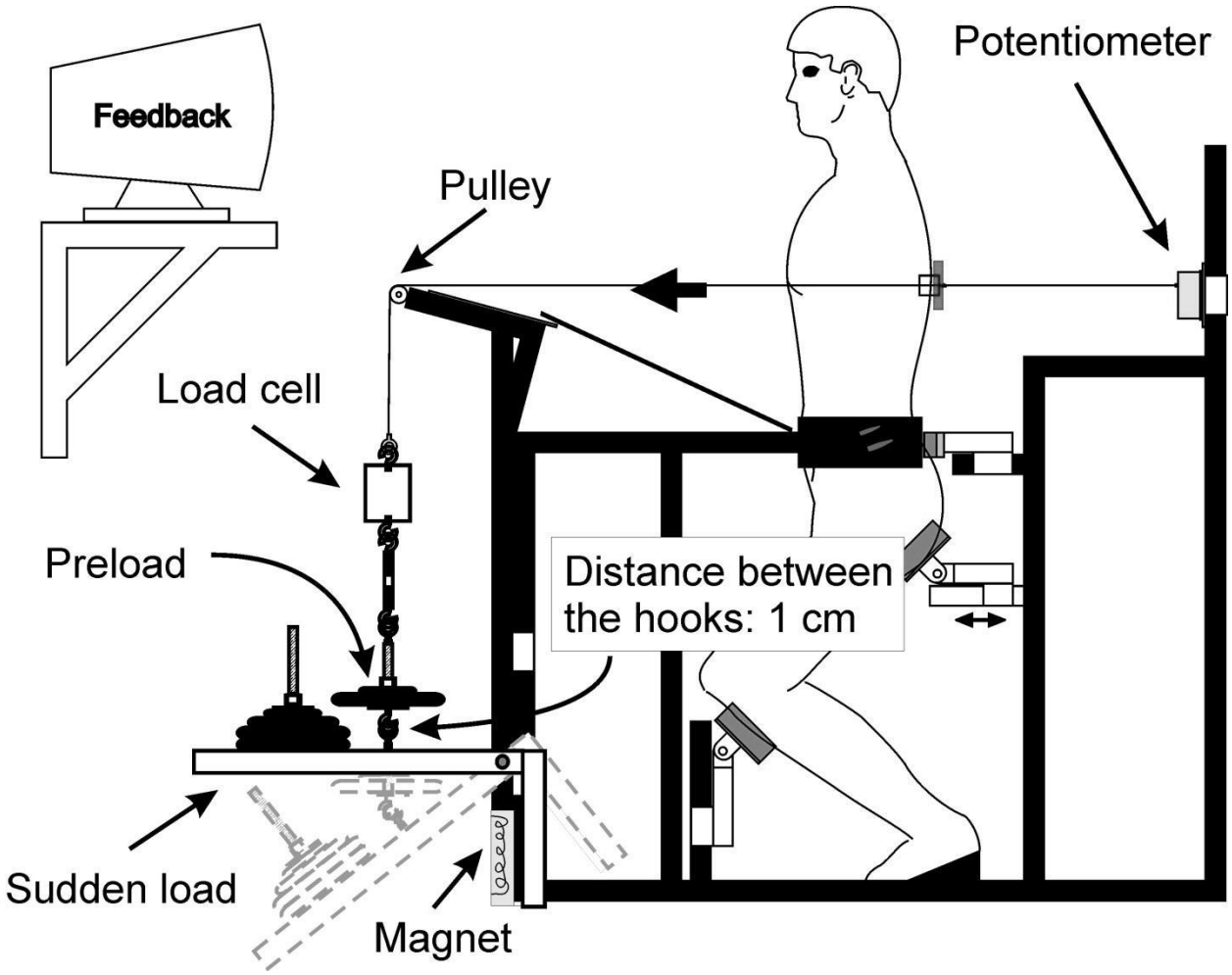

Figure 3.1 Experimental setup. Subjects performed tests while semi-seated in a perturbation apparatus with the pelvis fixed. A cable at the T8 level connected the harness to an arm system in front that supported the dropping weights. Load was measured by the load cell in front while displacement was measured by the potentiometer on the back. The weights dropped when the magnetic lock of the arm was triggered off by the experimenter. Before each perturbation, a screen provided the subject with his trunk position feedback and the EO normalized EMG activity when needed.

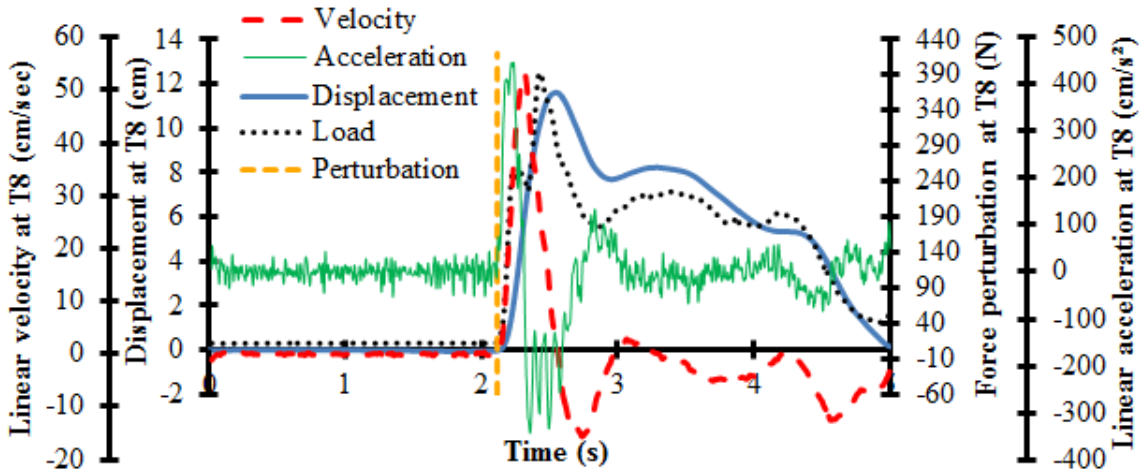

Figure 3.2 Measured trunk displacement and perturbation force profiles at the T8 level accompanied with calculated linear velocity and acceleration profiles at the T8 level. The demonstrated curves are for the subject 4, condition 6.

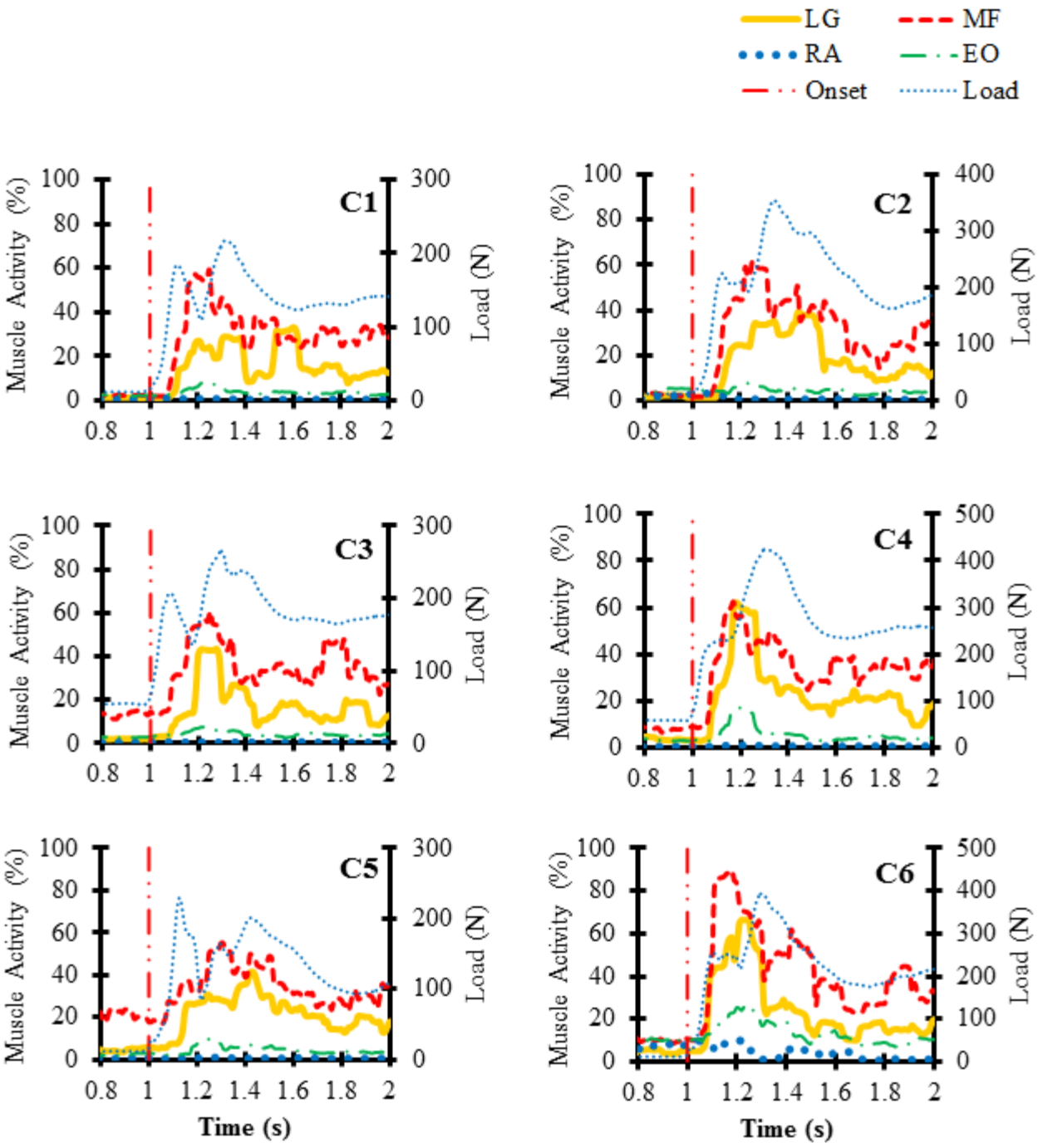

Figure 3.3 Normalized EMG of left LG, MF, RA and EO muscles during trial 5 of subject 4 for six conditions. Time axis in all conditions was shifted with the onset of perturbation (vertical dashed line) placed at 1 sec.

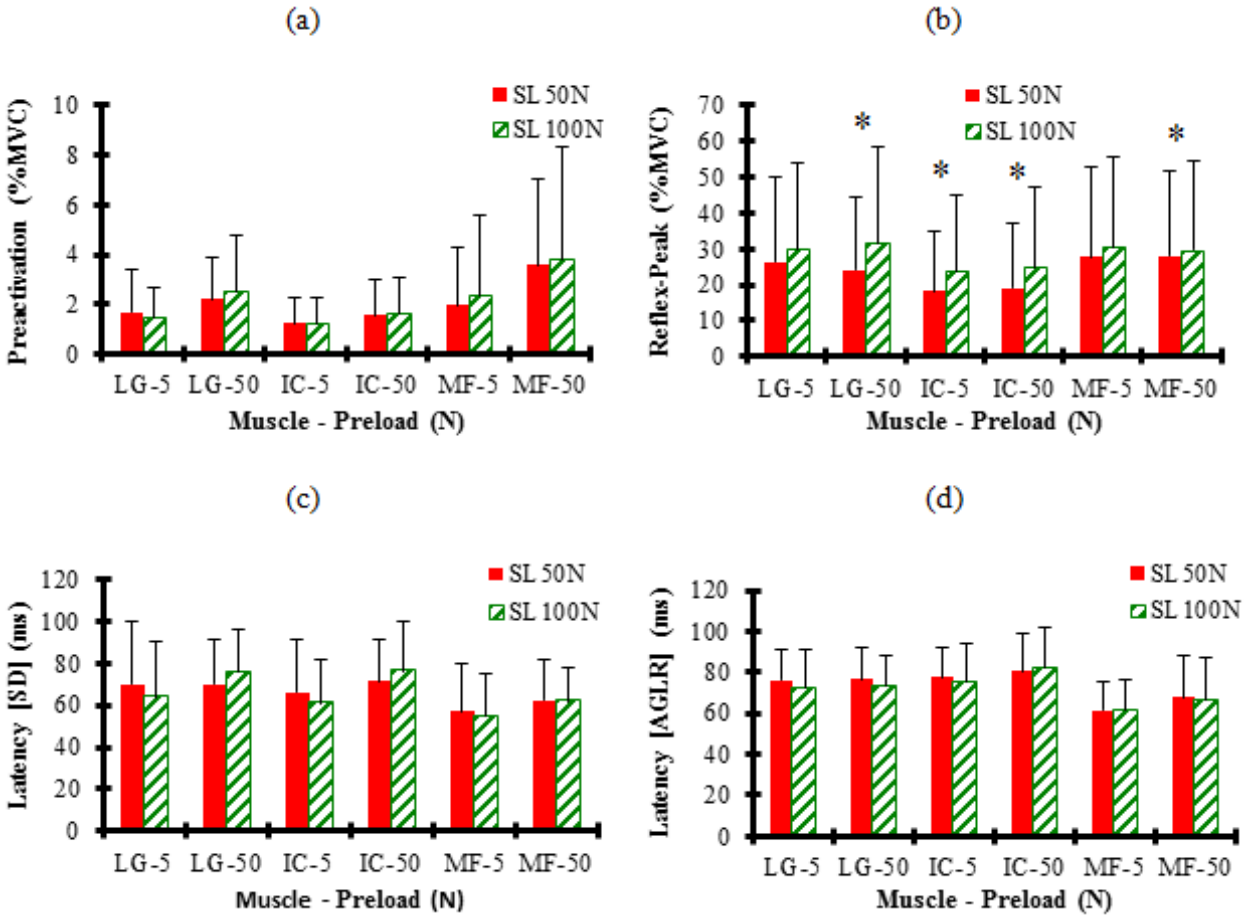

Figure 3.4 Parameters associated with the back muscle activity prior and after perturbation, presented for the two preloads (5 N and 50 N) and the two sudden loads (50 N and 100 N) in conditions 1-4. All values are averaged over 2 sides, 5 trials and 12 subjects. * ($p < 0.05$) indicates significant effect for the effect of sudden load.

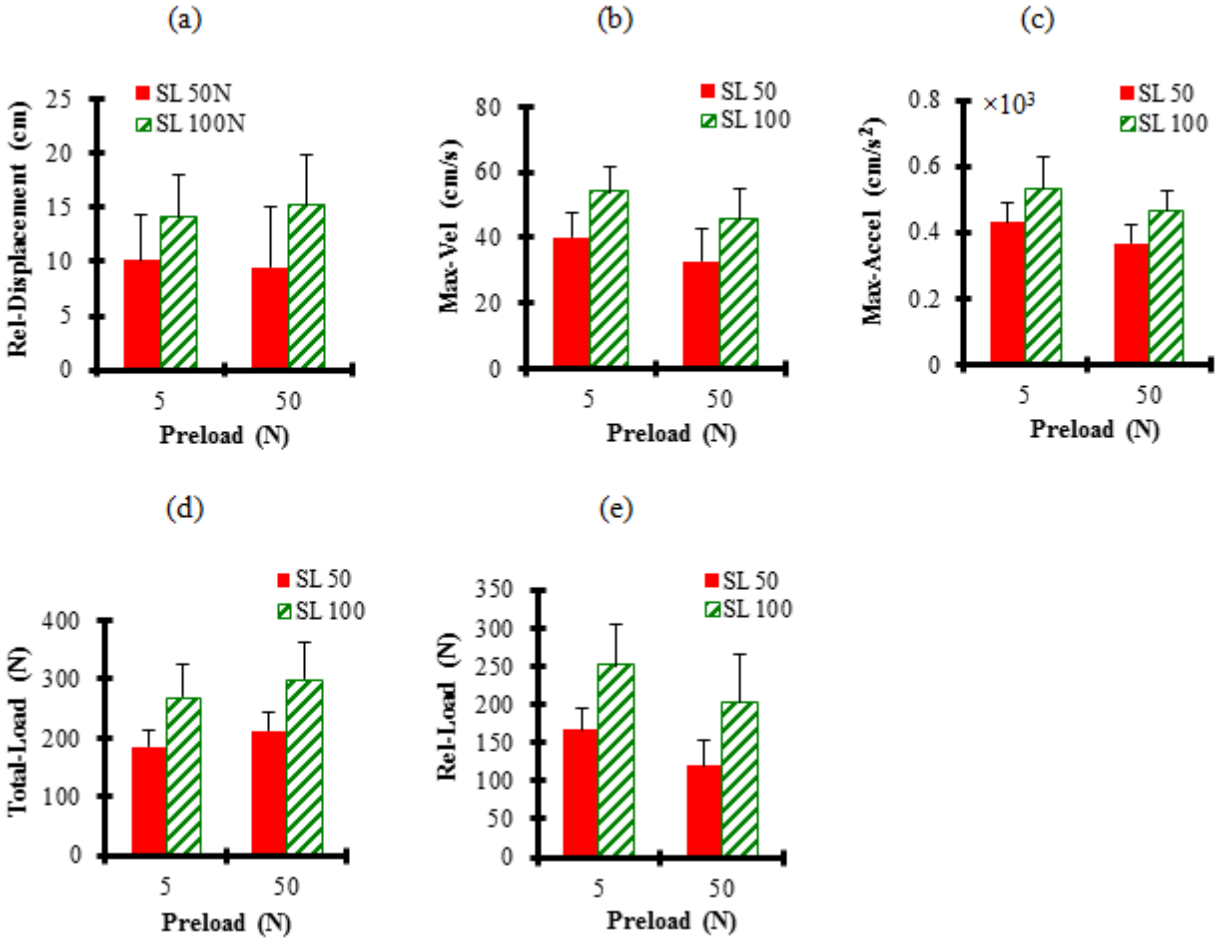

Figure 3.5 Kinematic parameters of the trunk movement for the two preloads (5 N and 50 N) and two sudden loads (50 N and 100 N) in conditions 1-4. All values are averaged across all subjects with error bars showing standard deviation.

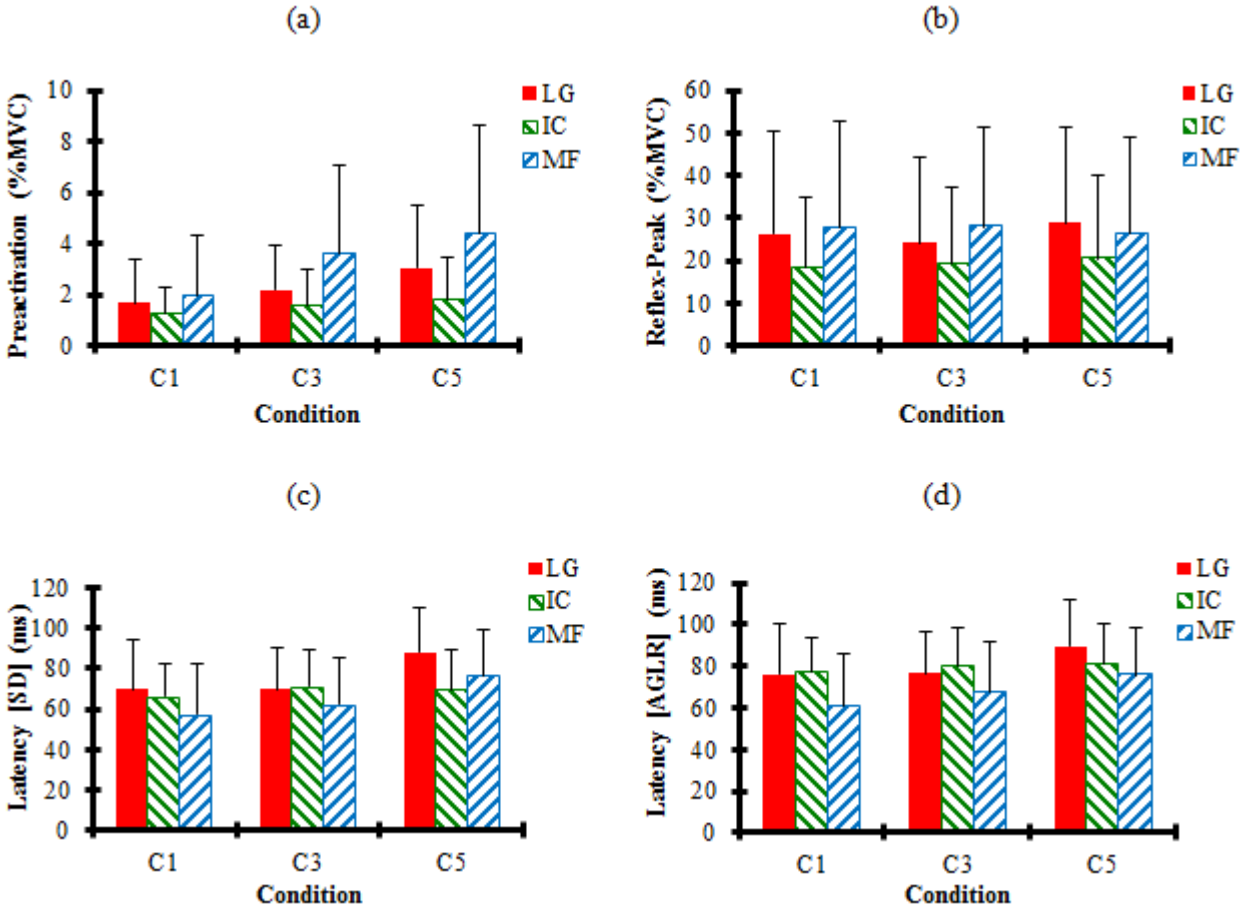

Figure 3.6 Parameters associated with the back muscle activity prior and after perturbation, presented for three conditions with 50 N sudden load: C1 (preload = 5 N), C3 (preload = 50 N) and C5 (initial trunk forward flexion). All values are averaged over 2 sides, 5 trials and 12 subjects.

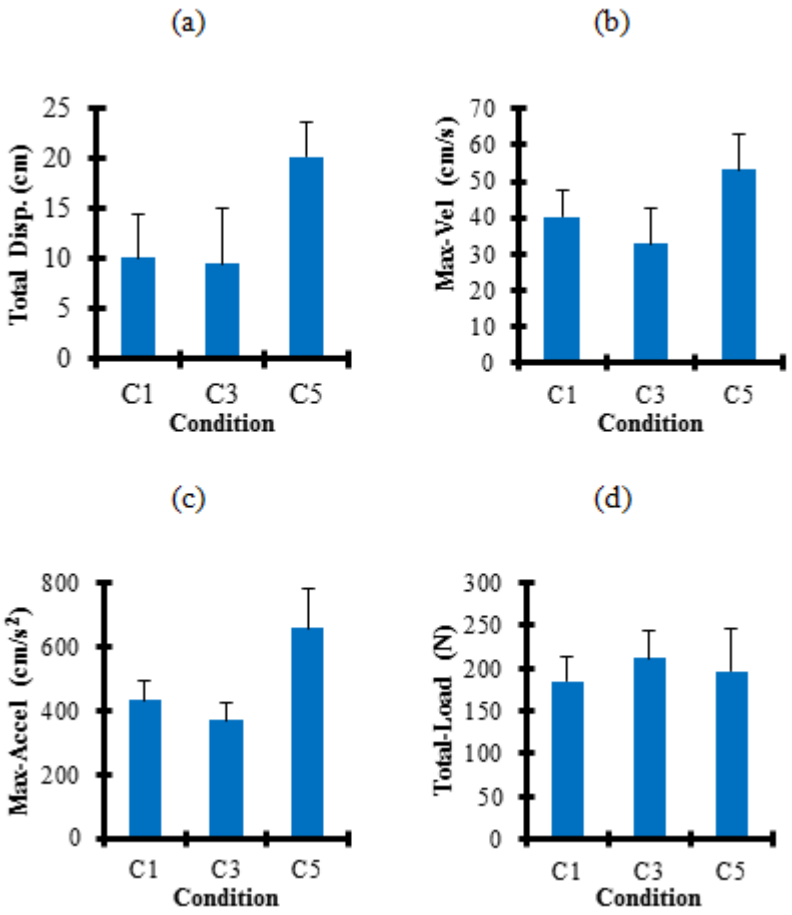

Figure 3.7 Kinematic and loading parameters of the trunk movement with 50 N sudden load when pre-perturbation condition changed: C1 (preload = 5 N), C3 (preload = 50 N) and C5 (initial trunk forward flexion). All values were averaged across all subjects with error bars showing standard deviation.

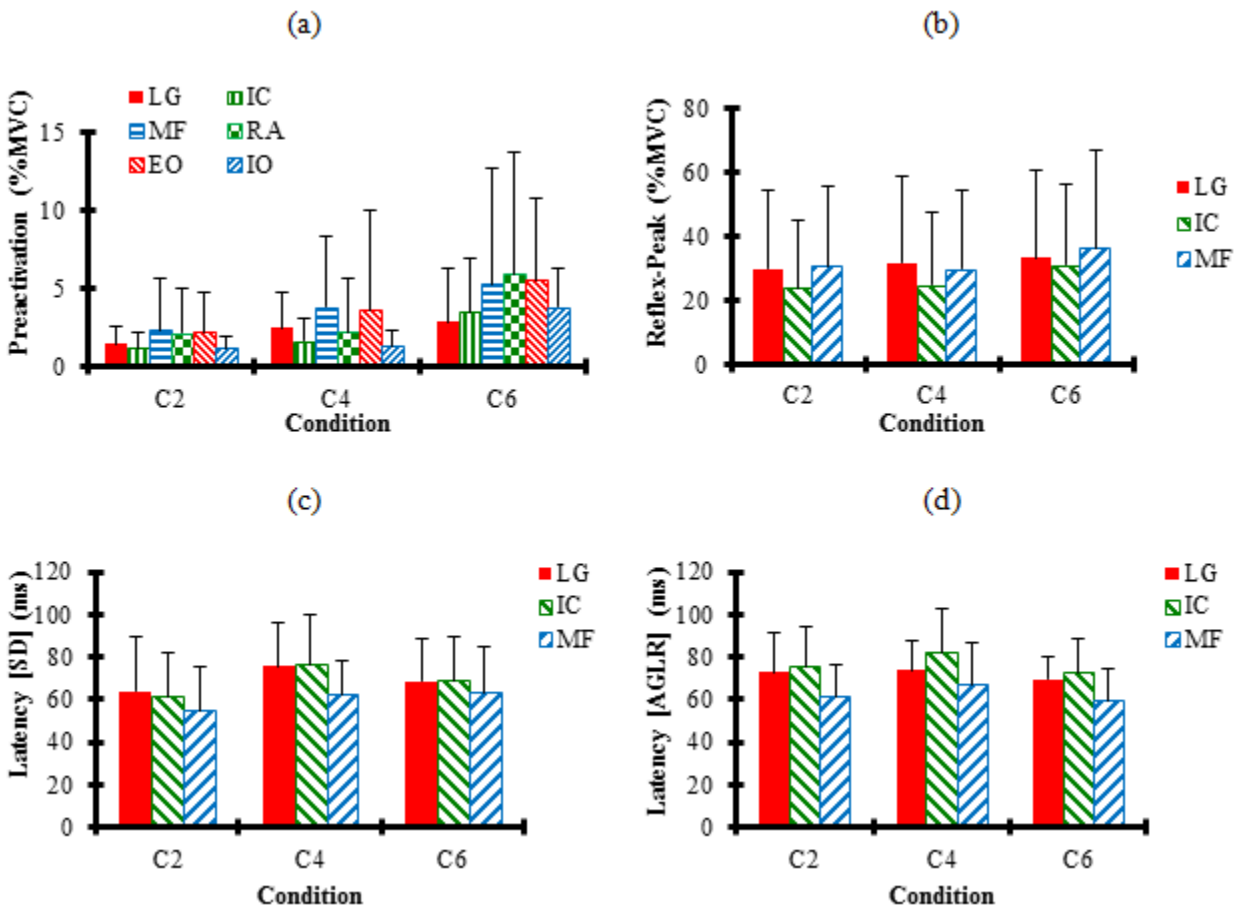

Figure 3.8 Parameters associated with the back muscle activity prior and after perturbation presented for three conditions with 100 N sudden load: C2 (preload = 5 N), C4 (preload = 50 N) and C6 (abdominal muscles preactivation). All the values averaged over 2 sides, 5 trials and 12 subjects.

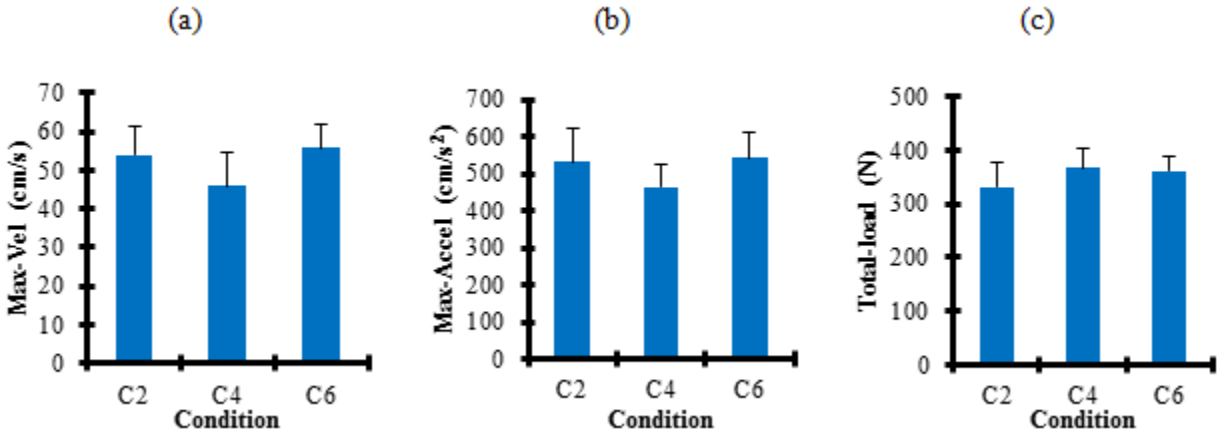

Figure 3.9 Kinematic and loading parameters of the trunk movement with 100 N sudden load when pre-perturbation condition changed: C2 (preload = 5 N), C4 (preload = 50 N) and C6 (abdominal muscles preactivation). All values were averaged across all subjects with error bars showing standard deviation.

CHAPTER 4 ARTICLE 2: TRUNK ACTIVE RESPONSE AND SPINAL FORCES IN SUDDEN FORWARD LOADING – ANALYSIS OF THE ROLE OF PERTURBATION LOAD AND PRE-PERTURBATION CONDITIONS BY A KINEMATICS-DRIVEN MODEL

Ali Shahvarpour [a], Aboulfazl Shirazi-Adl [a], Christian Larivière [b], Babak Bazrgari [c]

[a] Division of Applied Mechanics, Department of Mechanical Engineering, École Polytechnique, Montreal, Quebec, Canada

[b] Occupational Health and Safety Research Institute Robert-Sauvé, Montreal, Quebec, Canada

[c] Department of Biomedical Engineering, University of Kentucky, Lexington, KY, USA

Published in
Journal of Biomechanics (2015)

4.1. Abstract

Understanding the central nervous system (CNS) response strategy to trunk perturbations could help in prevention of back injuries and development of rehabilitation and treatment programs. This study aimed to investigate biomechanical response of the trunk musculoskeletal system under sudden forward loads, accounting for pre-perturbation conditions (preloading, initial posture and abdominal antagonistic coactivation) and perturbation magnitudes. Using a trunk kinematics-driven iterative finite element (FE) model, temporal profiles of measured kinematics and external load along with subjects' weights were prescribed to predict thoracolumbar muscle forces/latencies and spinal loads for twelve healthy subjects when tested in six conditions during pre- and post-perturbation periods. Results demonstrated that preloading the trunk significantly (i.e., $p< 0.05$) increased pre-perturbation back muscle forces but significantly decreased post-perturbation peak muscle active forces and muscle latencies. Initial trunk flexion significantly increased muscle active and passive forces before the perturbation and their peak values after the perturbation, which in turn caused much larger spinal loads. Abdominal muscles antagonistic pre-activation did not alter the internal variables investigated in this study. Increase

in sudden applied load increased muscle reflex activities and spinal forces; a 50 N increase in sudden load (i.e., when comparing 50 N to 100 N) increased the L5-S1 compression force by 1327 N under 5 N preload and by 1374 N under 50 N preload. Overall, forces on the spine and hence risk of failure substantially increased in sudden forward loading when the magnitude of sudden load increased and when the trunk was initially in a flexed posture. In contrast, a higher initial preload diminished reflex latencies and compression forces.

Keywords: Trunk, Sudden forward load, Preactivation, Kinematics-driven model, Reflex, Compression, Shear, latency

4.2. Introduction

Segmental compression and shear forces vary along the spinal column and depend on the external loads (gravity, load in hands and inertia), posture, passive ligamentous stiffness and activation level of trunk muscles. Due to large reflex responses and resulting spinal loads, unexpected alterations in loading and/or posture are recognized as risk factors for low back injuries (Lavender et al., 1989). Too low or too high magnitudes of and/or undue delays in reflex (feedback) activation in response to sudden perturbations are expected in patients with disordered CNS, injury or low back pain that likely exacerbate loads on spine and associated risk (Cholewicki et al., 2005; Panjabi, 1992; Reeves et al., 2008). The trunk response to sudden loads depends not only on the external perturbation itself but also on the internal pre-perturbation conditions associated with initial posture and muscle activity. Intrinsic trunk muscle and ligamentous passive stiffness values increase respectively with activation level (Bergmark, 1989b; Brown and McGill, 2010; Cholewicki and McGill, 1995) and greater trunk rotations and compression (Andersen et al., 2004; Arjmand and Shirazi-Adl, 2006a; Cholewicki et al., 2000b; Lee et al., 2007; Lee et al., 2006; Moorhouse and Granata, 2005; Shirazi-Adl, 2006). In accordance, higher trunk stiffness and muscle agonist/antagonist activities diminish trunk displacements under perturbations (Granata et al., 2004; Krajcarski et al., 1999; Stokes et al., 2000). Moreover, lower EMG reflex response along with smaller displacements were observed at higher pre-perturbation muscle activity (Vera-Garcia et al., 2006). Similarly, lower reflex response to perturbations were recorded at larger flexion angles (Granata and Rogers, 2007) emphasizing the marked role of the passive stiffness (Arjmand and Shirazi-Adl, 2006a; Granata and Wilson, 2001; McGill et al., 1994; Zeinali-Davarani et al., 2008).

Experimental set ups in earlier perturbation investigations, however, varied from one study to another, which tends to complicate attempts to compare findings and draw general conclusions. Changes include sudden load duration and temporal variations, perturbation load magnitude/direction/position, loading versus unloading, subject initial posture, muscle preactivation and anticipatory conditions. In our recent in vivo study on the effect of alterations in perturbation load and pre-perturbation trunk conditions (initial preload, posture and coactivation) (Shahvarpour et al., 2014), it was found that unlike peak displacement and reflex muscle responses, peak trunk velocity and acceleration were sensitive to changes in both perturbation load and initial conditions. In corroboration with our earlier findings (Bazrgari et al., 2009a), these sensitivities emphasize the potential of kinematics-driven models in decoding the complex and confounding roles of various initial conditions on the transient post-perturbation response of the human trunk. This also concurs with the fact that kinematics (velocity/acceleration profiles) and kinetics (external loads, body weight) that are used as input data in such models are recorded at greater accuracy as compared to EMG data. Effectively under sudden forward loading perturbations, back muscle reflex responses as recorded with surface EMG have shown poor to moderate reliability (Santos et al., 2011).

Following an unexpected perturbation, trunk muscles are reflexively activated to prevent lumbar instability but only after a delay period called reflex latency (Hodges and Bui, 1996; Santos et al., 2011; Staude, 2001; Vera-Garcia et al., 2006). An increase in reflex latency (in presence of prior back injuries for example) impairs adequate control and stability of the trunk (Cholewicki et al., 2005; Hodges and Richardson, 1996; Radebold et al., 2000). Any muscle activation on the other hand translates to a mechanical force only after an additional delay period called electromechanical delay (EMD). The rate of muscle force development during voluntary contractions was found to have inverse relation with EMD (Thelen et al., 1994; van Dieen et al., 1991). In addition, larger trunk flexion angles were reported to prolong EMD (Marras, 1987). In an earlier study (Bazrgari et al., 2009a), the time of muscle force onset (i.e., latency including EMD) was predicted using feed-forward simulations in a kinematics-driven FE model (Bazrgari et al., 2009a).

In the current study, the recently recorded trunk kinematics and applied sudden external force profiles along with body weight of 12 asymptomatic subjects under six different conditions

(Shahvarpour et al., 2014) were used to drive a validated musculoskeletal nonlinear FE model of the trunk (Arjmand and Shirazi-Adl, 2005, 2006a; Bazrgari et al., 2009a; Bazrgari et al., 2008c). All 12 subjects at six different experimental conditions were simulated and statistical analyses performed to identify the effects of perturbation (sudden load magnitude) and initial conditions (preload magnitude, initial posture and antagonistic preactivity) on muscle reflex responses (magnitude and delay) and spinal loads (compression and shear forces at the L5-S1). It was hypothesized that the kinematics-driven FE model would (1) be sensitive to the effect of various pre-perturbation and sudden loading conditions and (2) demonstrate that the trunk muscle reflex activity and spinal loads drop in conditions associated with higher pre-perturbation intrinsic stiffness.

4.3. Methods

Our recent in vivo study dataset used in the current simulations are briefly described here (Shahvarpour et al., 2014). Twelve young male subjects (weight 73.0 ± 3.9 Kg and height 177.7 ± 3.0 cm) participated. Isometric maximum voluntary contraction (MVC) trials were carried out for normalization of EMG data. Superficial EMG signals of 12 muscles were recorded bilaterally at longissimus (LG, at the L1 level), iliocostalis (IC, at the L3), multifidus (MF, at the L5), rectus abdominus (RA), external oblique (EO) and internal oblique (IO). Subjects were semi-seated in a perturbation apparatus with the pelvis fixed while pre-perturbation and sudden loads were applied via a cable connected at the T8 level to a harness. A load cell along the cable measured the load applied whereas a potentiometer connected to the harness on the back measured the translation at the T8 level. Muscles EMG and trunk displacement were recorded with the sampling frequency of 1024 Hz.

Six initial conditions were considered (Table 4.1). In conditions 1 to 4 (C1-C4) the effects of changes in preload (5 and 50 N) and sudden load (50 and 100 N) were investigated. In C5, subjects flexed forward (10 cm anterior translation at the T8 level causing ~20° of trunk flexion) before perturbation. Finally in C6, subjects preactivated abdominal muscles, attempting to maintain the activity level of EO at 10% of MVC using a visual biofeedback while in the upright posture similar to C1-C4. Recorded EMG showed significantly greater pre-perturbation activity in abdominals in C6 when compared to C2 and C4 (Shahvarpour et al., 2014). Five trials were

performed for each condition. The perturbation force was applied suddenly and randomly during 5 seconds.

4.3.1. FE model studies

For the sake of simulations, one trial was chosen randomly for each subject and condition as statistical analysis rejected the effect of learning between trials. Simulation durations covered periods starting 256 ms pre-perturbations and 1 s after. Recorded trunk displacement in this period was resampled to 50 Hz. With the pelvis fixed, sagittal rotations at the T12 and lumbar levels for each subject at 6 conditions were estimated based on the measured T8 translations (Shahvarpour et al., 2014) and intersegmental rotation ratios (Bazrgari et al., 2009a). Velocity and acceleration profiles were calculated from displacements. Due partly to the stiffening effect of the ribcage and in accordance with earlier studies (Belytschko et al., 1973; Nussbaum and Chaffin, 1996; Schultz et al., 1973), the T1-S1 motions are limited in the model to those at the T12-S1 levels thereby neglecting relative rotations at the T1-T12 levels. Some thoracic rotations at T1-T12, albeit much smaller than lumbar rotations, have nevertheless been reported (Gercek et al., 2008; Morita et al., 2014).

Iteratively and driven by angular velocity profiles at different levels as well as external load and subject-specific gravity forces distributed along the spinal height, the trunk FE model was iteratively analyzed to estimate muscle recruitment patterns and spinal loads during pre- and post-perturbation periods at all 6 conditions for all 12 subjects. The FE model (Bazrgari et al., 2009a; Bazrgari et al., 2008c) consisted of 7 rigid bodies representing sacrum, L5 to L1 vertebrae and thorax-head-hands segments (Figure 4.1). Six nonlinear shear-deformable beam elements, with mechanical properties based on previous studies (Oxland et al., 1992; Shirazi-Adl, 2006; Yamamoto et al., 1989), accounted for passive stiffness of motion segments. Seven connector elements parallel to beams accounted for intersegmental damping (Kasra et al., 1992; Markolf, 1970). Distributed mass and inertial properties at each vertebral level were based on the literature (de Leva, 1996; Pearsall et al., 1996; Zatsiorsky and Seluyanov, 1983).

Trunk musculature was represented by 46 local lumbar and 10 global thoracic muscles (Figure 4.1). For global extensor muscles, nonlinear trajectories (wrapping of muscles plus contact forces) were taken into account (Arjmand et al., 2006); global muscles were constrained

not to approach the T12 to L5 vertebral centers more than 90% of their respective initial distances at the undeformed configuration. In case of wrappings, muscle forces remained identical in various segments assuming frictionless contact at wrapping points (Shirazi-Adl, 1989, 2006; Shirazi-Adl and Parnianpour, 2000).Wrapping contact forces were applied as external forces in subsequent iteration. The trunk FE model of each of 12 subjects was driven by its angular velocity profiles at different levels (based on the measured translation profile at the T8) as well as external load profile and gravity forces distributed along the spinal height. It was iteratively analyzed to estimate muscle recruitment patterns and spinal loads at all times during pre- and post-perturbation periods under 6 conditions. The objective function of the minimum sum of the cubed muscle stresses at each vertebral level was considered (Arjmand and Shirazi-Adl, 2006c). All unknown muscle forces were bound to be greater than the muscle passive components (calculated based on the ratio of the muscle instantaneous lengths to their resting lengths at the upright position and a tension-length relationship (Davis et al., 2003)). Besides, muscle forces were also constrained to be smaller than the sum of their passive components plus maximum active forces (0.6 MPa times physiological cross-sectional area, PCSA) (Winter, 2009). Abdominal preactivation in C6 was simulated by setting a nonzero lower bound (3-5% of maximum force) on abdominal muscle active forces based on EMG measurements. Preliminary investigations showed that abdominal muscles coactivity lasted for ~1 s after the perturbation and slowly diminished thereafter. Accordingly, the prescribed lower bound for the abdominal muscles activity decreased linearly in 1 s from the pre-perturbation level to 1%. Analyses were performed using ABAQUS/Standard 6.10-1 (Simulia Corp., Providence, RI) and Optimtool toolbox of MATLAB 7.12 (The Mathworks Inc., Natick, Massachusetts). Implicit integration with unconditionally stable Hilber-Hughes-Taylor integration operator was used in FE analyses. Automatic time increment option of ABAQUS was used with 2 ms set as upper limit. Mesh refinement convergence was verified by taking twice more deformable beam elements in the model that resulted in almost the same muscle forces.

To estimate latency (i.e., onset of applied sudden load to muscle force initiation post perturbation), two methods were used to detect muscle reflex initiation; (1) AGLR (approximated generalized likelihood-ratio) method that indicates the probability of abrupt variation of the signal by evaluating log-likelihood ratio of variation in sliding windows along the signal (Staude, 2001; Staude and Wolf, 1999). Predicted forces in global extensor muscles (ICPT and LGPT,

Figure 4.1) were resampled with frequency of 1024 Hz. (2) Forward dynamic simulations were performed (only for the subject 4 at six conditions) with the kinematics-driven model taking muscle forces constant at their pre-perturbation values. The time at which the predicted T8 translation diverged from the measured T8 translation was identified as the onset of reflex activation (Bazrgari et al., 2009a).

4.3.2. Statistical analyses

Computed required moments (to be supported by muscles inserted at each level only), net moments (to be supported by all muscles), latencies (evaluated as delays in muscle force initiation post-perturbation), peak muscle active/passive forces and spinal loads for all 12 subjects and 6 conditions were statistically analyzed using NCSS software (NCSS 8. NCSS, LLC. Kaysville, Utah, USA. www.ncss.com), using a significance level (alpha) of 0.05. One- and two-way analyses of variance (ANOVA), involving one (initial trunk flexion or EO antagonistic preactivation) or two (preload and sudden load) within-factors, were carried out to test the effect of preload (C1-2 vs C3-4), sudden load (C1 and C3 vs C2 and C4), trunk flexion (C1 and C3 vs C5) and abdominal preactivation (C2 and C4 vs C6) on trunk kinematics, back muscle reflex/latency and spinal loads.

4.4. Results

Active/passive muscle forces along with spinal loads and required/net moments were computed at all times for 12 subjects at six conditions (Table 4.1). Typical input kinematics and perturbation load along with normalized profiles of predicted muscle forces and recorded EMG are presented pre- and post-perturbations for the subject 4 in Figures 3.2 and 3.3.

4.4.1. Preload and sudden load

Although the interaction between the preload and sudden load conditions did not affect any biomechanical parameters, larger perturbation load (100 N vs 50 N) increased significantly all post-perturbation parameters; from moments to muscle forces and spinal loads (Table 4.2, Figure 4.4). Higher preload significantly decreased the post-perturbation peak of required moment at the T12 (RM-T12) from 71.4 ± 11.0 Nm to 67.3 ± 12.6 Nm under 50 N sudden load and from 99.5 ± 13.1 Nm to 94.0 ± 15.5 Nm under 100 N sudden load. Accordingly, post-

perturbation total and active forces in global thoracic muscles significantly decreased under larger preload (Table 4.2 and Figure 4.4e). However, changes in preload did not affect post-perturbation required moments at local lumbar levels (L1: $p = 0.592$, L2: $p = 0.750$, L3: $p = 0.624$, L4: $p = 0.666$ and L5: $p = 0.644$), net moment at the S1, active force in lumbar muscles, passive force of all muscles and spinal loads (Table 4.2 and Figure 4.4). Higher preload significantly diminished latencies (AGLR method) though no effect of sudden load was observed (Table 4.2, Figure 4.4a). Latencies (feed-forward method for subject 4) were 180 ms (C1), 220 ms (C2), 210 ms (C3) and 190 ms (C4).

4.4.2. Pre-perturbation trunk flexion

Comparisons were made here between three conditions (C1, C3 and C5) with the same sudden load of 50 N (Table 4.1). In C5 with initial flexed posture, passive and active muscle forces were significantly higher pre-perturbation (Table 4.2 and Figure 4.5b). Total passive moment at the S1 (sum of moments resisted by passive muscles and ligamentous spine) prior to perturbation was 69.3 Nm in C5, which was far exceeding 36.5 Nm in C1 and 37.1 Nm in C3. Greater post-perturbation muscle forces (both global and local except at the L5), moments and spinal loads were also computed in C5 compared to C1 and C3 (Table 4.2 and Figure 4.5). The peak compression at the L5-S1 when normalized to its pre-perturbation value significantly decreased in C5 with respect to C1 and C3. The normalized shear in C5 was however only significantly lower than that of C1. Smaller muscle force latencies (AGLR method) were found in C3, although the differences were not statistically significant (Table 4.2 and Figure 4.5a). Latencies (feed-forward method for the subject 4) were 180, 210 and 170 ms for conditions C1, C3 and C5, respectively.

4.4.3. Abdominal preactivation

Here three conditions (C2, C4 and C6) were compared under a 100 N sudden load (Table 4.1). Pre-perturbation active muscle forces in C6 were significantly greater than those at C2 but smaller than those at C4 (Table 4.2 and Figure 4.6b) with no changes in passive forces. Post-perturbation, peak of required moment at the T12, net moment, muscles passive/active forces along with spinal loads did not significantly alter in C6 compared to C2 and C4. Significantly shorter AGLR latencies were found in C4 versus C6, but no difference was

observed between C2 and C6 (Table 4.2 and Figure 4.6a). Latencies (feed-forward method for subject 4) were 220, 190 and 210 ms in C2, C4 and C6, respectively.

4.5. Discussion

Kinematics and external loading temporal profiles measured under forward sudden perturbation of the trunk along with subject weight were prescribed into our trunk kinematics-driven FE model. A number of biomechanical parameters including required moments, muscle latencies, muscle passive/active forces and spinal loads were computed. Alterations in these variables were investigated while accounting for a number of independent variables: preload (5 N vs 50 N), sudden load (50 N vs 100 N), initial trunk posture (upright standing vs flexed posture) and abdominal antagonistic preactivation (none vs 10% of MVC at EO). Results demonstrated that preloading the trunk significantly increased pre-perturbation back muscle active forces and dropped the post-perturbation peak of muscle active forces and latencies. As a consequence, spinal loads diminished (though not significant). Pre-perturbation trunk flexion significantly increased muscle active/passive forces and spinal loads during both pre- and post-perturbation phases. With the exception of an increase in pre-perturbation active muscle forces, abdominal preactivation did not alter the biomechanical parameters investigated in this study. Increase in sudden load from 50 N to 100 N substantially increased all post-perturbation parameters but had no effect on muscles force latency. Results confirmed the potential of our kinematics-driven model in decoding the prescribed velocity profiles under measured external/gravity loads to yield estimates of neuromuscular strategies and internal spinal loads that are comparable with available measurement data.

Comparison of normalized superficial EMG activity (Shahvarpour et al., 2014) versus normalized muscle forces computed in the current study (see Figure 4.3) indicates a satisfactory agreement in trends. The time lags between recorded and computed profiles indicate the electromechanical delay. Cross-correlation between measured EMG data and predicted forces for the subject 4 varied in the range of 0.89-0.96 for C1-C6 (Figure 4.3). Apart from valid concerns on the crosstalk in recorded superficial EMG activities and any muscle EMG-force relationship, the magnitude of computed activity levels could have altered had we assumed a maximum muscle stress value different from 0.6 MPa. Indeed, greater values would drop the predicted activity levels for all conditions and at all times.

4.5.1. Preload and sudden load

No changes in passive muscle forces prior to perturbations were anticipated due to identical initial upright posture. However, during the pre-perturbation period, larger preload generated larger active muscle forces that in corroboration with previous works increased the initial spinal intrinsic stiffness (Bergmark, 1989b; Brown and McGill, 2010; Cholewicki and McGill, 1995; El-Rich et al., 2004). The associated drop in post-perturbation peak at T12 required moment and peak active forces in extensor global muscles (Figure 4.4e), despite comparable post-perturbation trunk motions, indicates an enhanced margin of trunk stability with lower demand on muscles reflexive response which is also in agreement with earlier studies (Brown and McGill, 2009; Brown and McGill, 2008; Granata et al., 2004; Moorhouse and Granata, 2007). Spinal loads also decreased slightly at the higher preload; L5-S1 compression/shear forces dropped, respectively, from 5184/2181 N to 5046/2115 N albeit the increase in the preload from 5 N to 50 N (Figure 4.4f). Despite agreement in higher normalized activity in LG compared to IC, measured surface EMG did not corroborate the predicted lower reflex response at higher preload (Figure 4.4d). In contrast to the T12 level, required moment at lumbar levels as well as peak active forces in local muscles were not affected by changes in the preload. Muscle force latencies significantly dropped at higher preload (Figure 4.4a) whereas recorded EMGs showed no effect of preload on onset of EMG (Shahvarpour et al., 2014). The latency periods estimated by forward dynamic simulations in subject 4 were in the range of 180-220 ms which were greater than those calculated by AGLR method for individual muscles of the same subject 4 (LG: 137 ms (C4) to 196 ms (C2), IC: 137 ms (C4) to 202 ms (C2)). It is to be noted that the forward dynamic latency was obtained via computed kinematics while AGLR latency was obtained from estimated muscle forces. These values are in agreement with earlier estimations (Bazrgari et al., 2009a).

Predictions demonstrated the significant influence of sudden load magnitude on biomechanical variables. Expectedly, larger sudden load magnitude (100 N vs 50 N) increased active muscle forces at all levels (Figure 4.4e) in agreement with our recorded EMG Reflex-Peak (Figure 4.4d) and earlier findings (Granata et al., 2004; Krajcarski et al., 1999). In addition, larger trunk displacements under larger sudden load (Shahvarpour et al., 2014) increased muscle passive forces (Figure 4.4c). Under 100 N sudden load, many local lumbar muscles were

activated at or near their maximum levels. Altogether, substantially larger spinal loads were estimated suggesting higher risk of back injury in presence of larger sudden loads (Lavender et al., 1989; Marras et al., 1987). It is interesting to note that a mere 50 N increase in sudden load (from 50 N to 100 N) substantially increased the L5-S1 compression force by 1327 N under 5 N preload and 1374 N under 50 N preload. In other words, every 1 N increase in the sudden load magnitude on top of an existing 50 N had on average a 27-fold magnification factor on the resulting spine compression. Earlier studies of lifting tasks reported lumbar compression forces exceeding 6 kN (Fathallah et al., 1999; Jager and Luttmann, 1991) and shear forces up to 1.8 kN (Arjmand et al., 2011; Fathallah et al., 1999; Granata and Marras, 1995).

4.5.2. Pre-perturbation trunk flexion

Larger muscle passive forces prior to perturbation was due to greater muscle elongation in the flexed posture. This along with greater pre-perturbation active forces (Figure 4.5b) augmented intrinsic spinal stiffness (Arjmand and Shirazi-Adl, 2006a; Granata and Rogers, 2007; Granata and Wilson, 2001; McGill et al., 1994). Despite larger intrinsic stiffness, pre- and post-perturbation, greater muscle reflex activities (in agreement with EMG measurements, Figure 4.5d) were computed that are due to larger gravity moments associated with the increase in prescribed trunk forward displacement. In accordance with larger moments and muscle forces in C5, spinal compression and shear forces also increased (Figure 4.5f). In this case the L5-S1 compression force of 3857 N in C1 with 5 N preload dropped by 186 N to 3671 N as the preload increased to 50 N in C3 but substantially increased by 1432 N to 5289 N in presence of pre-perturbation flexed posture. Lower ratio of peak compression to pre-perturbation compression in C5 when compared to C1 and C3 suggests a smaller relative increase in post-perturbation compression in C5. Similar to an increase in the magnitude of the sudden load, the initial flexed posture should hence be considered as a risk factor under sudden forward loading conditions. Initial flexed posture did not influence muscle force latencies (Figure 4.5a).

4.5.3. Abdominal preactivation

Although, based on the predictions (Figure 4.6) and EMG measurements (Shahvarpour et al., 2014), all back and abdominal muscles were activated prior to perturbation, no changes in the trunk movement and muscle response were found post-perturbation. This agrees with our earlier findings of no effect of antagonistic pre-activation on trunk displacement, velocity and

acceleration (Shahvarpour et al., 2014). The model did not predict changes in muscle active forces (Figure 4.6e) in contrast to the measurement of higher reflexive response in IC and MF muscles (Shahvarpour et al., 2014). Despite differences in pre-perturbation muscle forces (Figure 4.6b), no differences in spinal loads were found between C2, C4 and C6 (Figure 4.6f). Antagonistic preactivation did not significantly influence muscle force latencies (Figure 4.6a).

In summary, using a detailed trunk FE model some biomechanical parameters including moments, muscle passive/active forces and latencies as well as spinal loads were predicted while varying preload level, sudden load magnitude, initial trunk posture and abdominal antagonistic preactivation. Results demonstrated that preloading the trunk increased back muscle active forces prior to the perturbation. In contrast to EMG data, model-predicted forces however showed a decrease in both force and latency of muscles after perturbation. Initial flexion of the trunk increased muscle active/passive forces and spinal loads pre- and post-perturbations. Abdominal antagonistic preactivation did not affect the biomechanical variables. Results highlighted the much greater spinal loads and hence risk of injury as sudden applied load increased and in presence of initial forward flexed posture. In contrast, a higher initial preload is advantageous in diminishing latencies and compression forces.

Conflict of interest statement

None to declare.

Acknowledgements

This study has been supported by grants from the Institut de recherche Robert-Sauvé en santé et en sécurité du travail (IRSST-Québec) and the Natural Sciences and Engineering Research Council of Canada (NCERC-Canada). Authors thank Dr. André Plamondon and Mr. Hakim Mecheri for their advice, as well as Sophie Bellefeuille and Cynthia Appleby for their technical assistance during tests at the IRSST laboratory.

4.6. References

Andersen, T.B., Essendrop, M., Schibye, B., 2004. Movement of the upper body and muscle activity patterns following a rapidly applied load: the influence of pre-load alterations. European Journal of Applied Physiology 91, 488-492.

Arjmand, N., Plamondon, A., Shirazi-Adl, A., Larivière, C., Parnianpour, M., 2011. Predictive equations to stimate spinal loads in symmetric lifting tasks. Journal of Biomechanics 44, 84-91.

Arjmand, N., Shirazi-Adl, A., 2005. Biomechanics of changes in lumbar posture in static Lifting. Spine 30, 2637-2648.

Arjmand, N., Shirazi-Adl, A., 2006a. Model and in vivo studies on human trunk load partitioning and stability in isometric forward flexions. Journal of Biomechanics 39, 510-521.

Arjmand, N., Shirazi-Adl, A., 2006b. Sensitivity of kinematics-based model predictions to optimization criteria in static lifting tasks. Medical Engineering and Physics 28, 504-514.

Arjmand, N., Shirazi-Adl, A., Bazrgari, B., 2006. Wrapping of trunk thoracic extensor muscles influences muscle forces and spinal loads in lifting tasks. Clinical Biomechanics 21, 668-675.

Bazrgari, B., Shirazi-Adl, A., Lariviere, C., 2009. Trunk response analysis under sudden forward perturbations using a kinematics-driven model. Journal of Biomechanics 42, 1193-1200.

Bazrgari, B., Shirazi-Adl, A., Trottier, M., Mathieu, P., 2008. Computation of trunk equilibrium and stability in free flexion-extension movements at different velocities. Journal of Biomechanics 41, 412-421.

Belytschko, T.B., Andriacchi, T.P., Schultz, A.B., Galante, J.O., 1973. Analog studies of forces in the human spine: computational techniques. Journal of Biomechanics 6, 361-371.

Bergmark, A., 1989. Stability of the lumbar spine, A study in mechanical engineering. Acta Orthopaedica Scandinavica Supplementum 230, 1-54.

Brown, S.H., McGill, S.M., 2009. The intrinsic stiffness of the in vivo lumbar spine in response to quick releases: implications for reflexive requirements. Journal of Electromyography and Kinesiology 19, 727-736.

Brown, S.H.M., McGill, S.M., 2008. How the inherent stiffness of the in vivo human trunk varies with changing magnitudes of muscular activation. Clinical Biomechanics 23, 15-22.

Brown, S.H.M., McGill, S.M., 2010. The releationship between trunk muscle activation and trunk stiffness: examining a non-constant stiffness gain. Comput. Methods Biomech. Biomed. Eng. 13, 829-835.

Cholewicki, J., McGill, S.M., 1995. Relationship between muscle force and stiffness in the whole mammalian muscle: A simulation study Journal of Biomechanical Engineering 117, 339-342.

Cholewicki, J., Silfies, S.P., Shah, R.A., Greene, H.S., Reeves, N.P., Alvi, K., Goldberg, B., 2005. Delayed trunk muscle reflex responses increase the risk of low back injuries. Spine 30, 2614-2620.

Cholewicki, J., Simons, A.P.D., Radebold, A., 2000. Effects of external trunk loads on lumbar spine stability. Journal of Biomechanics 33, 1377-1385.

Davis, J., Kaufman, K.R., Lieber, R.L., 2003. Correlation between active and passive isometric force and intramuscular pressure in the issolated rabbit tibialis anterior muscle. Journal of Biomechanics 36, 505-512.

de Leva, P., 1996. Adustments to zatsiorsky-seluyanov's segment inertia parameters. Journal of Biomechanics 29, 1223-1230.

El-Rich, M., Shirazi-Adl, A., Arjmand, N., 2004. Muscle activity, internal loads, and stability of the human spine in standing postures: combined model and In vivo studies. Spine 29, 2633-2642.

Fathallah, F.A., Marras, W.S., Parnianpour, M., 1999. Regression models for predicting peak and continuous three-dimensional spinal loads during symmetric and asymmetric lifting tasks. Human Factors 41, 373-388.

Gercek, E., Hartmann, F., Kuhn, S., Dereif, J., Rommens, P.M., Ruding, L, 2008. Dynamic angular three-dimensional measurement of multisegmental thoracolumbar motion in vivo. Spine 33, 2326-2333.

Granata, K.P., Marras, W.S., 1995. An Emg-Assisted model of trunk loading during free-dynamic lifting. Journal of Biomechanics 28, 1309-1317.

Granata, K.P., Rogers, E.L., 2007. Torso flexion modulates stiffness and reflex response. Journal of Electromyography and Kinesiology 17, 384-392.

Granata, K.P., Slota, G.P., Bennett, B.C., 2004. Paraspinal muscle reflex dynamics. Journal of Biomechanics 37, 241-247.

Granata, K.P., Wilson, S.E., 2001. Trunk posture and spinal stability. Clinical Biomechanics 16, 650-659.

Hodges, P.W., Bui, B.H., 1996. A comparison of computer-based methods for the determination of onset of muscle contraction using electromyography. Electroencephalography and clinical Neurophysiology 101, 511-519.

Hodges, P.W., Richardson, C.A., 1996. Inefficient muscular stabilization of the lumbar spine associated with low back pain - A motor control evaluation of transversus abdominis. Spine 21, 2640-2650.

Jager, M., Luttmann, A., 1991. Compressive strength of lumbar spine elements related to age, gender and other influencing factors, in: Andersen, P.A., Hobart, D.J. (Eds.), Electromyographical Kinesiology. Elsevier Science, Amsterdam, pp. 291-294.

Kasra, M., Shirazi-Adl, A., Drouin, G., 1992. Dynamics of human intervertebral joints. Experimental and finite-element investigations. Spine 17.

Krajcarski, S.R., Potvin, J.R., Chiang, J., 1999. The in vivo dynamic response of the spine to perturbations causing rapid flexion: effects of pre-load and step input magnitude. Clinical Biomechanics 14, 54-62.

Lavender, S.A., Mirka, G.A., Schoenmarklin, R.W., Sommerich, C.M., Sudhakar, L.R., Marras, W.S., 1989. The effects of preview and task symmetry on trunk muscle response to sudden loading. Human Factors 31, 101-115.

Lee, P.J., Granata, K.P., Moorhouse, K.M., 2007. Active trunk stiffness during voluntary isometric flexion and extension exertions. Human Factors 49, 100-109.

Lee, P.J., Rogers, E.L., Granata, K.P., 2006. Active trunk stiffness increases with co-contraction. Journal of Electromyography and Kinesiology 16, 51-57.

Markolf, K.L., Year Stiffness and damping characteristics of thoracolumbar spine. In Proceeding of Workshop on Bioengineering Approaches to Problems of the Spine. Division of Research Grants. NIH, Bethesda.

Marras, W.S., 1987. Trunk motion during lifting: temporal relations among loading factors. International Journal of Industrial Ergonomics 1, 159-167.

Marras, W.S., Rangarajulu, S.L., Lavender, S.A., 1987. Trunk loading and expectation. Ergonomics 30, 551-562.

McGill, S.M., Marras, W.S., 1995. An Emg-Assisted model of trunk loading during free-dynamic lifting. Journal of Biomechanics 28, 1309-1317.

McGill, S.M., Seguin, J., Bennett, G., 1994. Passive stiffness of the lumbar torso in flexion, extension, lateral bending and axial rotation, Efect of belt wearing and breath holding. Spine 19, 696-704.

Moorhouse, K.M., Granata, K.P., 2005. Trunk stiffness and dynamics during active exertion extensions. Journal of Biomechanics 38, 2000-2007.

Moorhouse, K.M., Granata, K.P., 2007. Role of reflex dynamics in spinal stability: Intrinsic muscle stiffness alone is insufficient for stability. Journal of Biomechanics 40, 1058-1056.

Morita, D., Yukawa, Y., Nakashima, H., Ito, K., Yoshida, G., Kanbara, S., Iwase, T., Kato, F., 2014. Range of motion of thoracic spine in sagittal plane. European Spine Journal 23, 673-678.

Nussbaum, M.A., Chaffin, D.B., 1996. Development and evaluation of a scalable and deformable geometric model of the human torso. Clinical Biomechanics 11, 25-34.

Oxland, T., Lin, R.M., Panjabi, M.M., 1992. Three-dimensional mechanical properties of the thoracolumbar junction Journal of Orthopaedic Research 10, 573-580.

Panjabi, M.M., 1992. The stabilizing system of the spine. Part I. Function, dysfunction, adaptation, and enhancement. Journal of Spinal Disorders 5, 383-389.

Pearsall, D.J., Reid, J.G., Livingstone, L.A., 1996. Segmental inertial parameters of the human trunk as determined from computed tomography. Annals of Biomedical Engineering 24, 198-210.

Radebold, A., Cholewicki, J., Panjabi, M.M., Patel, T.C., 2000. Muscle response pattern to sudden trunk loading in healthy individuals and in patients with chronic low back pain. Spine 25, 947-954.

Reeves, N.P., Cholewicki, J., Milner, T., Lee, A.S., 2008. Trunk antagonistic co-activation is associated with impaired neuromuscular performance. Experimental Brain Research 188, 457-463.

Santos, B.R., Larivière, C., Belisle, A., McFadden, D., Plamondon, A., Imbeau, D., 2011. Sudden loading perturbation to determine the reflex response of different back muscles: A reliability study. Muscle & nerve 43, 348-359.

Schultz, A.B., Belytschko, T.B., Andriacchi, T.P., Galante, J.O., 1973. Analog studies of forces in the human spine: mechanical properties and motion segment. Journal of Biomechanics 6, 373-383.

Shahvarpour, A., Shirazi-Adl, A., Mecheri, H., Larivière, C., 2014. Trunk response to sudden forward perturbation - Effects of preload and sudden load magnitudes, posture and abdominal muscle preactivation. Journal of Electromyography and Kinesiology Under review.

Shirazi-Adl, A., 1989. Nonlinear finite element analysis of wrapping uniaxial elements. Computers & structures 32, 119-123.

Shirazi-Adl, A., 2006. Analysis of large compression loads on lumbar spine in flexion and in torsion using a novel wrapping element. Journal of Biomechanics 39, 267-275.

Shirazi-Adl, A., Parnianpour, M., 2000. Load-bearing and stress analysis of the human spine under a novel wrapping compression loading. Clinical Biomechanics 15, 718-725.

Staude, G.H., 2001. Precise onset detection of human motor responses using a whitening filter and the log-likelihood-ration test. IEEE Transactions on Biomedical Engineering 48, 1292-1305.

Staude, G.H., Wolf, W., 1999. Objective motor response onset detection in surface myoelectric signals. Medical Engineering and Physics 21, 449-467.

Stokes, I.A.F., Gardner-Morse, M.G., Henry, S.M., Badger, G.J., 2000. Decrease in trunk muscular response to perturbation with preactivation of lumbar spinal musculature. Spine 25, 1957-1964.

Thelen, D.G., Schultz, A.B., Ashton-Miller, J.A., 1994. Quentitative interpretation of lumbar muscle myoelectric signals during rapid cyclic attmpted trunk flexions and extensions. Journal of Biomechanics 27, 157-167.

van Dieen, J.H., Thissen, C.E.A.M., Ven, v.d., Toussaint, H.M., 1991. The electro-mechanical delay of the erector spinae muscle: influence of rate of force development, fatigue and electrode location. European Journal of Applied Physiology 63, 216-222.

Vera-Garcia, F.J., Brown, S.H., Gray, J.R., McGill, S.M., 2006. Effects of different levels of torso coactivation on trunk muscular and kinematic responses to posteriorly applied sudden loads. Clinical Biomechanics 21, 443-455.

Winter, D.A., 2009. Biomechanics and motor control of human movements, 4th ed. John wiley & Sons, Inc.

Yamamoto, I., Panjabi, M.M., Crisco, T., Oxland, T., 1989. Three-dimensional movements of the whole lumbar spine and Lumbosacral joint. Spine 14, 1256-1260.

Zatsiorsky, V.M., Seluyanov, V.N., 1983. The mass and inertia charachteristics of the main segments of the human body Biomechanics. Champaign: Human Kinetics Publishers, pp. 1152-1159.

Zeinali-Davarani, S., Hemami, H., Barin, K., Shirazi-Adl, A., Parnianpour, M., 2008. Dynamic stability of spine using stability-based optimization and muscle spindle reflex. IEEE Transactions on Neural Systems and Rehabilitation Engineering 16, 106-118.

Table 4.1 Independent parameters in the six experimental conditions considered in this work

Condition	Pre Load (N)	Sudden Load (N)	Initial posture	EO preactivation
C1	5	50	Upright	-
C2	5	100	Upright	-
C3	50	50	Upright	-
C4	50	100	Upright	-
C5	5	50	10 cm Anterior Translation	-
C6	5	100	Upright	10%

Table 4.2 Statistical results (ANOVA p-values) for the effects of preload, sudden load, pre-perturbation posture and abdominal preactivation on post-perturbation kinetic variables*

	Preload	Sudden load	Preload * sudden load	Pre-perturbation posture		Abdominal preactivation	
				C1 vs C5	C3 vs C5	C2 vs C6	C4 vs C6
RM-T12	**.045**	**<.001**	.707	**.001**	**.001**	.991	.363
Net moment at S1	.382	**<.001**	.973	**<.001**	**<.001**	.908	.502
LGPT active mean (pre-perturbation)	**<.001**	.266	.508	**<.001**	**<.001**	**.001**	**<.001**
LGPT/LGPL active peak (post-perturbation)	**.030**/.438	**<.001/<.001**	.623/.898	**.001/<.001**	**.001/<.001**	.841/.338	.229/-
ICPT/ICPL active peak (post-perturbation)	**.030**/0.194	**<.001/<.001**	.623/.470	**.001/<.001**	**.001 /<.001**	.684	-
LGPT passive mean (pre-perturbation)	.379	.327	.322	**.002**	**.002**	.256	.351
LGPT passive peak (post-perturbation)	.908	**<.001**	.490	**.008**	**.007**	.416	.173
Compression force at L5-S1	.205	**<.001**	.737	**<.001**	**<.001**	.963	.566
Shear at L5-S1	.310	**<.001**	.791	**.001**	**.001**	.897	.559
LGPT/LGPL latency	**<.001/<.001**	.459/.170	.548/.860	.862/**.041**	.206/.108	.270/.711	**.028/.003**
ICPT/ICPL latency	**<.001/.006**	.581/.384	.278/.990	.196/**<.001**	.186/**<.001**	.141/.595	**.002/.008**

*Statistics were carried out using C1 to C4 experimental conditions for the effect of preload and sudden load, C1, C3 and C5 for the effect of initial posture and C2, C4 and C6 for the effect abdominal preactivation; statistically significant differences ($p < 0.05$) are identified in bold characters. Latencies were obtained by AGLR method. RM-T12 refers to the required moment at the T12 level to be supported by global muscles, LGPT is the global thoracic LG (at the T12) and ICPT is the global thoracic IC (at the T12), LGPL here is for LG at the lumbar L1 level while ICPL here is the mean of the lumbar IC at the L1, L2 and L3 levels.

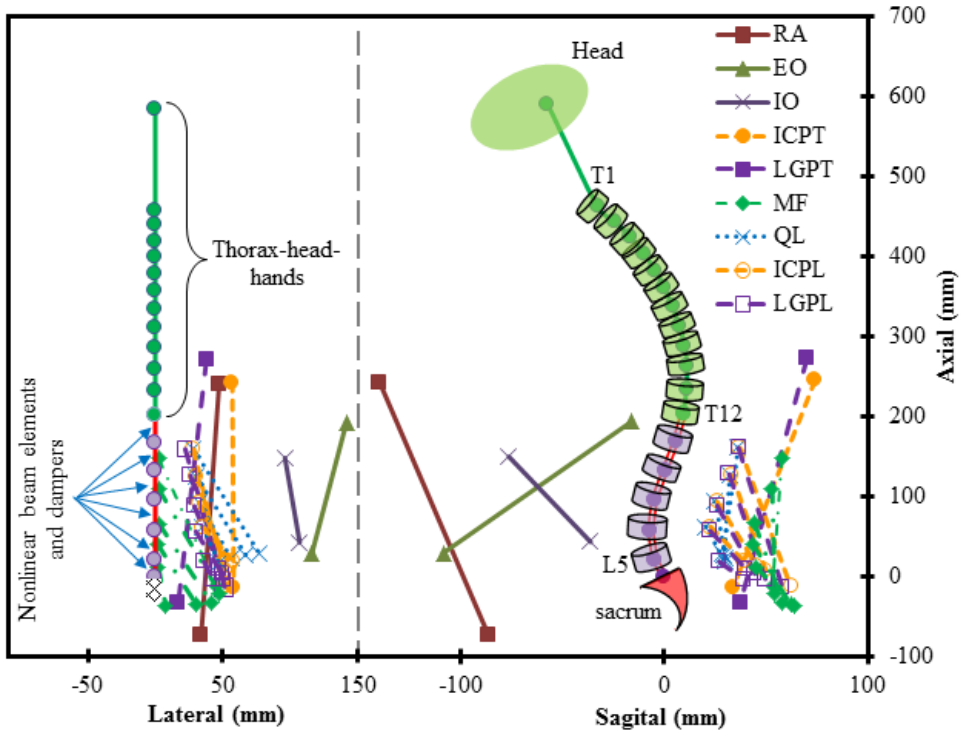

Figure 4.1 Schematic view of the trunk FE model (presented in upright posture with different horizontal and vertical scales) illustrating vertebral column as well as local and global musculature in the sagittal and lateral planes, RA: rectus abdominus, EO: external oblique, IO: internal oblique, ICPT: iliocostalis lumborum pars thoracic, LGPT: longissimus thoracis pars thoracic, MF: multifidus, QL: quadratus lumborum, ICPL: iliocostalis lumborum pars lumborum, LGPL: longissimus thoracis pars lumborum.

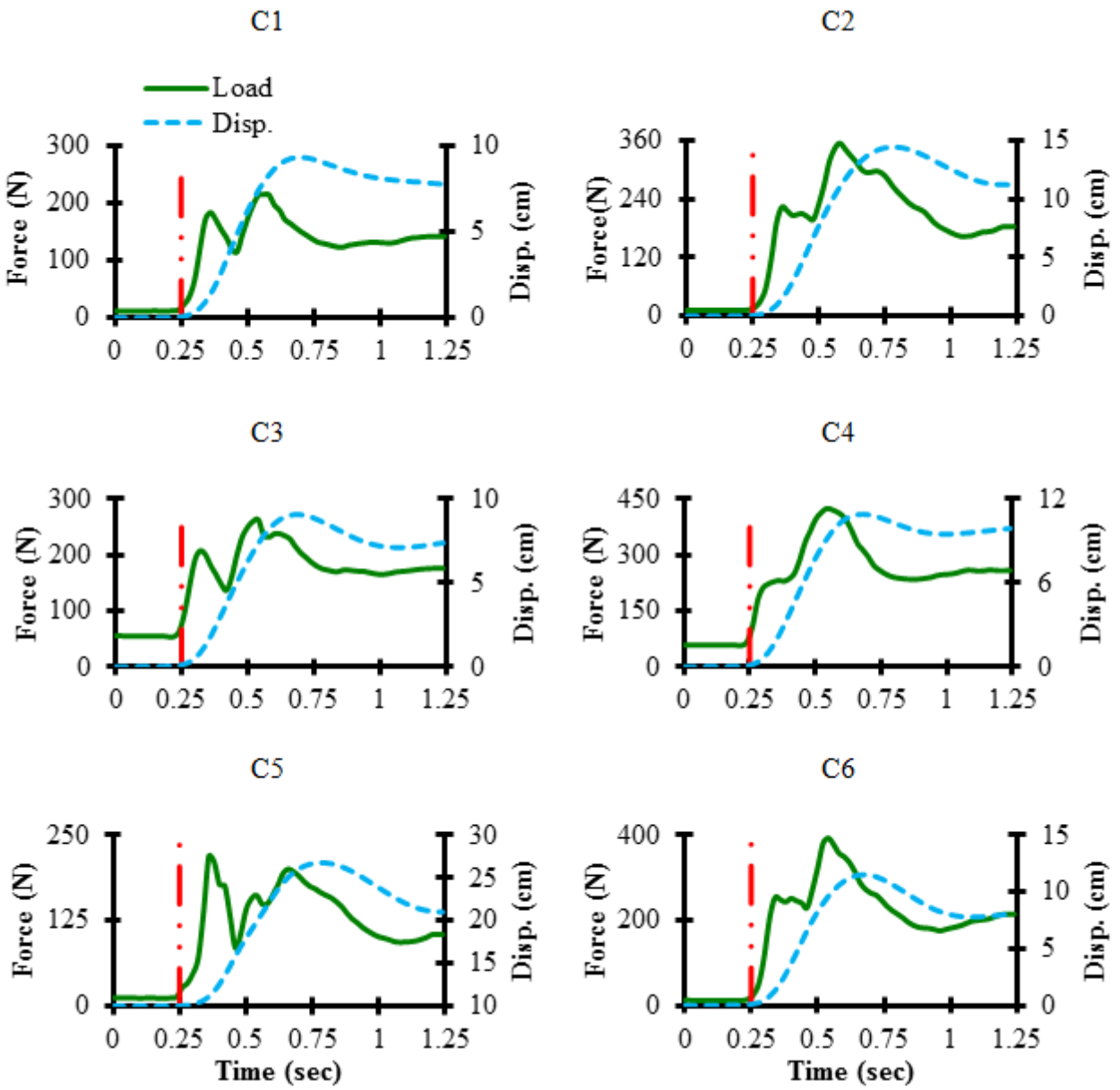

Figure 4.2 Measured (and prescribed in the FE model) perturbation load and displacement of the trunk relative to the upright posture for 6 conditions performed by the subject 4. Perturbation onset is identified by a vertical red line.

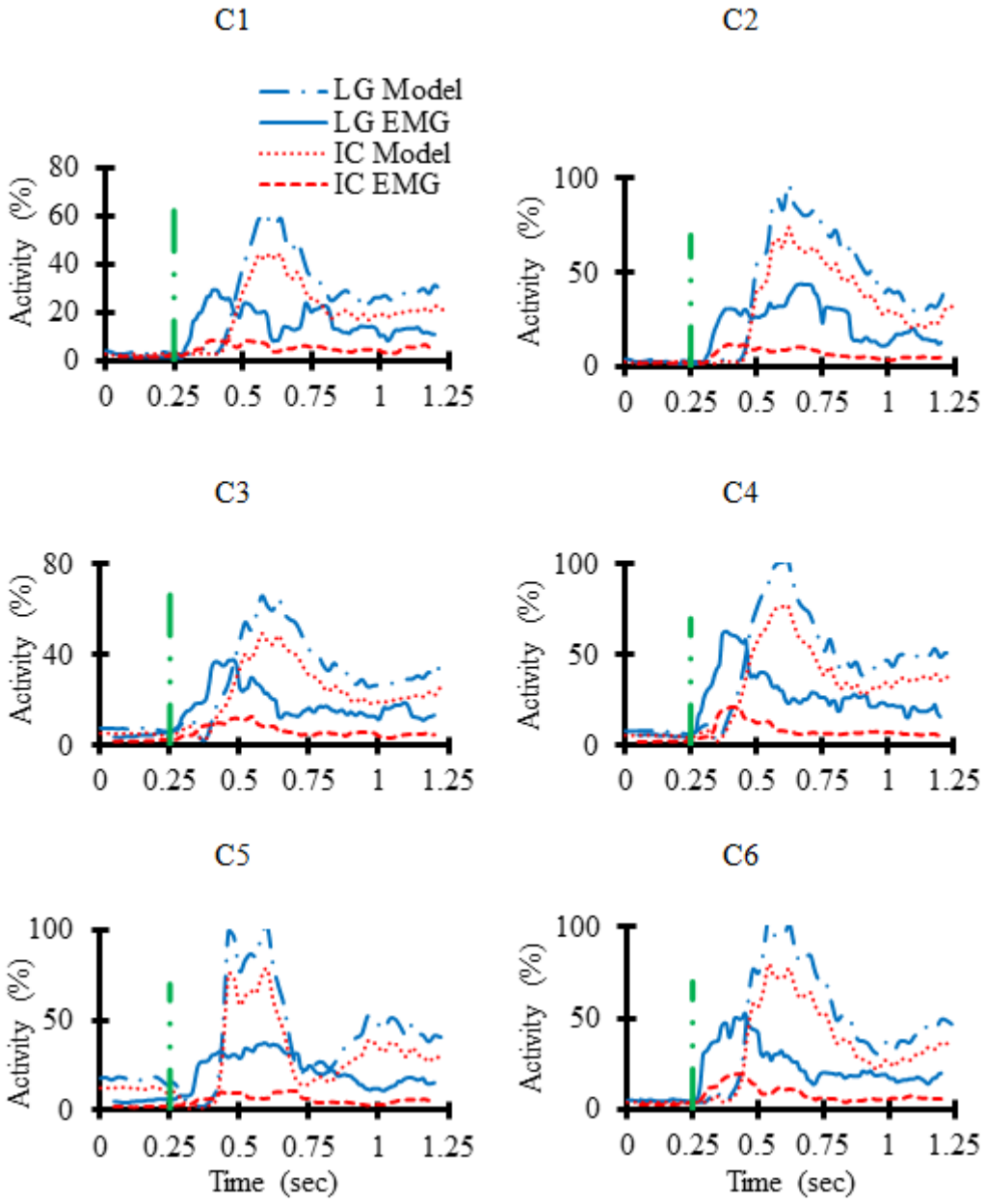

Figure 4.3 Normalized EMG (Shahvarpour et al., 2014) and model-predicted forces (normalized to maximum active forces of 0.6 MPa × PCSA) before and after the perturbation for 6 conditions performed by the subject 4. Perturbation onset is identified by a vertical green line.

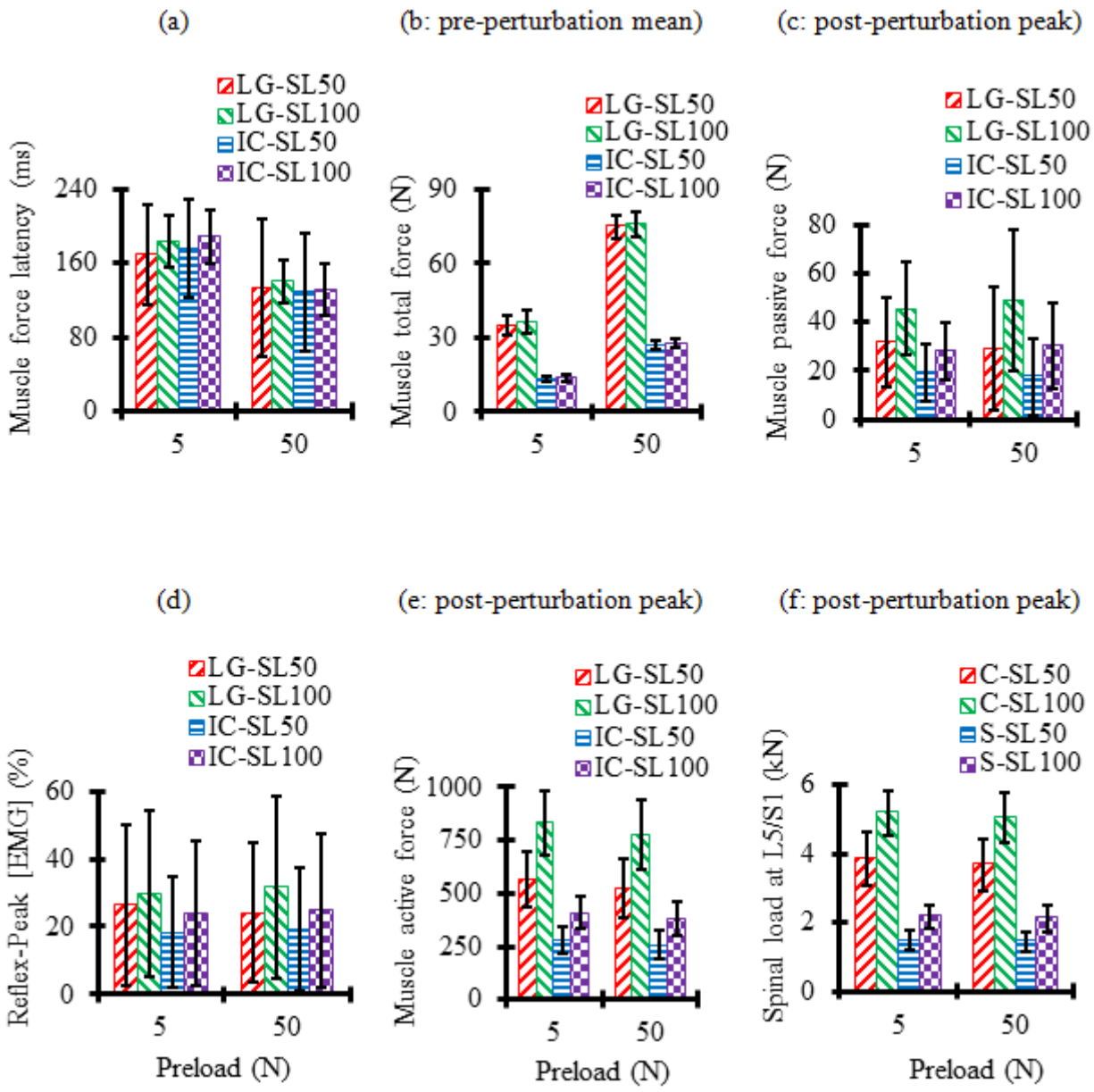

Figure 4.4 Biomechanical variables pre- and post-perturbation along with EMG reflexive response (Shahvarpour et al., 2014) presented for two preloads (5 N and 50 N) and two sudden loads (50 N and 100 N) in conditions C1-4. All biomechanical parameters were averaged over 12 subjects while Reflex-Peak [EMG] was averaged over left and right sides, 5 trials and 12 subjects. Latencies were obtained by AGLR method. Error bars represent standard deviation. (C: compression, S: shear in anterior direction, SL: sudden load, LG and IC in predictions refer to global muscles inserted into the T12).

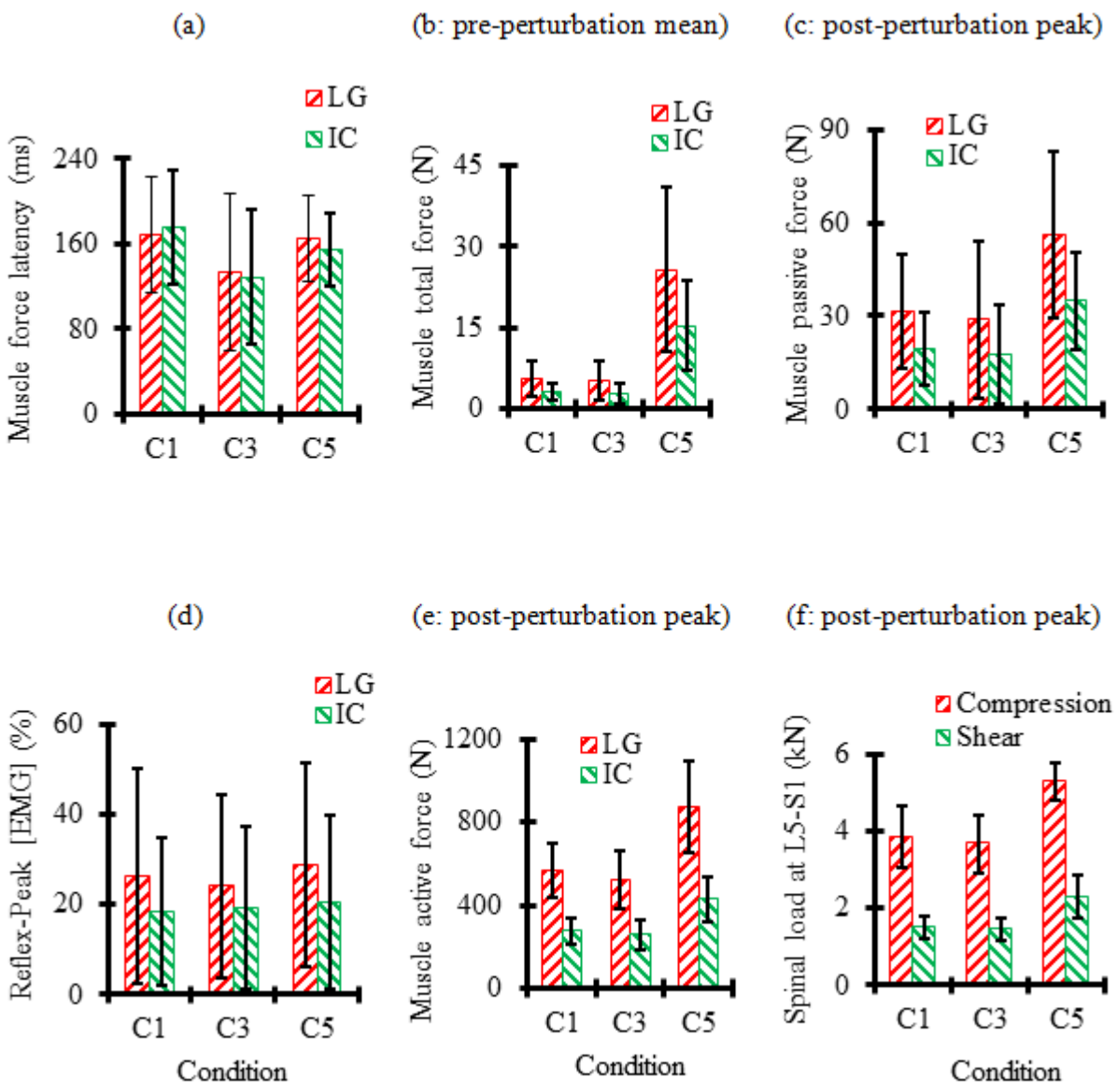

Figure 4.5 Biomechanical variables before and after perturbation along with EMG reflexive response (Shahvarpour et al., 2014) presented for three conditions with 50 N sudden load: C1 (preload = 5 N), C3 (preload = 50 N) and C5 (initial trunk forward flexion). All biomechanical parameters were averaged over 12 subjects while Reflex-Peak [EMG] was averaged over left and right sides, 5 trials and 12 subjects. Latencies were obtained by AGLR method. Error bars represent standard deviation (LG and IC in predictions refer to global muscles inserted into the T12).

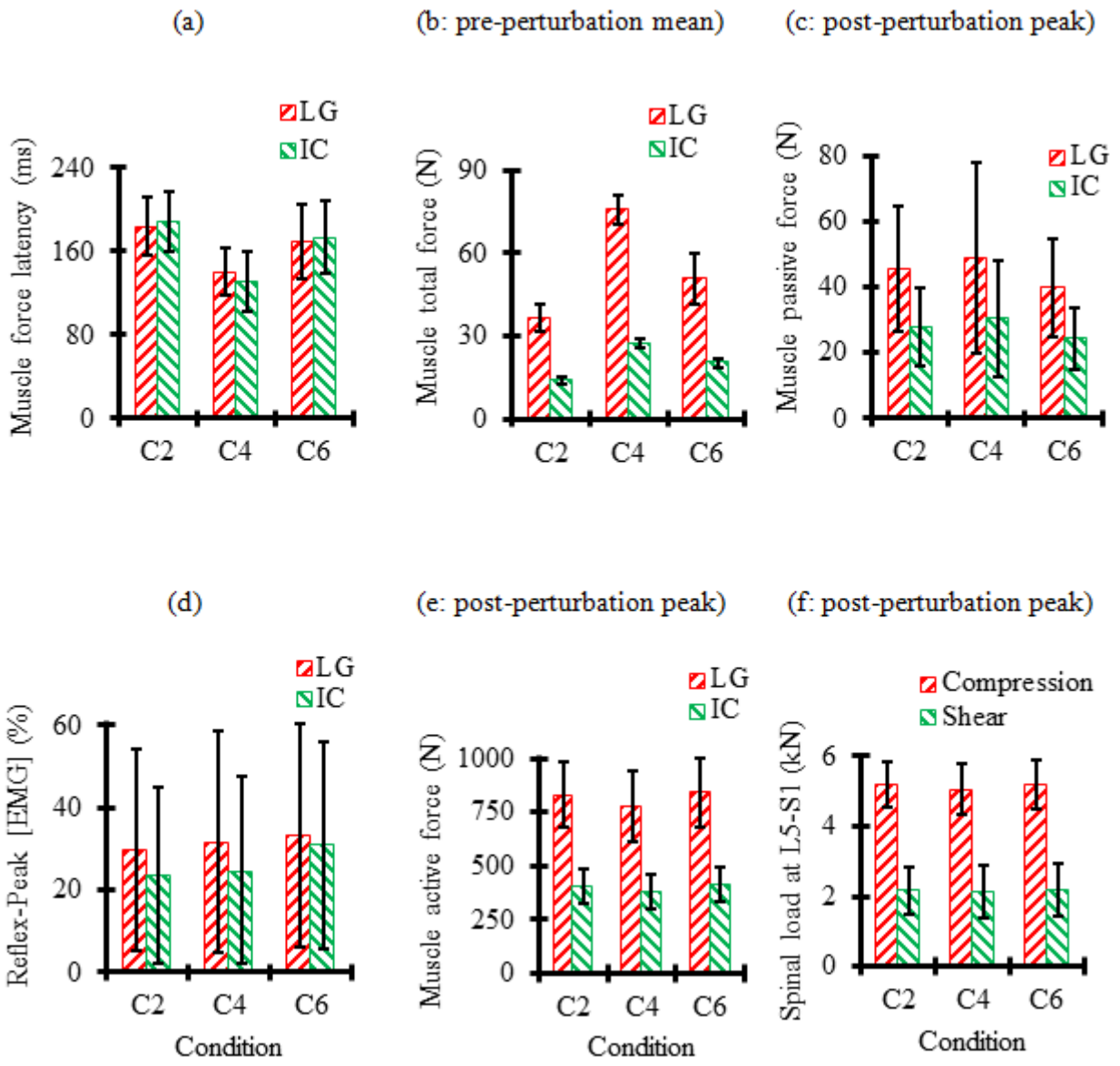

Figure 4.6 Biomechanical variables before and after perturbation along with EMG reflexive response (Shahvarpour et al., 2014) presented for three conditions with 100 N sudden load: C2 (preload = 5 N), C4 (preload = 50 N) and C6 (abdominal co-activation). All biomechanical parameters were averaged over 12 subjects while Reflex-Peak [EMG] was averaged over left and right sides, 5 trials and 12 subjects. Latencies were obtained by AGLR method. Error bars represent standard deviation (LG and IC in predictions refer to global muscles inserted into the T12).

CHAPTER 5 ARTICLE 3: COMPUTATION OF TRUNK STABILITY IN FORWARD PERTURBATIONS – EFFECTS OF PRELOAD, PERTURBATION LOAD, INITIAL FLEXION AND ABDOMINAL PREACTIVATION

Ali Shahvarpour [a], Aboulfazl Shirazi-Adl [a], Christian Larivière [b], Babak Bazrgari [c]

[a] Division of Applied Mechanics, Department of Mechanical Engineering, École Polytechnique, Montreal, Quebec, Canada

[b] Occupational Health and Safety Research Institute Robert-Sauvé, Montreal, Quebec, Canada

[c] Department of Biomedical Engineering, University of Kentucky, Lexington, KY, USA

Published in
Journal of Biomechanics (2015)

5.1. Abstract

Spine stability demand influences active-passive coordination of the trunk response, especially during sudden perturbations. The objective of this study was to look at the role of passive, stationary active and reflexive subsystems on spinal stability. Spine stability was evaluated here during pre- and post-perturbation phases by computing the minimum (i.e., critical) muscle stiffness coefficient required to maintain stability. The effects of pre-perturbation conditions (preloading, initial posture and abdominal antagonistic coactivation) as well as perturbation magnitude were studied. Results revealed that higher preload, initially flexed trunk posture and abdominal pre-activation enhanced pre-perturbation stiffness and stability. In contrast to the preload, however, larger sudden load, initial flexion and abdominal preactivation significantly increased post-perturbation stability margin. As a result, much lower critical muscle stiffness coefficient was required post-perturbation. Compared to the pre-perturbation phase, the trunk stiffness and stability substantially increased post-perturbation demanding thus a much lower critical muscle stiffness coefficient. Overall, these findings highlight the crucial role of the ligamentous spine and muscles (in both passive and active states) in augmenting the trunk

stiffness and hence stability during pre- and post-perturbation phases; a role much evident in the presence of initial trunk flexion.

Keywords: Trunk, Sudden forward load, Stability, Stiffness, Kinematics-driven model, Preload, Flexion, Co-activation

5.2. Introduction

Spinal instability manifests itself via excessive flexibility causing injuries and pain (Knutsson, 1944; White and Panjabi, 1990). Ligamentous thoracolumbar and lumbar spines devoid of musculature exhibit global instability (i.e., buckling) under compression forces as small as 20 N (Lucas and Bresler, 1960) and 88 N (Crisco, 1989), respectively. Much larger forces of about 5 kN have however been estimated in lifting, fast forward flexion and trunk strength exertion tasks (Bazrgari et al., 2008c; El Ouaaid et al., 2013; Fathallah et al., 1999) which underline the crucial role of the musculature and neural activity. Three distinct subsystems contribute to spinal stability (Panjabi, 1992, 2003); (1) ligamentous spine and musculature via their passive contributions; (2) musculature via its feed-forward activity and (3) the neuromuscular system via its feed-back reflexive response. Injury or dysfunction in these subsystems deteriorates stability and increases risk of injury and pain (Reeves et al., 2009).

Muscle stiffness increases at higher activation levels (Brown and McGill, 2005) as the number of cross-bridges increases (Cholewicki and McGill, 1995; Ma and Zahalak, 1985). Larger exertions in paraspinal muscles improve trunk stability under perturbation (Brown and McGill, 2009; Brown and McGill, 2008; Granata et al., 2004; Krajcarski et al., 1999; Moorhouse and Granata, 2007). Passive trunk stiffness, which is relatively small in the neighborhood of neutral upright posture, substantially increases with forward flexion and compression (Arjmand and Shirazi-Adl, 2006a; McGill et al., 1994; Shirazi-Adl, 2006). This enhances trunk stability under disturbances and lowers the demand for reflexive activity (Granata and Rogers, 2007), although the risk of injury may increase in flexed postures due to the overloading of the spine (Granata and Wilson, 2001). Similarly, antagonistic coactivation increases not only the trunk stiffness and stability margin (Brown and McGill, 2008; Brown et al., 2006; Gardner-Morse and Stokes, 1998; Van Dieen et al., 2003b) but also the spinal loads and the risk of injury (Arjmand and Shirazi-Adl, 2006a; Granata and Marras, 2000). Excessive antagonistic coactivity may however

deteriorate trunk stability due to resulting large compression forces on the spine (El Ouaaid et al., 2013).

Using in vivo and computational studies, it was found that the perturbation load and pre-perturbation conditions (initial load, posture and abdominal coactivation) influence the trunk velocity and acceleration as well as the reflexive response of back muscles and spinal loads (Shahvarpour et al., 2015; Shahvarpour et al., 2014). Trunk stability was however not quantified in these analyses. The critical coefficient of muscle stiffness (Bergmark, 1989b), q_{cr} as a surrogate measure of the trunk stability, is estimated in the current work using a kinematics-driven model (Bazrgari et al., 2009a). Trunk stability is quantified before and after forward perturbation while altering perturbation load magnitude, preload, trunk posture and abdominal preactivation. Pre-perturbation conditions and perturbation load are hypothesized to influence trunk stability.

5.3. Method

A detailed description of in vivo measurements used in this study is published elsewhere (Shahvarpour et al., 2014). In brief, 12 young male subjects (weight 73.0 ± 3.9 Kg and height 177.7 ± 3.0 cm) were semi-seated in a sudden forward perturbation apparatus. With the pelvis fixed, a harness was placed on their trunk at the T8 level. The load was applied anteriorly through a cable connected to the harness in front. A load cell placed between the load and the subject measured the applied load while a potentiometer connected to the harness from the back measured the trunk forward displacement. Six experimental conditions were tested (Table 5.1).

In our previous kinematics-driven FE model studies (Shahvarpour et al., 2015), a trial was chosen randomly among five for each subject and condition since statistical analyses confirmed no learning effect on trials. The simulation started 256 ms before perturbation and continued 1 s after. With the pelvis fixed, the T12-L5 vertebral rotations at each time instance were estimated using the anterior translation measured from the initial upright trunk position at the T8 and given partitioning among lumbar levels (Bazrgari et al., 2009a). Angular velocity profiles along with the perturbation load and distributed gravity forces were input into the FE model. The required moments at each level and time instance were partitioned among associated muscles by minimizing the sum of the cubed muscle stresses at each vertebral level (Arjmand and Shirazi-

Adl, 2006c). The FE model (Bazrgari et al., 2009a; Bazrgari et al., 2008c) consisted of 7 rigid bodies including sacrum, L5 to L1 vertebral level and thorax-head-hands segment. Six nonlinear shear-deformable beam elements and dampers represented stiffness and damping properties of the passive tissues (Kasra et al., 1992; Markolf, 1970). Trunk inertial and mass properties were taken from the literature (de Leva, 1996; Pearsall et al., 1996; Zatsiorsky and Seluyanov, 1983).

Forty six local muscles inserted into lumbar levels along with 10 global muscles inserted to the thorax accounted for the trunk musculature. Wrapping of global extensor muscles was simulated with a curved line of action and forces at contact points with vertebrae (Arjmand et al., 2006; Shirazi-Adl, 1989, 2006; Shirazi-Adl and Parnianpour, 2000). Abdominal preactivation of muscles in C6 (see Table 5.1) was simulated pre-perturbation using a nonzero lower constraint (3-5% of maximum active force) that dropped to 1% after 1s post-perturbation according to EMG measurements (Shahvarpour et al., 2014).

For the current stability analyses, muscle stiffness, K_i, was evaluated at each time instance by $K_i = q\frac{F_i}{L_i}$ (Bergmark, 1989b) in which F_i and L_i are instantaneous force and total length of muscle i. Muscle stiffness coefficient, q, was considered constant for all muscles. In the current stability phase of analyses, every muscle i was substituted with a spring with an stiffness K_i evaluated at each time step as a function of its force and length taken based on earlier equilibrium phase of analyses (Shahvarpour et al., 2015). Using linear modal vibration approach, the stability analyses determined the smallest (undamped) natural frequency of the system at all times and deformed configurations as a function of q. The critical stiffness coefficient, q_{cr}, was subsequently sought as this fundamental natural frequency approached zero. A lower q_{cr} at a time instance indicates a higher margin of stability for the entire system so that at the limit when q_{cr} reaches zero, the trunk does not require any stiffness contribution any more from muscles in order to maintain stability. An iterative procedure was exploited to calculate q_{cr} at each time instance. Analyses were performed by ABAQUS/Standard 6.10-1 (Simulia Corp., Providence, RI).

Temporal variation of q_{cr} showed small fluctuations before the perturbation but a sudden drop after the perturbation. Consequently, the average q_{cr} values were evaluated over four separate time intervals; (1) pre-q over 256 ms before perturbation, (2) post-q1 over 60 ms post-

perturbation set as the average reflex latency according to our earlier study (Shahvarpour et al., 2014), (3) post-q2 during 60-240 ms post-perturbation in which the reflex response translates into mechanical action (Shahvarpour et al., 2015) and finally (4) post-q3 from 240 ms to 1 s post-perturbation when the neural action was mostly voluntary.

5.3.1. Statistical analyses

The evaluated variables were statistically analyzed using NCSS software (NCSS 8. NCSS, LLC. Kaysville, Utah, USA. www.ncss.com), using a significance level (alpha) of 0.05. One- and two-way analyses of variance (ANOVA), involving one (initial trunk flexion or EO antagonistic preactivation) or two (preload and sudden load) within-factors, were performed to evaluate the effect of preload (C1-2 vs C3-4), sudden load (C1 and C3 vs C2 and C4), trunk flexion (C1 and C3 vs C5) and abdominal preactivation (C2 and C4 vs C6) on trunk stability. These were repeated at each time interval (pre-q and post-q1 - post-q3).

5.4. Results

The temporal variation of q_{cr} was calculated for 12 subjects and six experimental conditions (see Figure 5.1 for the subject 2). Statistical results revealed that the preload and sudden load did not have any interaction effect on q_{cr}, for any time interval (Table 5.2). Preload significantly increased Pre-q though sudden load did not influence this variable (Table 5.2 and Figure 5.2). Post-perturbation variables were not affected by preload. However, while only a trend was observed in post-q1 ($p = 0.082$), post-q2 ($p = 0.004$) and post-q3 ($p<0.001$) significantly dropped with greater sudden load (Figure 5.2).

Initial trunk flexion (C5) significantly decreased the q_{cr} pre-perturbation (pre-q) when compared to C1 (5-N preload) and C3 (50-N preload) (Table 5.2 and Figure 5.3). Despite identical sudden load of 50 N, all post-perturbation stability variables were also significantly smaller in C5 than in C1 and C3.

Preactivation of abdominal muscles significantly decreased q_{cr} pre-perturbation (pre-q) with respect to C2 (5-N preload) and C4 (50-N preload) (Table 5.2 and Figure 5.4). Post-q1 and post-q2 in C6 demonstrated a significant decrease vs C2 but not C4, although trends ($0.05 < p < 0.1$) were observed.

5.5. Discussion

The critical muscle stiffness coefficient, q_{cr}, modulates the stiffness of muscles and as such can be employed as a surrogate measure of the trunk stability margin. The stability margin at a loaded configuration denotes the residual load-carrying capacity of the system that can be resisted above and beyond the existing load before becoming unstable. Due to the crucial role of muscles in pre- and post-perturbation periods, this coefficient was chosen similar to our earlier studies (Bazrgari et al., 2009a; Bazrgari et al., 2008c). For a given set of muscle forces, the trunk stability margin grows as q_{cr} drops so that at the limit when $q_{cr} = 0$, the trunk requires no passive and active stiffness contributions from muscles in order to maintain stability although it continues to depend on muscle forces (but not muscle stiffnesses) for equilibrium and stability. This coefficient was calculated at all times pre- and post-perturbations and for all conditions (Table 5.1). The results demonstrated that higher preload significantly reduced the pre-perturbation q_{cr} indicating the effect of larger muscle forces and hence muscle stiffnesses in increasing trunk stability. Higher amplitude of sudden load significantly increased stability (i.e. smaller q_{cr}) post-perturbation (due to larger muscle forces/stiffness and greater passive stiffness at larger flexion) especially after the back muscles reflex onset. Trunk stability was also substantially improved throughout when the trunk was initially flexed forward highlighting the effective role of active-passive stiffness. Abdominal preactivation increased the trunk stiffness and stability (due to greater muscle forces/stiffness) at all instances except the final post-reflex phase. These findings supported the hypotheses on the marked effects of perturbation load and initial conditions on trunk stability.

5.5.1. Preload and sudden load

Larger preload and as a result larger muscle forces/stiffnesses increased the trunk stability during the pre-perturbation time interval, which corroborates previous findings (Cholewicki et al., 2000b; Gardner-Morse and Stokes, 2001; Moorhouse and Granata, 2005). This might explain why in our previous work, such an increase in the pre-perturbation stability diminished the back muscles reflexive response (Shahvarpour et al., 2015) as well as the velocity and acceleration of the trunk movement (Shahvarpour et al., 2014) after perturbation. The current results showed no effect of preload post-perturbation.

Larger sudden load significantly decreased q_{cr} post-perturbation after the back muscles reflex onset. The associated increase in reflexive muscle forces improved the trunk stability, which is in agreement with previous studies (Brown and McGill, 2009; Brown and McGill, 2010; Franklin and Granata, 2007; Moorhouse and Granata, 2007), but at the price of simultaneously increasing spinal loads (Shahvarpour et al., 2014) and hence the risk of back injury and pain.

All comparisons between the pre- and post-perturbation time intervals demonstrated that the post-perturbation trunk stability margin substantially increased compared to pre-perturbation (Figure 5.1). This was due to the increased muscle activity and ligamentous passive stiffness in post-perturbation forward flexion. Moreover and unlike post-perturbation periods, q_{cr} never approached zero during the pre-perturbation, which highlights the required contribution of muscles to maintain stability margin especially during the pre-perturbation time interval.

5.5.2. Pre-perturbation trunk flexion

With initial trunk flexion, q_{cr} dropped significantly during both pre- and post-perturbation time intervals indicating higher trunk stability margin at all periods (Figure 5.3). The larger trunk flexion substantially increases the trunk passive stiffness (Adams and Dolan, 1991; McGill et al., 1994; Shirazi-Adl, 2006). In addition, to offset the gravity moment in the flexed posture, larger back muscle activity was observed in the pre-perturbation time interval (Shahvarpour et al., 2014), which contributes to the trunk active stiffness (Granata and Wilson, 2001). Higher active-passive trunk stiffness improves trunk stability (Arjmand and Shirazi-Adl, 2006a) and lowers the demand for reflexive response to the perturbation (Granata and Rogers, 2007). Post-perturbation neuromuscular behavior in C5 demonstrated unchanged muscles reflex amplitude but longer muscles reflex latency when compared to C1 and C3, which supports the notion of lower demand for muscles reflexive response (Shahvarpour et al., 2014).

5.5.3. Abdominal preactivation

In support of earlier findings (Gardner-Morse and Stokes, 1998; Lee et al., 2006) and due to greater muscle forces/stiffness, the preactivation of abdominal muscles significantly reduced q_{cr}, thus improving spine stability during the pre-perturbation time interval. In accordance with a greater reflex activity of back muscles in C6 vs C2 and C4 (Shahvarpour et al., 2014), post-perturbation q_{cr} in C6 was smaller pointing to a more-stable condition."

In summary, the trunk stability, estimated via the critical muscle stiffness coefficient (q_{cr}) during pre- and post-perturbation time intervals, depends on a delicate interplay between the ligamentous passive spine, passive muscle contribution and muscle recruitment (reflexive or voluntary). Larger preload, initial trunk flexion and abdominal preactivation improved trunk stability pre-perturbation. Post-perturbation trunk stability was improved with higher perturbation load, initial flexion and abdominal pre-activation. When the trunk was initially flexed, passive tissue contribution played an important role in trunk stability pre- and post-perturbation.

Conflict of interest

None to declare.

Acknowledgements

This study has been supported by grants from the Institut de recherche Robert-Sauvé en santé et en sécurité du travail (IRSST-Québec) and the Natural Sciences and Engineering Research Council of Canada (NCERC-Canada). Authors thank Dr. André Plamondon and Mr. Hakim Mecheri for their advice, as well as Sophie Bellefeuille and Cynthia Appleby for their technical assistance during testing at IRSST's laboratory.

5.6. References

Adams, M.A., Dolan, P., 1991. A technique for quantifying the bending moment acting on the lumbar spine in vivo. Journal of Biomechanics 24, 11-126.

Arjmand, N., Shirazi-Adl, A., 2006a. Model and in vivo studies on human trunk load partitioning and stability in isometric forward flexions. Journal of Biomechanics 39, 510-521.

Arjmand, N., Shirazi-Adl, A., 2006b. Sensitivity of kinematics-based model predictions to optimization criteria in static lifting tasks. Medical Engineering and Physics 28, 504-514.

Arjmand, N., Shirazi-Adl, A., Bazrgari, B., 2006. Wrapping of trunk thoracic extensor muscles influences muscle forces and spinal loads in lifting tasks. Clinical Biomechanics 21, 668-675.

Bazrgari, B., Shirazi-Adl, A., Lariviere, C., 2009. Trunk response analysis under sudden forward perturbations using a kinematics-driven model. Journal of Biomechanics 42, 1193-1200.

Bazrgari, B., Shirazi-Adl, A., Trottier, M., Mathieu, P., 2008. Computation of trunk equilibrium and stability in free flexion-extension movements at different velocities. Journal of Biomechanics 41, 412-421.

Bergmark, A., 1989. Stability of the lumbar spine, A study in mechanical engineering. Acta Orthopaedica Scandinavica Supplementum 230, 1-54.

Brown, S.H., McGill, S.M., 2009. The intrinsic stiffness of the in vivo lumbar spine in response to quick releases: implications for reflexive requirements. Journal of Electromyography and Kinesiology 19, 727-736.

Brown, S.H.M., McGill, S.M., 2005. Muscle force-stiffness characteristics influence joint stability: A spine example. Clinical Biomechanics 20, 917-922.

Brown, S.H.M., McGill, S.M., 2008. How the inherent stiffness of the in vivo human trunk varies with changing magnitudes of muscular activation. Clinical Biomechanics 23, 15-22.

Brown, S.H.M., McGill, S.M., 2010. The releationship between trunk muscle activation and trunk stiffness: examining a non-constant stiffness gain. Comput. Methods Biomech. Biomed. Eng. 13, 829-835.

Brown, S.H.M., Vera-Garcia, F.J., McGill, S.M., 2006. Effects of abdominal muscle coactication on the externally preloaded trunk: Variations in motor control and its effect on spine stability. Spine 31, E387-E393.

Cholewicki, J., McGill, S.M., 1995. Relationship between muscle force and stiffness in the whole mammalian muscle: A simulation study Journal of Biomechanical Engineering 117, 339-342.

Cholewicki, J., Simons, A.P.D., Radebold, A., 2000. Effects of external trunk loads on lumbar spine stability. Journal of Biomechanics 33, 1377-1385.

Crisco, J.J., 1989. The biomechanical stability of the human lumbar spine: experimental and theoretical investigations. Yale University, New Haven, Connecticut.

de Leva, P., 1996. Adustments to zatsiorsky-seluyanov's segment inertia parameters. Journal of Biomechanics 29, 1223-1230.

El Ouaaid, Z., Shirazi-Adl, A., Plamondon, A., Larivière, C., 2013. Trunk strength, muscle activity and spinal loads in maximum isometric flexion and extension exersions: A combined in vivo computational study. Journal of Biomechanics Under press.

Fathallah, F.A., Marras, W.S., Parnianpour, M., 1999. Regression models for predicting peak and continuous three-dimensional spinal loads during symmetric and asymmetric lifting tasks. Human Factors 41, 373-388.

Franklin, T.C., Granata, K.P., 2007. Role of reflex gain and reflex delay in spinal stability-a dynamic simulation. Journal of Biomechanics 40, 1762-1767.

Gardner-Morse, M., Stokes, I.A.F., 1998. The effects of abdominal muscle co-activation on lumbar spine stability Spine 23, 86-91.

Gardner-Morse, M.G., Stokes, I.A.F., 2001. Trunk stiffness increases with steady-state effort. Journal of Biomechanics 34, 457-463.

Granata, K.P., Marras, W.S., 2000. Cost-benefit of muscle cocontraction in protecting against spinal instability. Spine 25, 1398-1404.

Granata, K.P., Rogers, E.L., 2007. Torso flexion modulates stiffness and reflex response. Journal of Electromyography and Kinesiology 17, 384-392.

Granata, K.P., Slota, G.P., Bennett, B.C., 2004. Paraspinal muscle reflex dynamics. Journal of Biomechanics 37, 241-247.

Granata, K.P., Wilson, S.E., 2001. Trunk posture and spinal stability. Clinical Biomechanics 16, 650-659.

Kasra, M., Shirazi-Adl, A., Drouin, G., 1992. Dynamics of human intervertebral joints. Experimental and finite-element investigations. Spine 17.

Knutsson, F., 1944. The instability associated with disk degeneration in the lumbar spine. Acta Radiolagica 25, 593-608.

Krajcarski, S.R., Potvin, J.R., Chiang, J., 1999. The in vivo dynamic response of the spine to perturbations causing rapid flexion: effects of pre-load and step input magnitude. Clinical Biomechanics 14, 54-62.

Lee, P.J., Rogers, E.L., Granata, K.P., 2006. Active trunk stiffness increases with co-contraction. Journal of Electromyography and Kinesiology 16, 51-57.

Lucas, B.D., Bresler, B., 1960. Stability of the ligamentous spine, Techtical Report Series. Biomechanics Laboratory, University of California, San Francisco.

Ma, S.P., Zahalak, G.I., 1985. The mechanical response of the active human triceps brachii muscle to very rapid stretch and shortening. Journal of Biomechanics 18, 585-598.

Markolf, K.L., Year Stiffness and damping characteristics of thoracolumbar spine. In Proceeding of Workshop on Bioengineering Approaches to Problems of the Spine. Division of Research Grants. NIH, Bethesda.

McGill, S.M., Seguin, J., Bennett, G., 1994. Passive stiffness of the lumbar torso in flexion, extension, lateral bending and axial rotation, Efect of belt wearing and breath holding. Spine 19, 696-704.

Moorhouse, K.M., Granata, K.P., 2005. Trunk stiffness and dynamics during active exertion extensions. Journal of Biomechanics 38, 2000-2007.

Moorhouse, K.M., Granata, K.P., 2007. Role of reflex dynamics in spinal stability: Intrinsic muscle stiffness alone is insufficient for stability. Journal of Biomechanics 40, 1058-1056.

Panjabi, M.M., 1992. The stabilizing system of the spine. Part I. Function, dysfunction, adaptation, and enhancement. Journal of Spinal Disorders 5, 383-389.

Panjabi, M.M., 2003. Clinical spinal instability and low back pain. Journal of Electromyography and Kinesiology 13, 371-379.

Pearsall, D.J., Reid, J.G., Livingstone, L.A., 1996. Segmental inertial parameters of the human trunk as determined from computed tomography. Annals of Biomedical Engineering 24, 198-210.

Reeves, N.P., Cholewicki, J., Narendra, K.S., 2009. Effects of reflex delays on postural control during unstable seated balance. Journal of Biomechanics 42, 164-170.

Shahvarpour, A., Shirazi-Adl, A., Larivière, C., Bazrgari, B., 2015, Trunk Active Response and Spinal Forces in Sudden Forward Loading – Analysis of the Role of Perturbation Load and Pre-perturbation Conditions by a Kinematics-Driven Model. Journal of Biomechanics 48: 44-52.

Shahvarpour, A., Shirazi-Adl, A., Mecheri, H., Larivière, C., 2014. Trunk response to sudden forward perturbation - Effects of preload and sudden load magnitudes, posture and abdominal muscle preactivation. Journal of Electromyography and Kinesiology 24, 394-403.

Shirazi-Adl, A., 1989. Nonlinear finite element analysis of wrapping uniaxial elements. Computers & structures 32, 119-123.

Shirazi-Adl, A., 2006. Analysis of large compression loads on lumbar spine in flexion and in torsion using a novel wrapping element. Journal of Biomechanics 39, 267-275.

Shirazi-Adl, A., Parnianpour, M., 2000. Load-bearing and stress analysis of the human spine under a novel wrapping compression loading. Clinical Biomechanics 15, 718-725.

Van Dieen, J.H., Kingma, I., van der Bug, J.C.E., 2003. Evidence for a role of antagonistic cocontraction in controlling trunk stiffness during lifting. Journal of Biomechanics 36, 1829-1836.

White, A.A., Panjabi, M.M., 1990. Clinical Biomechanics of the Spine. J.B. Lippincott, Philadelphia.

Zatsiorsky, V.M., Seluyanov, V.N., 1983. The mass and inertia characteristics of the main segments of the human body Biomechanics. Champaign: Human Kinetics Publishers, pp. 1152-1159.

Table 5.1 Parameters defining the six experimental conditions

Condition	Pre Load (N)	Sudden Load (N)	Initial posture	EO preactivation
C1	5	50	Upright	-
C2	5	100	Upright	-
C3	50	50	Upright	-
C4	50	100	Upright	-
C5	5	50	10 cm Anterior Translation*	-
C6	5	100	Upright	10%

* The anterior translation was measured from the initial upright trunk position.

Table 5.2 ANOVA *P* values for the effects of preload, sudden load, initial trunk flexion and abdominal preactivation on pre- and post-perturbation critical stiffness coefficient (q_{cr})*

Independent variables	ANOVA P values			
	Pre-q	Post-q1	Post-q2	Post-q3
Preload	**<0.001**	0.634	0.393	0.348
• (C1 and C2 vs C3 and C4)				
Sudden load	0.314	0.082	**0.004**	**<0.001**
• (C1 and C3 vs C2 and C4)				
Preload × Sudden load	0.282	0.105	0.127	0.759
Initial flexion				
• (C1 vs C5)	**<0.001**	**<0.001**	**<0.001**	**<0.001**
• (C3 vs C5)	**<0.001**	**0.001**	**<0.001**	**<0.001**
Abdominal Coactivation				
• (C2 vs C6)	**<0.001**	**0.003**	**0.013**	0.402
• (C4 vs C6)	**0.032**	0.072	0.060	0.070

*Statistically significant differences ($p < 0.05$) are identified in bold characters while trends ($0.05 < p < 0.1$) are underlined.

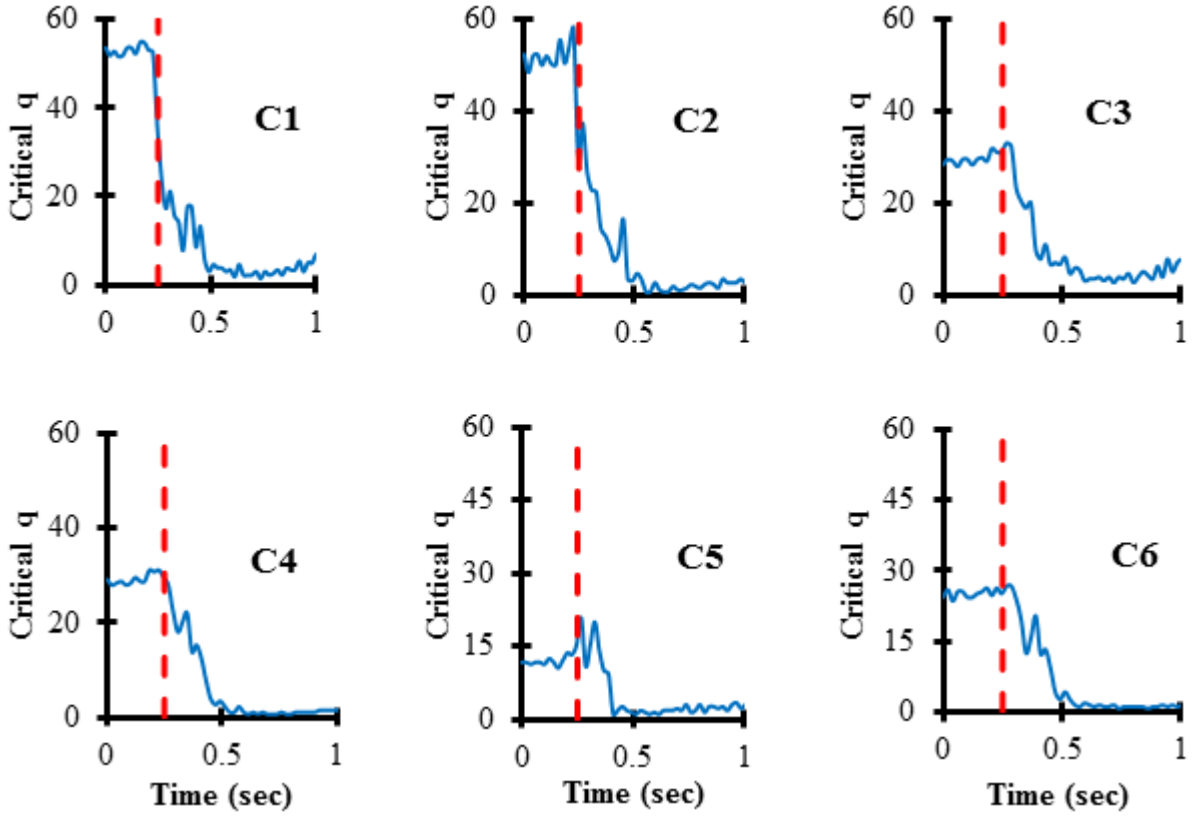

Figure 5.1 Pre- and post-perturbation temporal variations of the critical muscle stiffness coefficient for the six experimental conditions (Table 5.1) and subject 2. Perturbation instance is shown by the red broken line. Perturbation onset was estimated using AGLR (approximated generalized likelihood-ratio) method that indicates the probability of abrupt variation of the measured force signal by evaluating log-likelihood ratio of variation in sliding windows along the signal (Staude, 2001; Staude and Wolf, 1999).

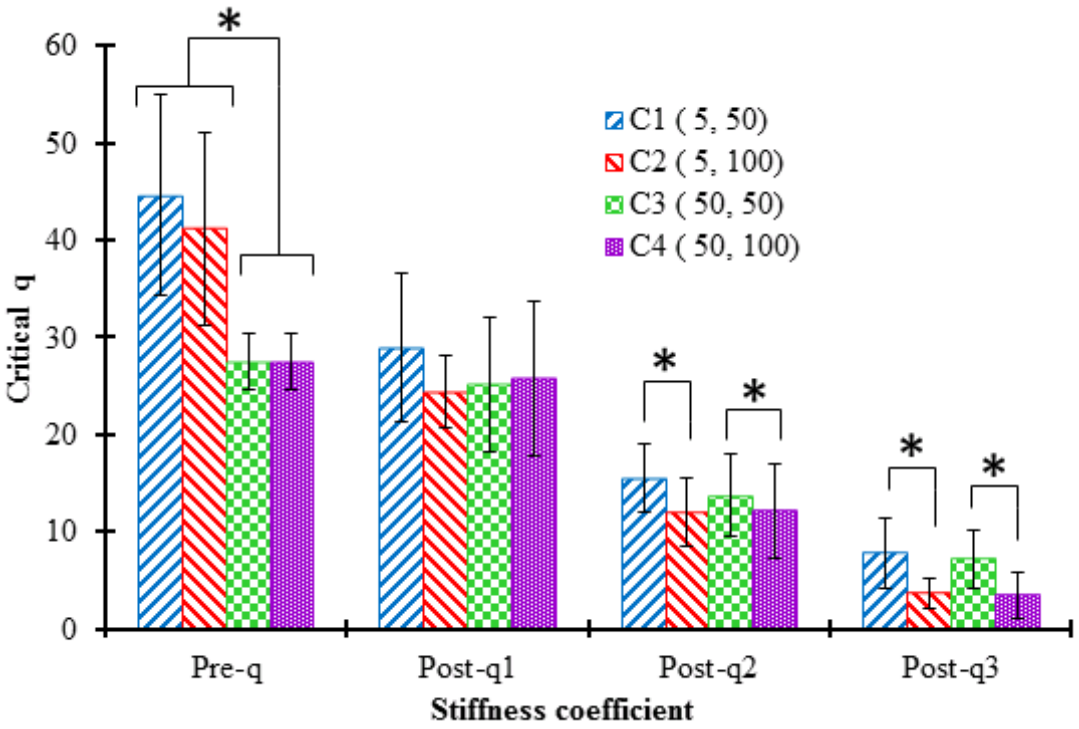

Figure 5.2 Averaged (n = 12 subjects) critical muscle stiffness coefficients, q_{cr}, during pre- and post-perturbation time intervals, for two preloads (5 N and 50 N) and two sudden loads (50 N and 100 N) corresponding to conditions C1 to C4. Variation bars are standard deviations. C1 (5, 50), C2 (5, 100), C3 (50, 50) and C4 (50, 100) refer to experimental conditions (Table 5.1) with preload and perturbation load listed in brackets in N, * indicates statistically significant difference.

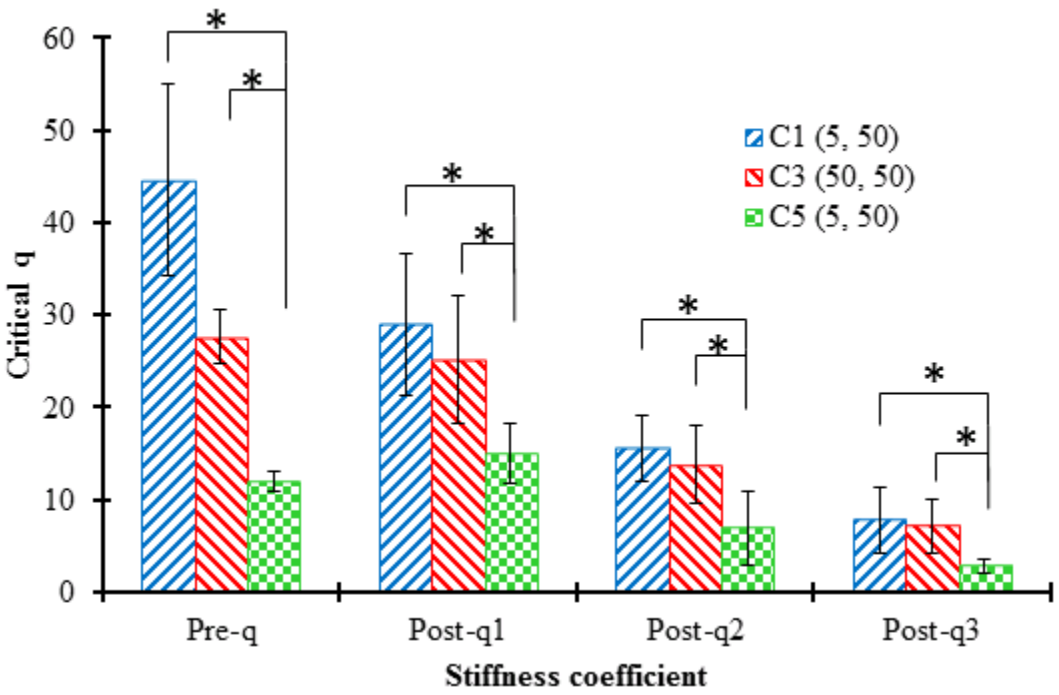

Figure 5.3 Averaged (n = 12 subjects) critical muscle stiffness coefficient, q_{cr}, during pre- and post-perturbation time intervals, for three conditions having the same 50-N sudden load: C1 (preload = 5 N), C3 (preload = 50 N) and C5 (initial trunk forward flexion). Variation bars are standard deviations. C1 (5, 50), C2 (5, 100) and C5 (5, 50) refer to experimental conditions (Table 5.1) with preload and perturbation load listed in brackets in N, * indicates statistically significant difference.

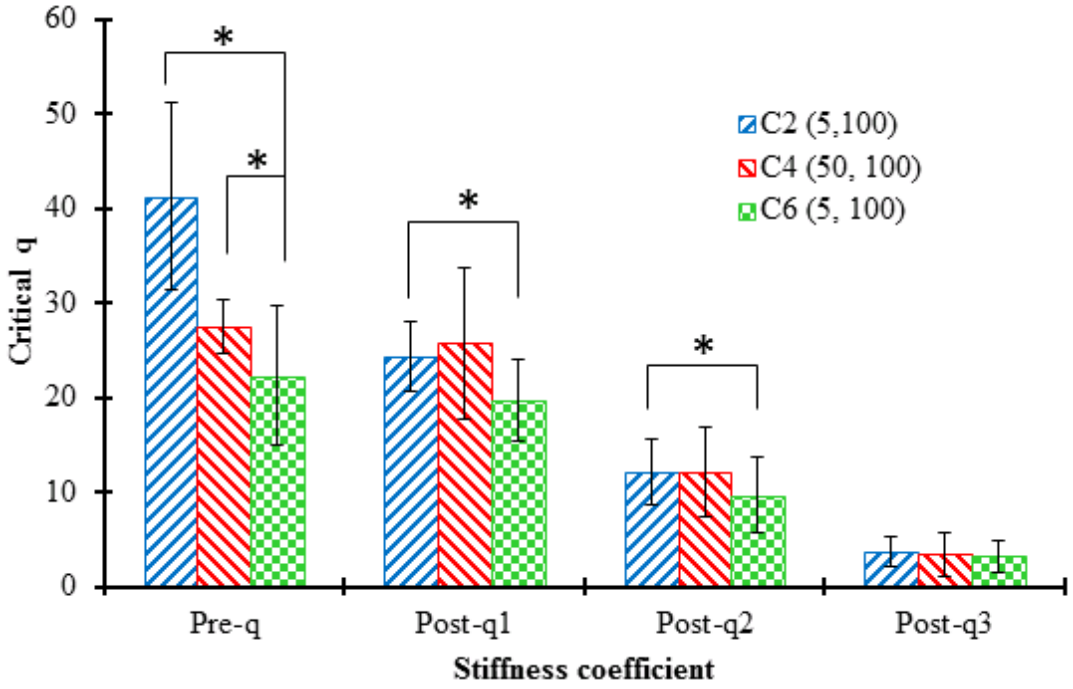

Figure 5.4 Averaged (n = 12 subjects) critical muscle stiffness coefficient, qcr, during pre- and post-perturbation time intervals, for three conditions having the same 100-N sudden load: C2 (preload = 5 N), C4 (preload = 50 N) and C6 (preactivation of abdominal muscles). Variation bars are standard deviations. C2 (5, 100), C4 (50, 100) and C6 (5, 100) refer to experimental conditions (Table 5.1) with preload and perturbation load listed in brackets in N. * demonstrates statistically significant difference.

CHAPTER 6 ARTICLE 4: ACTIVE-PASSIVE BIODYNAMICS OF THE HUMAN TRUNK WHEN SEATED ON A WOBBLE CHAIR

Ali Shahvarpour [a], Aboulfazl Shirazi-Adl [a], Christian Larivière [b]

[a] Division of Applied Mechanics, Department of Mechanical Engineering, École Polytechnique, Montreal, Quebec, Canada

[b] Robert-Sauvé Occupational Health and Safety Research Institute, Montreal, Quebec, Canada

Submitted to
Journal of Biomechanics (2015)

6.1. ABSTRACT

Unstable sitting on a wobble chair with different balance difficulty levels can be used as an effective tool in exercises as well as evaluation and therapeutic stages of rehabilitation. No data on muscle activity levels and spinal loads are however available to assess its safety compared to other regular daily activities. The goal of this study was to estimate muscle forces and spinal loads in a seated unstable wobble chair task. In vivo 3D kinematics of the trunk and seat collected in an earlier study were used here to drive computational trunk musculoskeletal models of 6 normal and 6 low-back pain subject groups sitting on a wobble chair for a duration of 10 s. Results revealed no significant differences between kinematics, muscle forces, spinal loads and force plate reaction forces when comparing these two groups. The estimated muscle forces and spinal loads were moderate though much larger than those in a stationary sitting posture. As an example and due to the prescribed trunk rotations, the initial static compression of 768 N (mean of 12 subjects) at the L5-S1 markedly increased to mean compression forces in the range of 938-1382 N. The wobble chair with characteristics considered in this study is found hence safe enough as a therapeutic exercise for both healthy and low-back pain subjects.

Keywords: Muscle forces, Spinal loads, Sitting, Wobble Chair, Center of Pressure

6.2. Introduction

Human body is subject to external perturbations during falls, tripping and sudden loading-unloading (Shahvarpour et al., 2014) as well as internal perturbations due to respiration (Hodges et al., 2002) and neuromuscular noise (Reeves et al., 2013). As a result, demands for muscles' passive, active and reflexive contributions increase in order both to satisfy the deteriorated transient equilibrium conditions and to maintain a sufficient margin of stability and balance to prevent falls and injuries (Panjabi, 1992). Unstable support environments such as those in standing and sitting on pivoted boards are helpful to assess and improve neuromuscular responses. Wobble chairs have been employed as a tool to investigate the trunk neuromuscular mechanisms involved in balance of the upper body in isolation from the confounding effects of the lower extremities (Cholewicki et al., 2000a). Trunk stability (Freddolini et al., 2014a; Tanaka et al., 2009; Tanaka et al., 2010), trunk stiffness (Freddolini et al., 2014c; Reeves et al., 2006), neuromuscular activity (Freddolini et al., 2014b; Reeves et al., 2006), reflexive response (Radebold et al., 2001; Reeves et al., 2009) and trunk motor behavioral differences between LBP patients and healthy subjects (Willigenburg et al., 2013) have been studied using such method of unbalanced sitting.

Previous iterative kinematics-driven computational trunk model studies under sudden dynamic loads and motions with high acceleration content estimated relatively high spinal compression forces (in the range of 3-6 kN) (Bazrgari et al., 2009a; Shahvarpour et al., 2015) and hence risk of low-back injuries. Initial flexed posture and antagonistic coactivity along with higher sudden load markedly increased spinal loads. Any dysfunction in the neuromuscular system associated with for example longer latency and/or muscle injury could further increase spinal loads and motions causing additional injuries. Furthermore, high spinal loads may aggravate pain in CLBP subjects that makes them excessively cautious due to the fear of pain when performing tasks (Greene et al., 2001; Khalil et al., 1987).

The primary aim of this study was to assess the safety of the wobble chair task. Despite the growing interest in unstable devices such as wobble chairs in exercises and rehabilitation therapies, no realistic model study of the trunk muscle forces and spinal loads has been carried out so far. Based on earlier in vivo measurements in which 18 healthy controls and 18 chronic low-back pain (CLBP) patients participated (Larivière et al., 2013), we simulated the trunk

response of 12 subjects (6 controls and 6 patients) under the associated personalized trunk masses and measured kinematics. Despite the fact that no significant differences in most recorded measures (range of motion, velocity, median frequency, etc.) were found in the in vivo study between healthy controls and patients (Larivière et al., 2015), a secondary aim (exploratory study) was to compare the biomechanical measures (angular velocities/accelerations, muscle forces, spinal loads) calculated by our kinematics-driven model in an attempt to discriminate between these two groups.

6.3. Method

6.3.1. Subjects and Measurements

Among 36 individuals volunteered for the in vivo study reported elsewhere (Larivière et al., 2013), 6 healthy and 6 CLBP male subjects with body height close to that in our FE model (vertical distance from the S1 to the C7 of 46.76 cm) were chosen (Table 6.1). A brief description of the in vivo study is provided here, with emphasis on elements specifically related to the current computational work. The inclusion criteria for CLBP subjects were: lumbar or lumbosacral pain with or without proximal radicular pain (limited distally at the knees) and presence of chronic pain defined as a daily or almost daily pain for at least 3 months. The exclusion criteria for the healthy controls were back pain in the previous year or back pain lasting longer than a week during the preceding years.

The subjects sat on the wobble chair with the feet on an adjustable platform attached to the chair and the arms crossed on the chest (Figure 6.1). To avoid excessive inter subject-chair movements, feet were strapped to the chair (footstep) and thighs were secured laterally with foam cubes attached with velcro. A ball and socket pivot supported the seat, allowing for a maximum tilt of 13 degrees in forward-backward and lateral directions (maximum range of motion allowed: 26°). The apparatus design restricted the axial rotation. Four springs (height = 4.5 cm, axial stiffness = 8467 N/m) with equal distances from the pivot were placed under the seat in front, back, right and left sides. The springs were just in contact with the seat at the beginning and did not stretch during tests as they were not attached to the seat. Kinematics of the wobble chair and trunk was measured using an Optotrak system (Northern Digital Inc., Waterloo, Ontario, Canada) at a sampling frequency of 50 Hz. Rigid marker clusters composed of three infrared light emitting

diodes were attached on the seat surface and the trunk of subjects at the S1, T12, C7 and head levels. A force plate placed (AMTI, model BP900900, Watertown, MA, USA) under the chair recorded the force and the center of pressure (CoP) at 1000-Hz sampling frequency (Figure 6.1).

A simple calibration protocol (Larivière et al., 2013; Slota et al., 2008) allowed for the positioning of the springs so as to reduce the influence of body size on recorded performance. The resulting spring positions defined hence a reference system that was considered neutrally stable for each specific subject. The task difficulty was subsequently determined by adjusting the spring positions relative to those set in the foregoing reference condition. In the current study the task difficulty was set at 60% (Larivière et al., 2013). The subject was instructed to keep the eyes closed during the task. Tests started after removing the stabilizing cushions placed under the chair, but due to technical limitations, recording started ~5 s after and lasted for 60 seconds.

6.3.2. FE model studies

The three-dimensional finite element (FE) model of the spine consisted of 7 rigid bodies representing sacrum, L1 to L5 lumbar vertebrae and thorax-head-arms (Figure 6.1) (Bazrgari et al., 2008c; Shahvarpour et al., 2015). Based on mesh refinement verifications, T12-L1 to L5-S1 intervertebral discs were represented by three quadratic shear-deformable beam elements with nonlinear deformation-load mechanical properties using published data (Oxland et al., 1992; Shirazi-Adl, 2006; Yamamoto et al., 1989). Six dampers (axial coefficient = 3600 Ns/m and rotational coefficient = 3.6 Ns/m) were added to intervertebral discs (Kasra et al., 1992; Markolf, 1970). Inertial properties along with corresponding mass centers for head, upper-lower limb segments, and trunk at different vertebral levels were considered based on published data (de Leva, 1996; Pearsall et al., 1996; Zatsiorsky and Seluyanov, 1983). Trunk musculature was represented by 46 local lumbar and 10 global thoracic muscles. Muscle passive properties were also considered (Davis et al., 2003). Wrapping of global extensor muscles were taken into account with muscles constrained not to approach T12-L5 vertebrae beyond 90% of their initial lever arms set at the undeformed configuration (see (Arjmand et al., 2006).

The final ten seconds (from 50 to 60 s) of the entire 60 s of recorded motion with sampling frequency of 50 Hz (step time 0.02 s) were deemed more suitable for analysis in all subjects because process stationarity is usually reached after 20 to 30 s during quiet standing

(Carroll and Freedman, 1993) or during sitting on a wobble chair having the same design (Lee and Granata, 2008). At the beginning of each simulation, the steady-state configuration of the model under gravity was altered slowly to reach the measured deformed position. The velocity profiles calculated from the measured rotations at the S1 and T12 vertebral levels were prescribed into the FE model at all levels from S1 to T12. The total lumbar rotation was partitioned among various lumbar levels at 22%, 25%, 19%, 15%, 11% and 8% for the caudal L5-S1 to the cranial T12-L1 level, respectively. The linear velocities at the S1 calculated from its measured translations were applied onto the S1 as base excitations. The FE analyses were carried out at each time frame using ABAQUS/Standard 6.10-1commercial program (Simulia Corp., Providence, RI, USA) using implicit integration with stable Hilber-Hughes-Taylor algorithm. Automatic time increment with no upper limit was considered. The muscle forces at each iteration were estimated separately out of the FE program by partitioning the required moments at different levels $\overrightarrow{RM}$ (calculated by the FE model for prescribed rotations) among the associated muscles through the following optimization problem (Arjmand and Shirazi-Adl, 2006c; Winter, 2009).

$$Min \sum_{i=1}^{m} \left(\frac{|\vec{F}_i|}{PCSA_i} \right)^3 \qquad \text{Eq. 1}$$

Subject to:

$$\sum_{i=1}^{m} (\vec{r}_i \times \vec{F}_i) - \overrightarrow{RM} = 0$$

$$PF_i < |\vec{F}_i| < PF_i + 0.6 \times PCSA_i$$

in which $\vec{F}_i$ and $\vec{r}_i$ are, respectively, the force vector and lever arm of muscle i with respect to the vertebral primary node at each level. $PCSA_i$ and PF_i are, respectively, the physiological cross sectional area and passive force magnitude of muscle i. The maximum stress of muscles was set at 0.6 MPa (Winter, 2009). The optimization was solved analytically at the beginning to set the initial spine posture in the sagittal plane. In the next steps of the simulation, with asymmetric

motions/loads and lack of an analytical solution, interior point algorithm (Pan, 2014) was applied by *fmincon* function from Optimtool toolbox of MATLAB 8.3 (The Mathworks Inc., Natrick, MA, USA) to solve the optimization problem. At each time step, the a-priori existing computed muscle forces were taken as the initial guesses for the next coming time step. The updated muscle forces were subsequently applied along with the gravity loads and base excitations. The iteration repeated in each time step till convergence was reached (i.e., negligible changes occurred in evaluated muscle forces in two consecutive iterations). The analysis proceeded then to the next time step. The same algorithm was used to calculate spinal loads at a stationary seated posture set by flattening the lumbar lordosis in upright standing posture by 8°. The corresponding estimated spinal loads were then compared to those subsequently evaluated during the challenged seated balance tasks.

Peak velocities and accelerations of the trunk at the S1 and T12 levels in three planes of motion (sagittal, frontal, and transverse) were calculated. Root mean square (RMS) of the estimated muscle forces and spinal loads as well as their peak magnitudes over 10 seconds of analysis were also determined. Unpaired t-test was carried out to detect the effect of normal versus CLBP subject groups on the biomechanical measures using NCSS software (NCSS 8. NCSS, LLC. Kaysville, Utah, USA. www.ncss.com) with the significance level (alpha) set at 0.05.

6.3.3. Validation

A free body diagram made of the seat (with four springs and a pivot underneath), lower extremities and buttocks (with the lower part of the trunk cut by an imaginary horizontal plane passing through the mid-point of the L5-S1 disc) was also developed (Figure 6.1). The measured rotation of the seat along with the computed spinal and muscle forces at the L5-S1 level at each time step were considered. The 10s temporal variations of the total vertical reaction force and its locus (i.e., center of pressure, CoP) were then estimated. These values were compared to those measured by the force plate. Moreover, Pearson's coefficient of correlation between the measured and computed CoP in both anterior-posterior (AP) and right-left (RL) directions were calculated.

6.4. Results

Computed and measured loci of CoP and magnitudes of the vertical reaction force on the force plate were found in good agreement, as shown for a healthy subject in Figure 6.2. Significant correlations (~0.90) across 10 subjects out of all 12 subjects between the estimated and measured loci of CoP in both AP and LR directions were found. No correlations (coefficients of 0.22 and 0.27 in the AP direction and 0.43 and 0.26 in the LR direction) were however calculated for the other 2 subjects.

Results on kinematics (rotation, angular velocity and acceleration) and kinetics (muscle forces and spinal loads) are shown only for one subject as an example (Figures 5.3-5.5). Statistical analyses revealed no significant between-group differences in kinematics variables. The peak angular velocity and acceleration of the CLBP group were higher in all directions except extension, although not at statistically significant levels (Figure 6.6). An earlier statistical study on recorded data of all 36 subjects revealed no significant difference in rotation and angular velocity between healthy and CLBP groups (Larivière et al., 2015).

Peak muscles activity level were found larger for patients, for all muscles, although the differences did not reach statistical significance (Figure 6.7). In contrast to RA for which negligible activity levels were computed, right and left EO and IO showed some activities to counterbalance lateral and axial moments. Larger moderate activities were estimated in thoracic extensor muscles (Figure 6.7). Local muscle forces were quite variable among-subjects, ranging between low (~5%) to high (> 40%) activity levels; with no statistical correlations between control and patient groups.

Spinal loads in local directions at the mid-height plane of the L5-S1 disc varied with time and showed a substantial change from their peaks (1473 N and 1720 N in compression, -691 N and -687 N in AP shear and 153 N and 208 N in RL shear, respectively, for healthy and CLBP groups) to those computed in the stationary sitting posture 768 N (mean of 12 subjects) in compression, -284 N in AP shear and 0 N in RL shear). No between-group significant effects of spinal loads were found (Figure 6.8).

6.5. Discussion

A nonlinear transient kinematics-driven FE model was used to estimate temporal profiles of muscle forces and spinal loads of 12 subjects seated on a wobble chair for a duration of 10 s. Measured individual kinematics and body weights collected for a total of 36 subjects in an earlier in vivo study were used to drive the current FE model studies for only 6 healthy controls and 6 CLBP subjects. No statistical differences in estimated biomechanical measures were found between healthy controls and CLBP patients. Overall, estimated spinal compression and shear forces remained moderate, indicating low risk of injury during this task. Satisfactory correlations were found for all subjects between measured and computed location of CoP and magnitude of the reaction force.

The statistical analyses showed the back pain status had no significant effect on the peak angular velocity and acceleration of the chair; likewise, an earlier study on the experimental data found no significant effect of back pain on the range of motion of the chair and the trunk (Larivière et al., 2015). Since the axial rotation of the seat was limited, its velocity and acceleration were smaller than those in the sagittal and lateral planes Figure 6.6. However, peak velocity and peak acceleration relatively increased at the S1 and T12 level that may indicate the strategy of the central nervous system (CNS) in exploiting the axial motion in order to keep balance in other planes. Although further investigation is needed; it is in line with previous studies that showed the control strategy of CNS is to allow variability in task-irrelevant, redundant dimensions (transverse plane in this study in which the system is always stable) in order to improve the control and stability in the relevant ones (sagittal and frontal planes in this study in which the system is unstable) (Todorov and Jordan, 2002). Granata and England (2006) also found more stability during asymmetric movements of the trunk than symmetric motions in the sagittal plane.

The peak angular velocity and acceleration of the trunk prescribed in the current model study were, respectively, 32 deg/s and 339 deg/s^2, both occurring in the frontal plane. These are noted to be much smaller than ~200 deg/s and ~1000 deg/s^2 recorded in the sagittal plane during fast voluntary flexion-extension movements (Bazrgari et al., 2008c). Consequently, the effect of inertia on muscle forces and spinal loads were relatively small. This is evident when comparing, in both measurements and computed results, the total axial reaction forces that include inertial

effects versus the body weight of the subjects (Figure 6.2). The relative differences between spinal forces estimated in stationary sitting and challenged seated balance task on wobble chair are due mainly to the trunk rotations, rather than inertial forces, that increase gravitational moments on spine and consequently the demand for muscle forces.

Muscle forces were found larger in CLBP groups although not at statistically significant levels. No significant activity was found in the RA muscle that is expected due to almost no net extension moment and its small role in resisting lateral and axial moments. In contrast, left and right EO and IO were more active to counterbalance the required moments in the frontal and transverse planes. Reported normalized EMG of paraspinal muscles recorded during challenged seated balance tasks remained always less than 10% (Reeves et al., 2006) while, in the current simulations, normalized abdominal and back muscles activity exceeded 20% and 35%, respectively. The tasks in other works might have been easier than those in the current study, thus affecting recorded values. Moreover and apart from concerns on the location of surface electrodes and normalization of EMG data in vivo, the normalization of predicted muscle forces in our study by 0.6 (MPa) × PCSA (mm^2) could influence such comparisons.

Spinal loads were neither statistically influenced by subjects' pain status. Due to higher activity/coactivity in paraspinal muscles under trunk rotations prescribed here, spinal forces exceeded their values in stationary seated position The root mean square (RMS) compression force at the L5-S1 during 10 s simulation duration was 1011 (±319) N and 1055 (±218) N in healthy and CLBP groups, respectively. The corresponding peaks reached 1473 (±534) N and 1720 (± 845) N, which exceeded the mean compression of 768 N computed at the stationary seated posture. Based on intradiscal pressure measurements, mean compression force of about 750 N is estimated at lower lumbar discs during sitting (Dreischarf et al., 2013; Nachemson and Morris, 1964; Sato et al., 1999; Shirazi-Adl and Drouin, 1988). Compression forces of 575 N and 690 N at the L5-S1 have also been reported respectively in steady state upright standing and flexed seated postures (Bazrgari et al., 2008a). In the current study, the marked increase in spinal loads on the wobble chair versus the steady state values in the seated configuration at the beginning is due mainly to the input trunk rotations that increase the gravitational moments on the spine. The current model did not account for antagonistic co-contraction, which could have increased the estimated spinal loads, especially in CLBP subjects (van Dieen et al., 2003a). The

foregoing estimated compression forces in subjects on wobble chair nevertheless remain much smaller than those computed in lifting and forward bending tasks. (Bazrgari et al., 2007; Bazrgari et al., 2008c).

The outlines of the model-estimated and measured loci of CoP were in good agreement. The mean correlations of CoP loci in AP and LR directions were 0.91 and 0.90, respectively. The excursions of the measured CoP in both AP and LR directions were however larger by 323% and 210% relative to the model-predicted ones (Figure 6.2, top). A number of parameters may influence these estimated values; the anthropometric data used in the models (i.e. mass, mass moment of inertia and the position of the center of masses) that were adjusted based only on the body mass of the subjects (de Leva, 1996). Moreover, the masses of the subject's shoes and measurement accessories, i.e. marker clusters, etc., were not considered in the model. The total vertical reaction force measured by the force plate and predicted by the model remained however in excellent correlation for all subjects (R=1.00) including those two subjects with apparently erroneous loci of CoP.

In summary, using measured asymmetric rotations of the trunk and seat in three planes in 6 healthy and 6 CLBP subjects on a wobble chair, time profiles of muscle forces and spinal loads for 10 s were estimated by a kinematics-driven FE model using the measured kinematics in an earlier study. No statistical differences in estimated biomechanical measures were observed between healthy controls and CLBP patients. Results revealed that the estimated muscle forces and spinal loads were relatively small but markedly larger than those in a flexed quasi-static sitting. The wobble chair with characteristics considered here is found hence safe enough as a therapeutic exercise for both healthy and CLBP subjects.

Conflict of interest

None to declare.

Acknowledgements

This study has been supported by grants from the Institut de recherche Robert-Sauvé en santé et en sécurité du travail (IRSST-Québec) and the Natural Sciences and Engineering Research Council of Canada (NCERC-Canada). Authors thank Dr. André Plamondon and Mr.

Hakim Mecheri for their advice, as well as Sophie Bellefeuille and Cynthia Appleby for their technical assistance during tests at the IRSST laboratory.

6.6. References

Arjmand, N., Shirazi-Adl, A., 2006. Sensitivity of kinematics-based model predictions to optimization criteria in static lifting tasks. Medical Engineering and Physics 28, 504-514.

Arjmand, N., Shirazi-Adl, A., Bazrgari, B., 2006. Wrapping of trunk thoracic extensor muscles influences muscle forces and spinal loads in lifting tasks. Clinical Biomechanics 21, 668-675.

Bazrgari, B., Shirazi-Adl, A., Arjmand, N., 2007. Analysis of squat and stoop dynamic liftings: muscle forces and internal spinal loads. European Spine Journal 16, 687-699.

Bazrgari, B., Shirazi-Adl, A., Kasra, M., 2008a. Computation of trunk muscle forces, spinal loads and stability in whole-body vibration. Journal of Sound and Vibration 318, 1334-1347.

Bazrgari, B., Shirazi-Adl, A., Lariviere, C., 2009. Trunk response analysis under sudden forward perturbations using a kinematics-driven model. Journal of biomechanics 42, 1193-1200.

Bazrgari, B., Shirazi-Adl, A., Trottier, M., Mathieu, P., 2008b. Computation of trunk equilibrium and stability in free flexion-extension movements at different velocities. Journal of Biomechanics 41, 412-421.

Carroll, J.P., Freedman, W., 1993. Nonstationary properties of postural sway. Journal of Biomechanics 26, 409-416.

Cholewicki, J., Polzhofer, G.A., Radebold, A., 2000. Postural control of trunk during unstable sitting. Journal of Biomechanics 22, 1733-1737.

Davis, J., Kaufman, K.R., Lieber, R.L., 2003. Correlation between active and passive isometric force and intramuscular pressure in the issolated rabbit tibialis anterior muscle. Journal of Biomechanics 36, 505-512.

de Leva, P., 1996. Adustments to zatsiorsky-seluyanov's segment inertia parameters. Journal of Biomechanics 29, 1223-1230.

Dreischarf, M., Rohlmann, A., Zhu, R., Schmidt, H., Zander, T., 2013. Is it possible to estimate the compressive force in the lumbar spine from intradiscal pressure measurements? A finite element evaluation. Medical Engineering & Physics 35, 1385-1390.

Freddolini, M., Strike, S., Lee, R.Y.W., 2014a. Dynamic Stability of the Trunk During Unstable Sitting in People With Low Back Pain. Spine 39, 785-790.

Freddolini, M., Strike, S., Lee, R.Y.W., 2014b. The role of trunk muscles in sitting balance control in people with low back pain. Journal of Electromyography and Kinesiology 24, 947-953.

Freddolini, M., Strike, S., Lee, R.Y.W., 2014c. Stiffness properties of the trunk in people with low back pain. Human Movement Science 36, 70-79.

Granata, K.P., England, S.A., 2006. Stability of dynamic trunk movement. Spine 31, E271-E276.

Greene, H.S., Cholewicki, J., Falloway, M.T., Nguyen, C.V., Radebold, A., 2001. A history of low back injury is a risk factor for recurrent back injuries in varsity athletes. The American Journal of Sports Medicine 29, 795-800.

Hodges, P.W., Gurfinkel, V.S., Brumangne, S., Smith, T.C., Cordo, P.C., 2002. Coexistance of stability and mobility in postural control : Evidance from postural compensation for respiration. Experimental Brain Research 144, 293-302.

Kasra, M., Shirazi-Adl, A., Drouin, G., 1992. Dynamics of human intervertebral joints. Experimental and finite-element investigations. Spine 17.

Khalil, T.M., Goldberg, M.L., Asfour, S.S., Moty, E.A., Rosomoff, R.S., Rosomoff, H.L., 1987. Acceptable maximum effort (AME). A psychophysical measure of strength in back pain patients. Spine 12, 372-376.

Larivière, C., Gagnon, D., Mecheri, H., 2015. Trunk postural control in unstable sitting: Effect of sex and low back pain status. Clinical Biomechanics 30, 933-939.

Larivière, C., Mecheri, H., Shahvarpour, A., Gagnon, D., Shirazi-Adl, A., 2013. Criterion validity and between-day reliability of an inertial-sensor-based trunk postural stability test during unstable sitting. Journal of Electromyography and Kinesiology 23, 899-907.

Lee, H., Granata, K.P., 2008. Process stationarity and reliability of trunk postural stability. Clinical Biomechanics 23, 735-742.

Markolf, K.L., Year Stiffness and damping characteristics of thoracolumbar spine. In Proceeding of Workshop on Bioengineering Approaches to Problems of the Spine. Division of Research Grants. NIH, Bethesda.

Nachemson, A., Morris, J.M., 1964. In vivo measurements of intradiscal pressure: Discometry, a method for the determination of pressure in the lower lumbar discs. Journal of Bone and Joint Surgery 46, 1077-1092.

Oxland, T., Lin, R.M., Panjabi, M.M., 1992. Three-dimensional mechanical properties of the thoracolumbar junction Journal of Orthopaedic Research 10, 573-580.

Pan, P.-Q., 2014. Linear Programming Computation. Springer-Verlag Berlin Heidelberg.

Panjabi, M.M., 1992. The stabilizing system of the spine. Part I. Function, dysfunction, adaptation, and enhancement. Journal of Spinal Disorders 5, 383-389.

Pearsall, D.J., Reid, J.G., Livingstone, L.A., 1996. Segmental inertial parameters of the human trunk as determined from computed tomography. Annals of Biomedical Engineering 24, 198-210.

Radebold, A., Cholewicki, J., Polzhofer, G.K., Greene, H.S., 2001. Impaired postural control of the lumbar spine is associated with delayed muscle response times in patients with chronic idiopathic low back pain. Spine 26, 724-730.

Reeves, N.P., Cholewicki, J., Narendra, K.S., 2009. Effects of reflex delays on postural control during unstable seated balance. Journal of Biomechanics 42, 164-170.

Reeves, N.P., Cholewicki, J., Pearcy, M., Parnianpour, M., 2013. How can models of motor control be useful for understanding low back pain?, in: Hodges, P.W., Cholewicki, J., Van Dieen, J.H. (Eds.), Spinal Control: The Rehabilitation of Back pain. Churchill Livingstone.

Reeves, N.P., Everding, V.Q., Cholewicki, J., Morrisette, C., 2006. The effects of trunk stiffness on postural control during unsatble seated balance. Experimental Brain Research 174, 694-700.

Sato, K., kikuchi, S., Yonezawa, T., 1999. In vivo intradiscal pressure measurement in healthy individuals and in patients with ongoing back problems. Spine 24, 2468-2474.

Shahvarpour, A., Shirazi-Adl, A., Larivière, C., Bazrgari, B., 2015. Trunk active response and spinal forces in sudden forward loading – Analysis of the role of perturbation load and pre-perturbation conditions by a kinematics-driven model. Journal of Biomechanics 48, 44-52.

Shahvarpour, A., Shirazi-Adl, A., Mecheri, H., Larivière, C., 2014. Trunk response to sudden forward perturbation - Effects of preload and sudden load magnitudes, posture and abdominal muscle preactivation. Journal of Electromyography and Kinesiology 24, 394-403.

Shirazi-Adl, A., 2006. Analysis of large compression loads on lumbar spine in flexion and in torsion using a novel wrapping element. Journal of Biomechanics 39, 267-275.

Shirazi-Adl, A., Drouin, G., 1988. Nonlinear gross response analysis of a lumbar motion segment in combined sagittal loadings. Journal of Biomechanical Engineering 110, 216-222.

Slota, G.P., Granata, K.P., Madigan, M.L., 2008. Effects of seated whole-body vibration on postural control of the trunk during unstable seated balance. Clinical Biomechanics 23, 381-386.

Tanaka, M.L., Nussbaum, M.A., Ross, S.D., 2009. Evaluation of the threshold of stability for the human spine. Journal of Biomechanics 42, 1017-1022.

Tanaka, M.L., Ross, S.D., Nussbaum, M.A., 2010. Mathematical modeling and simulation of seated stability. Journal of Biomechanics 43, 906-912.

Todorov, E., Jordan, M.I., 2002. Optimal feedback control as a theory of motor coordination. nature neuroscience 5, 1226-1235.

van Dieen, J.H., Cholewicki, J., Radebold, A., 2003. Trunk muscle recruitment patterns in patients with low back pain enhance the stability of the lumbar spine. Spine 28, 834-841.

Willigenburg, N.W., Kingma, I., Van Dieen, J.H., 2013. Center of pressure trajectories, trunk kinematics and trunk muscle activation during unstable sitting in low back pain patients. Gait and Posture 38, 625-630.

Winter, D.A., 2009. Biomechanics and motor control of human movements, 4th ed. John wiley & Sons, Inc.

Yamamoto, I., Panjabi, M.M., Crisco, T., Oxland, T., 1989. Three-dimensional movements of the whole lumbar spine and Lumbosacral joint. Spine 14, 1256-1260.

Zatsiorsky, V.M., Seluyanov, V.N., 1983. The mass and inertia characteristics of the main segments of the human body Biomechanics. Champaign: Human Kinetics Publishers, pp. 1152-1159.

Table 6.1 The anthropometric data of 12 male subjects considered in this model study

Subjects	**Body Mass (Kg) Mean (Range)**	**Body Height (cm) Mean (Range)**
Healthy controls	81.2 (29)	178 (9)
CLBP patients	82.8 (18.9)	179 (7)
All	82.0 (29)	178.5 (9)

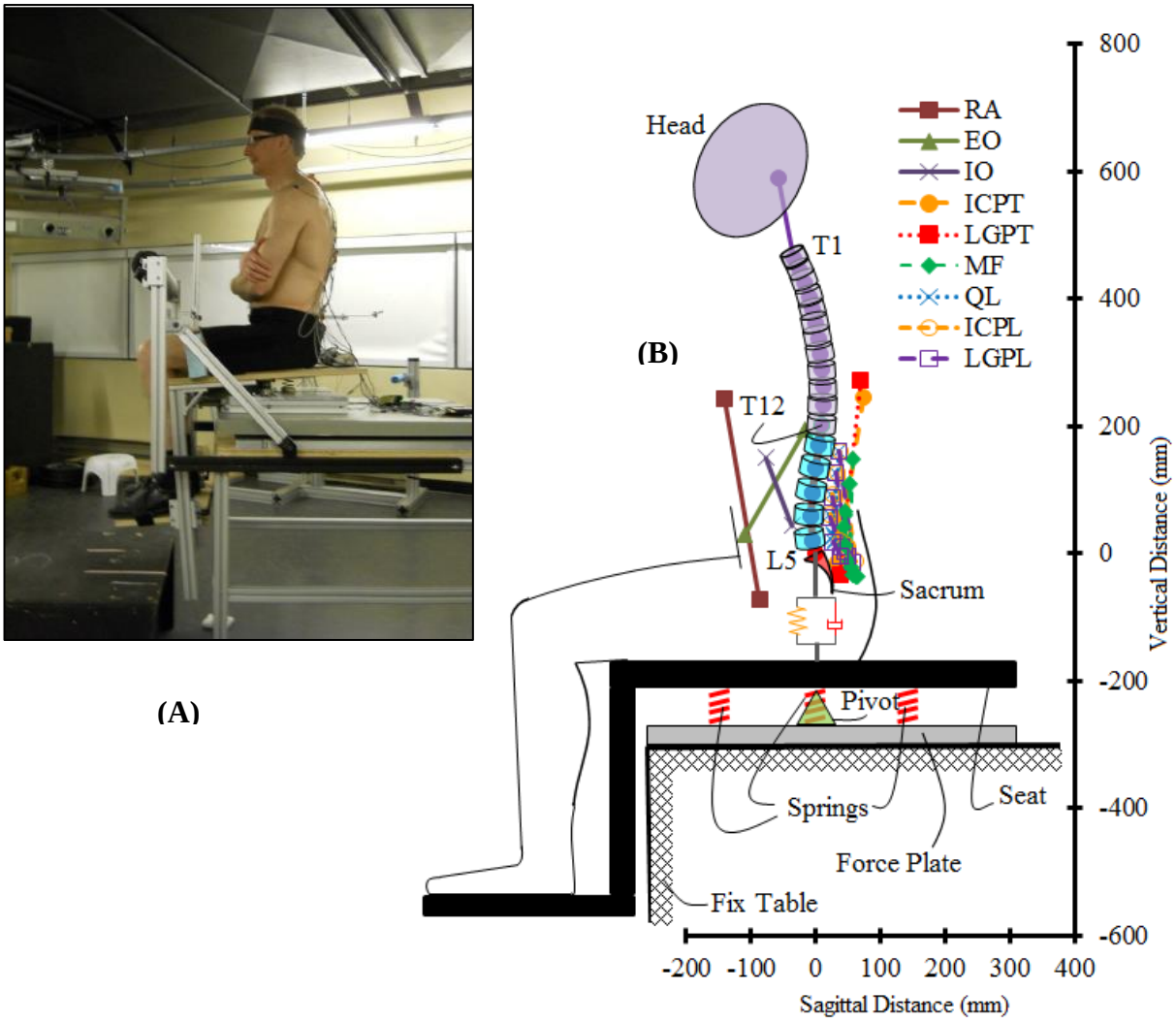

Figure 6.1 The side view photo of a subject sitting on the wobble chair (A) and a schematic sagittal view of the finite element model of the subject seated on the wobble chair. RA: rectus abdominus, EO: external oblique, IO: internal oblique, ICPT: iliocostalis lumborum pars thoracic, LGPT: longissimus thoracis pars thoracic, MF: multifidus, QL: quadratus lumborum, ICPL: iliocostalis lumborum pars lumborum, LGPL: longissimus thoracis pars lumborum.

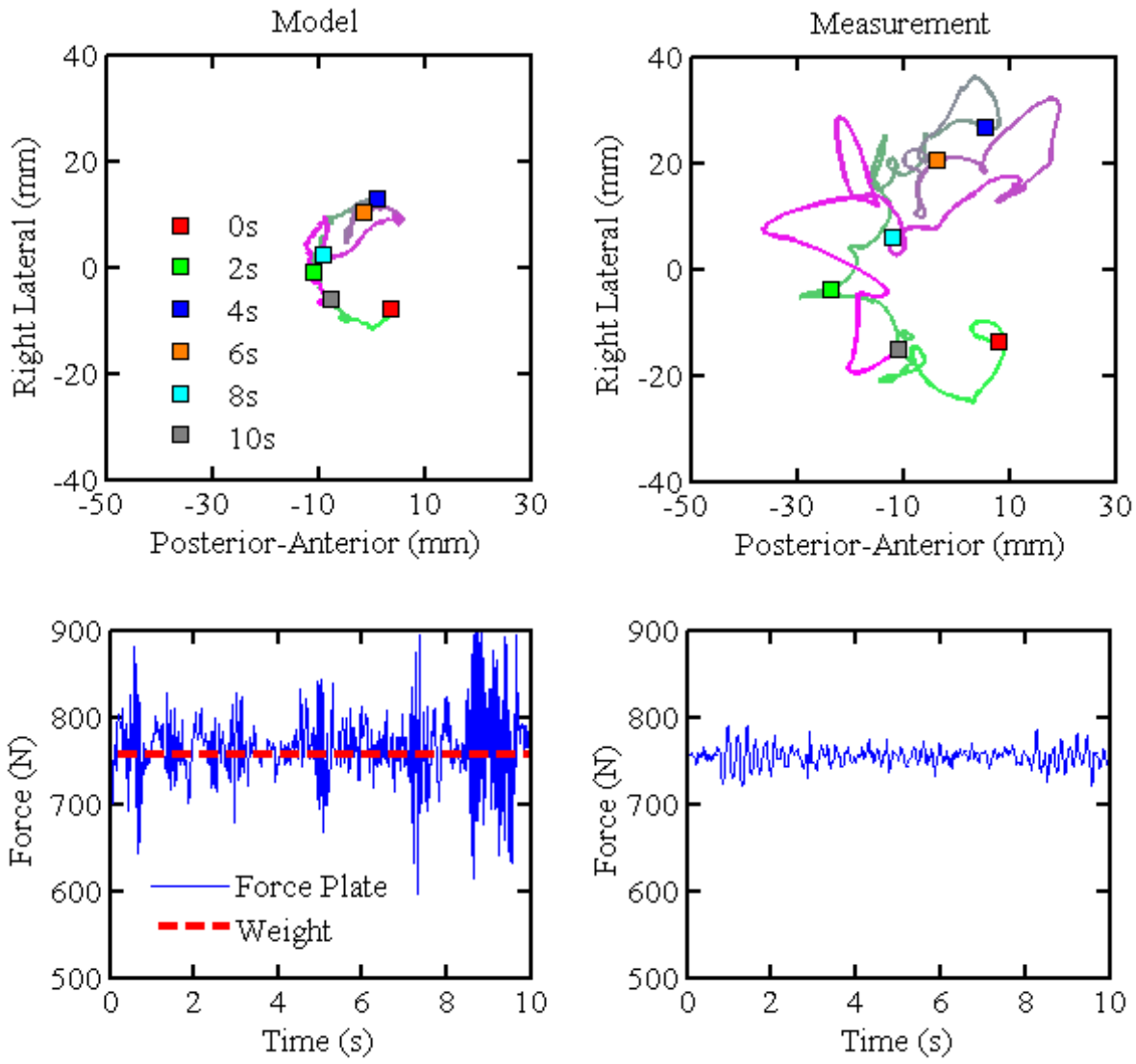

Figure 6.2 Model-estimated (left) and measured (right) loci of the center of pressure (top) and the vertical reaction force on the force plate (bottom) for a healthy subject (mass of 75.3 kg and height of 177 cm). The mass of the measurement accessories and subject's shoes is 1.94 kg (weight = (75.3+1.94) × 9.81 N). In top figures, the color at the beginning t = 0 s is light green that changes to dark green, pink and finally purple as time advances to 10 s. Squares show the time segments.

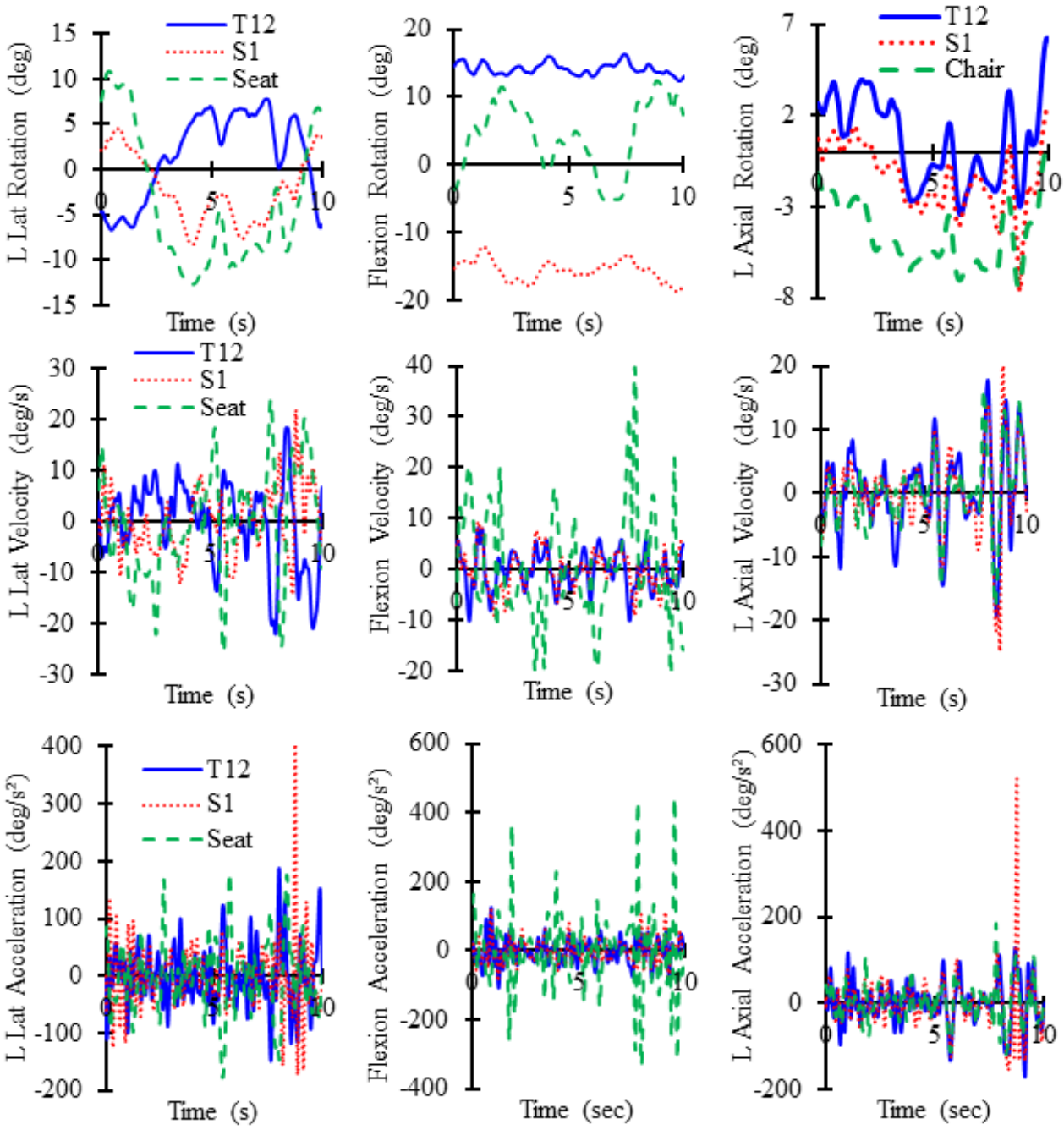

Figure 6.3 Flexion, left (L) lateral and axial rotations, angular velocity and angular acceleration (Ang. Accel.) of the seat and the trunk at T12 and S1 illustrated for a healthy subject (mass = 75.3 kg and height = 177 cm). The origin of rotation is set at relaxed sitting posture.

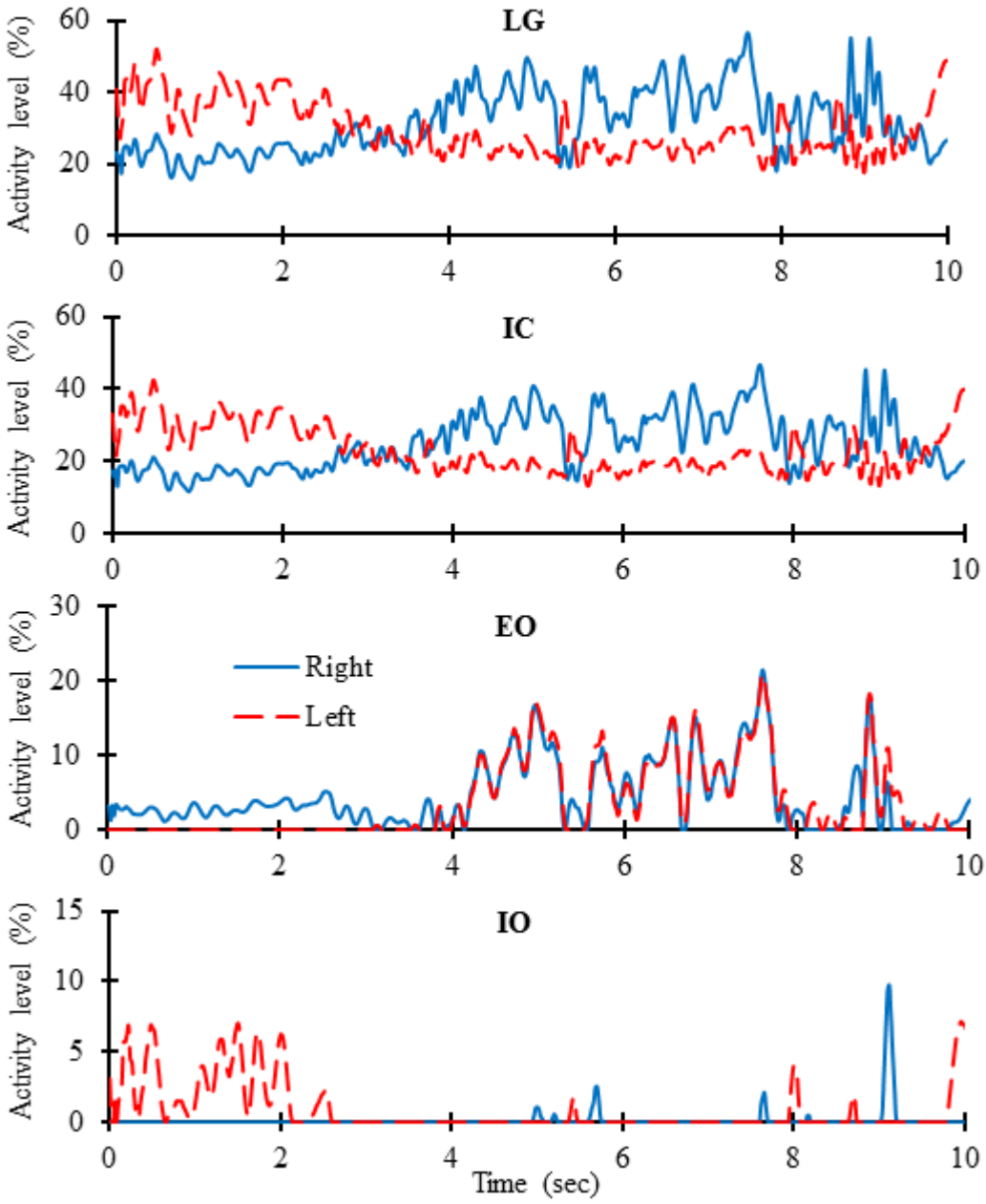

Figure 6.4 Activity of global muscles normalized to 0.6 (MPa) × PCSA (mm^2) illustrated for a healthy subject (mass = 75.3 kg and height = 177 cm). No activity was calculated for RA muscle.

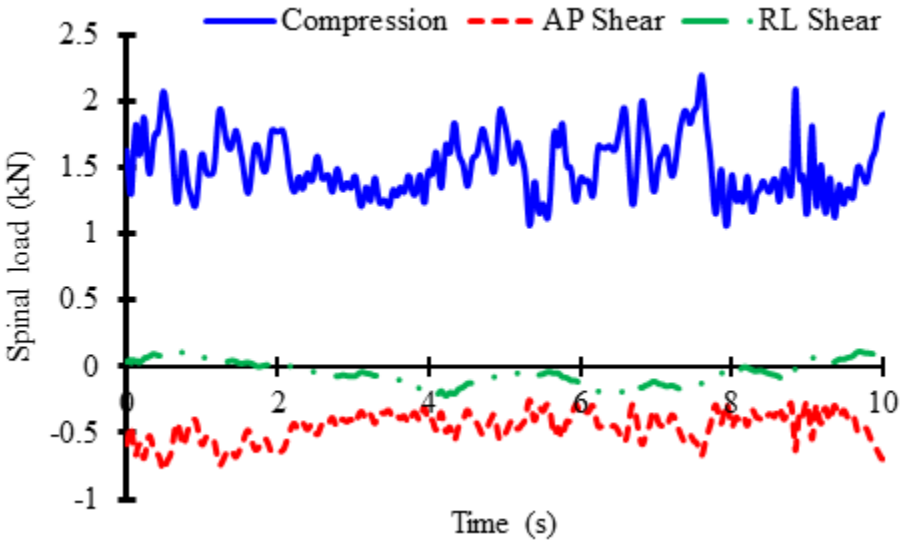

Figure 6.5 Predicted compression, AP shear and RL shear illustrated for a healthy subject (mass = 75.3 kg and height = 177 cm).

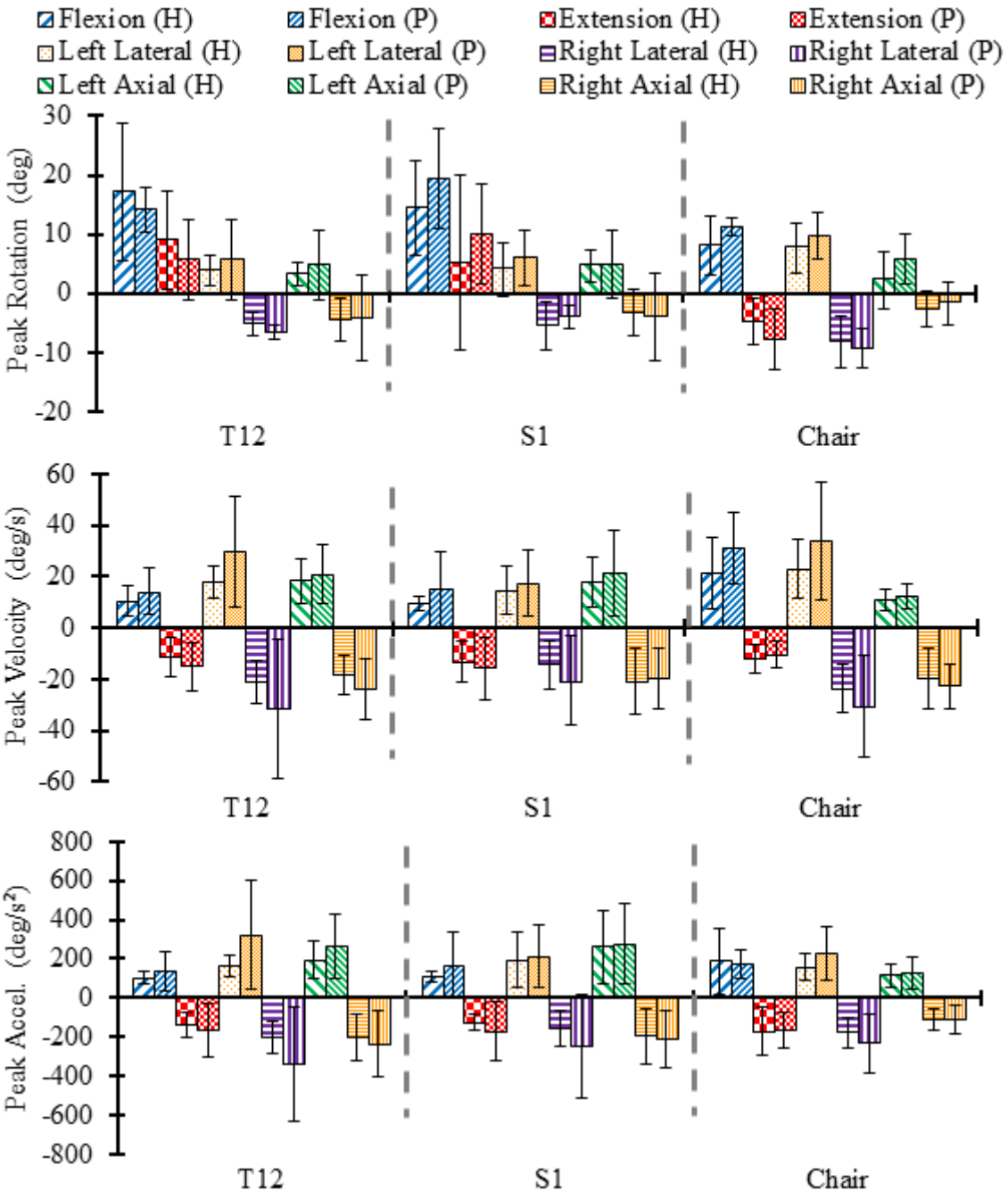

Figure 6.6 Peak rotation, angular velocity and acceleration (Accel.) (mean ± SD) of the seat and the trunk at the T12 and S1 levels in 3 directions (averaged over 6 healthy (H) controls and 6 patients (P)).

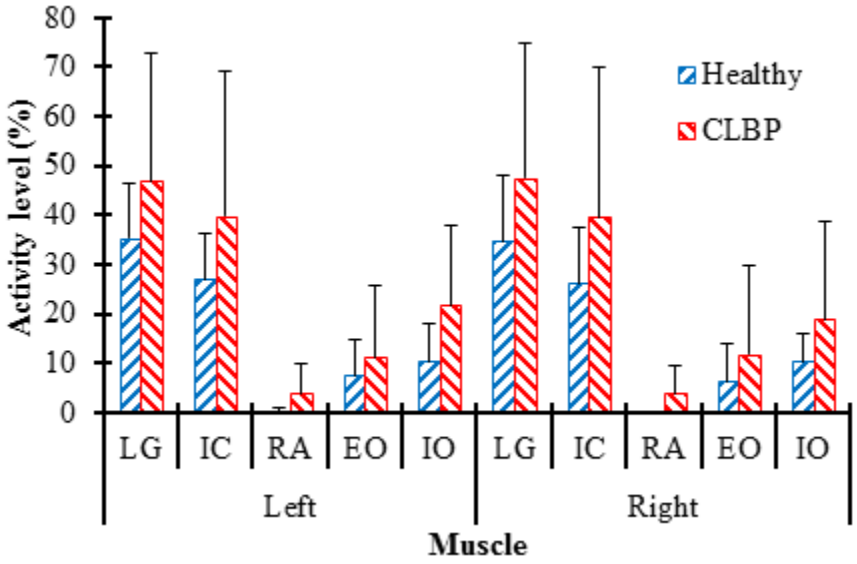

Figure 6.7 Peak estimated activity [normalized to 0.6 (MPa) × PCSA (mm^2)] of left and right global thoracic muscles averaged over 6 healthy and 6 CLBP subjects.

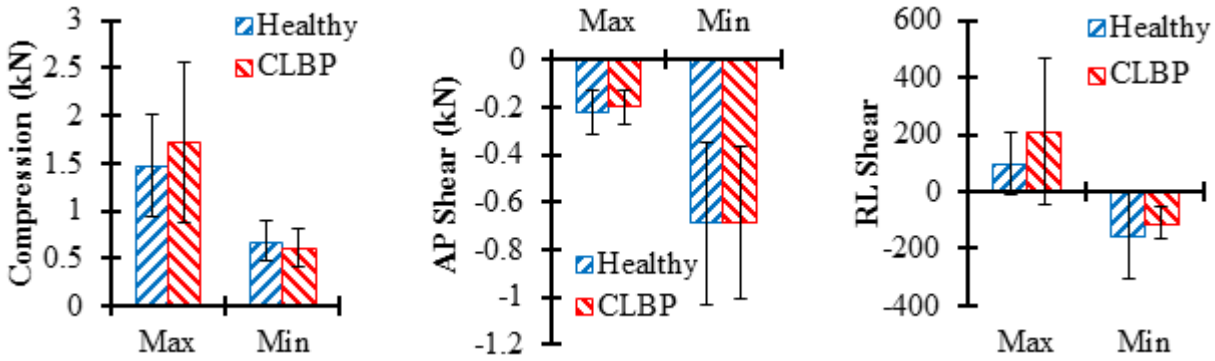

Figure 6.8 Maximum and minimum estimated compression, anterior-posterior (AP) shear and right-left (RL) shear forces at mid-height of the L5-S1 disc average across 6 healthy and 6 CLBP subjects illustrated.

CHAPTER 7 GENERAL DISCUSSION

Biodynamics of spine subject to external load perturbations was investigated in two separate studies. In the first combined experimental-model study of 12 asymptomatic subjects, the effect of pre-perturbation conditions, i.e. preload (5 N vs 50 N), initial trunk flexion (upright standing vs 20-degree flexion) and abdominal antagonistic preactivation (none vs 10% MVC at EO) and post-perturbation load (50 N vs 100 N) on trunk response, muscle forces, spinal loads and trunk stability was investigated. In the second study, using recorded data of measurements on 36 subjects (Larivière et al., 2015; Larivière et al., 2013), muscle forces and spinal loads were calculated for 12 subjects while maintaining their balance on a wobble chair. These studies were carried out to improve our understanding of the trunk functional biodynamics (i.e., muscle voluntary and reflex activities, spinal forces and stability) and parameters affecting them under sudden loading and seated balance-challenged conditions. These studies should help in evaluation and prevention of risk to injury as well as rehabilitation and treatment of spinal disorders.

7.1. Computational issues

Angular velocity profiles of the trunk, pelvis and lumbar vertebrae calculated by the derivative of measured displacements (sampling frequency = 50 HZ) were prescribed into the FE model as recommended by the package program itself (Abaqus tutorial). In the finite element model of the trunk, each intervertebral disc was modeled by shear-deformable quadratic beam elements. To determine the appropriate number of beam elements representing each intervertebral disc, mesh refinement was initially carried out in each simulation, i.e. in-sagittal sudden perturbation and spatial challenged seated-posture. Following preliminary convergence studies, each disc was represented by two beams in sudden perturbation studies while for 3D simulation of challenged seated balance three beams were used. Implicit integration with Hilber-Hughes-Taylor (HHT) integration algorithm (Hilber et al., 1977), which provides second order accuracy, has been used in FE analysis. Time increment was selected automatically by Abaqus, while the time increment was constrained to be greater than 10^{-5} and smaller than Δt = 0.02 sec.

At each time step and subject to prescribed kinematics-kinetics, the required moments at each vertebral level calculated by the nonlinear FE program were partitioned into muscle forces inserted into that level using an optimization algorithm. The optimization on minimum sum of

cubed muscle stresses was solved by fmincon function in Matlab that calculates the local minimum of the objective function with nonlinear constraints. This function uses interior point method to solve the optimization. The preliminary tests in 2D (in sagittal movements) revealed that this function was able to find the global minimum irrespective of the initial guess with high accuracy as the analytical solutions in 2D motions were available for comparison. However, to ensure that the calculated minimum at time t_n is the global minimum, the function was set to use the solution (muscle forces) of the previous time step, $t_{n-1} = t_n - \Delta t$, as the initial guess. Since the muscle force profiles and their derivatives are continuous, the solution at t_{n-1} is very close to the solution at t_n. Starting the search for minimum from a very close point to the global minimum helps the function to find the global minimum. This technic has been used in three-dimensional modeling as the analytical solution is not available.

7.2. Spine response under external perturbations

7.2.1. Preload

Results of experimental and model studies on the effect of trunk preload (50 N vs 5 N) on various parameters are listed in Table 7.1. Pre-perturbation back muscles activity (EMG) and predicted forces increased when trunk was preloaded. This was expected as back muscles maintained equilibrium against the anterior-directed preload. After the perturbation, additional muscle forces were required to maintain equilibrium. Muscles reflex latency was estimated at 30-129 ms range when reflex onset was detected by SD method and at 32-144 ms when the onset was detected by AGLR method. Neither muscles reflex latency nor muscles reflex amplitude calculated from the recorded EMG was affected by the preload except the latency of IC muscle when onset was detected by SD method. This observation is in agreement with studies that report no alterations in muscles reflexive response when trunk is preloaded (Andersen et al., 2004; Krajcarski et al., 1999; Stokes et al., 2000). However, our model studies find that both muscle force latency and muscles peak active force decrease significantly at higher preload. This could be due to lower critical stiffness coefficient pre-perturbation (Pre-q) that shows preloading the trunk increases trunk stiffness and enhances trunk stability pre-perturbation that decrease the demand for reflex response as observed by others as well (Brown and McGill, 2009; Brown and McGill, 2008; Granata et al., 2004; Moorhouse and Granata, 2007). Although the trunk displacement remained unchanged, lower peak velocity and acceleration of trunk after

perturbation might be due to this higher pre-perturbation stiffness. Previous studies reported lower rotation of trunk under preload (Granata et al., 2004; Krajcarski et al., 1999). Higher sensitivity in measured kinematics, particularly angular velocity and acceleration components, in comparison to surface EMG as preload changes indicates the power of our kinematics-driven model in more precise evaluation of trunk response.

In contrast to the T12 (thorax) level, required moments (moments resisted by forces in muscles) at lumbar levels as well as peak active forces in local muscles were not affected by changes in the preload. Small changes in spinal forces at the L5-S1 were estimated; compression reduced from 5184 N to 5046 N while shear force dropped from 2181 N to 2115 N (Figure 3.4f).

Table 7.1 Effect of preload, sudden load, initial trunk flexion and abdominal preactivation on muscles EMG and forces, kinematics, spinal loads and stability. All the listed effects are statistically significant except when indicated by NS (not significant).

	Variable	Preload	Initial Trunk Flexion	Abdominal Preactivation	Sudden load
EMG (Experiment)	Preactivation	↑	↑	↑	-
	Reflex latency	NS	↑ in LG and MF	NS	NS
	Reflex amplitude	NS	NS	↑ in IC and MF	↑
Muscle Force (Model)	Pre-pert. active	↑	↑	↑	-
	Force latency	↓	NS	NS	NS
	Post-pert. active	↑	↑	NS	↑
Kinematics	Displacement	NS	NS	NS	↑
	Velocity	↓	↑	NS	↑
	Acceleration	↓	↑	NS	↑
Spinal Load at L5-S1 (Model)	Compression	NS	↑	NS	↑
	AP shear	NS	↑	NS	↑
Stability (Model)	Pre-q	↓	↓	↓	NS
	Post-q1	NS	↓	↓	NS
	Post-q2	NS	↓	↓	↓
	Post-q3	NS	↓	NS	↓

7.2.2. Initial trunk flexion

Active and passive intrinsic trunk stiffness increased substantially (smaller Pre-q) due to large flexion angle and resulting higher activity in muscles (Adams and Dolan, 1991; Arjmand and Shirazi-Adl, 2006a; Granata and Rogers, 2007; Granata and Wilson, 2001; McGill et al., 1994; Shirazi-Adl, 2006). In spite of the expectation to see lower muscles reflexive activity due

to larger intrinsic stiffness before perturbation, muscle reflex amplitude (EMG) remained unchanged and model-predicted muscles active force amplitude increased. The reason could be the larger gravity moment acting in larger flexion angles. Trunk margin of stability was significantly larger through the entire time, pre- and post-perturbations. Larger spinal loads were estimated when trunk was initially flexed (Figure 4.5f). The peak compression force of 3857 N (at the L5-S1) found in the model with initial upright posture increased considerably by 1432 N to 5289 N in presence of initial trunk flexion. However, lower ratio of peak compression to pre-perturbation compression in presence of flexion suggests a smaller relative increase in post-perturbation compression in C5. Based on the results, initial flexion increases the risk of injury in forward perturbations. s

7.2.3. Abdominal antagonistic pre-activation

Biomechanical and stability variables at C6 (preload = 5 N, sudden load = 100 N and EO preactivation = 10%) were compared to C2 (preload = 5 N, sudden load = 100 N and no abdominal preactivation). Initial investigation of recorded EMG showed that back muscles were activated prior to the perturbation to counterbalance the moment generated by activated abdominal muscles. This observation was confirmed with FE modeling results. Higher muscles activation pre-perturbation decreased stiffness coefficient, Pre-q, indicating the effect muscles in improving stability.

After perturbation, peak normalized EMG of IC and MF were higher with respect to C2; however, peak muscle forces were not affected. Significantly smaller stiffness coefficients after perturbation, Post-q1 and Post-q2, indicate positive effect of muscles in enhancing spinal stability. The stabilizing effect of muscles however disappeared after 250 ms post-perturbation. Spinal loads as well as trunk displacement, velocity and acceleration were not affected post-perturbation.

7.2.4. Sudden load

Expectedly, sudden load did not affect the kinematics and muscle forces pre-perturbation; however, it affected kinematics, muscle forces and stability measures post-perturbation. Post-q1 was not affected as muscle forces have not yet kicked in to dynamics of motion during this period of time. Larger muscle reflexive forces generated in response to larger sudden load improved

trunk stability after the perturbation. Larger sudden load did not affect the reflex latency of EMG and muscle force. Due to larger muscle forces, spinal loads increased significantly with sudden load indicating higher risk of injury. Larger displacement, velocity and acceleration have been measured when sudden load was larger.

7.2.5. Validation

For validation of the results, model-predicted muscle forces were compared to the normalized recorded EMG of muscles. The temporal patterns of force and EMG were similar; however, the muscle force latency was ~120 ms (averaged for LG across 12 subjects and 6 conditions) delayed with respect to EMG. This value that was calculated as the difference between the onset of EMG and the onset of force was interpreted as the muscle electromechanical delay. It was not affected statistically by the any of the independent experimental variables.

7.3. Spine response in unstable sitting

A 3D nonlinear kinematics-driven FE model of spine was employed to calculate muscle forces and spinal loads when subjects were seated on a wobble chair attempting to maintain their balance. Among 36 male and female healthy and low back pain patients tested in a parallel study ((Larivière et al., 2015; Larivière et al., 2013)), 6 healthy and 6 CLBP males with close anthropometry to our FE model were selected. Driven by the measured velocity of trunk in three planes of motion, kinematics-driven finite element model calculated muscle forces at each intervertebral level using optimization. Spinal forces were then estimated at mid-height of each intervertebral disc.

Results revealed no statistical difference in estimated biomechanical measures between healthy controls and patients. Axial angular displacement, velocity and acceleration of the chair was smaller than those in other planes of motion due to constrained axial rotation of the chair. However, axial rotation, peak velocity and peak acceleration were greater at the T12 level relative to those in other planes indicating the likely control strategy of the CNS to maintain stability. The strategy of CNS in allowing variability in low-cost task-irrelevant directions (in this case task is stability maintenance) in order to control the high-cost task relevant directions has been suggested (Todorov and Jordan, 2002).

Pain status of subjects did not influence spinal loads. The mean compression of 12 subjects at mid-height of L5-S1 disc varied between 938 to 1382 N, which is higher than mean compressions in static sitting of 768 N predicted in this study 690 N computed elsewhere (Bazrgari et al., 2008a) and 900 N derived from in vivo IDP measurements (Nachemson and Morris, 1964; Sato et al., 1999). Higher spinal load is due to additional activity in muscles required for maintaining balance.

For validation, a model of chair, buttocks and lower extremities were developed and analyzed under loading calculated at the S1 and measured kinematics. Loci of CoP and the vertical reaction force on the force plate were calculated and compared to measured values. The outlines of the model-estimated CoP and the measured CoP were in good agreement such that mean correlations of CoP loci were found 0.91 and 0.9 in AP and LR directions, respectively. However, the excursions of the measured CoP in both AP and LR directions were much larger by 267% and 191% relative to the model-predicted excursions. This could be the effect of differences in the anthropometric data, i.e. mass, mass moment of inertia and the position of the center of masses, between the subjects and the FE model. Moreover, the masses of the subject`s shoes and measurement accessories, i.e. marker clusters, etc., were not considered in the model. Strong correlation was however found between the total vertical reaction forces measured by the force plate and predicted by the model.

7.4. Limitations

The geometry of the musculoskeletal FE model, i.e. body height, lumbar lordosis, sacral slope, plumb line, disc heights, musculature, etc., was fixed in spite of likely differences between subjects. Accordingly, muscle cross sectional areas, their insertion and origin points as well as muscle lever arms could vary from one subject to another (Hajihosseinali et al., 2015). Despite the fact that we chose subjects with body heights and weight as close as possible to those in our model, however, such variations could influence the predictions.

In addition, material properties of discs, facets, vertebrae and ligaments that alter due to changes in their properties, dimensions and degeneration state were taken identical for all subjects. Moreover, no viscoelastic effect was considered in modeling tissues. Predictions are likely affected by these assumptions.

The inertial properties of trunk, head and arms, i.e. mass, mass moments of inertia and center of mass, at each vertebral level were modeled based on mean values reported in the literature (de Leva, 1996; Pearsall et al., 1996; Zatsiorsky and Seluyanov, 1983). The inertial properties were remained constant in our simulations.

Moreover, wobbling of abdominal and chest soft tissues that may happen during fast movements such as perturbation or vibration was neglected in this study. It has been reported that neglecting the wobbling masses in modeling of trunk could amplify the impact of the perturbation load to the spine that increases the demand for muscle forces and overestimates the spinal loads in consequence (Bazrgari et al., 2011).

Another concern is in estimation of thorax, pelvis and lumbar vertebrae rotations through measured rotations of pelvis and trunk by the potentiometer or marker clusters and infra-red cameras. In trunk perturbation study, pelvis movement was restrained while trunk motion was measured by a potentiometer attached to the harness placed at the T8 level. Although the position of the harness was checked during the experiments, however, its slight slippage on the skin was likely during experiments. Measured displacement at the T8 level was mapped to the thorax rotation using our FE model assuming that a fixed pelvis. In simulating the three-dimensional movement of the trunk on a wobble chair, marker clusters were attached on the skin at the S1, T12, C7 and head. Motions of the clusters relative to the spine due to the relative movement of skin and soft tissues in between could influence the accuracy of recorded displacements. In all simulations of 2D perturbations in the sagittal plane and 3D challenged stability on the wobble chair, the total lumbar rotations in different planes were partitioned among the lumbar vertebrae based on the values reported in the literature (Bazrgari et al., 2009b).

Recorded muscles superficial EMG profiles were used for qualitative validation of the predicted muscle forces. Unfortunately, skin and the underneath fat tissues may influence the EMG signals recorded by electrodes. On the other hand, EMG of flat muscles such as external and internal oblique muscles could not be properly measured by single skin electrodes. And finally, recording EMG of deep muscles is limited due to their cross-talk with more superficial muscles. All these limitations plus subsequent filtering interventions could have influenced the recorded EMG of muscles during experiments and MVC tasks.

Back pain and spinal injuries may affect the muscles coordination, their response and neural control strategies in order to reduce or prevent the pain. In the wobble chair study, musculature properties (e.g., cross sectional area) were considered similar for both normal and LBP subjects that might have affected the results. The biomechanical measures of challenged seated balance were found only slightly different between healthy and CLBP groups, however, with no statistical significance. The low number of subjects in each group might have played a role.

Table 7.2 Pearson correlation coefficient (Corr.) and maximum difference (Max) between the measured rotations (by the skin markers in the wobble chair tests) at the T12 and the C7 levels in three planes of motion. * indicates clinical low back pain subjects

Subject	Flexion-Extension		Lateral Bending		Axial Rotation	
	Corr.	Max (deg)	Corr.	Max (deg)	Corr.	Max (deg)
1	0.83	8.2	0.06	5.2	0.12	5.0
2	0.26	3.4	0.03	5.3	0.31	4.7
3	0.83	9.3	0.65	11.7	0.41	11.8
4	0.93	3.2	0.92	7.3	0.85	5.1
5*	0.88	9.4	0.57	15.7	0.93	4.6
6*	0.79	9.0	0.79	14.3	0.52	15.6
7	0.81	3.3	0.50	6.4	0.88	5.6
8*	0.71	6.5	0.47	7.4	0.85	6.9
9*	0.71	3.7	0.43	6.83	0.57	9.1
10	0.89	3.3	-0.34	10.8	0.43	9.2
11*	0.66	11.5	-0.32	10.0	0.82	6.3
12*	0.35	12.5	0.34	6.6	0.37	3.9
Average (Healthy)	0.76	5.1	0.30	7.78	0.5	6.9
Average (CLBP)	0.69	8.2	0.37	9.8	0.6	7.6
Total Average	0.72	6.9	0.34	9.0	0.59	7.3

The measured rotations at the T12 and C7 were different (Table 7.2) in all three planes of motion indicating the deformability of the thoracic spine that was neglected in the model. No significant difference was seen between healthy and CLBP groups. The average Pearson correlation coefficient (across 12 subjects) between rotations at the C7 and at the T12 was maximum in the sagittal plane with 0.72 and minimum in the transverse plane with 0.59. No specific pattern was noted among the subjects; the correlation was strong (> 0.9) in some cases while it is even negative in some others. In the FE model the T1-T12, neck, head and hands were considered rigidly connected and the T12 rotations were applied to this upper trunk rigid body. This could be another limitation of this study as the thorax rotation could have been adjusted

accordingly or more degrees of freedom been added to the model as will be discussed in the next section on future works. A recent study measured the share of the T1-T12 segments in the total trunk forward flexion at 16-20% (Hajibozorgi and Arjmand, in press).

CHAPTER 8 CONCLUSION AND RECOMMENDATIONS

In the first study, the effect of preload, sudden load, initial flexion of trunk and abdominal antagonistic preactivation on kinematics, muscles EMG, muscle forces, spinal loads and stability were investigated using kinematics-driven detailed FE model of trunk. It was found that (1) trunk stability was enhanced due to larger contribution of active-passive components when preload, initial trunk flexion angle and abdominal preactivation increased; (2) initial (pre-perturbation) conditions influenced the trunk response both pre- and post-perturbation; (3) preload caused higher active intrinsic stiffness and decreased back muscles reflexive activity; (4) the demand for reflex response increased under initial flexed posture in spite of higher intrinsic active-passive stiffness as net moment and spinal loads increased significantly in consequence; (5) abdominal preactivation did not change muscle forces but the prolonged muscles coactivity that disappeared gradually after perturbation enhanced stability pre- and post-perturbation; (6) higher perturbation load magnitude increased both the margin of stability and the spinal loads; (7) higher sensitivity to independent variables found in trunk velocity and acceleration profiles as compared to collected muscle EMG, highlighted the capability of the kinematics-driven FE model in decoding the input kinematics and in predicting the effect of changing variables on muscle forces, spinal loads and stability.

Challenged seated balance task was investigated using a kinematics-driven FE model of trunk; muscle forces and spinal loads were evaluated. The effects of subjects pain status was investigated on muscle forces and spinal loads. The results revealed no statistical difference between healthy and CLBP groups. The root mean square (RMS) compression force at the L5-S1 during 10 s simulation duration was 1011 (±319) N and 1055 (±218) N in healthy and CLBP groups, respectively. The average spinal compression and shear forces increased (by about 50%) relative to those in relaxed sitting. They remained nevertheless low enough not to cause any injury.

8.1. Future works

Although the kinematics-driven FE model used in this study includes numerous physiological aspects of human spine, however, it makes also some assumptions that could influence predictions. The result of this study revealed that rotations at the T1 or C7 level could

be different from that at the T12 level (Table 7.2). Consideration of flexibility of the spinal column at the thoracic region, T1-T12, that is neglected in our model could improve the accuracy in computed muscle forces, spinal loads and stability margin. As indicated earlier, the contribution of the T1-T12 segments to the trunk flexion has been estimated at 16-20% (Hajibozorgi and Arjmand, in press).

One of the advantages of the kinematics-driven model is its ability to compute the muscle forces while optimizing sum of cubic or squared muscles stresses and satisfying equations of motion at all levels and directions. In addition, the model is driven by measured kinematics that makes it a biologic approach capable of capturing inter- and intra-subject variability in performance. Different methods of optimization however may change the muscle forces although equations of motions are still satisfied. In Dynamic motions, kinematics-driven model solves the optimization at very small time steps while marching ahead being driven by measured kinematics from the beginning to the end of motion. In this sense, the accuracy of collected kinematics and subsequent filtering modifications could influence model predictions. One concern is if CNS acts similarly by assigning muscle forces at each instance of time. Previous studies on motor behavior suggest that motor planning is based on noisy and delayed information of the state of the body, i.e. its position and velocity, final goal of the system and the routine performance developed due to learning and evolution (Jordan and Wolpert, 1999; Scott, 2004; Todorov, 2004; Todorov and Jordan, 2002). High-level neural control centers, such as cortex, modify the planned patterns as needed during the motion and low-level neural control centers, like spinal cord, interfere in case of error or perturbations. Based on these theories, trajectory-based forward optimization methods could unravel some physiologically-relevant results (Li and Todorov, 2007; Li et al., 2005).

In this study, spine stability was evaluated by replacing muscles with springs whose stiffness is calculated using Bergmark's formulation (Bergmark, 1989a) and testing the stability of the vertebral column by static or dynamic methods, such as buckling, perturbation and natural frequency analyses. In dynamic simulations, this algorithm is repeated at every time step from the beginning of motion to the end. The linear stiffness-force relation assumed here and an identical muscle coefficient q for all muscles remain of concern. Bergmark`s force-stiffness relationship is based on short-range stiffness of muscles (Morgan, 1977) that does not account for high-level control strategies and middle-level reflexive interferences. Therefore, temporal events such as

neuromuscular effect of noise are not considered in this formulation. Lyapunov exponents can measure stability of a system when its state is moving through a trajectory in a state space as time goes to infinity. It evaluates if the neighboring trajectories of the current trajectory are converging or diverging. The system is stable in case of convergence and it is unstable in case of divergence. Lyapunov exponents could provide an estimation of the eigenvalues of the state matrix of the linearized system (Shadden et al., 2005). Then a constrained trajectory-based optimization (as described in the previous paragraph) could be used to calculate muscle forces with the eigenvalues of the system's state matrix being equal to Lyapunov exponents.

BIBLIOGRAPHY

Acaroglu, E.R., Iatridis, J.C., Setton, L.A., Foster, R.J., Mow, V.C., Weidenbaum, M., 1995. Degeneration and aging affect the tensile behavior of human lumbar anulus fibrosus. Spine 20, 2690-2701.

Adams, M.A., Bogduk, N., Burton, K., Dolan, P., 2012. The Biomechanics of Back Pain, Third ed. Churchill Livingstone, Edinburgh.

Adams, M.A., Dolan, P., 1991. A technique for quantifying the bending moment acting on the lumbar spine in vivo. Journal of Biomechanics 24, 11-126.

Andersen, T.B., Essendrop, M., Schibye, B., 2004. Movement of the upper body and muscle activity patterns following a rapidly applied load: the influence of pre-load alterations. European Journal of Applied Physiology 91, 488-492.

Anderson, C.K., Chaffin, D.B., Herrin, G.D., Matthews, L.S., 1985. A biomechanical model of the lumbosacral joint during lifting activities. Journal of Biomechanics 18, 571-584.

Andersson, G.B., Ortengren, R., Nachemson, A., 1977. Intradiskal pressure, intra-abdominal pressure and myoelectric back muscle activity related to posture and loading. Clinical orthopaedics and related research, 156-164.

Andersson, T.B., Essendrop, M., Schibye, B., 2004. Movement oof the upper body and muscle activity patterns following a rapidly applying load: the influence of pre-load alterations. European Journal of Applied Physiology 91, 488-492.

Antoniou, J., Steffen, T., Nelson, F., Winterbottom, N., Hollander, A.P., Poole, R.A., Aebi, M., Alini, M., 1996. The human lumbar intervertebral discs: evidence for changes in the biosynthesis and denaturation of the extracellular matrix with growth, maturation, ageing, and degeneration. The Journal of Clinical Investigation 98, 996-1003.

Arjmand, N., 2006. Computatinal biomechanics of the human spine in static lifting tasks. École Polytechnique de Montréal, Montreal.

Arjmand, N., Plamondon, A., Shirazi-Adl, A., Larivière, C., Parnianpour, M., 2011. Predictive equations to stimate spinal loads in symmetric lifting tasks. Journal of Biomechanics 44, 84-91.

Arjmand, N., Shirazi-Adl, A., 2005. Biomechanics of changes in lumbar posture in static lifting. Spine 30, 2637-2648.

Arjmand, N., Shirazi-Adl, A., 2006a. Model and in vivo studies on human trunk load partitioning and stability in isometric forward flexions. Journal of Biomechanics 39, 510-521.

Arjmand, N., Shirazi-Adl, A., 2006b. Role of intra-abdominal pressure in the unloading and stabilization of the human spine during static lifting tasks. European Spine Journal 15, 1265-1275.

Arjmand, N., Shirazi-Adl, A., 2006c. Sensitivity of kinematics-based model predictions to optimization criteria in static lifting tasks. Medical Engineering and Physics 28, 504-514.

Arjmand, N., Shirazi-Adl, A., Bazrgari, B., 2006. Wrapping of trunk thoracic extensor muscles influences muscle forces and spinal loads in lifting tasks. Clinical Biomechanics 21, 668-675.

Arjmand, N., Shirazi-Adl, A., Parnianpour, M., 2007. Trunk biomechanical models based on equilibrium at a single-level violate equilibrium at other levels. European Spine Journal 16, 701-709.

Ashton-Miller, J.A., Schultz, A., 1997. Biomechanics of the Human Spine, in: Mow, V., Hayes, W. (Eds.), Basic Orthopaedic Biomechanics. Wolters Kluwer Publisher, Philadelphia, pp. 353-393.

Axler, C.T., McGill, S.M., 1997. Low back loads over a variety of abdominal exercises: Searching for the safest abdominal challenge. Medicine and Science in Sports and Exercise 29, 804-811.

Baloh, R.W., Jacobson, K.M., Enrietto, J.A., Corona, S., Honrubia, V., 1998. Balance disorders in older persons: Quantification with posturography. Otolaryngology - Head and Neck Surgery 119, 89-92.

Bazrgari, B., 2007. Biodynamics of the spine. École polytechnique, Montreal.

Bazrgari, B., Nussbaum, M.A., Madigan, M.L., Shirazi-Adl, A., 2011. Soft tissue wobbling affects trunk dynamic response in sudden perturbations. Journal of Biomechanics 44, 547-551.

Bazrgari, B., Shirazi-Adl, A., Arjmand, N., 2007. Analysis of squat and stoop dynamic liftings: muscle forces and internal spinal loads. European Spine Journal 16, 687-699.

Bazrgari, B., Shirazi-Adl, A., Kasra, M., 2008a. Computation of trunk muscle forces, spinal loads and stability in whole-body vibration. Journal of Sound and Vibration 318, 1334-1347.

Bazrgari, B., Shirazi-Adl, A., Kasra, M., 2008b. Seated whole body vibrations with high-magnitude accelerations - relative roles of inertia and muscle forces Journal of Biomechanics 41, 2639-2646.

Bazrgari, B., Shirazi-Adl, A., Lariviere, C., 2009a. Trunk response analysis under sudden forward perturbations using a kinematics-driven model. Journal of Biomechanics 42, 1193-1200.

Bazrgari, B., Shirazi-Adl, A., Parnianpour, M., 2009b. Transient analysis of trunk response in sudden release loading using kinematics-driven finite element model. Clinical Biomechanics 24, 341-347.

Bazrgari, B., Shirazi-Adl, A., Trottier, M., Mathieu, P., 2008c. Computation of trunk equilibrium and stability in free flexion-extension movements at different velocities. Journal of Biomechanics 41, 412-421.

Bean, J.C., Chaffin, D.B., Schultz, A.B., 1988. Biomechanical model calculation of muscle contraction forces: a double linear programming method. Journal of Biomechanics 21, 59-66.

Belytschko, T.B., Andriacchi, T.P., Schultz, A.B., Galante, J.O., 1973. Analog studies of forces in the human spine: computational techniques. Journal of Biomechanics 6, 361-371.

Bergmark, A., 1989a. Mechanical stability of the human lumbar spine. Journal of Biomechanics 22, 987.

Bergmark, A., 1989b. Stability of the lumbar spine, A study in mechanical engineering. Acta Orthopaedica Scandinavica Supplementum 230, 1-54.

Berkson, M.H., Nachemson, A., Schultz, A.B., 1979. Mechanical Properties of Human Lumbar Spine Motion Segments—Part II: Responses in Compression and Shear; Influence of Gross Morphology. Journal of Biomechanical Engineering 101, 53-57.

Blaszczyk, J.W., 2008. Sway ratio - a new measure for quantifying postural stability. Acta Neurobiologiae Experimentalis 68, 51-57.

Bogduk, N., 2012. Clinical and Radiological Anatomy of the Lumbar Spine, Fifth ed. Churchill Livingstone, Elsevier, China.

Bogduk, N., Amevo, B., Pearcy, M., 1995. A biological basis for instantaneous centres of rotation of the vertebral column. Proceedings of the Institution of Mechanical Engineers. Part H, Journal of engineering in medicine 209, 177-183.

Brinckmann, P., Frobin, W., Hierholzer, E., Horst, M., 1983. Deformation of the Vertebral End-plate Under Axial Loading of the Spine. Spine 8, 851-856.

Brinckmann, P., Grootenboer, H., 1991. Change of disk height, radial disk bulge, and intradiscal pressure from discectomy - an invitro investigation on human lumbar disks. Spine 16, 641-646.

Broberg, K.B., 1983. On the mechanical behavior of the intervertebral discs. Spine 8, 51-65.

Brown, S.H., McGill, S.M., 2009. The intrinsic stiffness of the in vivo lumbar spine in response to quick releases: implications for reflexive requirements. Journal of Electromyography and Kinesiology 19, 727-736.

Brown, S.H.M., Haumann, M.L., Potvin, J.R., 2003. The responces of leg and trunk muscles to sudden unloading of the hands: implications for balance and spine stability. Clinical Biomechanics 18, 812-820.

Brown, S.H.M., McGill, S.M., 2005. Muscle force-stiffness characteristics influence joint stability: A spine example. Clinical Biomechanics 20, 917-922.

Brown, S.H.M., McGill, S.M., 2008. How the inherent stiffness of the in vivo human trunk varies with changing magnitudes of muscular activation. Clinical Biomechanics 23, 15-22.

Brown, S.H.M., McGill, S.M., 2010. The releationship between trunk muscle activation and trunk stiffness: examining a non-constant stiffness gain. Comput. Methods Biomech. Biomed. Eng. 13, 829-835.

Brown, S.H.M., Potvin, J.R., 2005. Constraining spine stability levels in an optimization model leads to the prediction of trunk muscle cocontraction and improved spine compression force estimates. Journal of Biomechanics 38, 745-754.

Brown, S.H.M., Vera-Garcia, F.J., McGill, S.M., 2006. Effects of abdominal muscle coactication on the externally preloaded trunk: Variations in motor control and its effect on spine stability. Spine 31, E387-E393.

Bruijn, S.M., Bregman, D.J., Meijer, O.G., Beek, P.J., Van Dieen, J.H., 2012. Maximum Lyapunov exponents as predictors of global gait stability: A modelling approach. Medical Engineering and Physics 34, 428-436.

Bruijn, S.M., Dieen, J.H.v., Meijer, O.G., Beek, P.J., 2009. Is slow walking more stable? Journal of Biomechanics 42, 1506-1512.

Carroll, J.P., Freedman, W., 1993. Nonstationary properties of postural sway. Journal of Biomechanics 26, 409-416.

Cassidy, J.D., Carroll, L.J., Côté, P., 1998. The Saskatchewan health and back pain survey: the prevalence of low back pain and related disability in Saskatchewan adults. Spine 23, 1860-1866.

Cassidy, J.J., Hiltner, A., Baer, E., 1989. Hierarchical structure of the intervertebra-disk. Connect. Tissue Res. 23, 75-88.

Cavanagh, P.R., Komi, P.V., 1979. Electromechanical delay in human skeletal muscle under concentric and eccentric contractions. European Journal of Applied Physiology 42, 159-163.

Chaffin, D.B., 1969. A computerized biomechanical model-development of and use in studying gross body actions. Journal of Biomechanics 2, 429-441.

Cholewicki, J., McGill, S.M., 1994. EMG assisted optimization - A hybrid approach for estimating muscle forces in an indeterminant biomechanical model. Journal of Biomechanics 27, 1287-1289.

Cholewicki, J., McGill, S.M., 1995. Relationship between muscle force and stiffness in the whole mammalian muscle: A simulation study Journal of Biomechanical Engineering 117, 339-342.

Cholewicki, J., McGill, S.M., 1996. Mechanical stability of the in vivo lumbar spine: implications for injury and low back pain. Clinical Biomechanics 11, 1-15.

Cholewicki, J., McGill, S.M., Norman, R.W., 1991. Lumbar spine loads during the lifting of extremely heavy wights. Medicine and Science in Sports and Exercise 23, 1179-1186.

Cholewicki, J., McGill, S.M., Norman, R.W., 1995. Comparison of muscle forces and joint load from an optimization and EMG assisted lumbar spine model - Towards development of a hybrid approach. Journal of Biomechanics 28, 321-331.

Cholewicki, J., Polzhofer, G.A., Radebold, A., 2000a. Postural control of trunk during unstable sitting. Journal of Biomechanics 22, 1733-1737.

Cholewicki, J., Silfies, S.P., Shah, R.A., Greene, H.S., Reeves, N.P., Alvi, K., Goldberg, B., 2005. Delayed trunk muscle reflex responses increase the risk of low back injuries. Spine 30, 2614-2620.

Cholewicki, J., Simons, A.P.D., Radebold, A., 2000b. Effects of external trunk loads on lumbar spine stability. Journal of Biomechanics 33, 1377-1385.

Cresswell, A.G., Oddsson, L., Thorstensson, A., 1994. The influence of sudden perturbations on trunk muscle activity and intra-abdominal pressure while standing. Experimental Brain Research 98, 336-341.

Crisco, J.J., 1989. The biomechanical stability of the human lumbar spine: experimental and theoretical investigations. Yale University, New Haven, Connecticut.

Crow, W.T., Willis, D.R., 2009. Estimating Cost of Care for Patients With Acute Low Back Pain: A Retrospective Review of Patient Records. The Journal of the American Osteopathis Association 109, 229-233.

Crowninshield, R.D., Brand, R.A., 1981. A physiologically based criterion of muscle force prediction in locomotion. Journal of Biomechanics 14, 793-801.

Dagenais, S., Caro, J., Haldeman, S., 2008. A systematic review of low back pain cost of illness studies in the United States and internationally. The Spine Journal 8, 8-20.

Davis, J., Kaufman, K.R., Lieber, R.L., 2003. Correlation between active and passive isometric force and intramuscular pressure in the issolated rabbit tibialis anterior muscle. Journal of Biomechanics 36, 505-512.

Davis, K.G., Marras, W.S., Heaney, C.A., Waters, T.R., Gupta, P., 2002. The impact of mental processing and pacing on spine loading - 2002 Volvo Award in Biomechanics. Spine 27, 2645-2653.

De Foa, J.L., Forrest, W., Biedermann, H.J., 1989. Muscle fiber direction of longissimus, iliocostalis and multifidus: landmark-drived reference lines. Journal of Anatomy 163, 243-247.

de Leva, P., 1996. Adustments to zatsiorsky-seluyanov's segment inertia parameters. Journal of Biomechanics 29, 1223-1230.

Dreischarf, M., Rohlmann, A., Zhu, R., Schmidt, H., Zander, T., 2013. Is it possible to estimate the compressive force in the lumbar spine from intradiscal pressure measurements? A finite element evaluation. Medical Engineering & Physics 35, 1385-1390.

Dul, J., Johnson, G.E., Shiavi, R., Townsend, M.A., 1984. Muscular synergism--II. A minimum-fatigue criterion for load sharing between synergistic muscles. Journal of Biomechanics 17, 675-684.

Dupeyron, A., Perrey, S., Micallef, J.P., Pelissier, J., 2010. Influence of back muscle fatigue on lumbar reflex adaptation during sudden external force perturbations. Journal of Electromyography and Kinesiology 20, 426-432.

Edwards, W.T., Hayes, W.C., Posner, I., White, A.A., Mann, R.W., 1987. Variation of lumbar spine stiffness with load. Journal of Biomechanical Engineering 109, 35-42.

El-Rich, M., Shirazi-Adl, A., Arjmand, N., 2004. Muscle activity, internal loads, and stability of the human spine in standing postures: combined model and In vivo studies. Spine 29, 2633-2642.

El Ouaaid, Z., Arjmand, N., Shirazi-Adl, A., Parnianpour, M., 2009. A novel approach to evaluate abdominal coavtivities for optimal spinal stability and compression force in lifting. Computer Methods in Biomechanics and Biomechanical Engineering 12, 735-745.

El Ouaaid, Z., Shirazi-Adl, A., Plamondon, A., Larivière, C., 2013. Trunk strength, muscle activity and spinal loads in maximum isometric flexion and extension exersions: A combined in vivo computational study. Journal of Biomechanics Under press.

England, S.A., Granata, K.P., 2007. The influence of gait speed on local dynamic stability. Gait and Posture 25, 172-178.

Enrietto, J.A., Jacobson, K.M., Baloh, R.W., 1999. Aging effects on auditory and vestibular responses: A longitudinal study. Am. J. Otolaryngol. 20, 371-378.

Esposito, F., Limonta, E., Cé, E., 2011. Passive stretching effects on electromechanical delay and time course of recovery in human skeletal muscle: new insights from an electromyographic and mechanomyographic combined approach. European Journal of Applied Physiology 111, 485-495.

Fathallah, F.A., Marras, W.S., Parnianpour, M., 1999. Regression models for predicting peak and continuous three-dimensional spinal loads during symmetric and asymmetric lifting tasks. Human Factors 41, 373-388.

Ferguson, S., 2008. Biomechanics of the spine, Fundumentals of Diagnosis and Treatment, in: Boos, N., Aebi, M. (Eds.), Spinal Disorders. Springer - Verlag, Berlin Heidelberg, Germany.

Fernie, G.R., Gryfe, C.I., Holliday, P.J., Llewellyn, A., 1982. The relationship of postural sway in standing to the incidence of falls in generic susbjects. Age and Aging 11, 11-16.

Fitts, P.M., 1954. The information capacity of the human motor system in controlling the amplitude of movement. Journal of Experimental Physiology 47, 381-391.

Flash, T., Hogan, N., 1985. The coordination of arm movements: An experimentally confirmed mathematical model. The Journal of Neuroscience 5, 1688-1703.

Franklin, T.C., Granata, K.P., 2007. Role of reflex gain and reflex delay in spinal stability-a dynamic simulation. Journal of Biomechanics 40, 1762-1767.

Freddolini, M., Strike, S., Lee, R.Y.W., 2014a. Dynamic Stability of the Trunk During Unstable Sitting in People With Low Back Pain. Spine 39, 785-790.

Freddolini, M., Strike, S., Lee, R.Y.W., 2014b. The role of trunk muscles in sitting balance control in people with low back pain. Journal of Electromyography and Kinesiology 24, 947-953.

Freddolini, M., Strike, S., Lee, R.Y.W., 2014c. Stiffness properties of the trunk in people with low back pain. Human Movement Science 36, 70-79.

Gagnon, D., Larivière, C., Loisel, P., 2001. Comparative ability of EMG, optimization, and hybrid modelling approaches to predict trunk muscle forces and lumbar spine loading during dynamic sagittal plane lifting. Clinical Biomechanics 16, 359-372.

Galante, J.O., 1967. Tensile properties of the human lumbar annulus fibrosus. Acta Orthopaedica Scandinavica Supplementum No. 100.

Gardner-Morse, M., Stokes, I.A.F., 1998. The effects of abdominal muscle co-activation on lumbar spine stability Spine 23, 86-91.

Gardner-Morse, M., Stokes, I.A.F., Laible, J.P., 1995. Role of muscles in lumbar stability in maximum extesion efforts. Journal of Orthopaedic Research 13, 802-808.

Gardner-Morse, M.G., Stokes, I.A.F., 2001. Trunk stiffness increases with steady-state effort. Journal of Biomechanics 34, 457-463.

Gardner-Morse, M.G., Stokes, I.A.F., 2003. Physiologycal axial compressive preloads increase motion segment stiffness, linearity and hysteresis in all six degrees of freedom for small displacements about the neutral posture. Journal of Orthopaedic Research 21, 547-552.

Gardner-Morse, M.G., Stokes, I.A.F., 2004. Structrual behavior of human lumbar spinal motion segments. Journal of Biomechanics 37, 205-212.

Gercek, E., Hartmann, F., Kuhn, S., Degreif, J., Rommens, P.M., Rudig, L., 2008. Dynamic angular three-dimensional measurement of multisegmental thoracolumbar motion in vivo. Spine 33, 2326-2333.

Ghaffari, M., 2007. Low back pain among industrial workers, Occupational health studies on prevalence, incidence, and associations with work and lifestyle in I.R. Iran. Karolinska Institutet, Stockholm.

Ghaffari, M., Alipour, A., Jensen, I., Farshad, A.A., Vingard, E., 2006. Low back pain among iranian industrial workers. Occupational Medicine 56, 455-460.

Goel, V.K., 1987. Three-dimensional motion behavior of the human spine--a question of terminology. Journal of Biomechanical Engineering 109, 353-355.

Gracovetsky, S., Farfan, H.F., Lamy, C., 1977. A mathematical model of the lumbar spine using an optimized system to control muscles and ligaments. Orthopedic Clinics of North America 8, 135-153.

Graham, R.B., Sadler, E.M., Stevenson, J.M., 2011. Local dynamic stability of trunk movements during the repetitive lifting of loads Human Movement Science.

Granata, K.P., England, S.A., 2006. Stability of dynamic trunk movement. Spine 31, E271-E276.

Granata, K.P., Gottipati, P., 2008. Fatigue influences the dynamic stability of the torso. Ergonomics 51, 1258-1271.

Granata, K.P., Ikeda, A.J., Abel, M.F., 2000. Electromechanical delay and reflex response in spastic cerebral palsy. Archives of Physical Medicine and Rehabilitation 81, 888-894.

Granata, K.P., Marras, W.S., 1993. An Emg-assisted model of loads on the lumbar spine during asymetric trunk extensions. Journal of Biomechanics 26, 1429-1438.

Granata, K.P., Marras, W.S., 1995. An Emg-Assisted model of trunk loading during free-dynamic lifting. Journal of Biomechanics 28, 1309-1317.

Granata, K.P., Marras, W.S., 2000. Cost-benefit of muscle cocontraction in protecting against spinal instability. Spine 25, 1398-1404.

Granata, K.P., Marras, W.S., Davis, K.G., 1999. Variation in spinal load and trunk dynamics during repeated lifting exertions. Clinical Biomechanics 14, 367-375.

Granata, K.P., Orishimo, K.F., 2001. Response of trunk muscle coactivation to changes in spinal stability. Journal of Biomechanics 34, 1117-1123.

Granata, K.P., Orishimo, K.F., Sanford, A.H., 2001. Trunk muscle coactivation in preparation for sudden load. Journal of Electromyography and Kinesiology 11, 247-254.

Granata, K.P., Rogers, E.L., 2007. Torso flexion modulates stiffness and reflex response. Journal of Electromyography and Kinesiology 17, 384-392.

Granata, K.P., Slota, G.P., Bennett, B.C., 2004. Paraspinal muscle reflex dynamics. Journal of Biomechanics 37, 241-247.

Granata, K.P., Wilson, S.E., 2001. Trunk posture and spinal stability. Clinical Biomechanics 16, 650-659.

Greene, H.S., Cholewicki, J., Falloway, M.T., Nguyen, C.V., Radebold, A., 2001. A history of low back injury is a risk factor for recurrent back injuries in varsity athletes. The American Journal of Sports Medicine 29, 795-800.

Gsell, K.Y., Beaudette, S.M., Graham, R.B., Brown, S.H.M., 2015. The effect of different ranges of motion on local dynamic stability of the elbow during unloaded repetitive flexion-extension movements. Human Movement Science 42, 193-202.

Guerin, H.A.L., Elliott, D.M., 2006. Chapter 3 - Structure and Properties of Soft Tissues in the Spine, in: Kurtz, S.M., Edidin, A.A. (Eds.), Spine Technology Handbook. Academic Press, Burlington, pp. 35-62.

Hajibozorgi, M., Arjmand, N., in press. Sagittal range of motion of the thoracic spine using inertial tracking device and effect of measurement errors on model predictions. Journal of Biomechanics.

Hajihosseinali, M., Arjmand, N., Shirazi-Adl, A., 2015. Effect of body weight on spinal loads in various activities: A personalized biomechanical modeling approach. Journal of Biomechanics 48, 276-282.

Hajihosseinali, M., Arjmand, N., Shirazi-Adl, A., Farahmand, F., Ghiasi, M.S., 2014. A novel stability and kinematics-driven trunk biomechanical model to estimate muscle and spinal forces. Medical Engineering & Physics 36, 1296-1304.

Harris, C.M., Wolpert, D.M., 1998. Signal-dependent noise determines motor planning. Nature 394, 780-784.

Hilber, H.M., Hughes, T.J.R., Taylor, R.L., 1977. Improved numerical dissipation for time integration algorithms in structural dynamics. Earthquake Engineering & Structural Dynamics 5, 283-292.

Hill, A.V., Year The heat of shortening and the dynamic constraints of muscle. In Roryal Society Conference London, Britain.

Hilton, R.C., Ball, J., Benn, R.T., 1976. Vertebral end-plate lesions (Schmorl's nodes) in the dorsolumbar spine. Annals of the rheumatic diseases 35, 127-132.

Hodges, P.W., Bui, B.H., 1996. A comparison of computer-based methods for the determination of onset of muscle contraction using electromyography. Electroencephalography and clinical Neurophysiology 101, 511-519.

Hodges, P.W., Gurfinkel, V.S., Brumangne, S., Smith, T.C., Cordo, P.C., 2002. Coexistance of stability and mobility in postural control : Evidance from postural compensation for respiration. Experimental Brain Research 144, 293-302.

Hodges, P.W., Richardson, C.A., 1996. Inefficient muscular stabilization of the lumbar spine associated with low back pain - A motor control evaluation of transversus abdominis. Spine 21, 2640-2650.

Hoff, B.R., 1992. A computational description of the organization of human reaching and prehension. University of Southern California, CA, USA.

Hogan, N., 1984. An organizing principle for a class of voluntary movements. The Journal of Neuroscience 4, 2745-2754.

Horita, T., Ishiko, T., 1987. Relationships between muscle lactate accumulation and surface EMG activities during isokinetic contractions in man. European Journal of Applied Physiology 58, 1-7.

Houston, M.E., Norman, R.W., Froese, E.A., 1988. Mechanical measures during maximal velocity knee extension exercise and their relation to fibre composition of the human vastus lateralis muscle. European Journal of Applied Physiology 58, 1-7.

Hughes, R.E., 2000. Effect of optimization criterion on spinal force estimates during asymmetric lifting. Journal of Biomechanics 33, 225-229.

Iatridis, J.C., Kumar, S., Foster, R.J., Weidenbaum, M., Mow, V.C., 1999. Shear mechanical properties of human lumbar annulus fibrosus. Journal of Orthopaedic Research 17, 732-737.

Iatridis, J.C., Setton, L.A., Foster, R.J., Rawlins, B.A., Weidenbaum, M., Mow, V.C., 1998. Degeneration affects the anisotropic and nonlinear behaviors of human anulus fibrosus in compression. Journal of Biomechanics 31, 535-544.

Iatridis, J.C., Setton, L.A., Weidenbaum, M., Mow, V.C., 1997. Alterations in the mechanical behavior of the human lumbar nucleus pulposus with degeneration and aging. Journal of Orthopaedic Research 15, 318-322.

Jager, M., Luttmann, A., 1991. Compressive strength of lumbar spine elements related to age, gender and other influencing factors, in: Andersen, P.A., Hobart, D.J. (Eds.), Electromyographical Kinesiology. Elsevier Science, Amsterdam, pp. 291-294.

Janevic, J., Ashton-Miller, J.A., Schultz, A., 1991. Large compressive preloads decrease lumbar motion segment flexibility. Journal of Orthopaedic Research 9, 228-236.

Johnson, S.T., Kipp, K., Hoffman, M.A., 2012. Spinal motor control differences between the sexes. European Journal of Applied Physiology 112, 3859-3864.

Jordan, M.I., Wolpert, D.M., 1999. Computational motor control, in: Gazzaniga, M. (Ed.), The Cognitive Neurosciences. MIT Press, Cambridge, MA.

Joyce, G.C., Rack, P.M.H., 1969. Isotonic lengthening and shortening movements of cat soleus muscle. The Journal of Physiology 204, 475-491.

Kasra, M., Shirazi-Adl, A., Drouin, G., 1992. Dynamics of human intervertebral joints. Experimental and finite-element investigations. Spine 17.

Katz, J.N., 2006. Lumbar disc disorders and low-back pain: socioeconomic factors and conseqences. Journal of Bone and Joint Surgery 88(Suppl 2), 21-24.

Khalil, T.M., Goldberg, M.L., Asfour, S.S., Moty, E.A., Rosomoff, R.S., Rosomoff, H.L., 1987. Acceptable maximum effort (AME). A psychophysical measure of strength in back pain patients. Spine 12, 372-376.

Knutsson, F., 1944. The instability associated with disk degeneration in the lumbar spine. Acta Radiolagica 25, 593-608.

Kopperdahl, D.L., Keaveny, T.M., 1998. Yield strain behavior of trabecular bone. Journal of Biomechanics 31, 601-608.

Kopperdahl, D.L., Morgan, E.F., Keaveny, T.M., 2002. Quantitative computed tomography estimates of the mechanical properties of human vertebral trabecular bone. Journal of Orthopaedic Research 20, 801-805.

Krajcarski, S.R., Potvin, J.R., Chiang, J., 1999. The in vivo dynamic response of the spine to perturbations causing rapid flexion: effects of pre-load and step input magnitude. Clinical Biomechanics 14, 54-62.

Kurtz, S.M., 2006. Spine Technology Handbook. Elsevier Academic Press, Boston, MA, USA.

Kurtz, S.M., Edidin, A.A., 2006. The basic tools and terminology of spine treatment.

Laible, J.P., Pflaster, D.S., Krag, M.H., Simon, B.R., Haugh, L.D., 1993. A Poroelastic-Swelling Finite Element Model With Application to the Intervertebral Disc. Spine 18, 659-670.

Laible, J.P., Pflaster, D.S., Simon, B.R., Krag, M.H., Pope, M.H., Haugh, L.D., 1994. A Dynamic material parameter-estimation procedure for soft-tissue using a proelastic finit-element model. Journal of Biomechanical Engineering - Transaction of the ASME 116, 19-29.

Larivière, C., Forget, R., Vadeboncpeur, R., Bilodeau, M., Mecheri, H., 2010. The effect of sex and chronic low back pain on back muscle reflex responses. European Journal of Applied Physiology 109, 577-590.

Larivière, C., Gagnon, D., Genest, K., 2009. Offering proper feedback to control for out-of-plane lumbar moments influences the activity of trunk muscles during unidirectional isometric trunk exertions. Journal of Biomechanics 42, 1498-1505.

Larivière, C., Gagnon, D., Mecheri, H., 2015. Trunk postural control in unstable sitting: Effect of sex and low back pain status. Clinical Biomechanics 30, 933-939.

Larivière, C., Mecheri, H., Shahvarpour, A., Gagnon, D., Shirazi-Adl, A., 2013. Criterion validity and between-day reliability of an inertial-sensor-based trunk postural stability test during unstable sitting. Journal of Electromyography and Kinesiology 23, 899-907.

Lavender, S.A., Mirka, G.A., Schoenmarklin, R.W., Sommerich, C.M., Sudhakar, L.R., Marras, W.S., 1989. The effects of preview and task symmetry on trunk muscle response to sudden loading. Human Factors 31, 101-115.

Lawrence, B.M., Buckner, G.D., Mirka, G.A., 2006. An adaptive system identification model of the biomechanical response of the human trunk during sudden loading. Journal of Biomechanical Engineering 128, 235-241.

Lawrence, R.C., Helmick, C.G., Arnett, F.C., Deyo, R.A., Felson, D.T., Giannini, E.H., Heyse, S.P., Hirsch, R., Hochberg, M.C., Hunder, G.G., Liang, M.H., Pillemer, S.R., Steen, V.D., Wolfe, F., 1998. Estimates of the prevalence of arthritis and selected musculoskeletal disorders in the united states. Arthritis and Rheumatism 41, 778-799.

Lee, H., Granata, K.P., 2008. Process stationarity and reliability of trunk postural stability. Clinical Biomechanics 23, 735-742.

Lee, P., Helewa, A., Smythe, H.A., Bombardier, C., Goldsmith, C.H., 1985. Epidemiology of musculoskeletal disorders (complaints) and related disability in Canada. The Journal of Rheumatology 12, 1169-1173.

Lee, P.J., Granata, K.P., Moorhouse, K.M., 2007. Active trunk stiffness during voluntary isometric flexion and extension exertions. Human Factors 49, 100-109.

Lee, P.J., Rogers, E.L., Granata, K.P., 2006. Active trunk stiffness increases with co-contraction. Journal of Electromyography and Kinesiology 16, 51-57.

Li, W., Todorov, E., 2007. Iterative linearization methods for approximatly optimal control and estimation of non-linear stochastic system. International Journal of Control 80, 1439-1453.

Li, W., Todorov, E., Skelton, R.E., 2005. Estimation and control of systems with multiplicative noise via linear matrix inequalities, American Control Conference Portland, OR, USA, pp. 1811-1816.

Linton, S.J., Hellsing, A.L., Hallden, K., 1998. A population-based study of spinal pain among 35-45 year old individuals - Prevalence, sick leave, and health care use. 1998 23, 1457-1463.

Lucas, B.D., Bresler, B., 1960. Stability of the ligamentous spine, Techtical Report Series. Biomechanics Laboratory, University of California, San Francisco.

Ma, S.P., Zahalak, G.I., 1985. The mechanical response of the active human triceps brachii muscle to very rapid stretch and shortening. Journal of Biomechanics 18, 585-598.

Magnusson, M.L., Aleksiev, A.R., Wilder, D.G., Pope, M.H., Spratt, K., Lee, S.H., Goel, V.k., Weinstein, J.N., 1996. European Spine Society--the AcroMed Prize for Spinal Research 1995. Unexpected load and asymmetric posture as etiologic factors in low back pain. European Spine Journal 5, 23-35.

Magora, A., 1973. Investigation of the relation between low back pain and occupation 4. Physical requirements: bending, rotation, reaching and sudden maximal effort. Scandinavian Journal of Rehabilitative Medicine 5, 191-196.

Manning, D.P., Mitchell, R.G., Blanchfield, L.P., 1984. Body movements and events contributing to accidental and nonaccidental back injuries. Spine 9, 734-739.

Marchand, F., Ahmed, A.M., 1990. Investigation of the laminate structure of lumbar-disk anulus fibrosus. Spine 15, 402-410.

Markolf, K.L., Year Stiffness and damping characteristics of thoracolumbar spine. In Proceeding of Workshop on Bioengineering Approaches to Problems of the Spine. Division of Research Grants. NIH, Bethesda.

Markolf, K.L., 1972. Deformation of the Thoracolumbar Intervertebral Joints in Response to External Loads, A biomechanical study using autopsy material. Journal of Bone and Joint Surgery 54, 511-533.

Marras, W.S., 1987. Trunk motion during lifting: temporal relations among loading factors. International Journal of Industrial Ergonomics 1, 159-167.

Marras, W.S., Davis, K.G., Heaney, C.A., Maronitis, A.B., Allread, W.G., 2000. The influence of psychosocial stress, gender, and personality on mechanical loading of the lumbar spine. Spine 25, 3045-3054.

Marras, W.S., Davis, K.G., Jorgensen, M., 2002. Spine loading as a function of gender. Spine 27, 2514-2520.

Marras, W.S., Davis, K.G., Jorgensen, M., 2003. Gender influences on spine loads during complex lifting. The spine journal : official journal of the North American Spine Society 3, 93-99.

Marras, W.S., Ferguson, S.A., Burr, D., Davis, K.G., Gupta, P., 2004. Spine loading in patients with low back pain during asymmetric lifting exertions. The spine journal : official journal of the North American Spine Society 4, 64-75.

Marras, W.S., Granata, K.P., 1995. A biomechanical assessment and model of axial twisting in the thoracolumbar spine. Spine 20, 1440-1451.

Marras, W.S., Granata, K.P., 1997. Spine loading during trunk lateral bending motions. Journal of Biomechanics 30, 697-703.

Marras, W.S., Rangarajulu, S.L., Lavender, S.A., 1987. Trunk loading and expectation. Ergonomics 30, 551-562.

Marras, W.S., Sommerich, C.M., 1991. A 3-dimensional motion model of loads on the lumbar spine. 2. Model validation. Human Factors 33, 139-149.

Marshall, P., Murphy, B., 2003. The validity and reliability of surface EMG to assess the neuromucular response of the abdominal muscles to rapid limb movement. Journal of Electromyography and Kinesiology 13, 477-489.

McGill, S.M., 1991. Electromyographic activity of the abdominal and low back musculature during the generation of isometric and dynamic axial trunk torque: Implications for lumbar mechanics. Journal of Orthopaedic Research 9, 91-103.

McGill, S.M., 2007. Low Back Disorders: evidence-based prevention and rehabilitation, Second ed. Human Kinetics Publishers, USA.

McGill, S.M., Norman, R.W., Cholewicki, J., 1996. A simple polynomial that predicts low-back compression during complex 3-D tasks. Ergonomics 39, 1107-1118.

McGill, S.M., Seguin, J., Bennett, G., 1994. Passive stiffness of the lumbar torso in flexion, extension, lateral bending and axial rotation, Efect of belt wearing and breath holding. Spine 19, 696-704.

Meng, X., Bruno, A.G., Cheng, B., Wang, W., Bouxsein, M.L., Anderson, D.E., 2015. Effects of intervertebral joint stiffness magnitude and coupling on estimates of vertebral compressive loading and intervertebral translations. Journal of Biomechanical Engineering.

Miller, E.M., Slota, G.P., Agnew, M.J., Madigan, M.L., 2010. Females exibit shorter paraspinal reflex latencies than males in response to sudden trunk flexion perturbations. Clinical Biomechanics 25, 541-545.

Miller, J.A.A., Schultz, A.B., Warwick, D.N., Spencer, D.L., 1986. Mechanical properties of lumbar spine motion segments under large loads. Journal of Biomechanics 19, 79-84.

Mirka, G.A., Marras, W.S., 1993. A stochastic-model of trunk muscle coactivation during trunk bending. Spine 18, 1396-1409.

Mokhtarzadeh, H., Farahmand, F., Shirazi-Adl, A., Arjmand, N., Malekipour, F., Parnianpour, M., 2012. The effects of intra-abdominal pressure on the stability and unloading of the spine. J. Mech. Med. Biol. 12.

Moorhouse, K.M., Granata, K.P., 2005. Trunk stiffness and dynamics during active exertion extensions. Journal of Biomechanics 38, 2000-2007.

Moorhouse, K.M., Granata, K.P., 2007. Role of reflex dynamics in spinal stability: Intrinsic muscle stiffness alone is insufficient for stability. Journal of Biomechanics 40, 1058-1065.

Morgan, D.L., 1977. Separation of active and passive components of short-range stiffness of muscle. The Americarn Journal of Physiology 232, 45-49.

Morita, D., Yukawa, Y., Nakashima, H., Ito, K., Yoshida, G., Kanbara, S., Iwase, T., Kato, F., 2014. Range of motion of thoracic spine in sagittal plane. European Spine Journal 23, 673-678.

Morris, J.M., Lucas, B.D., Bresler, B., 1961. Role of the trunk in stability of the spine. Journal of Bone and Joint Surgery 43, 327-351.

Mosekilde, L., Mosekilde, L., 1986. Normal vertebral body size and compressive strength: Relations to age and to vertebral and iliac trabecular bone compressive strength. Bone 7, 207-212.

Moulton, A.W., 2009. Clinically Relevant Spinal Anatomy, in: Errico, T.J., Lonner, B.S., Moulton, A.W. (Eds.), Surgical Management of Spinal Deformities, 1st ed. Saunders Elsevier, Philadelphia, PA.

Nachemson, A., 1960. Lumbar intradiscal pressure. Experimental studies on post-mortem material. Acta orthopaedica Scandinavica. Supplementum 43, 1-104.

Nachemson, A., 1992. Lumbar mechanics as revealed by lumbar intradiscal pressure, in: Jaysön, M.I.V. (Ed.), The Lumbar Spine and Back Pain. Churchill Livingstone, pp. 381-396.

Nachemson, A., Elfström, G., 1970. Intravital dynamic pressure measurements in lumbar discs, A study of common movements, maneuvers and exercises. Scandinavian Journal of Rehabilitative Medicine Supplement 1.

Nachemson, A., Morris, J.M., 1964. In vivo measurements of intradiscal pressure: Discometry, a method for the determination of pressure in the lower lumbar discs. Journal of Bone and Joint Surgery 46, 1077-1092.

Nachemson, A.L., 1981. Disc pressure measurements. Spine 6, 93-97.

Nussbaum, M.A., Chaffin, D.B., 1996. Development and evaluation of a scalable and deformable geometric model of the human torso. Clinical Biomechanics 11, 25-34.

Oksuz, E., 2006. Prevalnce, risk factros, and preference-based health states of low back pain in a Turkish population. Spine 31, E968-E972.

Olson, M.W., 2014. Comparison of trunk muscle reflex activation patterns between active and passive trunk flexion-extension loading conditions. Human Movement Science 34, 12-27.

Overstall, P.W., Exton-Smith, A.N., Imms, F.J., Johnson, A.L., 1977. Falls in the elderly related postural imbalance. British Medical journal 1.

Oxland, T., Lin, R.M., Panjabi, M.M., 1992. Three-dimensional mechanical properties of the thoracolumbar junction Journal of Orthopaedic Research 10, 573-580.

Pan, P.-Q., 2014. Linear Programming Computation. Springer-Verlag Berlin Heidelberg.

Panagiotacopulos, N.D., Pope, M.H., Krag, M.H., Bloch, R., 1987. A mechanical model for the human intervertebral disc. Journal of Biomechanics 20, 839-850.

Panjabi, M.M., 1992. The stabilizing system of the spine. Part I. Function, dysfunction, adaptation, and enhancement. Journal of Spinal Disorders 5, 383-389.

Panjabi, M.M., 2003. Clinical spinal instability and low back pain. Journal of Electromyography and Kinesiology 13, 371-379.

Panjabi, M.M., Brand, R.A., Jr., White III, A.A., 1976. Three-dimensional flexibility and stiffness properties of the human thoracic spine. Journal of Biomechanics 9, 185-192.

Papageogiou, A.C., Croft, P.R., Ferry, S., Jayson, M.I.V., Silman, A.J., 1995. Estimating the prevalence of low-back-pain in the general population - Evidence from the south Manchester back pain survey Spine 20, 1889-1894.

Parnianpour, M., Wang, J.L., Shirazi-Adl, A., Sparto, P., Wilke, H.-J., 1997. The effect of variations in trunk models in predicting muscle strength and spinal loading. Journal of Musculoskeletal Research 01, 55-69.

Pearsall, D.J., Reid, J.G., Livingstone, L.A., 1996. Segmental inertial parameters of the human trunk as determined from computed tomography. Annals of Biomedical Engineering 24, 198-210.

Polga, D.J., Beaubien, B.P., Kallemeier, P.M., Schellhas, K.P., Lew, W.D., Buttermann, G.R., Wood, K.B., 2004. Measurement of in vivo intradiscal pressure in healthy thoracic intervertebral discs. Spine 29, 1320-1324.

Prieto, T.E., Myklebust, J.B., Hoffmann, R.G., Lovett, E.G., Myklebust, B.M., 1996. Measures of postural steadiness: Differences bteween healthy young and elderly adults. IEEE Transactions on Biomedical Engineering 43, 956-966.

Radebold, A., Cholewicki, J., Panjabi, M.M., Patel, T.C., 2000. Muscle response pattern to sudden trunk loading in healthy individuals and in patients with chronic low back pain. Spine 25, 947-954.

Radebold, A., Cholewicki, J., Polzhofer, G.K., Greene, H.S., 2001. Impaired postural control of the lumbar spine is associated with delayed muscle response times in patients with chronic idiopathic low back pain. Spine 26, 724-730.

Ramage-Morin, P.L., Gilmour, H., 2010. Chronic pain at ages 12 to 44, Health Reports. Statistics Canada.

Redfern, M.S., Hughes, R.E., Chaffin, D.B., 1993. High-pass filtering to remove electrocardiographic interference from torso EMG recording. Clinical Biomechanics 8, 44-48.

Reeves, N.P., Cholewicki, J., Milner, T., Lee, A.S., 2008. Trunk antagonistic co-activation is associated with impaired neuromuscular performance. Experimental Brain Research 188, 457-463.

Reeves, N.P., Cholewicki, J., Narendra, K.S., 2009. Effects of reflex delays on postural control during unstable seated balance. Journal of Biomechanics 42, 164-170.

Reeves, N.P., Cholewicki, J., Pearcy, M., Parnianpour, M., 2013. How can models of motor control be useful for understanding low back pain?, in: Hodges, P.W., Cholewicki, J., Van Dieen, J.H. (Eds.), Spinal Control: The Rehabilitation of Back pain. Churchill Livingstone.

Reeves, N.P., Everding, V.Q., Cholewicki, J., Morrisette, C., 2006. The effects of trunk stiffness on postural control during unsatble seated balance. Experimental Brain Research 174, 694-700.

Roaf, R., 1960. A study of the mechanics of spinal injuries. Journal of Bone & Joint Surgery, British Volume 42-B, 810-823.

Roberts, S., Menage, J., Urban, J.P.G., 1989. Biochemical and Structural Properties of the Cartilage End-Plate and its Relation to the Intervertebral Disc. Spine 14, 166-174.

Rohlmann, A., Dreischarf, M., Zander, T., Graichen, F., Strube, P., Schmidt, H., Bergmann, G., 2013. Monitoring the load on a telemeterised vertebral body replacement for a period of up to 65 months. European Spine Journal 22, 2575-2581.

Rohlmann, A., Pohl, D., Bender, A., Graichen, F., Dymke, J., Schmidt, H., Bergmann, G., 2014. Activities of everyday life with high spinal loads. PLoS One 9.

Rosenstein, M.T., Collins, J.J., De Luca, C.J., 1993. A practical method for calculating largest lyapunov exponents from small data sets. Physica D 65.

Ross, S.D., Tanaka, M.L., Senatore, C., 2010. Detecting dynamical boundaries from kinematic data in biomechanics. Chaos 20, 017507-017501.

Rousseau, M.A., Bradford, D.S., Hadi, T.M., Pedersen, K.L., Lotz, J.C., 2006. The instant axis of rotation influences facet forces at L5/S1 during flexion/extension and lateral bending. European Spine Journal 15, 299-307.

Sanchez-Zuriaga, D., Adams, M.A., Dolan, P., 2010. Is Activation of the Back Muscles Impaired by Creep or Muscle Fatigue? Spine 35, 517-525.

Santos, B.R., Larivière, C., Belisle, A., McFadden, D., Plamondon, A., Imbeau, D., 2011. Sudden loading perturbation to determine the reflex response of different back muscles: A reliability study. Muscle & nerve 43, 348-359.

Sato, K., kikuchi, S., Yonezawa, T., 1999. In vivo intradiscal pressure measurement in healthy individuals and in patients with ongoing back problems. Spine 24, 2468-2474.

Schmidt, H., Galbusera, F., Rohlmann, A., Shirazi-Adl, A., 2013. What have we learned from finite element model studies of lumbar intervertebral discs in the past four decades? Journal of Biomechanics 46, 2342-2355.

Schmidt, H., Heuer, F., Claes, L., Wilke, H.-J., 2008. The relation between the instantaneous center of rotation and facet joint forces – A finite element analysis. Clinical Biomechanics 23, 270-278.

Schultz, A., Andersson, G., Ortengren, R., Haderspeck, K., Nachemson, A., 1982. Loads on the lumbar spine. Validation of a biomechanical analysis by measurements of intradiscal pressures and myoelectric signals. The Journal of bone and joint surgery. American volume 64, 713-720.

Schultz, A.B., Belytschko, T.B., Andriacchi, T.P., Galante, J.O., 1973. Analog studies of forces in the human spine: mechanical properties and motion segment. Journal of Biomechanics 6, 373-383.

Schultz, A.B., Warwick, D.N., Berkson, M.H., Nachemson, A.L., 1979. Mechanical properties of human lumbar spine motion segments—Part I: Responses in flexion, extension, lateral bending, and torsion. Journal of Biomechanical Engineering 101, 46-52.

Scott, S.H., 2004. Optimality feedback control and the neural basis of volitional motor control. nature neuroscience 5, 534-546.

Shadden, S.C., Lekien, F., Marsden, J.E., 2005. Definition and properties of Lagrangian coherent structures from finite-time Lyapunov exponents in two-dimensional aperiodic flows. Physica D: Nonlinear Phenomena 212, 271-304.

Shahvarpour, A., Shirazi-Adl, A., Larivière, C., Bazrgari, B., 2015. Trunk active response and spinal forces in sudden forward loading – Analysis of the role of perturbation load and pre-perturbation conditions by a kinematics-driven model. Journal of Biomechanics 48, 44-52.

Shahvarpour, A., Shirazi-Adl, A., Mecheri, H., Larivière, C., 2014. Trunk response to sudden forward perturbation - Effects of preload and sudden load magnitudes, posture and abdominal muscle preactivation. Journal of Electromyography and Kinesiology 24, 394-403.

Shirazi-Adl, A., 1989. Nonlinear finite element analysis of wrapping uniaxial elements. Computers & structures 32, 119-123.

Shirazi-adl, A., 1994a. Biomechanics of the lumbar spine in sagittal/lateral moments. Spine 19, 2407-2414.

Shirazi-Adl, A., 1994b. Nonlinear stress-analysis of the whole lumbar spine in torsion - mechanics of facet articulation. Journal of Biomechanics 27, 289-&.

Shirazi-Adl, A., 2006. Analysis of large compression loads on lumbar spine in flexion and in torsion using a novel wrapping element. Journal of Biomechanics 39, 267-275.

Shirazi-Adl, A., Ahmed, A.M., Shrivastava, S.C., 1986a. A finite element study of a lumbar motion segment subjected to pure sagittal plane moments. Journal of Biomechanics 19, 331-350.

Shirazi-Adl, A., Ahmed, A.M., Shrivastava, S.C., 1986b. Mechanical response of a lumbar motion segment in axial torque alone and combined with compression. Spine 11, 914-927.

Shirazi-Adl, A., Drouin, G., 1987. Load-bearing role of facets in a lumbar segment under sagittal plane loading. Journal of Biomechanics 20, 601-613.

Shirazi-Adl, A., Drouin, G., 1988. Nonlinear gross response analysis of a lumbar motion segment in combined sagittal loadings. Journal of Biomechanical Engineering 110, 216-222.

Shirazi-Adl, A., Parnianpour, M., 2000. Load-bearing and stress analysis of the human spine under a novel wrapping compression loading. Clinical Biomechanics 15, 718-725.

Shirazi-Adl, A., Sadouk, S., Parnianpour, M., Pop, D., El-Rich, M., 2002. Muscle for evaluation and the role of posture in human lumbar spine under compression. European Spine Journal 11, 519-526.

Shirazi-Adl, A., Shrivastava, S.C., Ahmed, A.M., 1984. Stress analysis of the lumbar disc-body unit in compression: a three dimensional nonlinear finite element study Spine 9, 120-134.

Silva, M.J., Keaveny, T.M., Hayes, W.C., 1997. Load sharing between the shell and the centrum in the lumbar vertebral body. Spine 22, 140-150.

Simon, B.R., Wu, J.S., Carlton, M.W., Evans, J.H., Kazarian, L.E., 1985. Structural models for human spinal motion segments based on a poroelastic view of the intervertebral disk. Journal of Biomechanical Engineering - Transaction of the ASME 107, 327-335.

Slota, G.P., Granata, K.P., Madigan, M.L., 2008. Effects of seated whole-body vibration on postural control of the trunk during unstable seated balance. Clinical Biomechanics 23, 381-386.

Srbinoska, H., Dreischarf, M., Consmuller, T., Bergmann, G., Rohlmann, A., 2013. Correlation between back shape and spinal loads. Journal of Biomechanics 46, 1972-1975.

Staude, G.H., 2001. Precise onset detection of human motor responses using a whitening filter and the log-likelihood-ration test. IEEE Transactions on Biomedical Engineering 48, 1292-1305.

Staude, G.H., Wolf, W., 1999. Objective motor response onset detection in surface myoelectric signals. Medical Engineering and Physics 21, 449-467.

Stokes, I.A., Gardner-Morse, M., Churchill, D., Laible, J.P., 2002. Measurement of a spinal motion segment stiffness matrix. Journal of Biomechanics 35, 517-521.

Stokes, I.A.F., Gardner-Morse, M., 1999. Quantitative anatomy of the lumbar musculature. Journal of Biomechanics 32, 311-316.

Stokes, I.A.F., Gardner-Morse, M.G., 2003. Spinal stiffness increases with axial load: another stabilizing consequence of muscle action. Journal of Electromyography and Kinesiology 13, 397-402.

Stokes, I.A.F., Gardner-Morse, M.G., Henry, S.M., 2011. Abdominal muscle activation increases lumbar spinal stability: Analysis of contributions of different muscle groups. Clinical Biomechanics 26, 797-803.

Stokes, I.A.F., Gardner-Morse, M.G., Henry, S.M., Badger, G.J., 2000. Decrease in trunk muscular response to perturbation with preactivation of lumbar spinal musculature. Spine 25, 1957-1964.

Stokes, I.A.F., Henry, S.M., Single, R.M., 2003. Surface EMG electrodes do not accurately record from lumbar multifidus muscles. Clinical Biomechanics 19, 9-13.

Stokes, I.A.F., Iatridis, J.C., 2005. Biomechanics of the spine, in: Mow, V.C., Huiskes, R. (Eds.), Basic Orthopaedic Biomechanics and Mechano-Biology, 3rd ed. Lippincott Williams & Wilkins http://www.lww.com.

Sukthankar, A., Nerlich, A.G., Paesold, G., 2008. Age-Related Changes of the Spine, in: Boos, N., Aebi, M. (Eds.), Spinal Disorders. Springer-Verlag, Berlin Heidelberg, Germany.

Takahashi, I., Kikuchi, S., Sato, K., Sato, N., 2006. Mechanical load of the lumbar spine during forward bending motion of the trunk - A biomechanical study. Spine 31, 18-23.

Tanaka, M.L., Nussbaum, M.A., Ross, S.D., 2009. Evaluation of the threshold of stability for the human spine. Journal of Biomechanics 42, 1017-1022.

Tanaka, M.L., Ross, S.D., Nussbaum, M.A., 2010. Mathematical modeling and simulation of seated stability. Journal of Biomechanics 43, 906-912.

Thelen, D.G., Schultz, A.B., Ashton-Miller, J.A., 1994. Quentitative interpretation of lumbar muscle myoelectric signals during rapid cyclic attmpted trunk flexions and extensions. Journal of Biomechanics 27, 157-167.

Tjepkema, M., 2003. Repetitive strain injury Health Reports. Statistics Canada.

Todorov, E., 2004. Optimality principles in sensorimotor control. nature neuroscience 7, 907-915.

Todorov, E., Jordan, M.I., 2002. Optimal feedback control as a theory of motor coordination. nature neuroscience 5, 1226-1235.

Tsirakos, D., Baltzopoulos, V., Bartlett, R., 1997. Inverse optimization: Functional and physiological considerations related to the force-sharing problem. Crit. Rev. Biomed. Eng. 25, 371-407.

Uno, Y., Kawato, R., Suzuki, R., 1989. Formation and control of optimal trajectories in human multi arm joint movements: Minimum torque-change model. Biological Cybernetics 61, 89-101.

van Dieen, J.H., 1997. Are recruitment patterns of the trunk musculature compatible with a synergy based on the maximization of endurance? Journal of Biomechanics 30, 1095-1100.

van Dieen, J.H., Cholewicki, J., Radebold, A., 2003a. Trunk muscle recruitment patterns in patients with low back pain enhance the stability of the lumbar spine. Spine 28, 834-841.

van Dieen, J.H., de Looze, M.P., 1999. Sensitivity of single-equivalent trunk extensor muscle models to anatomical and functional assumptions. Journal of Biomechanics 32, 195-198.

van Dieen, J.H., Kingma, I., 2005. Effects of antagonistic co-contraction on differences between electromyography based and optimization based estimates of spinal forces. Ergonomics 48, 411-426.

Van Dieen, J.H., Kingma, I., van der Bug, J.C.E., 2003b. Evidence for a role of antagonistic cocontraction in controlling trunk stiffness during lifting. Journal of Biomechanics 36, 1829-1836.

van Dieen, J.H., Thissen, C.E.A.M., Ven, v.d., Toussaint, H.M., 1991. The electro-mechanical delay of the erector spinae muscle: influence of rate of force development, fatigue and electrode location. European Journal of Applied Physiology 63, 216-222.

Vera-Garcia, F.J., Brown, S.H., Gray, J.R., McGill, S.M., 2006. Effects of different levels of torso coactivation on trunk muscular and kinematic responses to posteriorly applied sudden loads. Clinical Biomechanics 21, 443-455.

Vieira, R.L.R., Arora, R., Schweitzer, M.E., 2009. Radiological Imaging of Spinal Deformaties, in: Errico, T.J., Lonner, B.S., Moulton, A.W. (Eds.), Surgical Management of Spinal Deformities, 1st ed. Saunders Elsevier, Philadelphia, PA.

Vos, E.J., Mullender, M.G., Schenau, v.I., 1990. Electromechanical delay in the vastus lateralis muscle during dynamic isometric contractions. European Journal of Applied Physiology 60, 467-471.

White, A.A., 3rd, Gordon, S.L., 1982. Synopsis: workshop on idiopathic low-back pain. Spine 7, 141-149.

White, A.A., Panjabi, M.M., 1978. The clinical biomechanics of the spine.

White, A.A., Panjabi, M.M., 1990. Clinical Biomechanics of the Spine. J.B. Lippincott, Philadelphia.

Wilder, D.C., Aleksiev, A.R., Magnusson, M.L., Pop, M.H., Spratt, K.F., Goel, V.k., 1996. Muscular response to sudden load, A tool to evaluate fatigue and rehabilitation. Spine 21, 2628-2639.

Wilke, H.-J., Krischak, S.T., Wenger, K.H., Claes, L.E., 1997. Load-displacement properties of the thoracolumbar calf spine: exprimental results and comparison to known human data. European Spine Journal 6, 129-137.

Wilke, H.-J., Neef, P., Caimi, M., Hoogland, T., Claes, L.E., 1999. New in vivo measurements of pressure in the intervertebral disc in daily life. Spine 24, 755-762.

Willigenburg, N.W., Kingma, I., Van Dieen, J.H., 2013. Center of pressure trajectories, trunk kinematics and trunk muscle activation during unstable sitting in low back pain patients. Gait and Posture 38, 625-630.

Wilson, E.L., Madigan, M.L., Davidson, B.S., Nussbaum, M.A., 2005. Postural strategy changes with fatigue of the lumbar extensor muscles. Gait and Posture 23, 348-354.

Winter, D.A., 2009. Biomechanics and motor control of human movements, 4th ed. John wiley & Sons, Inc.

Yamamoto, I., Panjabi, M.M., Crisco, T., Oxland, T., 1989. Three-dimensional movements of the whole lumbar spine and Lumbosacral joint. Spine 14, 1256-1260.

Zatsiorsky, V.M., Seluyanov, V.N., 1983. The mass and inertia characteristics of the main segments of the human body Biomechanics. Champaign: Human Kinetics Publishers, pp. 1152-1159.

Zedka, M., Kumar, S., Narayan, Y., 1998. Electromyographic response of the trunk muscles to postural perturbation in sitiing subjects. Journal of Electromyography and Kinesiology 8, 3-10.

Zedka, M., Prochazka, A., Knight, B., Gillard, D., Gauthier, M., 1999. Voluntary and reflex control of human back muscles during induced pain. Journal of Physiology 520, 591-604.

Zehra, U., Robson-Brown, K., Adams, M.A., Dolan, P., 2015. Prosity and thickness of the vertebral endplate depend on local mechanical loading. Spine 40, 1173-1180.

Zeinali-Davarani, S., Hemami, H., Barin, K., Shirazi-Adl, A., Parnianpour, M., 2008. Dynamic stability of spine using stability-based optimization and muscle spindle reflex. IEEE Transactions on Neural Systems and Rehabilitation Engineering 16, 106-118.

Zeinali-Davarani, S., Shirazi-Adl, A., Dariush, B., Hemami, H., Parnianpour, M., 2011. The effect of resistance level and stability demands on recruitment patterns and internal loading of spine in dynamic trunk flexion and extension movements. Comput. Methods Biomech. Biomed. Eng. 14, 645-656.

Zeinali-Davarani, S., Shirazi-Adl, A., Hemami, H., Mousavi, H.H., Parnianpour, M., 2007. Dynamic iso-resistive trunk extension simulation: contributions of the intrinsic and reflexive mechanisms to spinal stability. Technology and health care 15, 451-431.

Zhao, F.D., Pollintine, P., Hole, B.D., Adams, M.A., Dolan, P., 2009. Vertebral fractures usually affect the cranial endplate because it is thinner and supported by less-dense trabecular bone. Bone 44, 372-379.

APPENDIX A FINITE ELEMENT MODEL STUDY

A validated FE model of the trunk has been used to quantify the muscles recruitment patterns and forces, spinal loading and spinal stability (Arjmand, 2006; Bazrgari et al., 2009a; El-Rich et al., 2004). The model consists of 7 rigid bodies representing sacrum, L5 to T12 vertebrae and thorax-head-arms segments (Figure A.1). The vertebral rigid bodies are interconnected by 6 nonlinear shear-deformable beam elements which account for passive stiffness of the entire motion segments (discs, vertebral bodies, facets and ligaments). The nonlinear and direction-dependent load-displacement response of the deformable beam elements under single and combined axial/shear forces and sagittal, frontal, and transverse moments has been developed based on previous studies (Lee and Granata, 2008; Oxland et al., 1992; Shirazi-Adl, 2006; Shirazi-Adl et al., 2002; Yamamoto et al., 1989) (Figures A.2-4). Intersegmental damping characteristics of disc and other tissues around the vertebral column are represented as connector elements placed parallel to beam elements (Kasra et al., 1992; Markolf, 1970). Inertial properties of different segments are based on published results (Table A.1) (de Leva, 1996; Pearsall et al., 1996; Zatsiorsky and Seluyanov, 1983).

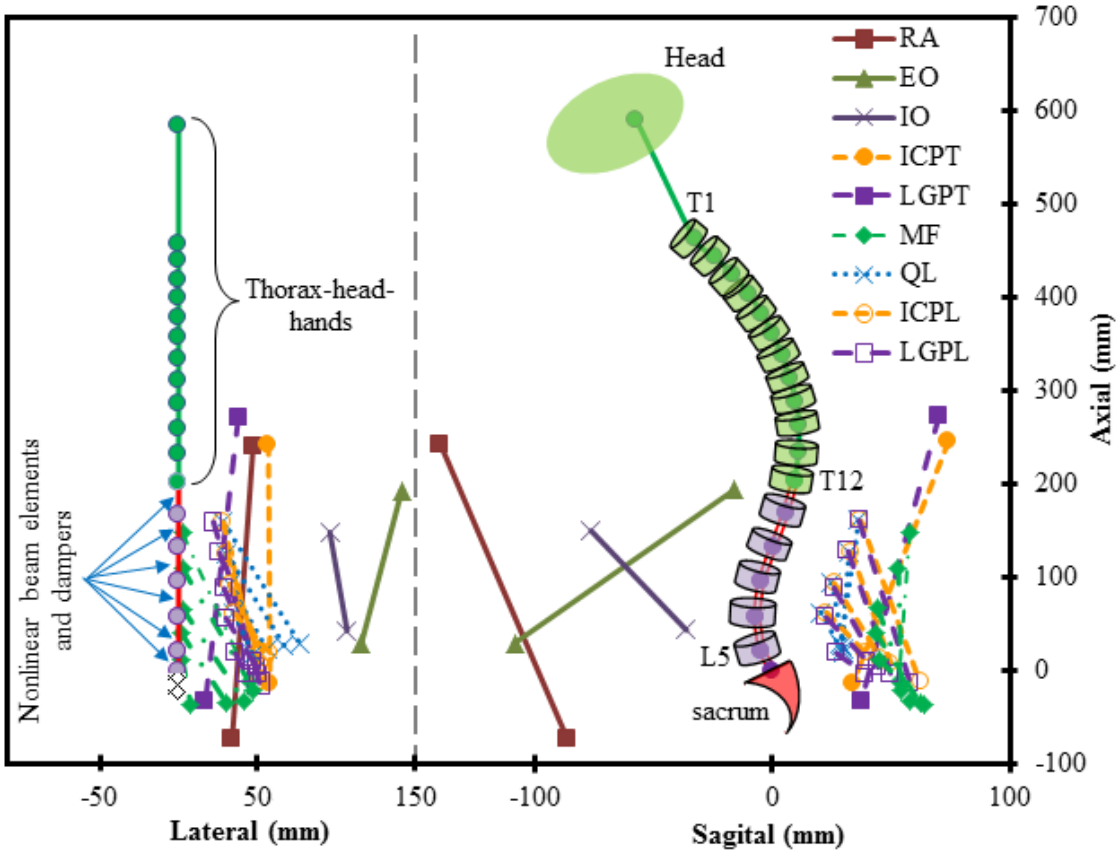

Figure A.1 Schematic view of the trunk FE model (presented in upright posture with different horizontal and vertical scales) illustrating vertebral column as well as local and global musculature in the sagittal and lateral planes, RA: rectus abdominus, EO: external oblique, IO: internal oblique, ICPT: iliocostalis lumborum pars thoracic, LGPT: longissimus thoracis pars thoracic, MF: multifidus, QL: quadratus lumborum, ICPL: iliocostalis lumborum pars lumborum, LGPL: longissimus thoracis pars lumborum.

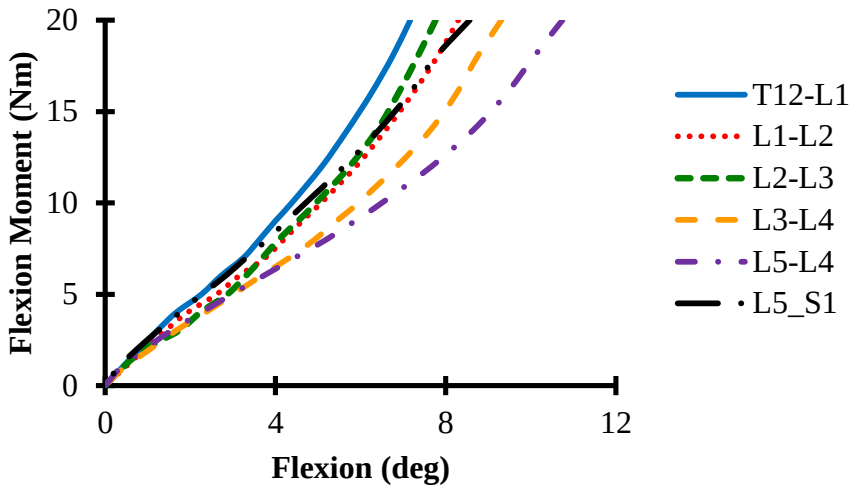

Figure A.2 Segmental nonlinear flexion moment-rotation relationship of various motion segments

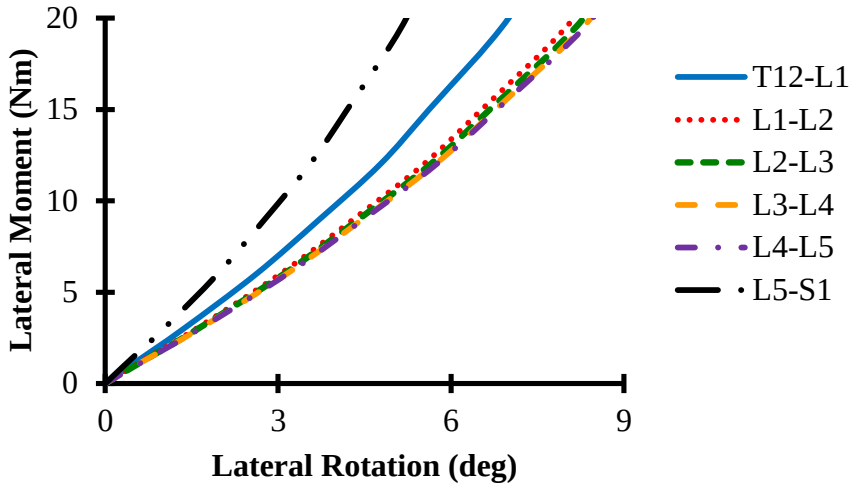

Figure A.3 Segmental nonlinear lateral bending moment-rotation relationship of various motion segments

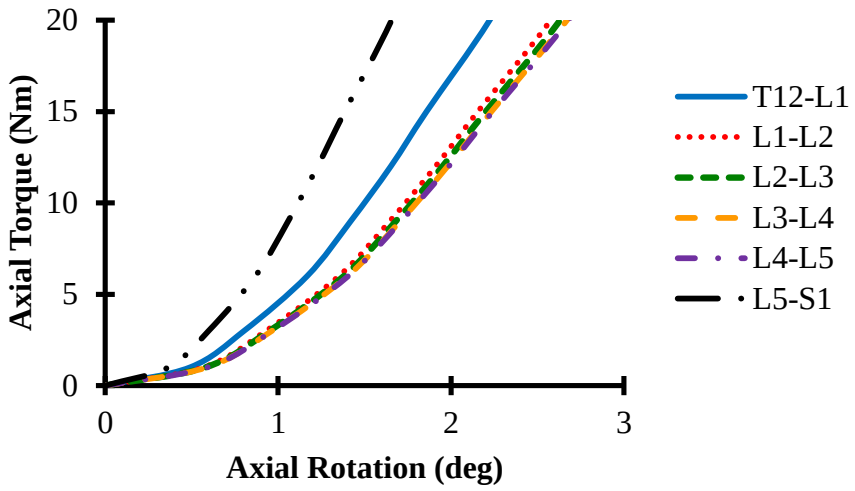

Figure A.4 Segmental nonlinear axial torque-rotation of various motion segments

To account for musculature and assuming sagittal symmetry, 46 local (inserted into lumbar vertebrae) muscles along with 10 global (inserted into thorax) muscles are considered (Stokes and Gardner-Morse, 1999) (Figure A.1 and Table A.2). The muscles are modeled like cables connecting the end points of each muscle; however, wrapping of muscles is taken into account in flexed postures (Arjmand et al., 2006). The Iliocostalis lumborum pars thoracic (ICpt) and Longissimus thoracis pars thoracic (LGpt) muscles are constrained not to approach the T12 to L5 vertebral centers more than 90% of their initial distances at the undeformed configuration. In other words, the minimum allowed distances between the vertebrae center, T12 to L5, and ICpt muscle are 58, 56, 56, 55, 52, and 45 mm, respectively, while their distances relative to LGpt are 53, 53, 55, 56, 54, and 48 mm, respectively. In case of wrapping at each level, the line of action of the associated muscle alters accordingly while a frictionless contact is assumed at the wrapping point. Identical force exists along the whole length of the wrapping muscle irrespective of the number of wrapping contacts (Shirazi-Adl, 1989; Shirazi-Adl and Parnianpour, 2000). The generated contact forces are considered as external forces in the finite element model. Muscle passive forces, F_p are calculated based on empirical data reported by (Bazrgari, 2007; Davis et al., 2003):

$$F_p/F_{Max} = 15.05\left(L/L_0\right)^2 - 30.238\left(L/L_0\right) + 15.194 \qquad \text{Eq. A.1}$$

in which L and L_0 are the instantaneous and resting lengths of muscles. In this study, the resting length was considered in neutral upright posture under gravity forces. F_{Max} is the maximum active muscle force, which is considered in this study as 0.6 MPa × *PCSA* (mm^2).

Table A.1 Mass and inertial properties of the human body segments; mass, mass moment of inertia, I_{xx}, I_{yy}, and I_{zz}, respectively, in sagittal, frontal and transverse planes and mass center at each segment.

Level	% Body Mass	I_{xx}	I_{yy}	I_{zz}	CG-Z	CG-X
Head-Neck	6.94	27.18	29.34	20.13	597.60	-10.00
Upper Arms	2×2.8	12.63	11.30	3.80	447.38	30.00
Lower Arms	2×1.6	6.45	5.99	1.20	426.85	30.00
Hands	2×0.6	1.31	0.88	0.50	405.81	30.00
T1	1.28	6.70	2.00	8.70	467.60	-8.00
T2	1.38	3.40	2.40	9.10	447.38	-12.00
T3	1.47	8.40	3.20	11.50	426.85	-20.00
T4	1.58	8.30	3.40	11.70	405.81	-28.00
T5	1.68	8.00	3.50	11.50	384.14	-33.00
T6	1.78	7.80	3.90	11.60	361.70	-39.00
T7	1.88	7.40	4.10	11.50	338.40	-43.00
T8	1.99	7.20	4.40	11.60	314.12	-45.00
T9	2.10	7.20	4.70	11.80	288.94	-48.00
T10	2.19	8.90	6.20	15.00	262.94	-48.00
T11	2.30	9.00	6.20	15.20	235.30	-46.00
T12	2.39	11.00	7.20	18.10	204.56	-44.00
L1	2.50	11.10	6.50	17.50	171.07	-37.01
L2	2.59	10.90	6.00	16.80	135.03	-29.00
L3	2.70	10.70	5.50	16.10	97.55	-17.00
L4	2.79	11.20	5.30	16.40	58.90	-10.00
L5	2.91	12.20	5.60	17.70	20.57	-6.00
S1	0.00	0.00	0.00	0.00	0.00	0.00
Pelvis	11.00	75.00	30.00	80.00	-89.00	0.00

Table A.2 The initial length, physiologic cross sectional area (PCSA), origin and insertion coordinates of global and local paraspinal muscles

Level	Muscle	Initial Length (mm)	PCSA (mm^2)	Cranial Insertion			Caudal Origin - pelvis		
				X(mm)	Y(mm)	Z(mm)	X(mm)	Y(mm)	Z(mm)
HEAD-T12	ICpt	250	600	84.9	57	235.3	34.9	58	-10
	LGpt	297	1100	85.6	37.8	262.9	40	17	-30
	RA	353	567	-126.7	47.3	269.8	-80	34	-80
	EO	239	1576	-13	141.5	200	-111	116	20
	IO	135	1345	-80	96	167	-40	107	40
L1	IP	276	252	12	10	174.3	-40	79	-88
	MF	158	96	96	54.9	2.5	145	54	45.2
	QL	137	88	34.8	28.3	159.3	26	77	32
	ICpl	170	108	35.7	28.3	159.3	63	52	-7
	LGpl	172	79	35	22.1	159.6	59	51.3	-8.4
L2	IP	241	295	-3	12.13	140.63	-40	79	-88
	MF	135	138	48.8	2.5	110	56	47.9	-16.5
	QL	104	80	28.6	30.5	126.9	27	67	30
	ICpl	118	154	29.8	30.5	126.9	49	52	12
	LGpl	132	91	28.4	26	128.2	50	50.7	0.1
L3	IP	206	334	-9	16.84	105.41	-40	79	-88
	MF	106	211	40.6	2.6	68.4	61	41.6	-28.3
	QL	74	75	21	32.3	95.3	28	56	26
	ICpl	84	182	21.9	23.3	95.3	44	55	18
	LGpl	88	103	22	28.9	90.1	44	49.6	7.3
L4	IP	169	311	-12.78	21.03	68.5	-40	79	-88
	MF	82	186	40.6	1.5	43.4	65	30.4	-29.5
	QL	46	70	17.1	35.1	63.9	28	47	21
	ICpl	50	189	19.3	35.1	63.9	37	58	23
	LGpl	52	110	19.3	30	58.6	39	47.1	13.3
L5	IP	132	182	-17.47	25.32	30.71	-40	79	-88
	MF	51	134	43.9	2.3	15.2	67	7.6	-30.4
	LGpl	25	116	25.7	36	20.6	39	42.9	0

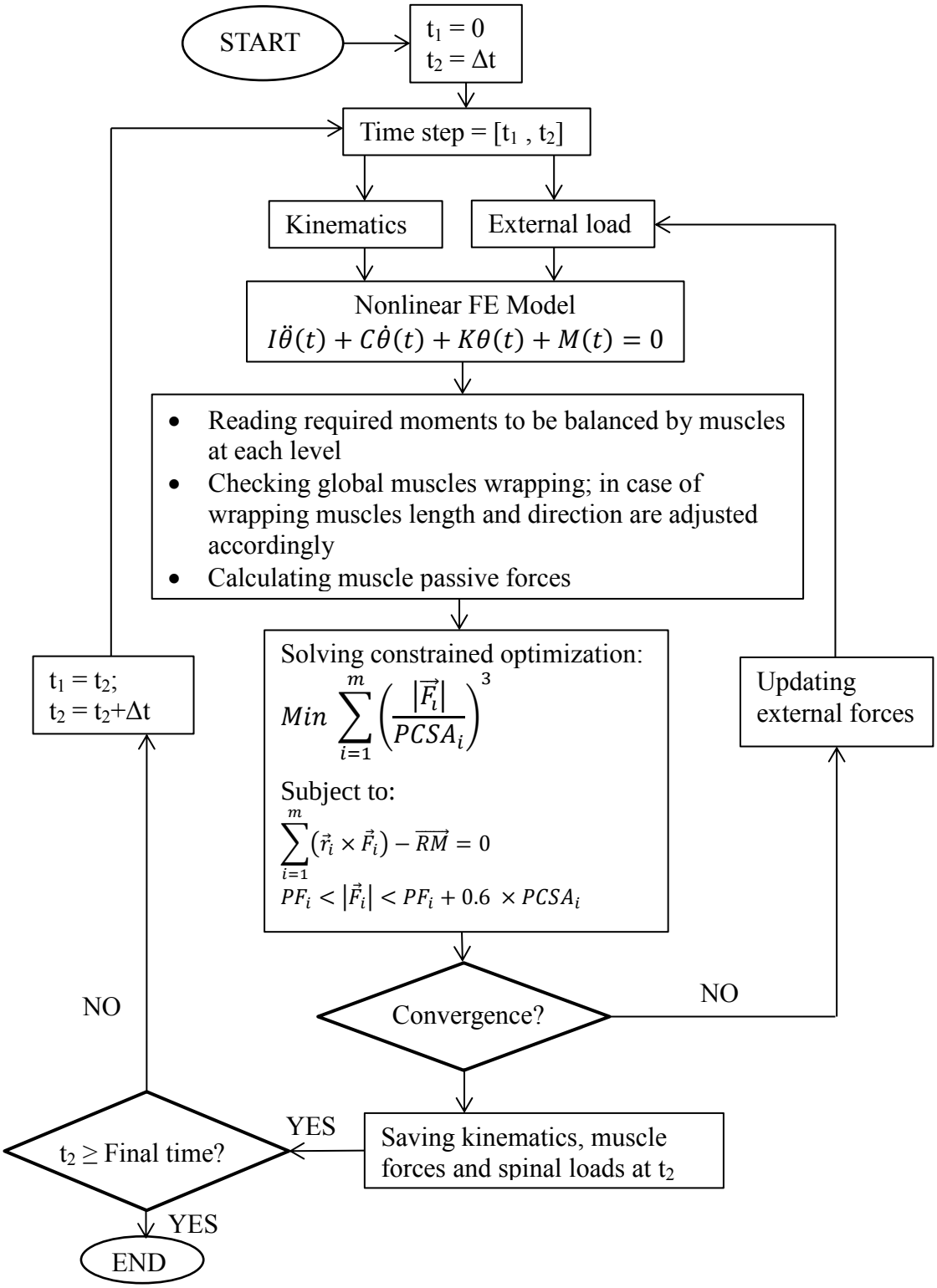

Figure A.5 The algorithm of the kinematics-driven model that starts with prescribing kinematics and external loading as input, and ends with muscle forces and spinal loading as outputs

The total lumbar rotation calculated from the measured rotations at the T12 and S1 is partitioned among the vertebral levels in accordance with proportions reported in earlier investigations (Bazrgari et al., 2008c): 22%, 25%, 19%, 15%, 11% and 8% for L5-S1 to T12-L1, respectively. The velocity profiles calculated as the first derivative of the rotations along with the external loads, i.e. gravity forces, pre- and perturbation loads, weights in hand and muscle forces, are prescribed into the FE model with the time step of Δt = 0.02 sec. The vector of required moments in three planes of motion at the end of each time step, which accounts for the required muscle forces for equilibrium, as well as the final configuration of the spine are obtained by executing the FE model. The following constrained optimization problem is solved to calculate the muscle forces.

$$Min \sum_{i=1}^{m} \left(\frac{|\vec{F_i}|}{PCSA_i} \right)^3 \qquad \text{Eq. A.2}$$

subject to

$$\sum_{i=1}^{m} (\vec{r_i} \times \vec{F_i}) - \overrightarrow{RM} = 0$$

$$PF_i < |\vec{F_i}| < PF_i + 0.6 \times PCSA_i$$

in which $\vec{F_i}$, $PCSA_i$, $\vec{r_i}$, $\overrightarrow{PF_i}$ are total force, physiological cross sectional area, level arm with respect to the center of vertebra and passive force of muscle *i*, respectively. $\overrightarrow{RM}$ is the vector of required moments in three planes of motion. This optimization is solved at each vertebral level separately to estimate corresponding muscle forces.

Analytical solution of this optimization is available for symmetric deformations in the sagittal plane including the upright neutral position under gravity forces. The optimization, however, is solved numerically using fmincon function of Matlab 7.12 and 8.3 (The Mathworks Inc., Natick, Massachusetts). The results e.g. muscle forces, obtained through the numerical optimization for movements in the sagittal plane have been compared to the analytical global solutions. It has revealed the accuracy of the numerical solutions irrespective of the initial guess. Therefore, for both 2D and 3D simulations numerical optimization method is used. However, to ensure that the solution (muscle forces) is the global minimum of the objective function, the solution of the

previous time step, t_{n-1} is used as the initial guess for subsequent optimization at t_n. Since the trunk is initially in the upright neutral posture, the analytical solution at t_0 is always available.

Using the calculated muscle forces, the external loading is updated and FE model is solved again. This procedure is repeated until convergence at which time the simulation proceeds to the next time step.

To assess spinal stability after muscle forces are estimated, all muscles are replaced with springs with stiffness, k, which is determined using the Bergmark's formulation (Bergmark, 1989b), $k = q\frac{F}{L}$, in which F and L are instantaneous muscle force and muscle length, respectively, (Figure A.5). The algorithm starts with a large q, and the goal is to find the minimum q called critical q for which the trunk is stable. Natural frequencies of the system are calculated using Abaqus. If the smallest natural frequency is found positive, the spine is stable. In this case, the q is decreased and the procedure is repeated until the minimum critical q for the trunk stability is found.

APPENDIX B THREE-DIMENSIONAL ROTATION

Abaqus FE package calculates Rodrigues rotations when defining spatial angular motions. So the input rotations should be based on Rodrigues formulation. In this study, however, the rotations are measured using Euler finite-rotation formulation. Therefore, the equivalent Rodrigues angles are calculated.

B.1. Euler angles

To define a three dimensional rotation in space from the primary angular position *(P)* to the final one *(F)*, three sequential Euler angles are defined (Figure B.1). The transformation matrix of rotation Θ_{x1} around axis *X* could be written as:

$$T_{P-1} = \begin{bmatrix} 1 & 0 & 0 \\ 0 & \cos\theta_{x1} & -\sin\theta_{x1} \\ 0 & \sin\theta_{x1} & \cos\theta_{x1} \end{bmatrix} \quad \text{Eq. B.1}$$

In the next step, the body rotates by Θ_{y2} around the rotated *Y* axis which is now *y1*. The transformation matrix of this rotation around y1 is:

$$T_{1-2} = \begin{bmatrix} \cos\theta_{y2} & 0 & \sin\theta_{y2} \\ 0 & 1 & 0 \\ -\sin\theta_{y2} & 0 & \cos\theta_{y2} \end{bmatrix} \quad \text{Eq. B.2}$$

Finally, the transformation matrix of rotation Θ_{z3} around the rotated axis z_2 is:

$$T_{2-F} = \begin{bmatrix} \cos\theta_{z3} & -\sin\theta_{z3} & 0 \\ \sin\theta_{z3} & \cos\theta_{z3} & 0 \\ 0 & 0 & 1 \end{bmatrix} \quad \text{Eq. B.3}$$

The total transformation matrix from the primary coordinate system (P) to the final coordinate system (F) is the multiplication of above matrices in the order of rotations x-y-z could be written in the following form.

$$T_{P-F} = \begin{bmatrix} 1 & 0 & 0 \\ 0 & \cos\theta_{x1} & -\sin\theta_{x1} \\ 0 & \sin\theta_{x1} & \cos\theta_{x1} \end{bmatrix} \times \begin{bmatrix} \cos\theta_{y2} & 0 & \sin\theta_{y2} \\ 0 & 1 & 0 \\ -\sin\theta_{y2} & 0 & \cos\theta_{y2} \end{bmatrix} \times \begin{bmatrix} \cos\theta_{z3} & -\sin\theta_{z3} & 0 \\ \sin\theta_{z3} & \cos\theta_{z3} & 0 \\ 0 & 0 & 1 \end{bmatrix}$$

$$T_{P-F} = \begin{bmatrix} c\theta_{y2}c\theta_{z3} & -c\theta_{y2}s\theta_{z3} & s\theta_{y2} \\ c\theta_{x1}s\theta_{z3} + c\theta_{z3}s\theta_{x1}s\theta_{y2} & c\theta_{x1}c\theta_{z3} - s\theta_{x1}s\theta_{y2}s\theta_{z3} & -c\,\theta_{y2}\,s\theta_{x1} \\ s\theta_{x1}s\theta_{z3} - c\theta_{x1}c\theta_{z3}s\theta_{y2} & c\theta_{z3}s\theta_{x1} + c\theta_{x1}s\theta_{y2}s\theta_{z3} & c\theta_{x1}c\theta_{y2} \end{bmatrix} \quad \text{Eq. B.4}$$

in which *c* and *s* represent cos and sin.

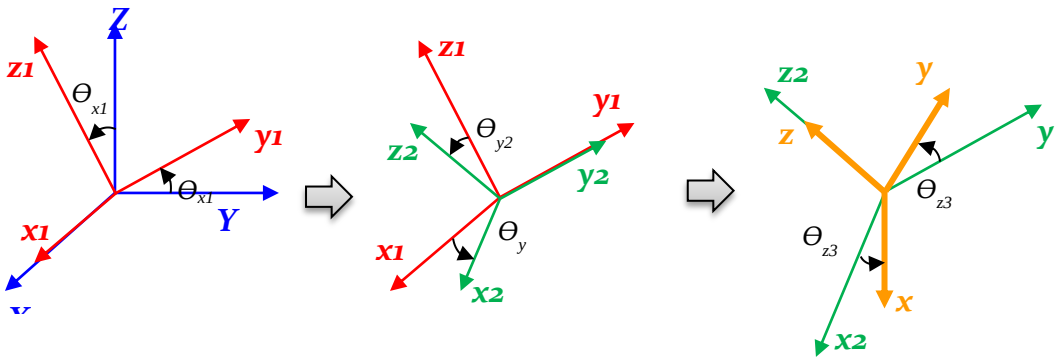

P-1 1-2 2-F

Figure B.1 Euler angles, Θ_{x1}, Θ_{y2} and Θ_{z3} are defined as the angles that rotate the body coordinate system in particular sequence around the rotated axes of a particular coordinate system. The body rotates from the primary position (P) to the final position (F).

B.2. Rodrigues angles

The three dimensional rotation of an object, such as vector a_0 in Figure B.2 could be defined as the rotation α around an axis of rotation $v(n_1,n_2,n_3)$, where n1, n2 and n3 are its cosine direction.

To derive the rotation matrix, the vector a_0 is decomposed into the a_p that is parallel to v and a_v that is perpendicular to v. Therefore, if k is the unit vector in the direction of v, we can write:

$$a_p = (a_0.k)k$$

and

$$a_v = a - a_p$$

The parallel component, a_p, does not rotate due to rotation α around v; however, a_v rotates as shown in Figure B.2.

The vector a_{v1} is the rotated form of a_v that is defined as

$$a_{v1} = (a_0 - (k.a_0)k)cos\alpha + (k \times a_0)sin\alpha$$

Since a_1, the rotated form of a_0, is the summation of a_{v1} and a_p, we may write:

$$a_1 = a_p + a_{v1} = (a_0 - (k.a_0)k)cos\alpha + (k \times a_0)sin\alpha + (k.a_0)k$$

Therefore:

$$a_1 = a_0 cos\alpha + (k \times a_0)sin\alpha + k(k.a_0)(1 - cos\theta) \qquad \text{Eq. B.5}$$

A matrix K is defined such that $Kv = k \times v$:

$$K = \begin{bmatrix} 0 & -n_3 & n_2 \\ n_3 & 0 & -n_1 \\ -n_2 & n_1 & 0 \end{bmatrix}$$

in which n_1, n_2 and n_3 are cosine directions of v and k. So Eq. B.5 could be rewritten as follows:

$$a_1 = a_0 cos\alpha + Ka_0 sin\alpha + k(k.a_0)(1 - cos\alpha)$$

After some mathematical operations:

$$a_1 = a_0 + Ka_0 sin\alpha + (k(k.a_0) - a_0)(1 - cos\alpha)$$

Then we write

$$a_1 = a_0 + (sin\alpha)Ka_0 + (1 - cos\alpha)K^2 a_0$$

The final rotation matrix would be:

$$R = I + (sin\alpha)K + (1 - cos\alpha)K^2$$

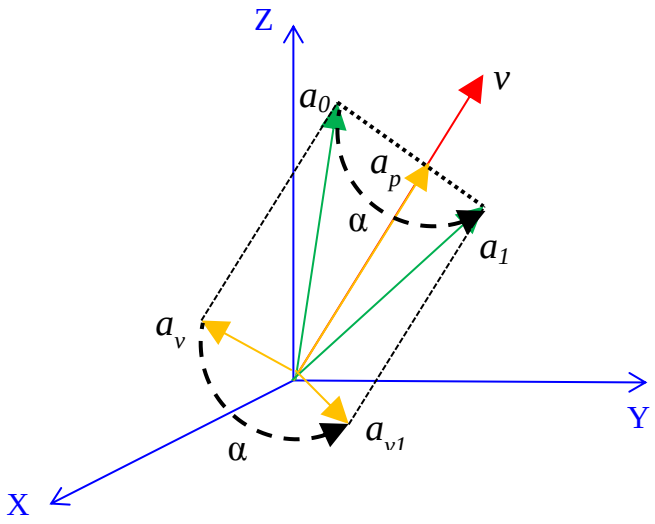

Figure B.2 Rodriguez angles are defined as the rotation α around a vector *v*.

This transformation matrix should be equivalent to that of Euler angles, $R=T_{P\text{-}F}$. So by solving this equation the rotations could be transformed from Euler to Rodrigues angles.